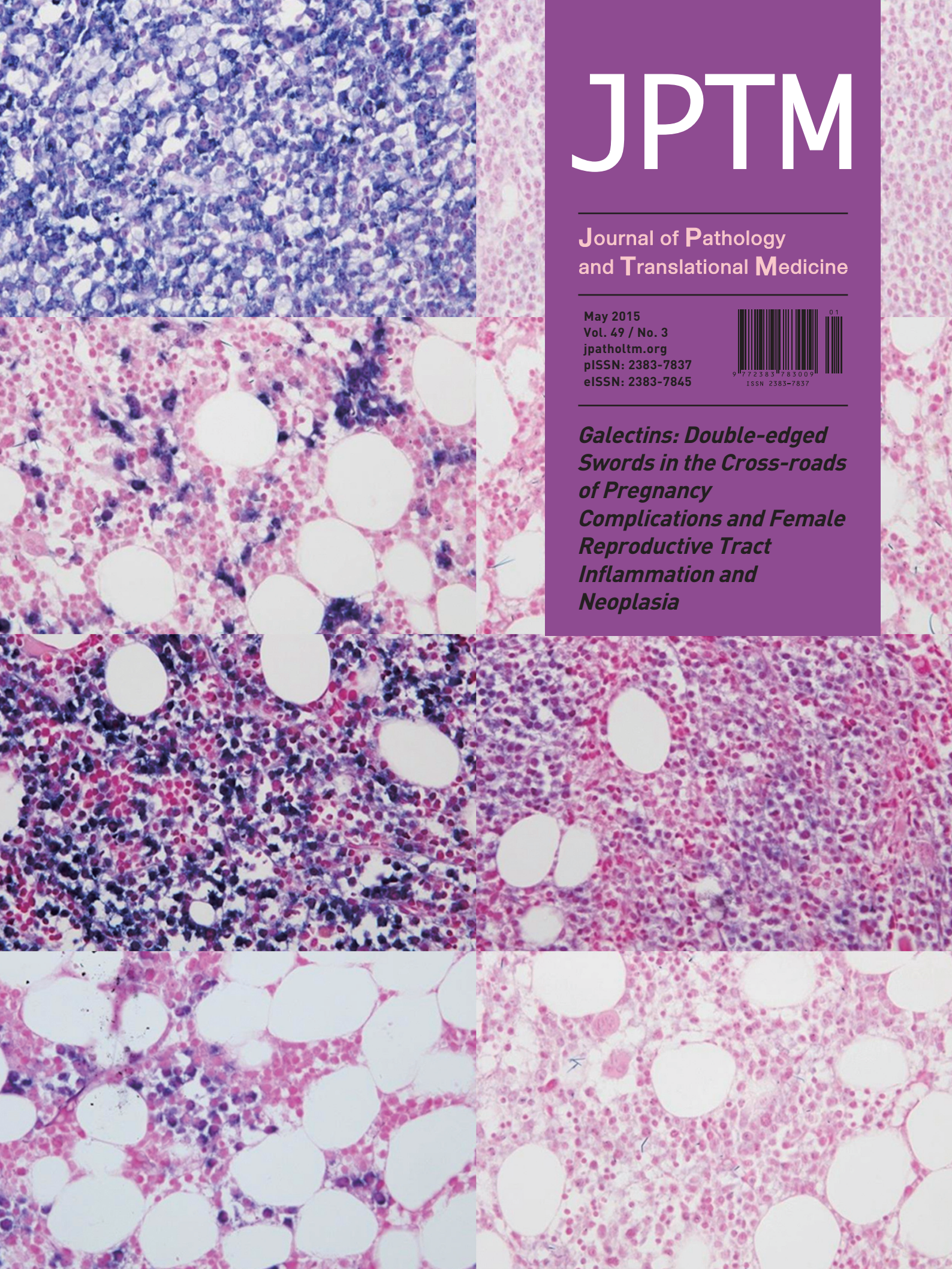

JPTM

Journal of Pathology and Translational Medicine

May 2015
Vol. 49 / No. 3
jpatholtm.org
pISSN: 2383-7837
eISSN: 2383-7845

Galectins: Double-edged Swords in the Cross-roads of Pregnancy Complications and Female Reproductive Tract Inflammation and Neoplasia

Journal of Pathology and Translational Medicine

Volume 49 • Number 3 • May 2015 (bimonthly)
Published since 1967
Printed on 11 May 2015 Published on 15 May 2015

J Pathol Transl Med
pISSN: 2383-7837
eISSN: 2383-7845

Aims & Scope

The Journal of Pathology and Translational Medicine is an open venue for the rapid publication of major achievements in various fields of pathology, cytopathology, and biomedical and translational research. The Journal aims to share new insights into the molecular and cellular mechanisms of human diseases and to report major advances in both experimental and clinical medicine, with a particular emphasis on translational research. The investigations of human cells and tissues using high-dimensional biology techniques such as genomics and proteomics will be given a high priority. Articles on stem cell biology are also welcome. The categories of manuscript include original articles, review and perspective articles, case studies, brief case reports, and letters to the editor.

Subscription Information

To subscribe to this journal, please contact the Korean Society of Pathologists/the Korean Society for Cytopathology. Full text PDF files are also available at the official website (http://jpatholtm.org). *Journal of Pathology and Translational Medicine* is indexed by PubMed, PubMed Central, Scopus, KoreaMed, KoMCI, WRPIM and CrossRef. Circulation number per issue is 700.

Contact the Korean Society of Pathologists/the Korean Society for Cytopathology

Publishers: Changsuk Kang, M.D., So Young Jin, M.D.
Editors-in-Chief: Soon Won Hong, M.D., Chong Jai Kim, M.D.
Published by the Korean Society of Pathologists/the Korean Society for Cytopathology

Editorial Office
Room 1209 Gwanghwamun Officia, 92 Saemunan-ro, Jongno-gu,
Seoul 110-999, Korea/#406 Lilla Swami Bldg, 68 Dongsan-ro,
Seocho-gu, Seoul 137-899, Korea
Tel: +82-2-795-3094/+82-2-593-6943
Fax: +82-2-790-6635/+82-2-593-6944
E-mail: office@jpatholtm.org

Printed by ML communications Co., Ltd.
Jungang Bldg. 18-8 Wonhyo-ro 89-gil, Yongsan-gu, Seoul 140-846, Korea
Tel: +82-2-717-5511 Fax: +82-2-717-5515 E-mail: ml@smileml.com

Manuscript Editing by InfoLumi Co.
210-202, 421 Pangyo-ro, Bundang-gu, Seongnam 463-926, Korea
Tel: +82-70-8839-8800 E-mail: infolumi.chang@gmail.com

Front cover image: Confocal laser endomicroscopic finding for normal mucosa. p213.

This paper meets the requirements of KS X ISO 9706, ISO 9706-1994 and ANSI/NISO Z.39.48-1992 (Permanence of Paper).
This journal was supported by the Korean Federation of Science and Technology Societies Grant funded by the Korean Government.

Journal of Pathology and Translational Medicine

J Pathol Transl Med
pISSN: 2383-7837
eISSN: 2383-7845

Volume 49, Number 3, May 2015

CONTENTS

REVIEWS

ORIGINAL ARTICLES

CASE REPORTS

CONTENTS CONTINUED

Instructions for Authors for *Journal of Pathology and Translational Medicine* are available at http://jpatholtm.org/authors/authors.php

Journal of Pathology and Translational Medicine 2015; 49: 181-208
http://dx.doi.org/10.4132/jptm.2015.02.25

■ REVIEW ■

Galectins: Double-edged Swords in the Cross-roads of Pregnancy Complications and Female Reproductive Tract Inflammation and Neoplasia

Nandor Gabor Than[1,2,3,4,5]
Roberto Romero[1] · Andrea Balogh[1,6]
Eva Karpati[3,6]
Salvatore Andrea Mastrolia[7,8]
Orna Staretz-Chacham[9]
Sinuhe Hahn[10] · Offer Erez[1,2,7]
Zoltan Papp[4] · Chong Jai Kim[1,11,12]

[1]Perinatology Research Branch, *Eunice Kennedy Shriver* National Institute of Child Health and Human Development, National Institutes of Health, Department of Health and Human Services, Detroit, MI, USA; [2]Department of Obstetrics and Gynecology, Wayne State University School of Medicine, Detroit, MI, USA; [3]Institute of Enzymology, Research Centre for Natural Sciences, Hungarian Academy of Sciences Budapest, Budapest, Hungary; [4]Maternity Private Department, Kutvolgyi Clinical Block, Semmelweis University, Budapest, Hangary; [5]First Department of Pathology and Experimental Cancer Research, Semmelweis University, Budapest, Hungary; [6]Department of Immunology, Eotvos Lorand University, Budapest, Hungary; [7]Department of Obstetrics and Gynecology, Ben-Gurion University, Beer-Sheva, Israel; [8]Department of Obstetrics and Gynecology, University of Bari Aldo Moro, Bari, Italy; [9]Department of Neonatology, Ben-Gurion University, Beer-Sheva, Israel; [10]Department of Biomedicine, University Hospital Basel, Basel, Switzerland; [11]Department of Pathology, Wayne State University, Detroit, MI, USA; [12]Department of Pathology, Asan Medical Center, University of Ulsan College of Medicine, Seoul, Korea

Received: February 18, 2015
Accepted: February 25, 2015

Corresponding Author
Nandor Gabor Than, M.D., Ph.D.
Institute of Enzymology, Research Centre for Natural Sciences, Hungarian Academy of Sciences, 2 Magyar Tudosok korutja, Budapest H-1117, Hungary
Tel: +36-1-382-6788
E-mail: than.gabor@ttk.mta.hu

Galectins are an evolutionarily ancient and widely expressed family of lectins that have unique glycan-binding characteristics. They are pleiotropic regulators of key biological processes, such as cell growth, proliferation, differentiation, apoptosis, signal transduction, and pre-mRNA splicing, as well as homo- and heterotypic cell-cell and cell-extracellular matrix interactions. Galectins are also pivotal in immune responses since they regulate host-pathogen interactions, innate and adaptive immune responses, acute and chronic inflammation, and immune tolerance. Some galectins are also central to the regulation of angiogenesis, cell migration and invasion. Expression and functional data provide convincing evidence that, due to these functions, galectins play key roles in shared and unique pathways of normal embryonic and placental development as well as oncodevelopmental processes in tumorigenesis. Therefore, galectins may sometimes act as double-edged swords since they have beneficial but also harmful effects for the organism. Recent advances facilitate the use of galectins as biomarkers in obstetrical syndromes and in various malignancies, and their therapeutic applications are also under investigation. This review provides a general overview of galectins and a focused review of this lectin subfamily in the context of inflammation, infection and tumors of the female reproductive tract as well as in normal pregnancies and those complicated by the great obstetrical syndromes.

Key Words: Alarmin; Epigenomics; Maternal-fetal interface; Neoplasms; Sex steroids

pISSN 2383-7837
eISSN 2383-7845

INTRODUCTION TO THE GALECTIN FAMILY

More than half of all human proteins are glycosylated,[1] and glycans are attached to various additional glycoconjugates (e.g. glycolipids) besides glycoproteins. Because of the abundance of glycans intra- and extracellularly and also their high complexity, glycans can store orders of magnitude larger biological information than other biomolecules (e.g. nucleic acids and proteins).[2,3] Lectins are sugar-binding proteins, which are not an antibody or an enzyme, and can specifically bind glycans without catalyzing their modification.[3,4] The interactions of lectins with glycans are pivotal in the regulation of a wide variety of interactions of cells with other cells, the extracellular matrix or pathogens.[2-4]

Galectins belong to a subfamily of lectins based on their unique structural and sugar-binding characteristics, since their carbohydrate-recognition domains (CRDs) contain consensus amino acid sequences and they specifically bind beta-galactoside–containing glycoconjugates.[5-8] Galectins are the most widely expressed animal lectins; they have been found in species ranging from sponges to humans.[7-9] They regulate a wide variety of key biological processes, such as cell growth, proliferation and differentiation, apoptosis, signal transduction, pre-mRNA splicing, as well as cell-cell and cell-extracellular matrix interactions.[2,5-9] Galectins are also pivotal in immune responses since they regulate host-pathogen interactions, acute and chronic inflammation, and immune tolerance (Fig. 1).[8,10-13] Moreover, some galectins are central to the regulation of angiogenesis in the placenta and in tumors.[14,15] Interestingly, galectins can have opposing functions, and the same galectin can also have varying or contrasting effects based on the biological context and the microenvironment since their functions depend on the differentiation or activation status of the cell, the dynamic changes of their glycan partners on the cell surfaces, the redox and oligomerization status of the galectin, or its intra- or extracellular localization.[8,11,16,17] Thus, galectins' double-edged action may sometimes be beneficial or harmful to the organism.

The fundamental functions of galectins indicate that they are strongly associated with reproductive functions as well as the establishment and maintenance of pregnancy.[10,18-28] Indeed, some galectins are highly expressed at the maternal-fetal interface,[10,18-39] and these are evolutionarily linked to placental evolution in eutherian mammals.[5,7,9,26,27,40] Moreover, the dysregulated expression of these galectins in pregnancy complications has been increasingly documented.[10,23,32-36,38,41-51] Galectins have also been implicated in inflammatory, infectious and malignant diseases of the reproductive tracts. Of importance, the same galectins may be functional in pathways commonly shared by physiological and pathological, placental, and tumor developmental processes (e.g. cell invasion, angiogenesis, and immune tolerance). This review aims to give a general overview of galectins and also a focused review of them in the context of inflammation, infection and tumors in the female reproductive tract as well as in normal and complicated pregnancies.

Structural features of mammalian galectins

Galectins were originally termed "S-type lectins," where "S" refers to their free cysteine residues.[6,8] Galectins or galectin-like proteins were also discovered in fungi, viruses, and even plants.[8,9] Because of the diversity between mammalian and non-mammalian galectins, their nomenclature has diverged as mammalian galectins have been named using sequential numbering, while non-mammalian galectins have retained specific names (Table 1).[6] Nineteen galectins have been identified in mammals to date, 13 of which were found in humans.[9,27] These galectins can be divided into three structural groups:[5-8] (1) "proto-type" galectins (-1, -2, -5, -7, -10, -13, -14, -15, -16, -17, -19, -20) contain a single CRD of ~130 amino acids, which homodimerize;[5-8,52] (2) "tandem-repeat-type" galectins (-4, -6, -8, -9, -12) contain two homologous CRDs connected by a short linker sequence. These may differ in their sugar-binding affinities and enable multivalent binding activity;[5-7,52] and (3) "chimera-type" galectin-3, which contains a C-terminal CRD and an N-terminal non-lectin domain important for multimerization and cross-linking as well as functional regulation.[5-7,52]

Although the amino acid sequences of galectins have diverged during evolution, the topologies of their CRDs are very similar, often described as "jelly-roll;" these are β-sandwiches consisting of five- and six-stranded anti-parallel β-sheets (Fig. 1).[6-8,53-55] Highly conserved in galectin CRDs are eight residues, which are involved in glycan-binding by hydrogen-bonds as well as electrostatic and van der Waals interactions.[53,55] All galectins specifically bind beta-galactosides[5-8] except galectin-10, which has more affinity to beta-mannosides.[53] Of interest, some galectins have high affinity for poly-N-acetyllactosamine or ABO blood-group containing glycans, and the latter is responsible for their hemagglutinin activity.[52,56-58]

Functional characteristics of mammalian galectins

Galectins have multiple functions both inside and outside the cell (Table 1).[8,59,60] Intracellularly, certain galectins can modulate cell growth, differentiation, apoptosis, and migration[8,59,60] via protein-protein interactions.[8,59,60] Some galectins (-1 and -3)

 http://dx.doi.org/10.4132/jptm.2015.02.25

shuttle into the nucleus where they function in pre-mRNA splicing.[8,59] In spite of the fact that they do not have a secretory signal sequence, galectins can be secreted from cells via a non-classical pathway, avoiding the endoplasmic reticulum and Golgi apparatus, which is characteristic of only a small set of proteins (e.g. high-mobility group box 1 protein, interleukin-1β).[61] Extracellularly, galectins predominantly localize to lipid rafts on cell surfaces[8,52,62] where they exert their functions through binding to cell-surface or extracellular matrix molecules, which carry their glycan ligands.[2,7,8,11,13,52,63,64] They can form multivalent galectin-glycan arrays, so-called lattices, by cross-linking their ligands on cell surfaces, and these lattices can organize lipid raft domains and modulate cell signaling for cell growth, metabolic functions, cytokine secretion, and survival, as well as many other intracellular and extracellular interactions.[8,11,13,17,52,65] Some galectins can also affect cell adhesion and apoptosis, and activate or inhibit immune responses.[8,11,13,63] An interesting trait of galectins is that their secretion is heightened upon response to stress conditions (e.g. inflammation and infection) and cellular damage (e.g. necrosis); therefore, galectins have been implicated as "alarmins" which signal tissue damage and elicit effector responses from immune cells, thereby promoting the activation and/or resolution of immune responses.[12,35,64,66]

Expression profile of human galectins

Accumulating evidence in various species shows that galectins have distinct but overlapping tissue expression patterns in mammals including humans (Table 1).[6,8,27,67,68] Among prototype galectins, galectin-1 and galectin-3 have a wide expression pattern in humans, galectin-1 being the most abundant in the endometrium/decidua.[8,26,67] Among tandem-repeat-type galectins, galectin-8 and galectin-9 have a broad and complex expression pattern. Alternatively spliced isoforms of galectin-8 are differentially expressed in various tissues[8,39,67] similar to galectin-9, which is encoded by three genes.[67] These galectins are highly expressed in the female reproductive tract and at the maternal-fetal interface.[8,10,18-23,25,27,32,34,35,37-39,69] Some galectins (-2, -4, -5, -6, -7, -12) have more restricted tissue distribution.[8,67] Of note, the expression of galectins in the chromosome 19 cluster is very restricted. Among these, galectin-10 is expressed in T regulatory (Treg) cells, as well as eosinophil and basophil lineages, and forms the so-called Charcot-Leyden crystals at sites of eosinophil-associated inflammation.[53,70] The expression of galectin-13, -14 and -16 is predominant in the placenta, while galectin-17 expression is low in any tissues.[27,29,67,71] Interestingly, these galectins (-10, -13, -14, -16, -17), which are expressed from the chromosome 19 cluster, emerged via birth-and-death evolution in anthropoid primates and may regulate unique aspects of pregnancies, including maternal-fetal immune regulation and tolerance in these species.[16,27,72]

GALECTINS IN INFECTION AND INFLAMMATION OF THE FEMALE REPRODUCTIVE TRACT

Due to the multiple functions of galectins, they have been implicated in pathways and processes fundamental for reproductive functions in both the pregnant and non-pregnant state. Data on the expression profile and functions of galectins regarding female reproductive tissues has recently emerged. Accordingly, a growing body of evidence suggests that galectins play important roles in immune responses in inflammatory and infectious diseases and in the development of various tumors of the female reproductive tract.

Galectins in infection of the female reproductive tract

Recent evidence suggests that the outcome of infection is also significantly influenced by galectins (Fig. 1) as these glycan-binding proteins acts as regulators of host-pathogen interactions.[12] Similar to alarmins, upon tissue damage and/or prolonged infection, cytosolic galectins can be passively released from dying cells or actively secreted by inflammation-activated cells through the non-classical 'leaderless' secretory pathway.[12] Once exported, galectins act as soluble or membrane-bound 'damage associated molecular patterns'[12,66] or 'pathogen associated molecular patterns.' The latter, due to their CRDs, can specifically recognize pathogen cell surface antigens like pattern recognition receptors.[12,66,73] Indeed, various galectins have been shown to bind a wide range of pathogens, which display their ligands on the surfaces, such as Gram-positive bacteria (e.g. *Streptococcus pneumoniae*), Gram-negative bacteria (e.g. *Klebsiella pneumoniae*, *Neisseria meningitidis*, *Neisseria gonorrhoeae*, *Haemophilus influenzae*, *Pseudomonas aeruginosa*, *Porphyromonas gingivalis*, and *Escherichia coli*), enveloped viruses (Nipah and Hendra paramyxoviruses, human immunodeficiency virus [HIV]-1, and influenza virus A), fungi (*Candida albicans*) and parasites (*Toxoplasma gondii*, *Leishmania major*, *Schistosoma mansoni*, *Trypanosoma cruzi*, and *Trichomonas vaginalis*).[12,74-82]

It is interesting that the co-evolution of microbes and host glycocalyx components is a continuously ongoing process, and the evolutionary arms race, the "Red Queen effect," has strongly impacted pathogenic and invasive properties of those microbes in

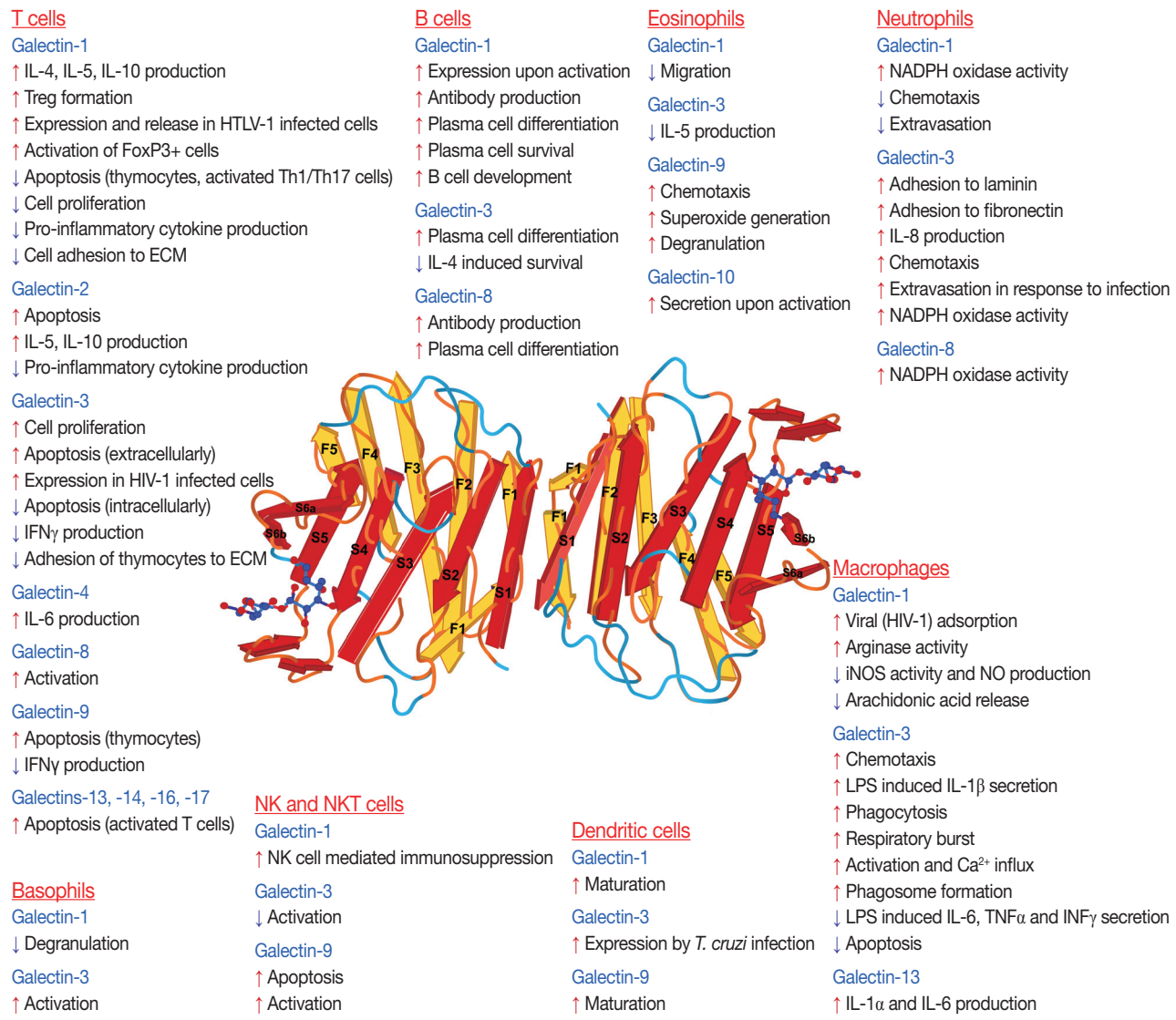

Fig. 1. Galectins in inflammation and infection. The effects and expression changes of galectins in immune cells are depicted around the three-dimensional model of galectin-1 (Protein Data Bank accession number: 1GZW).[35,55] Galectins' effects are biological-context and microenvironment dependent and relate to the differentiation or activation status of the cell, the dynamic changes of the glycan partners of galectins on cell surfaces, the redox and oligomerization status of the galectin, or its intracellular or extracellular localization. ECM, extracellular matrix; HIV-1, human immunodeficiency virus 1; iNOS, inducible nitric oxide synthase; IFN, interferon; IL, interleukin; LPS, lipopolysaccharide; NK, natural killer; TNF, tumor necrosis factor. Parts of the figure are adapted from Than *et al*. Trends Endocrinol Metab 2012; 23: 23-31, with permission of Elsevier.[16]

relation to glycocalyx components that now infect our species.[73,83] For example, it has been observed that galectin-3 provides advantage for *Helicobacter pylori* in binding to gastric epithelial cells, and thus, enhances the rate of infection.[78] Similarly, galectin-1 increases the spread of human T-cell leukemia virus type I by stabilizing both virus-cell and uninfected-infected T cell interactions.[79] Interestingly, due to their ligand-binding specificity, galectin-1, but not galectin-3, can influence the sexual transmission of HIV-1 through the increase of viral adsorption kinetics on monocyte-derived macrophages.[77,84] Based on this data, the progress of microbial infections seems to depend on the expression and localization of various galectins in the route of infection.

The most studied galectin in infections of the female reproductive tract is galectin-3. It is expressed on the apical side of the non-ciliated epithelial cells in the Fallopian tube and can bind the lipooligosaccharides on *Neisseria gonorrhoeae*. Since galectin-3 participates in several endocytotic processes, such as its own reuptake, it can facilitate the invasion of human epithelial cells by gonococci.[74] Interestingly, in response to gonococcal infection, tumor necrosis factor α production increases in the Fallopian

http://dx.doi.org/10.4132/jptm.2015.02.25

Table 1. Mammalian galectins

Galectin	Species	Human tissue and cell localization	Participation in biological processes relevant to tumors and pregnancy in mammals
Galectin-1	From fishes	Adipose tissue, bone marrow, central nervous system, endocrine glands, endothelia, female and male reproductive systems, immune cells, lymphatic organs, placenta, respiratory system, skin, smooth muscle	Angiogenesis, apoptosis, cell adhesion, proliferation, migration and invasion, inflammation and infection, immune tolerance, immune surveillance
Galectin-2	From fishes	Blood, bone marrow, digestive tract, immune cells, lymphatic organs, placenta, urinary tract	Apoptosis, inflammation and infection, tumor cell adhesion
Galectin-3	From fishes	Adipose tissue, bone marrow, central nervous system, digestive tract, endocrine glands, female and male reproductive systems, heart muscle, immune cells, lymphatic organs, placenta, respiratory system, skin, smooth muscle, urinary tract	Apoptosis, cell proliferation, migration and invasion, inflammation and infection, immune tolerance, immune surveillance, tumor and immune cell adhesion
Galectin-4	From amphibians	Digestive tract, male reproductive system, skin	Inflammation, tumor cell adhesion
Galectin-5	Only in rodents	-	-
Galectin-6	Only in rodents	-	-
Galectin-7	From mammals	Digestive tract, female reproductive system, hearth, lymphatic organs	Apoptosis, cell proliferation
Galectin-8	From amphibians	Bone marrow, digestive tract, endocrine glands, female and male reproductive systems, immune cells, lymphatic organs, placenta, urinary tract	Infection, tumor and immune cell adhesion
Galectin-9	From fishes	Adipose tissue, bone marrow, digestive tract, endocrine glands, female reproductive system, immune cells, lymphatic organs, placenta, respiratory system, skin, smooth muscle	Apoptosis, cell proliferation, migration, inflammation and infection
Galectin-10	From primates	Bone marrow, immune cells, lymphatic organs	Inflammation, immune regulation
Galectin-12	From amphibians	Adipose tissue, bone marrow, female reproductive system, immune cells	Apoptosis, cell proliferation
Galectin-13	From primates	Placenta	Apoptosis, immune regulation, immune tolerance
Galectin-14	From primates	Placenta	Apoptosis, immune regulation, immune tolerance
Galectin-15	Ruminants	-	-
Galectin-16	From primates	Placenta	Apoptosis, immune regulation, immune tolerance
Galectin-17	From primates	Placenta	Apoptosis, immune regulation, immune tolerance
Galectin-19	New World Monkeys	-	-
Galectin-20	New World Monkeys	-	-

tube and induces apoptosis of cells not protected by galectin-3. Since the presence of gonococci is limited mainly to galectin-3–positive non-ciliated cells, galectin-3 promotes the survival of this pathogen.[74] The induction of this anti-apoptotic effect of galectin-3 can be observed when it is phosphorylated in response to infection, which increases the ability of galectin-3 to induce arrest in the G1 growth phase[85] and to perpetuate the survival and proliferation of infected cells.[78]

Besides galectin-3, galectin-1 and -7 can also bind *Trichomonas vaginalis*. Surprisingly, the interaction of galectin-7 with this pathogen is not carbohydrate-mediated, in contrast to galectin-1, which is expressed by human cervical and vaginal epithelial cells, the placenta, as well as endometrial and decidual tissues.[80,81] Galectin-1 and -3 are capable of binding purified lipophosphoglycan, which covers the whole surface of *Trichomonas vaginalis*.[86] Galectin-1 is thought to be a general attachment factor for this parasite and promotes the colonization of the female and male reproductive tracts, which could lead to vaginitis, bacterial vaginosis, increased risk of cervical cancer, human papillomavirus and HIV infection in females, endometritis, infertility, preterm birth, and low birth weight.[81] In addition, female infants could get infected during birth and then would remain symptomless until puberty.[87]

In contrast to the harmful roles of galectins during *Trichomonas vaginalis* infection, upon invasion of this parasite, vaginal epithelial cells release galectin-1 and -3, and these galectins modulate vaginal epithelial cell inflammatory responses by triggering resident immune cells, and thus, contribute to the elimination of this pathogen.[81] In addition, secreted galectin-3 initiates the trafficking of phagocytic cells to the site of infection by supporting neutrophil adhesion to the endothelial cell layer, and this also increases its phagocytic activity.[78,88]

Galectins in inflammation of the female reproductive tract

Among various inflammatory diseases of the female reproductive tract, endometriosis has been the most studied in regard to

galectins. Endometriosis is an inflammatory disease of reproductive-aged women, and it is strongly related to consequent infertility.[89] The pathophysiology of endometriosis involves chronic dysregulation of inflammatory and vascular signaling,[90] processes in which galectins are operational. Not surprisingly, galectin-1 and -3 are overexpressed in various forms of endometriotic tissues.[91-94] Moreover, higher galectin-3 concentrations are also detected in peritoneal fluid samples from women with endometriosis than from controls.[93] Functionally, it has been shown that corticotropin releasing hormone (CRH) and urocortin, two neuropeptides that are also overexpessed in endometriosis, are involved in the up-regulation of galectin-1, acting through CRH receptor 1, in a human endometrial adenocarcinoma cell line and in mouse macrophages.[94] This up-regulation of galectin-1 may contribute to T cell apoptosis favoring the establishment, persistence and immune escape of endometriotic foci.[90] Moreover, galectin-1 may promote the vasculogenesis of endometriotic tissues since it orchestrates vascular networks in endometriotic lesions as demonstrated in mice with or without galectin-1 deficiency,[92] and a neutralizing antibody against galectin-1 reduces the size and vascularized area of endometriotic lesions within the peritoneal compartment.[92]

Recent data have suggested that galectin-3 may play a role in the development of pain due to endometriosis since it is involved in myelin phagocytosis, Wallerian degeneration of neurons, and triggers neuronal apoptosis induction after nerve injury.[95] In fact, galectin-3, overexpressed in endometriotic foci, could induce nerve degeneration, since there is a close morphological relationship between nerves and endometriotic foci by means of perineurial and endoneurial invasion, especially in the most painful form of the disease.[96] Interestingly, neurotrophin, a nerve growth factor strongly expressed in endometriosis, up-regulates galcetin-3 expression.[91] These data underline the importance of galectin-1 and -3 in the pathogenesis of endometriosis.

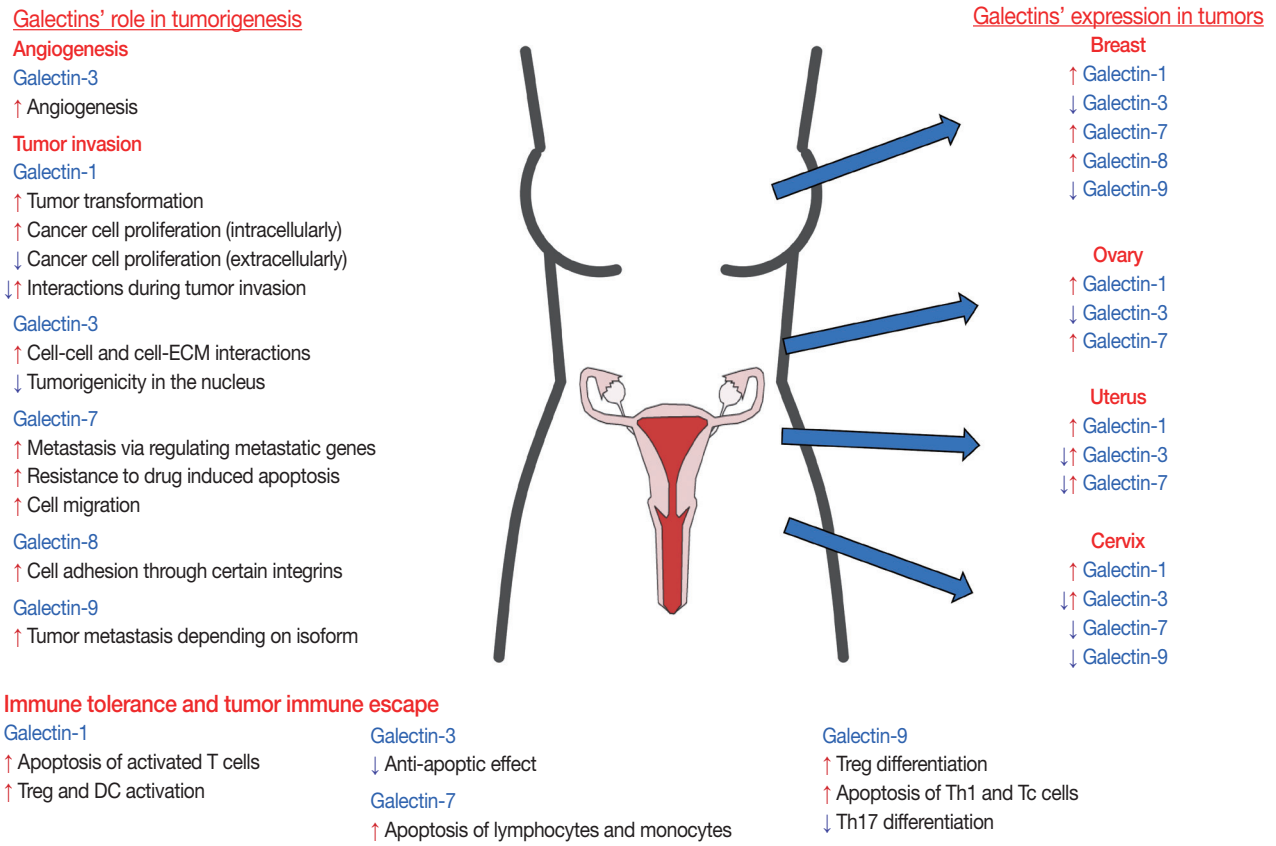

Fig. 2. Galectins in neoplasia of the female reproductive tract. The functional effects of various galectins in tumorigenesis and their expression changes in certain types of female tract neoplasia are depicted. The effects of galectins are biological-context and microenvironment dependent. Galectins' expression changes can be different according to the stage and type of various neoplasia as well as the type of the expressing cell. DC, dendritic cell.

http://dx.doi.org/10.4132/jptm.2015.02.25

GALECTINS IN TUMORS OF THE FEMALE REPRODUCTIVE TRACT

The multifunctional role of galectins in cell growth, differentiation, apoptosis, adhesion, invasion, and angiogenesis explains why they are associated with different tumors. Indeed, many cancers have differential galectin expression compared to healthy controls, including tumors of the female reproductive tract (Fig. 2).[97] Of interest, certain galectins have been functionally implicated in dysregulated pathways in tumor developmental processes, which are physiologically tightly regulated during placental development (e.g. invasion, angiogenesis, and immune tolerance).[14,16,17,98] In addition, galectins may also be dysregulated in tumor-associated stromal cells or endothelial cells,[15,99] and their glycan ligand expression and/or glycosylation pattern can also be affected.[100,101] Most of these studies focused on galectin-1 and -3, but an increasing number of recent studies also investigated galectin-7, -8, and -9.

Galectin-1 is differentially expressed in several tumors in the female reproductive tract. An increased expression of galectin-1 protein is found in endometrial,[102,103] breast,[104] ovarian,[105] and cervical[106] cancers. The intensity of galectin-1 expression also increases according to the pathologic grade of cervical[106] or breast[104] cancer and correlates with the depth of invasion of the cervical cancer and in lymph node metastases.[107] In breast cancers, not only tumor cells but also cancer-associated stromal cells have elevated galectin-1 expression.[99] In squamous cell carcinoma (SCC) of the uterine cervix, the intracellular expression of galectin-1 in tumor cells is higher than in the tumor-associated stroma, and galectin-1 is an independent prognostic factor associated with local recurrence and cancer-specific survival in stage I–II cervical cancer patients undergoing definitive radiation therapy.[108] It has been suggested that galectin-1 mediates radio-resistance through the H-Ras signaling pathway that is involved in DNA damage repair in cervical carcinoma cells,[109] underlining the importance of galectin-1 in tumorigenesis and therapy.

Galectin-3 is down-regulated in cervical carcinomas, and its expression is correlated to histopathologic grades.[110] It is also down-regulated in advanced uterine adenocarcinoma cells compared to normal adjacent endometrial cells.[102,103] Moreover, galectin-3 expression is predominantly detected in the cytoplasm and/or nucleus of uterine or breast cancer cells.[102,111,112] Of note, those uterine endometrioid adenocarcinomas, where galectin-3 is detected only in the cytoplasm, are characterized by deeper invasion of the myometrium.[102] In addition, the neoplastic epithelium within 'MELF' (microcystic, elongated, and fragmented glands) areas shows a consistent reduction in galectin-3 protein expression, often contrasting with the adjacent galectin-3–positive conventional glands and reactive stromal cells. Conversely, intravascular tumor foci often show cytoplasmic and nuclear galectin-3 immunoreactivity.[112] On the contrary, in some ovarian and endometrial carcinomas, including clear cell, serous, endometrioid, and mucinous ovarian carcinomas, higher galectin-3 expression is seen either by immunohistochemistry[113-116] or by reverse transcription polymerase chain reaction.[117] Which biological functions of galectin-3 are utilized by tumor cells depends on the localization of this galectin: nuclear galectin-3 may function in mRNA splicing, cell growth and cell cycle regulation; cytoplasmic galectin-3 may induce apoptosis resistance; and secreted galectin-3 modulates cellular adhesion and signaling, immune response, angiogenesis and tumorigenesis by binding to cell surface glycoconjugates such as laminin, fibronectin, collagen I and mucin-1.[111,118-121] For example galectin-3 may mediate chemoresistance via regulating the cell cycle as responders to chemotherapy have a higher proliferation activity than non-responders. This finding was strengthened by experimental results after knocking down galectin-3, which increases the fraction of cells in the S-phase of the cell cycle and decreases the expression of p27 cyclin dependent kinase inhibitor in clear cell carcinoma cell lines.[114] Moreover, the ability of galectin-3 to protect cells against apoptosis induced by various agents, working through different mechanisms, suggests that galectin-3 acts in a common central pathway of the apoptotic cascade, involving protection of mitochondrial integrity and caspase inhibition.[85,122-128] Of importance, a galectin-3 polymorphism, the substitution of a proline with histidine (P64H), results in susceptibility to matrix metalloproteinase cleavage and acquisition of resistance to drug-induced (e.g. doxorubicin, staurosporine, and genistein) apoptosis,[129-131] and homozygosity for this H allele is associated with increased breast cancer risk.[130] On the other hand, the Pro64 variant and phosphorylation of galectin-3 at Ser6 seems to be important in tumor necrosis factor-related apoptosis-inducing ligand (TRAIL)–induced apoptosis of human breast carcinoma cells.[131,132] Interestingly, nicotine induces the expression of galectin-3 in breast cancer cells and in primary tumors from breast cancer patients through its receptor and STAT3 expression, increasing the anti-apoptotic effect of galectin-3, and suggesting detrimental effects of smoking.[133]

Galectin-7 up-regulation in cervical cancer is associated with better overall survival after definitive radiation treatment,[134] and similar observations were made in other cancers (e.g. urothelial and colon), as well.[135-138] On the other hand, galectin-7 induces

chemoresistance in breast cancer cells via impairing p53[139] or via mutant p53-induced galectin-7 expression.[140]

Galectin-8 is expressed by various ovarian and breast cancer cell lines;[141] however, only one study reported that breast cancer tissues constitute the only group of tissue to exhibit a higher immunohistochemical galectin-8 expression in the malignant, as opposed to the benign, tumors.[142]

Galectin-9 can be detected in normal epithelium and endocervical glands, and it has decreased expression in cervical intraepithelial neoplasia and SCC. High-grade intraepithelial lesions express less galectin-9 than low-grade lesions. Unexpectedly, galectin-9 expression is higher in well-differentiated SCC compared to moderate or poorly differentiated SCCs. These results imply the involvement of galectin-9 in the differentiation of cervical cancer cells.[143,144] Recently, galectin-9 has been implicated as a prognostic factor in breast cancer.[145] The various roles of galectin-9 in tumorigenesis, including the participation in apoptosis, cell cycle control, adhesion, aggregation, migration, invasion, metastasis, angiogenesis, and immune escape, have recently been summarized in a review.[146]

Galectins in tumor invasion

The invasive and metastatic phenotype of cancer cells is presumably associated with a specific pattern of expression of cell adhesion molecules that allows for crossing through the basement membranes and creating distant metastases. Emerging data demonstrate the role of galectins in metastasis events, although the data is conflicting, possibly due to the various effects that galectins may have according to the microenvironmental and physicochemical changes.

Galectin-1, a laminin-binding molecule, may contribute to the invasiveness of cancer cells, since higher galectin-1 binding to cancerous epithelial cells was observed in stage III/IV endometrial carcinomas than in lower stage tumors.[102,147] Indeed, the down-regulation of galectin-1 by siRNA results in the inhibition of cell growth, proliferation and invading ability of various cervical cancer cell lines.[107]

Galectin-3, when localized to the cell surface, is involved in Thomsen-Friedenreich antigen (Galβ1-3GalNAcα1 disaccharide)-dependent homotypic cell adhesion and heterotypic cancer cell-endothelial cell contact.[148,149] Therefore, the decreased expression of this lectin could reflect the ability of cancer cells to detach from each other before invasion. Nuclear and cytoplasmic presence of galectin-3 implies that its localization and phosphorylation status is correlated with the proliferation status of the cells.[150] All aspects of this topic have been reviewed elsewhere.[151]

Galectin-7 is also involved in the regulation of tumor growth and invasion. A recent *in vitro* study in human cervical SCC cell lines revealed that knocking down galectin-7 enhances tumor cell invasion and tumor cell viability against paclitaxel-induced apoptosis likely through increasing the matrix metallopeptidase (MMP)-9 expression and activating the phosphoinositide 3-kinase/Akt signaling pathway.[152] However, more studies demonstrated that the expression of MMP-9 is increased by galectin-7 in cervical or ovarian cancer cell lines through the p38 mitogen activated protein kinase signaling pathway or mutant p53, respectively, resulting in increased cell invasion.[153,154] In accord with this earlier study, high expression levels of galectin-7 are found exclusively in high-grade breast carcinomas; in a preclinical mouse model of breast cancer, high expression of galectin-7 significantly increases the ability of cancer cells to metastasize to lung and bone.[155]

Galectins in tumor angiogenesis

Galectin-3 is involved in tumor angiogenesis and invasion, as vascular endothelial growth factor C (VEGF-C)-mediated nuclear factor kB signaling pathway promotes invasion of cervical cancer cells via VEGF-C–enhanced interaction between VEGF receptor-3 and galectin-3.[156] Moreover, the cleavage of galectin-3 and its subsequent release into the tumor microenvironment leads to breast cancer angiogenesis and progression as supported by the findings with BT-549-H(64) cells, in which galectin-3 increases chemotaxis, invasion and cancer cell–endothelial cell interactions resulting in angiogenesis and 3D morphogenesis. It is suggested that this *in vitro* angiogenic activity of galectin-3 is related to its ability to induce the migration of endothelial cells.[157] An *in vivo* study in immunocompromised mice transplanted with human breast cancer cells that overexpress galectin-3 showed increased density of capillaries surrounding the tumors, supporting that galectin-3 secreted by tumor cells induces angiogenesis.[158]

In addition, endothelial cells also express several galectins (-1, -3, -8, and -9) that may regulate tumor angiogenesis. For example, galectin-9 splice variants are expressed by endothelial cells, and their expression is regulated during endothelial cell activation. It is suggested that galectin-9 is possibly involved in attracting various immune cells (e.g. dendritic cells, DCs), which release angiogenic growth factors like VEGF, and its altered expression in the endothelium may interfere with a proper anti-tumor immune response.[146] Additional data that has started to emerge on the role of galectins in tumor angiogenesis is reviewed elsewhere.[15]

 http://dx.doi.org/10.4132/jptm.2015.02.25

Galectins in tumor immune tolerance

Studies published to date mainly address the involvement of galectin-1 in tumor immune escape. Galectin-1 is involved in CD4+CD25+Foxp3+ Treg cell[104] and tolerogenic DC activation, which may contribute to immune escape of tumor cells.[159] Th1 cells are important in anti-tumor immune responses[160] in all cancer types, and galectin-1 induces the selective apoptosis of Th1, Th17, and Tc lymphocytes in mice[161] and humans.[25] Of note, anti–galectin-1 antibody treatment in combination with cell therapy in a cervical cancer mouse model is more effective than the treatment with tumor infiltrating lymphocytes alone.[162] This shows that inhibition of galectin-1 results in decreased immune escape of tumor cells. In addition, galectin-1 silencing in a breast cancer mouse model results in a marked reduction in tumor growth and lung metastases.[104] These results suggest that galectin-1 blockade may be a good therapeutic approach, and further aspects on the roles of galectin-1 in tumor formation and progression are reviewed elsewhere.[163]

Extracellular galectin-3 and galectin-7 induces apoptosis of T cells and peripheral blood mononuclear cells after binding to cell surface glycoconjugate receptors through carbohydrate-dependent interactions.[154,164] In the case of galectin-3, CD7 and CD29 are identified as its apoptosis-inducing receptors. Furthermore, galectin-3–negative cell lines are significantly more sensitive to exogenous galectin-3 than those expressing this lectin. This suggests crosstalk between the anti-apoptotic activity of intracellular galectin-3 and the pro-apoptotic activity of extracellular galectin-3, providing a new insight for the immune escape mechanisms of cancer cells.

Galectin-9 has immunosuppressive activity similar to galectin-1;[146] however, its role in tumor immune escape remains largely unexplored. Galectin-9 suppresses Th17 cell differentiation and induces the apoptosis of Th1 and Tc cells, while it enhances CD4+CD25+Treg cell differentiation, suggesting immunosuppressive functions of this lectin. On the other hand, galectin-9 was shown to induce the expansion of DCs and the subsequent potentiation of natural killer (NK) and Tc cell–mediated anti-tumor immunity in melanoma and sarcoma models, respectively, showing that galectin-9 may have various effects on immune escape.[146]

Galectins implicated as blood biomarkers of tumors

A few studies have focused on determining the concentrations of certain galectins (-1, -2, -3, -4, -8, -9)[159,165,166] or galectin ligands[167] in the sera of healthy people and cancer patients. The serum concentrations of galectin-2, -3, -4, and -8 were up to 31-fold higher in patients with breast cancer than in controls, in particular those with metastasis.[166] It is important, since the presence of galectin-3 promotes cancer cell-endothelium adhesion *in vitro* via the interaction with the T antigen on cancer-associated mucin 1. In addition, galectin-2, -4, and -8 induce endothelial secretion of pro-inflammatory cytokines and chemokines *in vitro*, leading to the expression of endothelial cell surface adhesion molecules, and consequently increase cancer-endothelial adhesion and endothelial tube formation.[159]

Serum from breast cancer patients also contains an almost two-fold higher concentration of galectin-1 ligand glycoproteins.[167] The most abundant ones are α-2-macroglobulin, IgM and haptoglobin. In accordance, galectin-1–bound and non-bound haptoglobin uptake was also analyzed, and a dramatic difference was found in intracellular targeting, with the galectin-1 non-binding fraction targeted into lysosomes, while the galectin-1 binding fraction targeted into larger, galectin-1–positive granules. This suggests a major regulatory step in the scavenging of hemoglobin by haptoglobin, which can be altered in cancer.[167]

Galectin-3 concentrations in urine of various (e.g. breast, cervical, and ovarian) cancer patients and healthy controls showed a strong correlation between the stages of the disease and galectin-3 concentration.[168]

GALECTINS IN PREGNANCY

Pregnancy poses a substantial challenge to the maternal immune system. The semi-allogeneic fetus, placenta and chorioamniotic membranes continuously interact with maternal immune cells in the uterus, which is an immune privileged site,[169] and those in the maternal circulation.[170] During implantation and placentation, there is a continuous immune recognition and modulation of the maternal immune system by trophoblasts at the maternal-fetal interface.[171-174] Moreover, there is a continuous deportation of fetal cells and trophoblastic debris into the maternal circulation, which leads to microchimerism and an increase in systemic inflammation in the mother during pregnancy.[175-179] Therefore, normal pregnancy is associated with a mild inflammatory state, especially by neutrophils of the innate immune system.[180,181] This is significantly pronounced in preeclampsia, where the activation state of neutrophils is higher than in sepsis.[182,183] Overtly activated neutrophils are also implicated in recurrent fetal loss or bacterially induced abortions.[181] It was also revealed that other great obstetrical syndromes (e.g. intrauterine growth restriction [IUGR] and preterm labor) are also associated with various changes in the phenotypes as well as the behavior of maternal peripheral

blood leukocytes and systemic inflammation.[183-186] Since several galectins are expressed at the maternal-fetal interface, the site of contact between maternal and fetal cells that varies among different species,[171,187-190] they are proposed to promote maternal-fetal immune tolerance and regulate local and systemic inflammation and infection.[10,16,17,26,27] Indeed, changes in the expression of galectins[23,32-38] have been reported in the great obstetrical syndromes (e.g. preterm labor, preeclampsia),[191] which are related to local and/or systemic inflammation and infection, and are responsible for most perinatal mortality and morbidity.[192-205]

Galectin expression at the maternal-fetal interface in normal pregnancy

The human maternal-fetal interfaces dynamically change during gestation.[190] First, the syncytiotrophoblast is in direct contact with maternal cells in the decidua for a few days post-implantation and then with cells in the intervillous space. The latter is also the site of the interaction between the syncytiotrophoblast and maternal blood cells by the end of the first trimester, while invasive extravillous cytotrophoblasts in the placental bed and trophoblasts in the chorion laeve come into contact with maternal cells in the decidua.[190] In this dynamic context, the expression of several galectins is also spatio-temporally regulated during development (Fig. 3).[8] Galectin-1, -3, and -9 are broadly expressed during human and mouse embryogenesis, suggesting that they may play a role in embryo development in mammals.[8] Despite that, galectin-1 or galectin-3 knock out (KO) mice are viable,[206] possibly due to the redundancy in galectin functions.[8] In addition, galectin-1, -3, -8, -9, -13, -14, and -16 are also strongly expressed at the maternal-fetal interface in various mammals, some in a developmentally regulated fashion.[16,18,19,21,23,27,32-34,39]

For example, galectin-1 expression is strong in the differentiated syncytiotrophoblast but not in the cytotrophoblast during first and third trimesters,[19,207,208] and its expression in the extravillous trophoblast is developmentally regulated during the first-trimester.[19,209] This latter phenomenon is also true for galectin-3, which also localizes to villous cytotrophoblasts.[19,208] Galectin-4 has weaker placental expression,[27] which is down-regulated during trophoblast differentiation in rats.[210] Galectin-8 has expression in villous and extravillous trophoblasts,[39] while galectin-9 is mainly located in the decidua.[16] RNA and protein evidence have shown that galectins in the chromosome 19 cluster (-13, -14, -16, and -17) are predominantly expressed by the syncytiotrophoblast but not by the underlying cytotrophoblasts.[27,28,31,33,46,58] This is supported by galectin-13 immunolocalization to the multinucleated luminal trophoblasts within converted decidual spiral arterioles in the first trimester.[28] A recent study demonstrated that the expression of galectin-13, -14, and -16 is related to the differentiation and syncytialization of the villous trophoblast,[72] which is important in the production of placental hormones and immune proteins to control fetal development and immune tolerance.[189,211,212] *In vitro* assays demonstrated that the expression of these galectins is related to syncytium formation induced by cAMP.[72] Interestingly, the promoter evolution and the insertion of a primate-specific transposable element into the 5' untranslated region of an ancestral galectin gene introduced several binding sites for transcription factors fundamental in syncytiotrophoblastic gene expression, leading to the gain of placental expression of these chromosome 19 cluster galectins.[72,213] Of note, DNA methylation also regulates the developmental expression of these genes[72] similar to other galectins.[214] Of interest, galectin-1, -7, -9, -13, -14, -16, and -17 are also expressed in the chorioamniotic membranes, but the developmental aspects of their regulation at this site have not yet been revealed.[16,27,34,37,38]

Galectins in embryo implantation

Embryonic implantation can be considered a pro-inflammatory response in the decidua, which involves the chemotaxis of leukocytes and their active participation in the regulation of implantation via secreted immune and angiogenic factors.[215-218] Decidual cell-derived factors also have a key role in implantation.[219] Of importance, several galectins are expressed by the uterine endometrium and decidua in mammals and are strictly regulated by sex steroids.[18,22,220-222] The peak expression of these galectins coincides with the implantation time window; therefore, their possible roles in blastocyst attachment and in the regulation of immune cell functions during implantation have been implicated (Fig. 3).[18,21,22]

For example, a temporal expression change of galectin-1, dependent on estrogen and progesterone, has been observed during the estrus cycle in mice.[10,18] In humans, the expression of galectin-1, -2, -3, -4, -8, -9, and -12 is described in the endometrium[21,22,98,113,223-225] where galectin-1 and galectin-3 are highly expressed during the implantation time window.[22,221] Galectin-3 expression is increased in glandular epithelial cells in the secretory phase, while galectin-1 expression is increased in stromal cells in the late secretory phase and further increased in the decidua.[22] Interestingly, galectin-1 is also expressed in the trophectoderm and inner cell mass of human pre-implantation stage embryos, where it may be involved in the attachment to the uterine epithelium.[226] In spite of the identification of galectin-3 in trophoblasts, its role in implantation has not been well de-

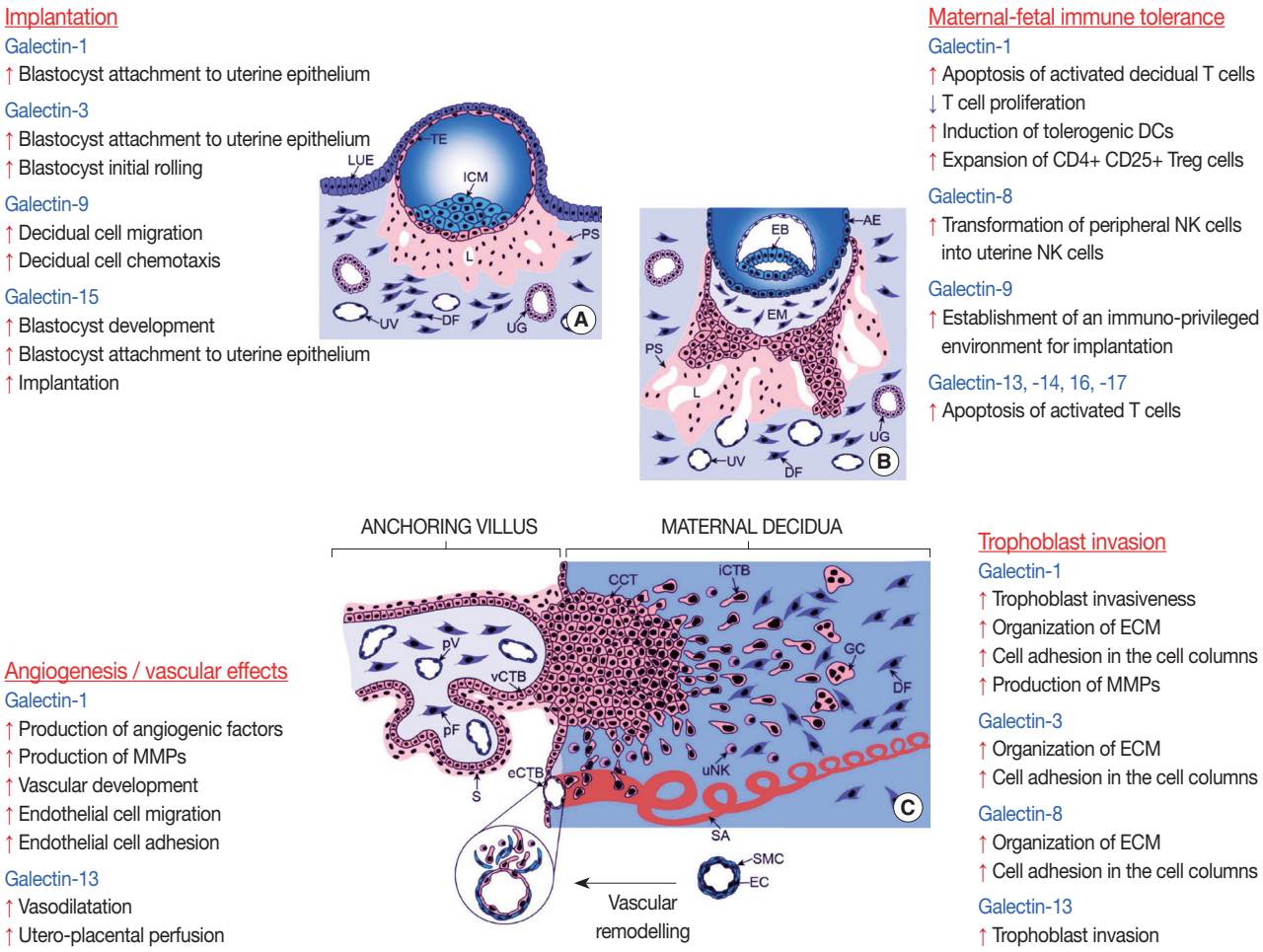

Fig. 3. Physiological aspects of galectins at the maternal-fetal interface. The figure represents multiple roles of galectins in implantation, angiogenesis, maternal-fetal immune tolerance and trophoblast invasion. (A) Embryo implantation. (B) Formation of primary villi by proliferative cytotrophoblasts. (C) Formation of tertiary villi, placental angiogenesis, extravillous trophoblast invasion and spiral artery remodeling. AE, amniotic epithelium; CCT, cell column trophoblast; DC, dendritic cell; DF, decidual fibroblast; EB, embryoblast; EC, endothelial cell; ECM, extracellular matrix; EM, extraembryonic mesoderm; eCTB, endovascular cytotrophoblast; GC, giant cell; ICM, inner cell mass, iCTB, interstitial cytotrophoblast; LUE, luminal uterine epithelium; L, lacunae; MMP, matrix metalloproteinase; NK, natural killer; pF, placental fibroblast; PS, primitive syncytium; pV, placental vessel; SA, spiral artery; S, syncytium; SMC, smooth muscle cell; TE, trophectoderm; UG, uterine gland; uNK, uterine NK cell; UV, uterine vessel; vCTB, villous cytotrophoblast. Cartoons are adapted from Knofler and Pollheimer. Front Genet 2013; 4: 190, under the terms of the Creative Commons Attribution License.[217]

fined.

Data in humans and mice support that galectin-9 is also involved in implantation. In mouse models, galectin-9 is associated with cell-to-cell interactions and the establishment of an immuno-privileged local environment for implantation and early fetal development as well as the mediation of decidual cell migration and chemotaxis.[223] In humans, galectin-9 is expressed by the endometrial glandular epithelial cells during the implantation time window as well as by the human decidua during early pregnancy.[21] Electron microscopy clarified its localization on the apical projections of the human endometrial epithelium called uterodomes,[223] which are membrane projections that exclusively feature the receptive endometrium during the implantation time window. The contribution of galectin-9 to the development of pregnancy is supported by the observation that normal pregnancy and cases of spontaneous abortions differ significantly in terms of endometrial galectin-9 splice variant profiles in both mice and humans.[227]

Galectins in trophoblast invasion

A growing body of evidence suggests that human galectins play key roles in placentation events beyond implantation. For example, galectin-1, -3, and -8 are expressed in the extravillous trophoblast in the first trimester[19,39] throughout the invasive

pathway of trophoblast differentiation.[212,217,228] These galectins are expressed in extravillous trophoblast cell columns, where they actively deposit extracellular matrix and can bind to major structural glycans of the placental bed (e.g. fibronectin and laminin).[8,19,39,229] Thus, galectin-1, -3, and -8 may play a role in the organization of the extracellular matrix and the modulation of cell adhesion in the cell columns.[19,39] In addition, galectin-1 and -3 may have a role in the regulation of the extravillous trophoblast cell cycle since they are absent from the differentiated, non-proliferating, interstitially migrating, highly invasive cytotrophoblasts (Fig. 3).[19]

Not only the expression pattern of galectin-1 in the first trimester placenta but also the findings that blocking galectin-1 substantially abrogates migration of primary trophoblasts and HTR8/SVneo cells cultured in matrigel[19,209] suggest that galectin-1 modulates the invasive pathway of trophoblast differentiation and enhances trophoblast invasiveness. Extravillous trophoblastic galectin-3[19,208] may interact between cell and extracellular matrix components, modulating adhesive interactions and immune reactions as observed in a murine model.[230]

In the case of galectin-13 (PP13), a different mechanism is proposed to promote trophoblast invasion.[28] Galectin-13 is secreted by the syncytiotrophoblast to the maternal circulation, from where it is transferred into the decidua in the first trimester, coinciding with the time of early trophoblast invasion. Interestingly, galectin-13 forms crystal-like aggregates in the decidua, where it attracts, activates and kills maternal immune cells, diverting them from spiral arterioles and invading trophoblasts.[28] In this manner, PP13 may serve to establish a decoy inflammatory response, sequestering maternal immune cells away from the site of extravillous trophoblast spiral artery modification.

Galectins in maternal-fetal immune tolerance

In eutherian mammals multiple immune mechanisms exist which support the establishment and maintenance of immunological privilege in the pregnant uterus, as well as antigen-specific, local and systemic maternal-fetal tolerance.[10,26,27,171-174,192] These mechanisms are strongly affected by the type of placentation and the interactions between fetal trophoblasts and maternal immune cells at the maternal-fetal interfaces.[171,187,189] In this regard, it is important to note that galectins are also expressed by maternal immune cells, which infiltrate the decidua and play key roles in mammalian pregnancies (Fig. 3).[20,25,51,70,231]

For example, galectin-1 is strongly expressed by uterine natural killer (uNK) cells compared to peripheral blood NK cells.[20] These CD56+ galectin-1+ uNK cells comprise ~70% of maternal leukocytes at the implantation site, promote angiogenesis and trophoblast invasion[20,171] and are pivotal for the maternal adaptation to pregnancy.[232] Galectin-1, secreted by human uNK cells, induces apoptosis of activated decidual T cells,[25] which is supported by data indicating that galectin-1 can selectively induce apoptosis of Th1 and Th17 cells[25,63] and contribute to maternal immune-tolerance to the semi-allogeneic fetus.[10,25,26] In addition, galectin-1 is among the immunosuppressive molecules secreted by villous trophoblasts, which were identified by a proteomics study and found to inhibit T lymphocyte proliferation and adaptive immune responses.[69] The villous trophoblast secretes other galectins, expressed from the chromosome 19 galectin cluster (-13, -14, and -16), which induce the apoptosis of activated T cells, and thus, are assumed to exert special homeostatic and immunobiological functions at the maternal-fetal interface.[16,27]

As *in vivo* evidence for the pivotal functions of human galectin-1, a proteomics study identified it to be down-regulated in villous placenta in early pregnancy loss, reflecting abnormalities in the support for the maintenance of pregnancy.[23] Other *in vivo* evidence comes from a mouse model of stress-induced fetal loss in which the decidual expression of galectin-1 decreased, and these mice, similar to galectin-1 KO mice, had a higher rate of fetal loss in allogeneic pregnancies.[10] This effect was reversed by the administration of recombinant galectin-1 and also by progesterone treatment, supporting the progesterone-dependent regulation of decidual galectin-1 expression. Galectin-1 treatment also prevents the drop in progesterone and progesterone-induced blocking factor serum concentrations in stressed animals, suggesting a synergistic effect of galectin-1 and progesterone in pregnancy maintenance.[10] It was also elucidated that galectin-1 exerts its immune modulatory effect through the induction of tolerogenic DCs, which in turn trigger the expansion of interleukin-10 expressing CD4+ CD25+ Treg cells *in vivo*.[10] Subsequently, it was determined that Treg cells, which normally expand during pregnancy and suppress the maternal allogeneic response directed against the fetus,[187] also overexpress galectin-10, which has an important role in suppressive functions.[70,231]

The galectin-9/TIM-3 (T-cell immunoglobulin domain and the mucin domain 3) pathway has been recognized as central in the regulation of Th1 immunity and tolerance induction.[233,234] Very recently, galectin-9 was also implicated in the regulation of uNK cell function and the maintenance of normal pregnancy[235] as galectin-9, secreted by human trophoblast cells, induces the transformation of peripheral NK cells into uNK-like cells via the interaction with TIM-3. In addition, a decreased number of

TIM-3+uNK cells was detected in human miscarriages and abortion-prone murine models, and a Th2/Th1 imbalance was detected in TIM-3+uNK cells in human and mouse miscarriages, suggesting the importance of the galectin-9/TIM-3 pathway.[235] Moreover, Treg cells increase their galectin-9 expression with advancing gestational age in accord with the increasing galectin-9 concentrations in maternal blood, suggesting that galectin-9 expressing Treg cells may have important roles in the maintenance of pregnancy.[236]

Galectins in placental angiogenesis

Aside from modulating the immune system and trophoblast invasion, human galectins have been implicated in key roles in angiogenesis (Fig. 3). This is not surprising in light of the pivotal role of galectin-glycan interactions in angiogenesis[237] and the angiostimulatory roles of several galectins reviewed elsewhere.[14] The most studied galectin, with respect to placental angiogenesis, is galectin-1. When this lectin is added exogeneously in a rodent model of reduced angiogenesis, it enhances the production of pro-angiogenic factors (e.g. angiogenin, heparin-binding epidermal growth factor, and fibroblast growth factor-basic) and matrix metallopeptidases (MMP-3, MMP-8, and MMP-9) to promote normal vascular development, to rescue implantation and to support healthy placentation.[238] Galectin-1 acts via the NRP-1–VEGF–VEGF-R2 signaling pathway,[239,240] which is important in promoting angiogenesis during implantation, decidualization and placentation.[241,242] Galectin-1 binding to neuropilin-1 promotes VEGF–VEGF-R2 interactions, and consequently, endothelial cell migration and adhesion,[239,241,243] and these effects can be blocked by an NRP-1 neutralizing antibody, which inhibits VEGF–VEGF-R2 signaling.[238,240]

Although several other galectins (-3, -8, and -9) have been implicated in angiogenesis and endothelial cell biology,[14] their involvement in placental angiogenesis has not yet been elucidated. The effect of galectin-13 has recently been tested on rat vasculature, and it was found that recombinant galectin-13 reduces blood pressure and increases utero-placental perfusion *in vivo*, while it promotes vasodilation in isolated arteries *in vitro*.[244,245]

Galectins in local inflammation in the womb

Term parturition is characterized by local pro-inflammatory changes in the decidua and chorioamnion, which play fundamental roles in the initiation of labor and myometrial contractions.[37,246-249] Evidence from microarray studies have shown that galectins may also play a role in pathways leading to term labor as galectin-7 is up-regulated in the amnion in oxytocin-induced labor, and galectin-9 is down-regulated in the chorion at the site of rupture (Fig. 4).[37]

Preterm parturition is a syndrome that has many etiologies, predominantly those associated with intra-amniotic infection and inflammation.[193,205,250] The pathways initiated in preterm parturition are different from those in term labor, whereas the terminal pathway of cervical effacement and dilatation, chorio-decidual, as well as myometrial activation, are shared between the two.[193,205,246,250] Interestingly, proteomics studies show that galectin-1 is upregulated in the fetal membranes in preterm parturition,[38] reflecting heightened local inflammation.

Preterm premature rupture of the membranes (PPROM) is a syndrome in which approximately 32%–75% of the cases are associated with microbial invasion of the amniotic cavity.[193,195,196] To date, only galectin-1 expression has been studied in PPROM using detailed gene and protein expression profiling;[34] it is increased in the chorioamniotic membranes in patients with histologic chorioamnionitis, but not in those without this condition. Galectin-1 expression is increased[34] in a temporal and spatial fashion in amnion epithelial cells, maternal neutrophils and chorioamniotic macrophages and myofibroblasts[251] with advancing inflammation. Since galectin-1 is associated with the up-regulation of genes encoding for MMPs in DCs,[252] it has been proposed that the overexpression of galectin-1 in the chorioamniotic membranes may be the link between inflammation, tissue remodeling, and membrane weakening, which may contribute to the membrane rupture.[34] Moreover, the increased expression of galectin-1 by chorioamniotic macrophages upon inflammation suggests a role for galectin-1 in the active barrier functions of the membranes, protecting the fetus from bacterial infection and promoting the recognition and phagocytic removal of invading maternal neutrophils.[34] This hypothesis is supported by findings that (1) activated macrophages are present in the fetal membranes in association with fetal inflammatory response upon infection,[253-255] (2) the chorioamniotic membranes have antimicrobial properties,[256] (3) galectin-1 expression is up-regulated in activated macrophages[257] where it regulates macrophage effector functions,[258] (4) galectin-1 decreases macrophage inducible nitric oxide synthase expression and inhibits lipopolysaccharide-induced NO metabolism,[259] and (5) it regulates the cell surface expression of FcγRI.[258]

Galectins in inflammatory conditions in the neonate

Due to galectins' roles in immune responses, their relevant roles in term and preterm parturition in the neonate have also been investigated, mainly regarding galectin-1 and galectin-3

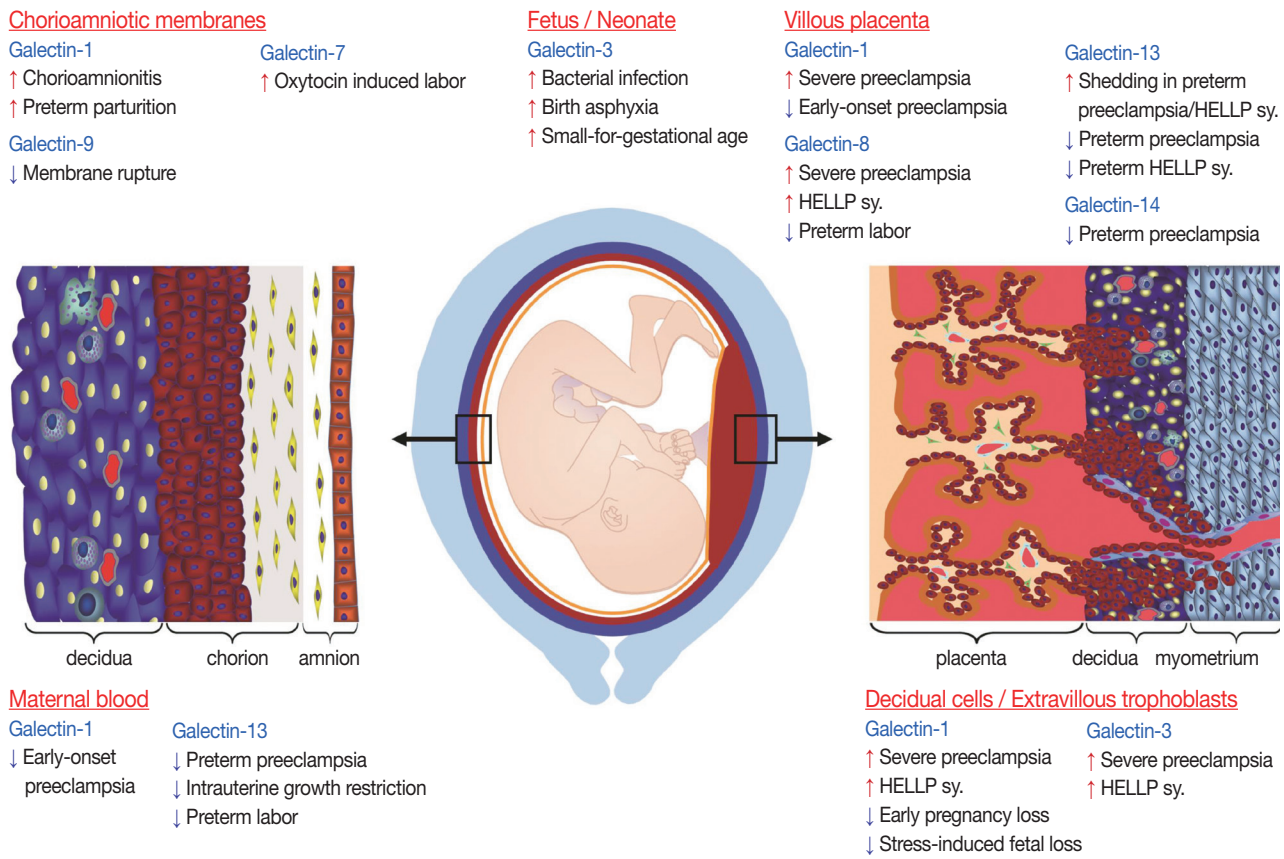

Fig. 4. Galectin expression at the maternal-fetal interface. The figure represents the maternal-fetal interfaces where maternal and fetal cells appose each other from the end of the first trimester of human pregnancy. The villous syncytiotrophoblast (depicted with gold) is bathed in maternal blood, whereas invasive extravillous trophoblasts in the placental bed (depicted in red) and chorionic trophoblasts in the fetal membranes (depicted in red) are in contact with maternal cells in the decidua (depicted in dark blue). The differential expression of galectins is depicted according to the interface where observed in normal pregnancy and in pregnancy complications. Sy., syndrome, Cartoon was adapted from Than *et al*. Trends Endocrinol Metab 2012; 23: 23-31, with permission of Elsevier.[16]

(Fig. 4).[260-262]

In term parturition, in spite of the physiological systemic inflammation in the mother at the time of normal delivery, cord blood plasma contains more galectin-3 than maternal plasma, regardless of the delivery mode.[262] In addition, cord blood neutrophils show priming in comparison to maternal neutrophils by responding to galectin-3 with reactive oxygen species (ROS) production, suggesting that inflammatory stimuli associated with labor promotes neutrophils to develop a reactive phenotype with extensive priming features.[262] Indeed, when cord blood leukocytes are stimulated by invasive bacteria, there is an induction of galectin-3 expression, suggesting its importance for innate immunity in the neonate.[260] Although galectin-1 is also expressed in cord blood, lymphocytes expressing galectin-1 were not determined to have a major role in immune reactivity in cord blood.[263]

In preterm parturition, the earlier preterm birth occurs, the higher the rate of intra-amniotic infection and inflammation.[193] Since 5%–13% of pregnancies are affected by preterm parturition,[194] the resulting severe complications (i.e. intraventricular hemorrhage, cystic periventricular leukomalacia, bronchopulmonary dysplasia [BPD], and cerebral palsy) have disastrous short-term and life-long impacts on the neonate, and the healthcare and social impacts are immense.[193,205] In regard to these, galectin-3 concentrations are elevated in the cerebrospinal fluid of infants suffering from birth asphyxia, and even higher in those with abnormal outcomes.[261] Since galectin-3 is produced by activated microglia/macrophages and activates NADPH oxidase, leading to neurotoxic production of ROS and contributing to hypoxic brain injury in an animal model,[264] it has been proposed to serve as a marker for abnormal outcomes.[261] In addition, in a small preliminary study, galectin-3 concentrations in tracheal aspirates of premature infants tended to be elevated in the first week of life in those who later developed BPD (Staretz *et al*., personal communication).

IUGR is one of the most heterogeneous syndromes in obstetrics; it is associated with fetal malformations and chromosomal abnormalities, as well as maternal autoimmune disorders and placental dysfunction resulting from poor implantation, making the understanding of an IUGR fetus a challenge. In addition, neonates may be small-for-gestational age (SGA) due to a normal condition in short-stature couples.[265] Of interest, a recent report showed that galectin-3 concentrations in cord blood have a positive correlation with gestational age, and SGA neonates have higher concentrations of galectin-3 than those that are appropriate for gestational age,[260] which may be a sign of an inflammatory condition.

Galectins in preeclampsia, a systemic inflammatory state

Based on the above data, it is not surprising that galectins have been implicated in the development of preeclampsia, a syndrome with impaired trophoblast invasion, an anti-angiogenic state and an exaggerated maternal systemic immune response.[190,266] Preeclampsia is a severe complication of pregnancy, which affects 5%–7% of pregnant women and is a leading cause of maternal and perinatal morbidity and mortality.[267,268] It also confers a high risk to the mother and fetus for metabolic and cardiovascular diseases later in life.[269-272] Preeclampsia is a syndrome with a spectrum of phenotypes, which may present at various gestational ages, with different degrees of severity at clinical onset, and also with or without the involvement of the fetus.[272-274]

It is a multi-stage disease that has placental origins[190,275-277] due to the failure of extravillous trophoblast invasion into the uterine tissues[278,279] and impaired villous trophoblastic syncytialization.[72,280,281] Subsequent rheological changes in uterine blood flow, metabolic changes, and ischemic stress of the villous placenta lead to the liberation of anti-angiogenic molecules, highly inflammatory placental debris, and cell-free fetal DNA that may also be pro-inflammatory and cause an exaggerated maternal systemic inflammatory response, anti-angiogenic conditions and end-organ damage.[179,181,190,192,271,275-277,282-291] Other, less severe pathologies are also implicated that result in the terminal pathway of systemic inflammation and an anti-angiogenic state.[292] Importantly, several members of the galectin family have been implicated in the development of various stages of this syndrome (Fig. 4).

Impaired extravillous trophoblast invasion

Indirect evidence of galectin involvement is the up-regulation of galectin-1 and -3 in the extravillous trophoblasts in the placental bed during preeclampsia and HELLP syndrome,[38,158] which is associated with the failure of extravillous trophoblast invasion.[32] It was also observed that low galectin-13 expression is associated with deficient trophoblast invasion, failure of spiral arteriole conversion, and the development of preeclampsia.[28]

Impaired villous trophoblastic syncytialization

Galectin-13 and galectin-14 mRNA expression is decreased in the syncytiotrophoblast in preeclampsia associated with or without HELLP syndrome at the time of clinical onset, predominantly in the early-onset forms.[28,33,72] Importantly, decreased galectin-13 mRNA expression can be detected as early as the first trimester in laser captured specimens of chorionic villous trophoblasts as well as decreased galectin-13 protein and mRNA concentrations in first trimester maternal serum sampled from patients destined to develop preeclampsia.[36] This phenomenon possibly reflects abnormal villous trophoblast syncytialization starting from early pregnancy and may be one of the earliest placental indicators for the subsequent development of preeclampsia. A recent study[72] revealed that GCM1 and ESRRG, two transcription factors that regulate villous trophoblastic syncytialization and metabolic functions, are down-regulated in the placenta in preeclampsia. Functional and evolutionary evidence also implicates these two factors in regulating trophoblastic expression of chromosome 19 galectin cluster genes. This is supported by the observation of decreased GCM1-mediated trophoblast fusion in impaired galectin gene expression in preeclampsia.[72] Furthermore, the differential methylation of *LGALS13* and *LGALS14* is also found in the villous trophoblast in preterm preeclampsia, suggesting that potential additional disease-mechanisms may account for the trophoblastic pathology in preterm preeclampsia.[72]

Villous placental stress

Galectin-1 and -8 are overexpressed in the villous trophoblast in preeclampsia and HELLP syndrome,[32,35] where increased placental stress occurs preceding exaggerated maternal systemic inflammation.[275,276,290,293,294] It is possible that galectins may function as "alarmins" in this condition.[12,35] Alarmins are endogenous danger signals secreted by activated cells via non-classical pathways or released from necrotic cells, which signal tissue damage and contribute to the activation and/or resolution of immune responses.[66] Galectin-13 may also be considered a placental alarmin since it is excessively secreted or shed from the syncytiotrophoblast at the time of the clinical onset of preeclampsia and HELLP syndrome.[33,64] Interestingly, the syncytiotrophoblast microvillous membrane and microvesicles, which are shed from the

syncytiotrophoblast, stain strongly for galectin-13, suggesting that the increased release of galectin-13–positive microvesicles from the syncytiotrophoblast may lead to elevated maternal serum galectin-13 concentrations when the clinical symptoms appear.[33,46]

Anti-angiogenesis

Placental and maternal blood galectin-1 expression is downregulated in patients with early-onset preeclampsia, and *Lgals1* KO mice exhibit preeclampsia-like symptoms, probably due to the inhibition of pro-angiogenic effects of galectin-1.[238] Moreover, blocking galectin-1–mediated angiogenesis with anginex, a synthetic peptide, also promotes preeclampsia-like symptoms in mice and inhibits human extravillous trophoblast functions *in vitro*.[238,295]

Maternal systemic inflammation

The number of galectin-1–expressing NK cells and Treg cells is decreased in preeclampsia,[51,296,297] which may reflect a failure of immune tolerance in this syndrome.[298] Recently, the involvement of galectin-9 and its TIM-3 ligand has been implicated in maternal systemic inflammation in preeclampsia.[299] In this regard, decreased TIM-3 expression by T cells, cytotoxic T cells, NK cells, and CD56dim NK cells, as well as increased frequency of galectin-9+ peripheral lymphocytes, is detected in women with early-onset preeclampsia, suggesting that the impairment of the galectin-9/TIM-3 pathway can result in an enhanced systemic inflammatory response including the activation of Th1 lymphocytes in preeclampsia.[299]

Galectins implicated as maternal blood biomarkers in obstetrical syndromes

Due to the dysregulation of some galectins at the maternal-fetal interface and in maternal blood in various obstetrical syndromes, investigations have been expanded on their possible value as diagnostic, predictive and prognostic biomarkers of these pregnancy complications. Most data is available for galectin-13, also known as PP13, which has been widely investigated by international collaborative studies (Fig. 4).[41-50,58] The changes in the expression patterns of galectin-13 in the placenta during gestation in normal and preeclamptic pregnancies, the fact that galectin-13 is expressed only in the placenta,[27] and it is not detected in non-pregnant patients (Madar-Shapiro *et al.*, personal communication), make this galectin a suitable and promising first trimester maternal blood biomarker for the prediction of preterm preeclampsia. In addition, genetic studies found certain single nucleotide polymorphisms, including an exonic variant (221delT) in the *LGALS13* gene, which may increase the risk for preterm labor and preeclampsia.[300] Recent advancement in the field has also facilitated the study of the potential use of this galectin as a therapeutic drug for preeclampsia.[244,245] The utilization of other galectins as biomarkers has recently been started.

In the first trimester of pregnancy, there is a lower PP13 mRNA content in maternal blood in preeclampsia compared to controls;[301,302] however, the predictive value of the detected maternal blood PP13 mRNA species is currently limited due to the varying and low amounts of trophoblastic mRNA reaching the maternal circulation. Much more promising results were derived from studies on maternal blood PP13 concentrations in the first trimester for the prediction of preeclampsia, which were analyzed by a recent meta-analysis.[303] The results were pooled from 19 studies on singleton pregnancies, which were included in prospective or nested case-control studies or fully prospective studies in which a total of 16,153 pregnant women were tested for PP13 between 6 and 14 weeks of gestation.[42-48,50,58,304-313] For all cases of preeclampsia, the mean detection rate (DR) for predicting preeclampsia was 47% (95% confidence interval [CI], 43 to 65) at a 10% false-positive rate (FPR). For preterm preeclampsia, the DR was 66% (95% CI, 48 to 78); for early-onset preeclampsia, the DR was 83% (95% CI, 25 to 100). For all cases of preeclampsia, the positive likelihood ratio (LR) [sensitivity/(1-specificity)] was 5.82, while the negative LR [(1-sensitivity)/specificity] was 0.46. For preterm preeclampsia, both of these indices were better (positive LR, 6.94; negative LR, 0.34).

Of interest, the introduction of maternal ABO blood groups into the prediction model could improve the DRs for preeclampsia, which can be explained by the differential binding of PP13 onto ABO blood group antigen-containing cell surfaces and the varying bioavailability of PP13 in maternal blood depending on the ABO blood type.[58] Moreover, the performance of the first trimester PP13 test could further be improved by the inclusion of PP13 into panels of multiple biomarkers (e.g. ADAM metallopeptidase domain 12 [ADAM12], pregnancy associated plasma protein A [PAPP-A], placenta growth factor [PlGF]),[50,314] which is necessitated in light of the syndromic nature of preeclampsia.[48,314] In addition, risk predictions based on combining PP13 and uterine artery Doppler pulsatility index (PI) also showed increased prediction accuracy.[42,44,304,306,314-316] Moreover, the combination of PP13, Doppler PI, and maternal artery stiffness (MAP) increased the DR of preeclampsia to 93% for early-onset preeclampsia and to 86% for all cases of preeclampsia at 10% FPR.[49] This is in line with comprehensive risk algorithms based on combined multi-marker analysis of back-

ground risks, MAP, Doppler PI, and a panel of blood biomarkers that can yield much higher predictive value and accuracy than individual markers,[306] especially for early-onset (< 34 weeks) and preterm (< 37 weeks) preeclampsia. Therefore, the introduction of a broad biomarker panel for the evaluation of preeclampsia and other obstetrical syndromes in the first trimester is suggested in order to change antenatal care as formulated by the inverted pyramid model of perinatal evaluation in pregnancy.[317]

In the second trimester of pregnancy, galectin-13 does not have much diagnostic or predictive value due to the sharp increase in PP13 maternal blood concentrations in preeclampsia between the first and third trimesters compared to the moderate change in women with normal pregnancy.[318] Interestingly, galectin-1 has recently emerged as a potential preclinical biomarker for preeclampsia since a prospective study detected decreased galectin-1 maternal blood concentrations and placental expression in early-onset preeclampsia compared to normal pregnancy in mid pregnancy.[238] Of note, placental galectin-1 expression is increased in preterm and severe preeclampsia compared to normal pregnancy.[35,238]

In the third trimester of pregnancy, galectin-13 may have diagnostic significance for the clinical development of preeclampsia according to a recent meta-analysis.[318] This included eight clinical studies that contained third trimester maternal blood PP13 data from 2750 pregnant women.[33,45,46,58,319,320] Maternal blood PP13 was higher in women who subsequently developed preeclampsia compared to unaffected women. The mean DR at 10% FPR for all preeclampsia cases was 59.4% (95% CI, 49.7 to 64.5), and for preterm preeclampsia was 71.7% (95% CI, 60.3 to 75.3). Interestingly, the DR appeared to be related to the severity of the cases in a given study, showing that the higher the hypertension and proteinuria, the higher the third trimester PP13 in maternal blood. A combined algorithm of PP13, MAP and proteinuria yielded a 95% DR for preterm preeclampsia and 85% for all preeclampsia at 5% FPR. The positive LR for all cases of preeclampsia was 5.94 and the negative LR was 0.45, providing an overall LR of 26.24. The positive LR for preterm preeclampsia was 7.17 and the negative LR was 0.31, providing an overall LR of 37.99. Therefore, the meta-analysis indicates that higher third trimester maternal blood PP13, among women who subsequently developed preeclampsia, reached clinical diagnostic levels.[318]

CONCLUSION

Galectins are an evolutionarily ancient family of lectins that have pleiotropic functions in the regulation of key biological processes. Galectins are pivotal in immune responses, angiogenesis, cell migration and invasion, and due to these functions, they have double-edged functions in shared and unique pathways of embryonic and tumor development. Recent advances facilitate the use of galectins as biomarkers in obstetrical syndromes and in various malignancies, and their therapeutic applications are also under investigation.

Conflicts of Interest

No potential conflict of interest relevant to this article was reported.

Acknowledgments

We thank Szilvia Szabo, Zsolt Gelencser and Balint Peterfia (Hungarian Academy of Sciences), Krisztian Papp (Eotvos Lorand University), Pat Schoff and Russ Price (Perinatology Research Branch), and Valerie Richardson (Yale University) for their technical assistance and/or art work, and Sara Tipton (Wayne State University) for critical reading of the manuscript. Figs. 1 and 4 were adapted from reference 16 with kind permission from Elsevier. Fig. 3 was adapted from reference 217 under the terms of the Creative Commons Attribution License and with kind permission from Martin Knofler and Jurgen Pollheimer. Original research conducted by the authors in the topic and the writing of this manuscript was supported, in part, by the Perinatology Research Branch, Division of Intramural Research, *Eunice Kennedy Shriver* National Institute of Child Health and Human Development (NICHD), National Institutes of Health (NIH), Department of Health and Human Services (DHHS); Federal funds from the NICHD under Contract No. HHSN275201300006C; the European Union FP6 Grant "Pregenesys 037244"; the Hungarian OTKA-PD Grant "104398"; and the Hungarian Academy of Sciences Momentum Grant "LP2014-7/2014".

REFERENCES

1. Apweiler R, Hermjakob H, Sharon N. On the frequency of protein glycosylation, as deduced from analysis of the SWISS-PROT database. Biochim Biophys Acta 1999; 1473: 4-8.
2. Gabius HJ, André S, Kaltner H, Siebert HC. The sugar code: functional lectinomics. Biochim Biophys Acta 2002; 1572: 165-77.
3. Varki A, Cummings RD, Esko JD, *et al*. Essentials in glycobiology. Cold Spring Harbor: Cold Spring Harbor Laboratory Press, 2008.
4. Barondes SH. Bifunctional properties of lectins: lectins redefined.

Trends Biochem Sci 1988; 13: 480-2.
5. Hirabayashi J, Kasai K. The family of metazoan metal-independent beta-galactoside-binding lectins: structure, function and molecular evolution. Glycobiology 1993; 3: 297-304.
6. Barondes SH, Cooper DN, Gitt MA, Leffler H. Galectins. Structure and function of a large family of animal lectins. J Biol Chem 1994; 269: 20807-10.
7. Kasai K, Hirabayashi J. Galectins: a family of animal lectins that decipher glycocodes. J Biochem 1996; 119: 1-8.
8. Cummings RD, Liu FT. Galectins. In: Varki A, Cummings R, Esko JD, *et al*., eds. Essentials of glycobiology. 2nd ed. Cold Spring Harbor: Cold Spring Harbor Laboratory Press, 2009; 475-88.
9. Cooper DN. Galectinomics: finding themes in complexity. Biochim Biophys Acta 2002; 1572: 209-31.
10. Blois SM, Ilarregui JM, Tometten M, *et al*. A pivotal role for galectin-1 in fetomaternal tolerance. Nat Med 2007; 13: 1450-7.
11. Rabinovich GA, Toscano MA. Turning 'sweet' on immunity: galectin-glycan interactions in immune tolerance and inflammation. Nat Rev Immunol 2009; 9: 338-52.
12. Sato S, St-Pierre C, Bhaumik P, Nieminen J. Galectins in innate immunity: dual functions of host soluble beta-galactoside-binding lectins as damage-associated molecular patterns (DAMPs) and as receptors for pathogen-associated molecular patterns (PAMPs). Immunol Rev 2009; 230: 172-87.
13. Liu FT, Rabinovich GA. Galectins: regulators of acute and chronic inflammation. Ann N Y Acad Sci 2010; 1183: 158-82.
14. Blois SM, Conrad ML, Freitag N, Barrientos G. Galectins in angiogenesis: consequences for gestation. J Reprod Immunol 2015; 108: 33-41.
15. Griffioen AW, Thijssen VL. Galectins in tumor angiogenesis. Ann Transl Med 2014; 2: 90.
16. Than NG, Romero R, Kim CJ, McGowen MR, Papp Z, Wildman DE. Galectins: guardians of eutherian pregnancy at the maternal-fetal interface. Trends Endocrinol Metab 2012; 23: 23-31.
17. Blidner AG, Rabinovich GA. 'Sweetening' pregnancy: galectins at the fetomaternal interface. Am J Reprod Immunol 2013; 69: 369-82.
18. Choe YS, Shim C, Choi D, Lee CS, Lee KK, Kim K. Expression of galectin-1 mRNA in the mouse uterus is under the control of ovarian steroids during blastocyst implantation. Mol Reprod Dev 1997; 48: 261-6.
19. Vicovac L, Janković M, Cuperlović M. Galectin-1 and -3 in cells of the first trimester placental bed. Hum Reprod 1998; 13: 730-5.
20. Koopman LA, Kopcow HD, Rybalov B, *et al*. Human decidual natural killer cells are a unique NK cell subset with immunomodulatory potential. J Exp Med 2003; 198: 1201-12.
21. Popovici RM, Krause MS, Germeyer A, Strowitzki T, von Wolff M. Galectin-9: a new endometrial epithelial marker for the mid- and late-secretory and decidual phases in humans. J Clin Endocrinol Metab 2005; 90: 6170-6.
22. von Wolff M, Wang X, Gabius HJ, Strowitzki T. Galectin fingerprinting in human endometrium and decidua during the menstrual cycle and in early gestation. Mol Hum Reprod 2005; 11: 189-94.
23. Liu AX, Jin F, Zhang WW, *et al*. Proteomic analysis on the alteration of protein expression in the placental villous tissue of early pregnancy loss. Biol Reprod 2006; 75: 414-20.
24. Lewis SK, Farmer JL, Burghardt RC, *et al*. Galectin 15 (LGALS15): a gene uniquely expressed in the uteri of sheep and goats that functions in trophoblast attachment. Biol Reprod 2007; 77: 1027-36.
25. Kopcow HD, Rosetti F, Leung Y, Allan DS, Kutok JL, Strominger JL. T Cell apoptosis at the maternal-fetal interface in early human pregnancy, involvement of galectin-1. Proc Natl Acad Sci U S A 2008; 105: 18472-7.
26. Than NG, Romero R, Erez O, *et al*. Emergence of hormonal and redox regulation of galectin-1 in placental mammals: implication in maternal-fetal immune tolerance. Proc Natl Acad Sci U S A 2008; 105: 15819-24.
27. Than NG, Romero R, Goodman M, *et al*. A primate subfamily of galectins expressed at the maternal-fetal interface that promote immune cell death. Proc Natl Acad Sci U S A 2009; 106: 9731-6.
28. Kliman HJ, Sammar M, Grimpel YI, *et al*. Placental protein 13 and decidual zones of necrosis: an immunologic diversion that may be linked to preeclampsia. Reprod Sci 2012; 19: 16-30.
29. Than NG, Sumegi B, Than GN, Berente Z, Bohn H. Isolation and sequence analysis of a cDNA encoding human placental tissue protein 13 (PP13), a new lysophospholipase, homologue of human eosinophil Charcot-Leyden Crystal protein. Placenta 1999; 20: 703-10.
30. Bozić M, Petronijević M, Milenković S, Atanacković J, Lazić J, Vicovać L. Galectin-1 and galectin-3 in the trophoblast of the gestational trophoblastic disease. Placenta 2004; 25: 797-802.
31. Than NG, Pick E, Bellyei S, *et al*. Functional analyses of placental protein 13/galectin-13. Eur J Biochem 2004; 271: 1065-78.
32. Jeschke U, Mayr D, Schiessl B, *et al*. Expression of galectin-1, -3 (gal-1, gal-3) and the Thomsen-Friedenreich (TF) antigen in normal, IUGR, preeclamptic and HELLP placentas. Placenta 2007; 28: 1165-73.
33. Than NG, Abdul Rahman O, Magenheim R, *et al*. Placental protein 13 (galectin-13) has decreased placental expression but increased shedding and maternal serum concentrations in patients presenting with preterm pre-eclampsia and HELLP syndrome. Virchows Arch 2008; 453: 387-400.
34. Than NG, Kim SS, Abbas A, *et al*. Chorioamnionitis and increased galectin-1 expression in PPROM: an anti-inflammatory response

in the fetal membranes? Am J Reprod Immunol 2008; 60: 298-311.
35. Than NG, Erez O, Wildman DE, *et al*. Severe preeclampsia is characterized by increased placental expression of galectin-1. J Matern Fetal Neonatal Med 2008; 21: 429-42.
36. Sekizawa A, Purwosunu Y, Yoshimura S, *et al*. PP13 mRNA expression in trophoblasts from preeclamptic placentas. Reprod Sci 2009; 16: 408-13.
37. Nhan-Chang CL, Romero R, Tarca AL, *et al*. Characterization of the transcriptome of chorioamniotic membranes at the site of rupture in spontaneous labor at term. Am J Obstet Gynecol 2010; 202: 462.e1-41.
38. Shankar R, Johnson MP, Williamson NA, *et al*. Molecular markers of preterm labor in the choriodecidua. Reprod Sci 2010; 17: 297-310.
39. Kolundžić N, Bojić-Trbojević Z, Radojćić L, Petronijević M, Vićovac L. Galectin-8 is expressed by villous and extravillous trophoblast of the human placenta. Placenta 2011; 32: 909-11.
40. Houzelstein D, Goncalves IR, Fadden AJ, *et al*. Phylogenetic analysis of the vertebrate galectin family. Mol Biol Evol 2004; 21: 1177-87.
41. Burger O, Pick E, Zwickel J, *et al*. Placental protein 13 (PP-13): effects on cultured trophoblasts, and its detection in human body fluids in normal and pathological pregnancies. Placenta 2004; 25: 608-22.
42. Nicolaides KH, Bindra R, Turan OM, *et al*. A novel approach to first-trimester screening for early pre-eclampsia combining serum PP-13 and Doppler ultrasound. Ultrasound Obstet Gynecol 2006; 27: 13-7.
43. Chafetz I, Kuhnreich I, Sammar M, *et al*. First-trimester placental protein 13 screening for preeclampsia and intrauterine growth restriction. Am J Obstet Gynecol 2007; 197: 35.e1-7.
44. Spencer K, Cowans NJ, Chefetz I, Tal J, Meiri H. First-trimester maternal serum PP-13, PAPP-A and second-trimester uterine artery Doppler pulsatility index as markers of pre-eclampsia. Ultrasound Obstet Gynecol 2007; 29: 128-34.
45. Gonen R, Shahar R, Grimpel YI, *et al*. Placental protein 13 as an early marker for pre-eclampsia: a prospective longitudinal study. BJOG 2008; 115: 1465-72.
46. Huppertz B, Sammar M, Chefetz I, Neumaier-Wagner P, Bartz C, Meiri H. Longitudinal determination of serum placental protein 13 during development of preeclampsia. Fetal Diagn Ther 2008; 24: 230-6.
47. Romero R, Kusanovic JP, Than NG, *et al*. First-trimester maternal serum PP13 in the risk assessment for preeclampsia. Am J Obstet Gynecol 2008; 199: 122.e1-11.
48. Akolekar R, Syngelaki A, Beta J, Kocylowski R, Nicolaides KH. Maternal serum placental protein 13 at 11-13 weeks of gestation in preeclampsia. Prenat Diagn 2009; 29: 1103-8.
49. Khalil A, Cowans NJ, Spencer K, Goichman S, Meiri H, Harrington K. First-trimester markers for the prediction of pre-eclampsia in women with a-priori high risk. Ultrasound Obstet Gynecol 2010; 35: 671-9.
50. Wortelboer EJ, Koster MP, Cuckle HS, Stoutenbeek PH, Schielen PC, Visser GH. First-trimester placental protein 13 and placental growth factor: markers for identification of women destined to develop early-onset pre-eclampsia. BJOG 2010; 117: 1384-9.
51. Molvarec A, Blois SM, Stenczer B, *et al*. Peripheral blood galectin-1-expressing T and natural killer cells in normal pregnancy and preeclampsia. Clin Immunol 2011; 139: 48-56.
52. Brewer FC. Binding and cross-linking properties of galectins. Biochim Biophys Acta 2002; 1572: 255-62.
53. Swaminathan GJ, Leonidas DD, Savage MP, Ackerman SJ, Acharya KR. Selective recognition of mannose by the human eosinophil Charcot-Leyden crystal protein (galectin-10): a crystallographic study at 1.8 Å resolution. Biochemistry 1999; 38: 13837-43.
54. Visegrády B, Than NG, Kilár F, Sümegi B, Than GN, Bohn H. Homology modelling and molecular dynamics studies of human placental tissue protein 13 (galectin-13). Protein Eng 2001; 14: 875-80.
55. López-Lucendo MF, Soliś D, André S, *et al*. Growth-regulatory human galectin-1: crystallographic characterisation of the structural changes induced by single-site mutations and their impact on the thermodynamics of ligand binding. J Mol Biol 2004; 343: 957-70.
56. Horlacher T, Oberli MA, Werz DB, *et al*. Determination of carbohydrate-binding preferences of human galectins with carbohydrate microarrays. Chembiochem 2010; 11: 1563-73.
57. Stowell SR, Arthur CM, Dias-Baruffi M, *et al*. Innate immune lectins kill bacteria expressing blood group antigen. Nat Med 2010; 16: 295-301.
58. Than NG, Romero R, Meiri H, *et al*. PP13, maternal ABO blood groups and the risk assessment of pregnancy complications. PLoS One 2011; 6: e21564.
59. Liu FT, Patterson RJ, Wang JL. Intracellular functions of galectins. Biochim Biophys Acta 2002; 1572: 263-73.
60. Camby I, Le Mercier M, Lefranc F, Kiss R. Galectin-1: a small protein with major functions. Glycobiology 2006; 16: 137R-57R.
61. Nickel W. Unconventional secretory routes: direct protein export across the plasma membrane of mammalian cells. Traffic 2005; 6: 607-14.
62. Danielsen EM, Hansen GH. Lipid raft organization and function in brush borders of epithelial cells. Mol Membr Biol 2006; 23: 71-9.
63. Hernandez JD, Baum LG. Ah, sweet mystery of death! Galectins and control of cell fate. Glycobiology 2002; 12: 127R-36R.
64. Balogh A, Pozsgay J, Matkó J, *et al*. Placental protein 13 (PP13/galectin-13) undergoes lipid raft-associated subcellular redistribution in the syncytiotrophoblast in preterm preeclampsia and HELLP syndrome. Am J Obstet Gynecol 2011; 205: 156.e1-14.
65. Dennis JW, Nabi IR, Demetriou M. Metabolism, cell surface orga-

nization, and disease. Cell 2009; 139: 1229-41.
66. Bianchi ME. DAMPs, PAMPs and alarmins: all we need to know about danger. J Leukoc Biol 2007; 81: 1-5.
67. Su AI, Wiltshire T, Batalov S, *et al*. A gene atlas of the mouse and human protein-encoding transcriptomes. Proc Natl Acad Sci U S A 2004; 101: 6062-7.
68. Saal I, Nagy N, Lensch M, *et al*. Human galectin-2: expression profiling by RT-PCR/immunohistochemistry and its introduction as a histochemical tool for ligand localization. Histol Histopathol 2005; 20: 1191-208.
69. Dong M, Ding G, Zhou J, Wang H, Zhao Y, Huang H. The effect of trophoblasts on T lymphocytes: possible regulatory effector molecules: a proteomic analysis. Cell Physiol Biochem 2008; 21: 463-72.
70. Kubach J, Lutter P, Bopp T, e*t al*. Human CD4+CD25+ regulatory T cells: proteome analysis identifies galectin-10 as a novel marker essential for their anergy and suppressive function. Blood 2007; 110: 1550-8.
71. Yang QS, Ying K, Yuan HL, *et al*. Cloning and expression of a novel human galectin cDNA, predominantly expressed in placenta. Biochim Biophys Acta 2002; 1574: 407-11.
72. Than NG, Romero R, Xu Y, *et al*. Evolutionary origins of the placental expression of chromosome 19 cluster galectins and their complex dysregulation in preeclampsia. Placenta 2014; 35: 855-65.
73. Vasta GR. Roles of galectins in infection. Nat Rev Microbiol 2009; 7: 424-38.
74. John CM, Jarvis GA, Swanson KV, *et al*. Galectin-3 binds lactosaminylated lipooligosaccharides from Neisseria gonorrhoeae and is selectively expressed by mucosal epithelial cells that are infected. Cell Microbiol 2002; 4: 649-62.
75. Rabinovich GA, Gruppi A. Galectins as immunoregulators during infectious processes: from microbial invasion to the resolution of the disease. Parasite Immunol 2005; 27: 103-14.
76. Kasamatsu A, Uzawa K, Shimada K, *et al.* Elevation of galectin-9 as an inflammatory response in the periodontal ligament cells exposed to Porphylomonas gingivalis lipopolysaccharide *in vitro* and *in vivo*. Int J Biochem Cell Biol 2005; 37: 397-408.
77. Ouellet M, Mercier S, Pelletier I, *et al*. Galectin-1 acts as a soluble host factor that promotes HIV-1 infectivity through stabilization of virus attachment to host cells. J Immunol 2005; 174: 4120-6.
78. Fowler M, Thomas RJ, Atherton J, Roberts IS, High NJ. Galectin-3 binds to Helicobacter pylori O-antigen: it is upregulated and rapidly secreted by gastric epithelial cells in response to H. pylori adhesion. Cell Microbiol 2006; 8: 44-54.
79. Gauthier S, Pelletier I, Ouellet M, *et al*. Induction of galectin-1 expression by HTLV-I Tax and its impact on HTLV-I infectivity. Retrovirology 2008; 5: 105.
80. Okumura CY, Baum LG, Johnson PJ. Galectin-1 on cervical epithelial cells is a receptor for the sexually transmitted human parasite *Trichomonas vaginalis*. Cell Microbiol 2008; 10: 2078-90.
81. Fichorova RN. Impact of *T. vaginalis* infection on innate immune responses and reproductive outcome. J Reprod Immunol 2009; 83: 185-9.
82. Hepojoki J, Strandin T, Hetzel U, *et al*. Acute hantavirus infection induces galectin-3-binding protein. J Gen Virol 2014; 95(Pt 11): 2356-64.
83. Varki A. Nothing in glycobiology makes sense, except in the light of evolution. Cell 2006; 126: 841-5.
84. Mercier S, St-Pierre C, Pelletier I, Ouellet M, Tremblay MJ, Sato S. Galectin-1 promotes HIV-1 infectivity in macrophages through stabilization of viral adsorption. Virology 2008; 371: 121-9.
85. Kim HR, Lin HM, Biliran H, Raz A. Cell cycle arrest and inhibition of anoikis by galectin-3 in human breast epithelial cells. Cancer Res 1999; 59: 4148-54.
86. Ryan CM, Mehlert A, Richardson JM, Ferguson MA, Johnson PJ. Chemical structure of *Trichomonas vaginalis* surface lipoglycan: a role for short galactose (beta1-4/3) N-acetylglucosamine repeats in host cell interaction. J Biol Chem 2011; 286: 40494-508.
87. Smith LM, Wang M, Zangwill K, Yeh S. *Trichomonas vaginalis* infection in a premature newborn. J Perinatol 2002; 22: 502-3.
88. Sato S, Ouellet N, Pelletier I, Simard M, Rancourt A, Bergeron MG. Role of galectin-3 as an adhesion molecule for neutrophil extravasation during streptococcal pneumonia. J Immunol 2002; 168: 1813-22.
89. Lebovic DI, Mueller MD, Taylor RN. Immunobiology of endometriosis. Fertil Steril 2001; 75: 1-10.
90. Omwandho CO, Konrad L, Halis G, Oehmke F, Tinneberg HR. Role of TGF-betas in normal human endometrium and endometriosis. Hum Reprod 2010; 25: 101-9.
91. Noël JC, Chapron C, Borghese B, Fayt I, Anaf V. Galectin-3 is overexpressed in various forms of endometriosis. Appl Immunohistochem Mol Morphol 2011; 19: 253-7.
92. Bastón JI, Barañao RI, Ricci AG, *et al*. Targeting galectin-1-induced angiogenesis mitigates the severity of endometriosis. J Pathol 2014; 234: 329-37.
93. Caserta D, Di Benedetto L, Bordi G, D'Ambrosio A, Moscarini M. Levels of galectin-3 and stimulation expressed gene 2 in the peritoneal fluid of women with endometriosis: a pilot study. Gynecol Endocrinol 2014; 30: 877-80.
94. Vergetaki A, Jeschke U, Vrekoussis T, *et al*. Galectin-1 overexpression in endometriosis and its regulation by neuropeptides (CRH, UCN) indicating its important role in reproduction and inflammation. PLoS One 2014; 9: e114229.

95. Chen HL, Liao F, Lin TN, Liu FT. Galectins and neuroinflammation. Adv Neurobiol 2014; 9: 517-42.
96. Borghese B, Vaiman D, Mondon F, *et al*. Neurotrophins and pain in endometriosis. Gynecol Obstet Fertil 2010; 38: 442-6.
97. Ebrahim AH, Alalawi Z, Mirandola L, *et al*. Galectins in cancer: carcinogenesis, diagnosis and therapy. Ann Transl Med 2014; 2: 88.
98. Jeschke U, Hutter S, Heublein S, et al. Expression and function of galectins in the endometrium and at the human feto-maternal interface. Placenta 2013; 34: 863-72.
99. Jung EJ, Moon HG, Cho BI, *et al.* Galectin-1 expression in cancer-associated stromal cells correlates tumor invasiveness and tumor progression in breast cancer. Int J Cancer 2007; 120: 2331-8.
100. Moiseeva EV, Rapoport EM, Bovin NV, *et al*. Galectins as markers of aggressiveness of mouse mammary carcinoma: towards a lectin target therapy of human breast cancer. Breast Cancer Res Treat 2005; 91: 227-41.
101. Ferrer CM, Reginato MJ. Sticking to sugars at the metastatic site: sialyltransferase ST6GalNAc2 acts as a breast cancer metastasis suppressor. Cancer Discov 2014; 4: 275-7.
102. van den Brule FA, Buicu C, Berchuck A, *et al*. Expression of the 67-kD laminin receptor, galectin-1, and galectin-3 in advanced human uterine adenocarcinoma. Hum Pathol 1996; 27: 1185-91.
103. Ege CB, Akbulut M, Zekioğlu O, Ozdemir N. Investigation of galectin-3 and heparanase in endometrioid and serous carcinomas of the endometrium and correlation with known predictors of survival. Arch Gynecol Obstet 2011; 284: 1231-9.
104. Dalotto-Moreno T, Croci DO, Cerliani JP, *et al*. Targeting galectin-1 overcomes breast cancer-associated immunosuppression and prevents metastatic disease. Cancer Res 2013; 73: 1107-17.
105. van den Brule F, Califice S, Garnier F, Fernandez PL, Berchuck A, Castronovo V. Galectin-1 accumulation in the ovary carcinoma peritumoral stroma is induced by ovary carcinoma cells and affects both cancer cell proliferation and adhesion to laminin-1 and fibronectin. Lab Invest 2003; 83: 377-86.
106. Kohrenhagen N, Volker HU, Kapp M, Dietl J, Kammerer U. Increased expression of galectin-1 during the progression of cervical neoplasia. Int J Gynecol Cancer 2006; 16: 2018-22.
107. Kim HJ, Do IG, Jeon HK, *et al*. Galectin 1 expression is associated with tumor invasion and metastasis in stage IB to IIA cervical cancer. Hum Pathol 2013; 44: 62-8.
108. Huang EY, Chanchien CC, Lin H, Wang CC, Wang CJ, Huang CC. Galectin-1 is an independent prognostic factor for local recurrence and survival after definitive radiation therapy for patients with squamous cell carcinoma of the uterine cervix. Int J Radiat Oncol Biol Phys 2013; 87: 975-82.
109. Huang EY, Chen YF, Chen YM, *et al*. A novel radioresistant mechanism of galectin-1 mediated by H-Ras-dependent pathways in cervical cancer cells. Cell Death Dis 2012; 3: e251.
110. Lee JW, Song SY, Choi JJ, *et al*. Decreased galectin-3 expression during the progression of cervical neoplasia. J Cancer Res Clin Oncol 2006; 132: 241-7.
111. Logullo AF, Lopes AB, Nonogaki S, *et al*. C-erbB-2 expression is a better predictor for survival than galectin-3 or p53 in early-stage breast cancer. Oncol Rep 2007; 18: 121-6.
112. Stewart CJ, Crook ML. Galectin-3 expression in uterine endometrioid adenocarcinoma: comparison of staining in conventional tumor glands and in areas of MELF pattern myometrial invasion. Int J Gynecol Pathol 2010; 29: 555-61.
113. Brustmann H, Riss D, Naudé S. Galectin-3 expression in normal, hyperplastic, and neoplastic endometrial tissues. Pathol Res Pract 2003; 199: 151-8.
114. Oishi T, Itamochi H, Kigawa J, *et al*. Galectin-3 may contribute to cisplatin resistance in clear cell carcinoma of the ovary. Int J Gynecol Cancer 2007; 17: 1040-6.
115. Kim MK, Sung CO, Do IG, *et al*. Overexpression of galectin-3 and its clinical significance in ovarian carcinoma. Int J Clin Oncol 2011; 16: 352-8.
116. Min KW, Park MH, Hong SR, *et al*. Clear cell carcinomas of the ovary: a multi-institutional study of 129 cases in Korea with prognostic significance of Emi1 and galectin-3. Int J Gynecol Pathol 2013; 32: 3-14.
117. Lee JH, Zhang X, Shin BK, Lee ES, Kim I. Mac-2 binding protein and galectin-3 expression in mucinous tumours of the ovary: an annealing control primer system and immunohistochemical study. Pathology 2009; 41: 229-33.
118. Dagher SF, Wang JL, Patterson RJ. Identification of galectin-3 as a factor in pre-mRNA splicing. Proc Natl Acad Sci U S A 1995; 92: 1213-7.
119. Honjo Y, Nangia-Makker P, Inohara H, Raz A. Down-regulation of galectin-3 suppresses tumorigenicity of human breast carcinoma cells. Clin Cancer Res 2001; 7: 661-8.
120. Dumic J, Dabelic S, Flögel M. Galectin-3: an open-ended story. Biochim Biophys Acta 2006; 1760: 616-35.
121. Baptiste TA, James A, Saria M, Ochieng J. Mechano-transduction mediated secretion and uptake of galectin-3 in breast carcinoma cells: implications in the extracellular functions of the lectin. Exp Cell Res 2007; 313: 652-64.
122. Yang RY, Hsu DK, Liu FT. Expression of galectin-3 modulates T-cell growth and apoptosis. Proc Natl Acad Sci U S A 1996; 93: 6737-42.
123. Akahani S, Nangia-Makker P, Inohara H, Kim HR, Raz A. Galectin-3: a novel antiapoptotic molecule with a functional BH1 (NWGR) domain of Bcl-2 family. Cancer Res 1997; 57: 5272-6.

124. Matarrese P, Tinari N, Semeraro ML, Natoli C, Iacobelli S, Malorni W. Galectin-3 overexpression protects from cell damage and death by influencing mitochondrial homeostasis. FEBS Lett 2000; 473: 311-5.
125. Moon BK, Lee YJ, Battle P, Jessup JM, Raz A, Kim HR. Galectin-3 protects human breast carcinoma cells against nitric oxide-induced apoptosis: implication of galectin-3 function during metastasis. Am J Pathol 2001; 159: 1055-60.
126. Lin HM, Pestell RG, Raz A, Kim HR. Galectin-3 enhances cyclin D (1) promoter activity through SP1 and a cAMP-responsive element in human breast epithelial cells. Oncogene 2002; 21: 8001-10.
127. Yu F, Finley RL Jr, Raz A, Kim HR. Galectin-3 translocates to the perinuclear membranes and inhibits cytochrome c release from the mitochondria: a role for synexin in galectin-3 translocation. J Biol Chem 2002; 277: 15819-27.
128. Choi JH, Chun KH, Raz A, Lotan R. Inhibition of N-(4-hydroxyphenyl)retinamide-induced apoptosis in breast cancer cells by galectin-3. Cancer Biol Ther 2004; 3: 447-52.
129. Nangia-Makker P, Raz T, Tait L, Hogan V, Fridman R, Raz A. Galectin-3 cleavage: a novel surrogate marker for matrix metalloproteinase activity in growing breast cancers. Cancer Res 2007; 67: 11760-8.
130. Balan V, Nangia-Makker P, Raz A. Galectins as cancer biomarkers. Cancers (Basel) 2010; 2: 592-610.
131. Mazurek N, Byrd JC, Sun Y, Ueno S, Bresalier RS. A galectin-3 sequence polymorphism confers TRAIL sensitivity to human breast cancer cells. Cancer 2011; 117: 4375-80.
132. Mazurek N, Sun YJ, Liu KF, *et al*. Phosphorylated galectin-3 mediates tumor necrosis factor-related apoptosis-inducing ligand signaling by regulating phosphatase and tensin homologue deleted on chromosome 10 in human breast carcinoma cells. J Biol Chem 2007; 282: 21337-48.
133. Guha P, Bandyopadhyaya G, Polumuri SK, *et al*. Nicotine promotes apoptosis resistance of breast cancer cells and enrichment of side population cells with cancer stem cell-like properties via a signaling cascade involving galectin-3, alpha9 nicotinic acetylcholine receptor and STAT3. Breast Cancer Res Treat 2014; 145: 5-22.
134. Tsai CJ, Sulman EP, Eifel PJ, e*t al*. Galectin-7 levels predict radiation response in squamous cell carcinoma of the cervix. Gynecol Oncol 2013; 131: 645-9.
135. Ueda S, Kuwabara I, Liu FT. Suppression of tumor growth by galectin-7 gene transfer. Cancer Res 2004; 64: 5672-6.
136. Saussez S, Kiss R. Galectin-7. Cell Mol Life Sci 2006; 63: 686-97.
137. Matsui Y, Ueda S, Watanabe J, Kuwabara I, Ogawa O, Nishiyama H. Sensitizing effect of galectin-7 in urothelial cancer to cisplatin through the accumulation of intracellular reactive oxygen species. Cancer Res 2007; 67: 1212-20.
138. St-Pierre Y, Campion CG, Grosset AA. A distinctive role for galectin-7 in cancer? Front Biosci (Landmark Ed) 2012; 17: 438-50.
139. Grosset AA, Labrie M, Gagné D, *et al*. Cytosolic galectin-7 impairs p53 functions and induces chemoresistance in breast cancer cells. BMC Cancer 2014; 14: 801.
140. Campion CG, Labrie M, Lavoie G, St-Pierre Y. Expression of galectin-7 is induced in breast cancer cells by mutant p53. PLoS One 2013; 8: e72468.
141. Lahm H, Andre S, Hoeflich A, *et al*. Tumor galectinology: insights into the complex network of a family of endogenous lectins. Glycoconj J 2004; 20: 227-38.
142. Danguy A, Rorive S, Decaestecker C, *et al*. Immunohistochemical profile of galectin-8 expression in benign and malignant tumors of epithelial, mesenchymatous and adipous origins, and of the nervous system. Histol Histopathol 2001; 16: 861-8.
143. Liang MY, Lu YM, Zhang Y, Zhang SL. Serum galectin-9 in cervical cancer. Zhonghua Yi Xue Za Zhi 2008; 88: 2783-5.
144. Liang CH, Wu CY. Glycan array: a powerful tool for glycomics studies. Expert Rev Proteomics 2009; 6: 631-45.
145. Irie A, Yamauchi A, Kontani K, *et al*. Galectin-9 as a prognostic factor with antimetastatic potential in breast cancer. Clin Cancer Res 2005; 11: 2962-8.
146. Heusschen R, Griffioen AW, Thijssen VL. Galectin-9 in tumor biology: a jack of multiple trades. Biochim Biophys Acta 2013; 1836: 177-85.
147. Mylonas I, Mayr D, Walzel H, *et al*. Mucin 1, Thomsen-Friedenreich expression and galectin-1 binding in endometrioid adenocarcinoma: an immunohistochemical analysis. Anticancer Res 2007; 27: 1975-80.
148. Khaldoyanidi SK, Glinsky VV, Sikora L, *et al*. MDA-MB-435 human breast carcinoma cell homo- and heterotypic adhesion under flow conditions is mediated in part by Thomsen-Friedenreich antigen-galectin-3 interactions. J Biol Chem 2003; 278: 4127-34.
149. Yu LG, Andrews N, Zhao Q, *et al*. Galectin-3 interaction with Thomsen-Friedenreich disaccharide on cancer-associated MUC1 causes increased cancer cell endothelial adhesion. J Biol Chem 2007; 282: 773-81.
150. Inohara H, Akahani S, Raz A. Galectin-3 stimulates cell proliferation. Exp Cell Res 1998; 245: 294-302.
151. Song L, Tang JW, Owusu L, Sun MZ, Wu J, Zhang J. Galectin-3 in cancer. Clin Chim Acta 2014; 431: 185-91.
152. Zhu H, Wu TC, Chen WQ, *et al*. Roles of galectin-7 and S100A9 in cervical squamous carcinoma: Clinicopathological and *in vitro* evidence. Int J Cancer 2013; 132: 1051-9.
153. Park JE, Chang WY, Cho M. Induction of matrix metalloprotein-

ase-9 by galectin-7 through p38 MAPK signaling in HeLa human cervical epithelial adenocarcinoma cells. Oncol Rep 2009; 22: 1373-9.
154. Labrie M, Vladoiu MC, Grosset AA, Gaboury L, St-Pierre Y. Expression and functions of galectin-7 in ovarian cancer. Oncotarget 2014; 5: 7705-21.
155. Demers M, Rose AA, Grosset AA, *et al*. Overexpression of galectin-7, a myoepithelial cell marker, enhances spontaneous metastasis of breast cancer cells. Am J Pathol 2010; 176: 3023-31.
156. Liu J, Cheng Y, He M, Yao S. Vascular endothelial growth factor C enhances cervical cancer cell invasiveness via upregulation of galectin-3 protein. Gynecol Endocrinol 2014; 30: 461-5.
157. Nangia-Makker P, Wang Y, Raz T, *et al*. Cleavage of galectin-3 by matrix metalloproteases induces angiogenesis in breast cancer. Int J Cancer 2010; 127: 2530-41.
158. Liu FT, Rabinovich GA. Galectins as modulators of tumour progression. Nat Rev Cancer 2005; 5: 29-41.
159. Chen C, Duckworth CA, Fu B, Pritchard DM, Rhodes JM, Yu LG. Circulating galectins -2, -4 and -8 in cancer patients make important contributions to the increased circulation of several cytokines and chemokines that promote angiogenesis and metastasis. Br J Cancer 2014; 110: 741-52.
160. Fridman WH, Pagès F, Sautès-Fridman C, Galon J. The immune contexture in human tumours: impact on clinical outcome. Nat Rev Cancer 2012; 12: 298-306.
161. Toscano MA, Bianco GA, Ilarregui JM, *et al*. Differential glycosylation of TH1, TH2 and TH-17 effector cells selectively regulates susceptibility to cell death. Nat Immunol 2007; 8: 825-34.
162. Li H, Wang Y, Zhou F. Effect of *ex vivo*-expanded γδ-T cells combined with galectin-1 antibody on the growth of human cervical cancer xenografts in SCID mice. Clin Invest Med 2010; 33: E280-9.
163. Rabinovich GA. Galectin-1 as a potential cancer target. Br J Cancer 2005; 92: 1188-92.
164. Fukumori T, Takenaka Y, Yoshii T, *et al*. CD29 and CD7 mediate galectin-3-induced type II T-cell apoptosis. Cancer Res 2003; 63: 8302-11.
165. Iurisci I, Tinari N, Natoli C, Angelucci D, Cianchetti E, Iacobelli S. Concentrations of galectin-3 in the sera of normal controls and cancer patients. Clin Cancer Res 2000; 6: 1389-93.
166. Barrow H, Guo X, Wandall HH, *et al*. Serum galectin-2, -4, and -8 are greatly increased in colon and breast cancer patients and promote cancer cell adhesion to blood vascular endothelium. Clin Cancer Res 2011; 17: 7035-46.
167. Carlsson MC, Balog CI, Kilsgård O, *et al*. Different fractions of human serum glycoproteins bind galectin-1 or galectin-8, and their ratio may provide a refined biomarker for pathophysiological conditions in cancer and inflammatory disease. Biochim Biophys Acta 2012; 1820: 1366-72.
168. Balasubramanian K, Vasudevamurthy R, Venkateshaiah SU, Thomas A, Vishweshwara A, Dharmesh SM. Galectin-3 in urine of cancer patients: stage and tissue specificity. J Cancer Res Clin Oncol 2009; 135: 355-63.
169. Jerzak M, Bischof P. Apoptosis in the first trimester human placenta: the role in maintaining immune privilege at the maternal-foetal interface and in the trophoblast remodelling. Eur J Obstet Gynecol Reprod Biol 2002; 100: 138-42.
170. Petty HR, Kindzelskii AL, Espinoza J, Romero R. Trophoblast contact deactivates human neutrophils. J Immunol 2006; 176: 3205-14.
171. Moffett A, Loke C. Immunology of placentation in eutherian mammals. Nat Rev Immunol 2006; 6: 584-94.
172. Erlebacher A. Immune surveillance of the maternal/fetal interface: controversies and implications. Trends Endocrinol Metab 2010; 21: 428-34.
173. Mor G, Cardenas I. The immune system in pregnancy: a unique complexity. Am J Reprod Immunol 2010; 63: 425-33.
174. Arck PC, Hecher K. Fetomaternal immune cross-talk and its consequences for maternal and offspring's health. Nat Med 2013; 19: 548-56.
175. Bianchi DW. Current knowledge about fetal blood cells in the maternal circulation. J Perinat Med 1998; 26: 175-85.
176. Nelson JL. Pregnancy, persistent microchimerism, and autoimmune disease. J Am Med Womens Assoc 1998; 53: 31-2, 47.
177. Lapaire O, Hösli I, Zanetti-Daellenbach R, *et al*. Impact of fetal-maternal microchimerism on women's health: a review. J Matern Fetal Neonatal Med 2007; 20: 1-5.
178. Redman CW, Sargent IL. Microparticles and immunomodulation in pregnancy and pre-eclampsia. J Reprod Immunol 2007; 76: 61-7.
179. Redman CW, Sargent IL. Circulating microparticles in normal pregnancy and pre-eclampsia. Placenta 2008; 29 Suppl A: S73-7.
180. Naccasha N, Gervasi MT, Chaiworapongsa T, *et al*. Phenotypic and metabolic characteristics of monocytes and granulocytes in normal pregnancy and maternal infection. Am J Obstet Gynecol 2001; 185: 1118-23.
181. Hahn S, Giaglis S, Hoesli I, Hasler P. Neutrophil NETs in reproduction: from infertility to preeclampsia and the possibility of fetal loss. Front Immunol 2012; 3: 362.
182. Redman CW, Sacks GP, Sargent IL. Preeclampsia: an excessive maternal inflammatory response to pregnancy. Am J Obstet Gynecol 1999; 180(2 Pt 1): 499-506.
183. Gervasi MT, Chaiworapongsa T, Pacora P, *et al*. Phenotypic and metabolic characteristics of monocytes and granulocytes in preeclampsia. Am J Obstet Gynecol 2001; 185: 792-7.
184. Gervasi MT, Chaiworapongsa T, Naccasha N, *et al*. Phenotypic and metabolic characteristics of maternal monocytes and granulo-

cytes in preterm labor with intact membranes. Am J Obstet Gynecol 2001; 185: 1124-9.
185. Gervasi MT, Chaiworapongsa T, Naccasha N, *et al*. Maternal intravascular inflammation in preterm premature rupture of membranes. J Matern Fetal Neonatal Med 2002; 11: 171-5.
186. Ogge G, Romero R, Chaiworapongsa T, *et al*. Leukocytes of pregnant women with small-for-gestational age neonates have a different phenotypic and metabolic activity from those of women with preeclampsia. J Matern Fetal Neonatal Med 2010; 23: 476-87.
187. Aluvihare VR, Kallikourdis M, Betz AG. Regulatory T cells mediate maternal tolerance to the fetus. Nat Immunol 2004; 5: 266-71.
188. Wildman DE, Chen C, Erez O, Grossman LI, Goodman M, Romero R. Evolution of the mammalian placenta revealed by phylogenetic analysis. Proc Natl Acad Sci U S A 2006; 103: 3203-8.
189. Aplin JD. Developmental cell biology of human villous trophoblast: current research problems. Int J Dev Biol 2010; 54: 323-9.
190. Redman CW, Sargent IL. Immunology of pre-eclampsia. Am J Reprod Immunol 2010; 63: 534-43.
191. Romero R. Prenatal medicine: the child is the father of the man. 1996. J Matern Fetal Nonatal Med 2009; 22: 636-9.
192. Redman CW, Sargent IL. Latest advances in understanding preeclampsia. Science 2005; 308: 1592-4.
193. Romero R, Espinoza J, Kusanovic JP, *et al*. The preterm parturition syndrome. BJOG 2006; 113 Suppl 3: 17-42.
194. Goldenberg RL, Culhane JF, Iams JD, Romero R. Epidemiology and causes of preterm birth. Lancet 2008; 371: 75-84.
195. DiGiulio DB, Romero R, Amogan HP, *et al*. Microbial prevalence, diversity and abundance in amniotic fluid during preterm labor: a molecular and culture-based investigation. PLoS One 2008; 3: e3056.
196. Kim MJ, Romero R, Gervasi MT, *et al*. Widespread microbial invasion of the chorioamniotic membranes is a consequence and not a cause of intra-amniotic infection. Lab Invest 2009; 89: 924-36.
197. Kim CJ, Romero R, Kusanovic JP, *et al*. The frequency, clinical significance, and pathological features of chronic chorioamnionitis: a lesion associated with spontaneous preterm birth. Mod Pathol 2010; 23: 1000-11.
198. Ogge G, Romero R, Lee DC, *et al*. Chronic chorioamnionitis displays distinct alterations of the amniotic fluid proteome. J Pathol 2011; 223: 553-65.
199. Lee J, Romero R, Xu Y, *et al*. A signature of maternal anti-fetal rejection in spontaneous preterm birth: chronic chorioamnionitis, anti-human leukocyte antigen antibodies, and C4d. PLoS One 2011; 6: e16806.
200. Lee J, Romero R, Xu Y, *et al*. Maternal HLA panel-reactive antibodies in early gestation positively correlate with chronic chorioamnionitis: evidence in support of the chronic nature of maternal anti-fetal rejection. Am J Reprod Immunol 2011; 66: 510-26.
201. Xu Y, Tarquini F, Romero R, *et al*. Peripheral CD300a+CD8+ T lymphocytes with a distinct cytotoxic molecular signature increase in pregnant women with chronic chorioamnionitis. Am J Reprod Immunol 2012; 67: 184-97.
202. Lee J, Romero R, Chaiworapongsa T, *et al*. Characterization of the fetal blood transcriptome and proteome in maternal anti-fetal rejection: evidence of a distinct and novel type of human fetal systemic inflammatory response. Am J Reprod Immunol 2013; 70: 265-84.
203. Lee J, Romero R, Xu Y, *et al*. Detection of anti-HLA antibodies in maternal blood in the second trimester to identify patients at risk of antibody-mediated maternal anti-fetal rejection and spontaneous preterm delivery. Am J Reprod Immunol 2013; 70: 162-75.
204. Romero R, Miranda J, Chaiworapongsa T, *et al*. Prevalence and clinical significance of sterile intra-amniotic inflammation in patients with preterm labor and intact membranes. Am J Reprod Immunol 2014; 72: 458-74.
205. Romero R, Dey SK, Fisher SJ. Preterm labor: one syndrome, many causes. Science 2014; 345: 760-5.
206. Colnot C, Fowlis D, Ripoche MA, Bouchaert I, Poirier F. Embryonic implantation in galectin 1/galectin 3 double mutant mice. Dev Dyn 1998; 211: 306-13.
207. Walzel H, Neels P, Bremer H, *et al*. Immunohistochemical and glycohistochemical localization of the beta-galactoside-binding S-type lectin in human placenta. Acta Histochem 1995; 97: 33-42.
208. van den Brule FA, Fernandez PL, Buicu C, *et al*. Differential expression of galectin-1 and galectin-3 during first trimester human embryogenesis. Dev Dyn 1997; 209: 399-405.
209. Kolundžić N, Bojić-Trbojević Ž, Kovačević T, Stefanoska I, Kadoya T, Vićovac L. Galectin-1 is part of human trophoblast invasion machinery: a functional study in vitro. PLoS One 2011; 6: e28514.
210. Arikawa T, Simamura E, Shimada H, *et al*. Expression pattern of Galectin 4 in rat placentation. Placenta 2012; 33: 885-7.
211. Than GN, Bohn H, Szabo DG. Advances in pregnancy-related protein research: functional and clinical applications. Boca Raton: CRC Press, 1993.
212. Bischof P, Irminger-Finger I. The human cytotrophoblastic cell, a mononuclear chameleon. Int J Biochem Cell Biol 2005; 37: 1-16.
213. Ahmed MS, Aleksunes LM, Boeuf P, *et al*. IFPA Meeting 2012 Workshop Report II: epigenetics and imprinting in the placenta, growth factors and villous trophoblast differentiation, role of the placenta in regulating fetal exposure to xenobiotics during pregnancy, infection and the placenta. Placenta 2013; 34 Suppl: S6-10.
214. Chiariotti L, Salvatore P, Frunzio R, Bruni CB. Galectin genes: reg-

ulation of expression. Glycoconj J 2004; 19: 441-9.
215. Segerer S, Kammerer U, Kapp M, Dietl J, Rieger L. Upregulation of chemokine and cytokine production during pregnancy. Gynecol Obstet Invest 2009; 67: 145-50.
216. Hammer A. Immunological regulation of trophoblast invasion. J Reprod Immunol 2011; 90: 21-8.
217. Knöfler M, Pollheimer J. Human placental trophoblast invasion and differentiation: a particular focus on Wnt signaling. Front Genet 2013; 4: 190.
218. Lima PD, Zhang J, Dunk C, Lye SJ, Croy BA. Leukocyte driven-decidual angiogenesis in early pregnancy. Cell Mol Immunol 2014; 11: 522-37.
219. Godbole G, Suman P, Gupta SK, Modi D. Decidualized endometrial stromal cell derived factors promote trophoblast invasion. Fertil Steril 2011; 95: 1278-83.
220. Phillips B, Knisley K, Weitlauf KD, Dorsett J, Lee V, Weitlauf H. Differential expression of two beta-galactoside-binding lectins in the reproductive tracts of pregnant mice. Biol Reprod 1996; 55: 548-58.
221. Lee VH, Lee AB, Phillips EB, Roberts JK, Weitlauf HM. Spatiotemporal pattern for expression of galectin-3 in the murine uteroplacental complex: evidence for differential regulation. Biol Reprod 1998; 58: 1277-82.
222. Yang H, Lei C, Zhang W. Expression of galectin-3 in mouse endometrium and its effect during embryo implantation. Reprod Biomed Online 2012; 24: 116-22.
223. Shimizu Y, Kabir-Salmani M, Azadbakht M, Sugihara K, Sakai K, Iwashita M. Expression and localization of galectin-9 in the human uterodome. Endocr J 2008; 55: 879-87.
224. Yang H, Lei CX, Zhang W. Human chorionic gonadotropin (hCG) regulation of galectin-3 expression in endometrial epithelial cells and endometrial stromal cells. Acta Histochem 2013; 115: 3-7.
225. Blois SM, Barrientos G. Galectin signature in normal pregnancy and preeclampsia. J Reprod Immunol 2014; 101-102: 127-34.
226. Tirado-González I, Freitag N, Barrientos G, *et al*. Galectin-1 influences trophoblast immune evasion and emerges as a predictive factor for the outcome of pregnancy. Mol Hum Reprod 2013; 19: 43-53.
227. Heusschen R, Freitag N, Tirado-González I, *et al*. Profiling Lgals9 splice variant expression at the fetal-maternal interface: implications in normal and pathological human pregnancy. Biol Reprod 2013; 88: 22.
228. Knöfler M, Pollheimer J. IFPA Award in Placentology lecture: molecular regulation of human trophoblast invasion. Placenta 2012; 33 Suppl: S55-62.
229. Elola MT, Chiesa ME, Alberti AF, Mordoh J, Fink NE. Galectin-1 receptors in different cell types. J Biomed Sci 2005; 12: 13-29.
230. Crider-Pirkle S, Billingsley P, Faust C, Hardy DM, Lee V, Weitlauf H. Cubilin, a binding partner for galectin-3 in the murine utero-placental complex. J Biol Chem 2002; 277: 15904-12.
231. Garin MI, Chu CC, Golshayan D, Cernuda-Morollon E, Wait R, Lechler RI. Galectin-1: a key effector of regulation mediated by CD4+CD25+ T cells. Blood 2007; 109: 2058-65.
232. Karimi K, Arck PC. Natural killer cells: keepers of pregnancy in the turnstile of the environment. Brain Behav Immun 2010; 24: 339-47.
233. Zhu C, Anderson AC, Schubart A, *et al*. The Tim-3 ligand galectin-9 negatively regulates T helper type 1 immunity. Nat Immunol 2005; 6: 1245-52.
234. Wang F, Wan L, Zhang C, Zheng X, Li J, Chen ZK. Tim-3-Galectin-9 pathway involves the suppression induced by CD4+CD25+ regulatory T cells. Immunobiology 2009; 214: 342-9.
235. Li YH, Zhou WH, Tao Y, *et al*. The galectin-9/Tim-3 pathway is involved in the regulation of NK cell function at the maternal-fetal interface in early pregnancy. Cell Mol Immunol 2015 Jan 12 [Epub]. http://dx.doi.org/10.1038/cmi.2014.126.
236. Meggyes M, Miko E, Polgar B, *et al*. Peripheral blood TIM-3 positive NK and CD8+ T cells throughout pregnancy: TIM-3/galectin-9 interaction and its possible role during pregnancy. PLoS One 2014; 9: e92371.
237. Nangia-Makker P, Baccarini S, Raz A. Carbohydrate-recognition and angiogenesis. Cancer Metastasis Rev 2000; 19: 51-7.
238. Freitag N, Tirado-González I, Barrientos G, *et al*. Interfering with Gal-1-mediated angiogenesis contributes to the pathogenesis of preeclampsia. Proc Natl Acad Sci U S A 2013; 110: 11451-6.
239. Hsieh SH, Ying NW, Wu MH, *et al*. Galectin-1, a novel ligand of neuropilin-1, activates VEGFR-2 signaling and modulates the migration of vascular endothelial cells. Oncogene 2008; 27: 3746-53.
240. Douglas NC, Tang H, Gomez R, *et al*. Vascular endothelial growth factor receptor 2 (VEGFR-2) functions to promote uterine decidual angiogenesis during early pregnancy in the mouse. Endocrinology 2009; 150: 3845-54.
241. Halder JB, Zhao X, Soker S, *et al*. Differential expression of VEGF isoforms and VEGF(164)-specific receptor neuropilin-1 in the mouse uterus suggests a role for VEGF(164) in vascular permeability and angiogenesis during implantation. Genesis 2000; 26: 213-24.
242. Baston-Buest DM, Porn AC, Schanz A, Kruessel JS, Janni W, Hess AP. Expression of the vascular endothelial growth factor receptor neuropilin-1 at the human embryo-maternal interface. Eur J Obstet Gynecol Reprod Biol 2011; 154: 151-6.
243. Soker S, Takashima S, Miao HQ, Neufeld G, Klagsbrun M. Neuropilin-1 is expressed by endothelial and tumor cells as an isoform-specific receptor for vascular endothelial growth factor. Cell 1998; 92: 735-45.
244. Gizurarson S, Huppertz B, Osol G, Skarphedinsson JO, Mandala

M, Meiri H. Effects of placental protein 13 on the cardiovascular system in gravid and non-gravid rodents. Fetal Diagn Ther 2013; 33: 257-64.

245. Sammar M, Nisamblatt S, Gonen R, *et al*. The role of the carbohydrate recognition domain of placental protein 13 (PP13) in pregnancy evaluated with recombinant PP13 and the DelT221 PP13 variant. PLoS One 2014; 9: e102832.
246. Romero R, Espinoza J, Gonçalves LF, Kusanovic JP, Friel LA, Nien JK. Inflammation in preterm and term labour and delivery. Semin Fetal Neonatal Med 2006; 11: 317-26.
247. Hassan SS, Romero R, Tarca AL, *et al*. The transcriptome of cervical ripening in human pregnancy before the onset of labor at term: identification of novel molecular functions involved in this process. J Matern Fetal Neonatal Med 2009; 22: 1183-93.
248. Hassan SS, Romero R, Tarca AL, *et al*. The molecular basis for sonographic cervical shortening at term: identification of differentially expressed genes and the epithelial-mesenchymal transition as a function of cervical length. Am J Obstet Gynecol 2010; 203: 472.e1-14.
249. Mittal P, Romero R, Tarca AL, *et al*. Characterization of the myometrial transcriptome and biological pathways of spontaneous human labor at term. J Perinat Med 2010; 38: 617-43.
250. Romero R, Mazor M, Munoz H, Gomez R, Galasso M, Sherer DM. The preterm labor syndrome. Ann N Y Acad Sci 1994; 734: 414-29.
251. Kim SS, Romero R, Kim JS, *et al*. Coexpression of myofibroblast and macrophage markers: novel evidence for an *in vivo* plasticity of chorioamniotic mesodermal cells of the human placenta. Lab Invest 2008; 88: 365-74.
252. Fulcher JA, Hashimi ST, Levroney EL, *et al*. Galectin-1-matured human monocyte-derived dendritic cells have enhanced migration through extracellular matrix. J Immunol 2006; 177: 216-26.
253. Sutton L, Mason DY, Redman CW. HLA-DR positive cells in the human placenta. Immunology 1983; 49: 103-12.
254. Eis AL, Brockman DE, Myatt L. Immunolocalization of the inducible nitric oxide synthase isoform in human fetal membranes. Am J Reprod Immunol 1997; 38: 289-94.
255. Benirschke K, Kaufmann P, Baergen RN. Pathology of the human placenta. 5th ed. New York: Springer-Verlag, 2006.
256. Espinoza J, Chaiworapongsa T, Romero R, *et al*. Antimicrobial peptides in amniotic fluid: defensins, calprotectin and bacterial/permeability-increasing protein in patients with microbial invasion of the amniotic cavity, intra-amniotic inflammation, preterm labor and premature rupture of membranes. J Matern Fetal Neonatal Med 2003; 13: 2-21.
257. Gil CD, Cooper D, Rosignoli G, Perretti M, Oliani SM. Inflammation-induced modulation of cellular galectin-1 and -3 expression in a model of rat peritonitis. Inflamm Res 2006; 55: 99-107.
258. Barrionuevo P, Beigier-Bompadre M, Ilarregui JM, *et al*. A novel function for galectin-1 at the crossroad of innate and adaptive immunity: galectin-1 regulates monocyte/macrophage physiology through a nonapoptotic ERK-dependent pathway. J Immunol 2007; 178: 436-45.
259. Correa SG, Sotomayor CE, Aoki MP, Maldonado CA, Rabinovich GA. Opposite effects of galectin-1 on alternative metabolic pathways of L-arginine in resident, inflammatory, and activated macrophages. Glycobiology 2003; 13: 119-28.
260. Demmert M, Faust K, Bohlmann MK, *et al*. Galectin-3 in cord blood of term and preterm infants. Clin Exp Immunol 2012; 167: 246-51.
261. Savman K, Heyes MP, Svedin P, Karlsson A. Microglia/macrophage-derived inflammatory mediators galectin-3 and quinolinic acid are elevated in cerebrospinal fluid from newborn infants after birth asphyxia. Transl Stroke Res 2013; 4: 228-35.
262. Sundqvist M, Osla V, Jacobsson B, Rudin A, Sävman K, Karlsson A. Cord blood neutrophils display a galectin-3 responsive phenotype accentuated by vaginal delivery. BMC Pediatr 2013; 13: 128.
263. Kollar S, Sandor N, Molvarec A, *et al*. Prevalence of intracellular galectin-1-expressing lymphocytes in umbilical cord blood in comparison with adult peripheral blood. Biol Blood Marrow Transplant 2012; 18: 1608-13.
264. Doverhag C, Keller M, Karlsson A, *et al*. Pharmacological and genetic inhibition of NADPH oxidase does not reduce brain damage in different models of perinatal brain injury in newborn mice. Neurobiol Dis 2008; 31: 133-44.
265. Bamberg C, Kalache KD. Prenatal diagnosis of fetal growth restriction. Semin Fetal Neonatal Med 2004; 9: 387-94.
266. Matthiesen L, Berg G, Ernerudh J, Ekerfelt C, Jonsson Y, Sharma S. Immunology of preeclampsia. Chem Immunol Allergy 2005; 89: 49-61.
267. ACOG Committee on Practice Bulletins--Obstetrics. ACOG practice bulletin. Diagnosis and management of preeclampsia and eclampsia. Number 33, January 2002. Obstet Gynecol 2002; 99: 159-67.
268. Sibai B, Dekker G, Kupferminc M. Pre-eclampsia. Lancet 2005; 365: 785-99.
269. Barker DJ. Fetal nutrition and cardiovascular disease in later life. Br Med Bull 1997; 53: 96-108.
270. Irgens HU, Reisaeter L, Irgens LM, Lie RT. Long term mortality of mothers and fathers after pre-eclampsia: population based cohort study. BMJ 2001; 323: 1213-7.
271. Powe CE, Levine RJ, Karumanchi SA. Preeclampsia, a disease of the maternal endothelium: the role of antiangiogenic factors and implications for later cardiovascular disease. Circulation 2011; 123: 2856-69.
272. Than NG, Vaisbuch E, Kim CJ, *et al*. Early-onset preeclampsia and

HELLP syndrome: an overview. In: Preedy VR, ed. Handbook of growth and growth monitoring in health and disease. New York: Springer, 2012; 1867-91.
273. Ness RB, Roberts JM. Heterogeneous causes constituting the single syndrome of preeclampsia: a hypothesis and its implications. Am J Obstet Gynecol 1996; 175: 1365-70.
274. von Dadelszen P, Magee LA, Roberts JM. Subclassification of preeclampsia. Hypertens Pregnancy 2003; 22: 143-8.
275. Burton GJ, Jauniaux E. Placental oxidative stress: from miscarriage to preeclampsia. J Soc Gynecol Investig 2004; 11: 342-52.
276. Burton GJ, Woods AW, Jauniaux E, Kingdom JC. Rheological and physiological consequences of conversion of the maternal spiral arteries for uteroplacental blood flow during human pregnancy. Placenta 2009; 30: 473-82.
277. Roberts JM, Hubel CA. The two stage model of preeclampsia: variations on the theme. Placenta 2009; 30 Suppl A: S32-7.
278. Brosens IA, Robertson WB, Dixon HG. The role of the spiral arteries in the pathogenesis of preeclampsia. Obstet Gynecol Annu 1972; 1: 177-91.
279. Brosens I, Pijnenborg R, Vercruysse L, Romero R. The "Great Obstetrical Syndromes" are associated with disorders of deep placentation. Am J Obstet Gynecol 2011; 204: 193-201.
280. Lee X, Keith JC Jr, Stumm N, *et al*. Downregulation of placental syncytin expression and abnormal protein localization in pre-eclampsia. Placenta 2001; 22: 808-12.
281. Chen CP, Chen CY, Yang YC, Su TH, Chen H. Decreased placental GCM1 (glial cells missing) gene expression in pre-eclampsia. Placenta 2004; 25: 413-21.
282. Roberts JM, Taylor RN, Musci TJ, Rodgers GM, Hubel CA, McLaughlin MK. Preeclampsia: an endothelial cell disorder. Am J Obstet Gynecol 1989; 161: 1200-4.
283. Sacks GP, Studena K, Sargent K, Redman CW. Normal pregnancy and preeclampsia both produce inflammatory changes in peripheral blood leukocytes akin to those of sepsis. Am J Obstet Gynecol 1998; 179: 80-6.
284. Maynard SE, Min JY, Merchan J, *et al*. Excess placental soluble fms-like tyrosine kinase 1 (sFlt1) may contribute to endothelial dysfunction, hypertension, and proteinuria in preeclampsia. J Clin Invest 2003; 111: 649-58.
285. Chaiworapongsa T, Romero R, Espinoza J, *et al*. Evidence supporting a role for blockade of the vascular endothelial growth factor system in the pathophysiology of preeclampsia. Young Investigator Award. Am J Obstet Gynecol 2004; 190: 1541-7.
286. Gupta AK, Hasler P, Holzgreve W, Gebhardt S, Hahn S. Induction of neutrophil extracellular DNA lattices by placental microparticles and IL-8 and their presence in preeclampsia. Hum Immunol 2005; 66: 1146-54.
287. Levine RJ, Lam C, Qian C, *et al*. Soluble endoglin and other circulating antiangiogenic factors in preeclampsia. N Engl J Med 2006; 355: 992-1005.
288. Venkatesha S, Toporsian M, Lam C, *et al*. Soluble endoglin contributes to the pathogenesis of preeclampsia. Nat Med 2006; 12: 642-9.
289. Rusterholz C, Holzgreve W, Hahn S. Oxidative stress alters the integrity of cell-free mRNA fragments associated with placenta-derived syncytiotrophoblast microparticles. Fetal Diagn Ther 2007; 22: 313-7.
290. Burton GJ, Yung HW, Cindrova-Davies T, Charnock-Jones DS. Placental endoplasmic reticulum stress and oxidative stress in the pathophysiology of unexplained intrauterine growth restriction and early onset preeclampsia. Placenta 2009; 30 Suppl A: S43-8.
291. Rusterholz C, Messerli M, Hoesli I, Hahn S. Placental microparticles, DNA, and RNA in preeclampsia. Hypertens Pregnancy 2011; 30: 364-75.
292. Redman CW, Sargent IL, Staff AC. IFPA Senior Award Lecture: making sense of pre-eclampsia - two placental causes of preeclampsia? Placenta 2014; 35 Suppl: S20-5.
293. Webster RP, Roberts VH, Myatt L. Protein nitration in placenta: functional significance. Placenta 2008; 29: 985-94.
294. Burton GJ, Yung HW. Endoplasmic reticulum stress in the pathogenesis of early-onset pre-eclampsia. Pregnancy Hypertens 2011; 1: 72-8.
295. Thijssen VL, Postel R, Brandwijk RJ, *et al*. Galectin-1 is essential in tumor angiogenesis and is a target for antiangiogenesis therapy. Proc Natl Acad Sci U S A 2006; 103: 15975-80.
296. Sasaki Y, Darmochwal-Kolarz D, Suzuki D, *et al*. Proportion of peripheral blood and decidual CD4(+) CD25(bright) regulatory T cells in pre-eclampsia. Clin Exp Immunol 2007; 149: 139-45.
297. Toldi G, Saito S, Shima T, *et al*. The frequency of peripheral blood CD4+ CD25high FoxP3+ and CD4+ CD25- FoxP3+ regulatory T cells in normal pregnancy and pre-eclampsia. Am J Reprod Immunol 2012; 68: 175-80.
298. Saito S, Sakai M, Sasaki Y, Nakashima A, Shiozaki A. Inadequate tolerance induction may induce pre-eclampsia. J Reprod Immunol 2007; 76: 30-9.
299. Miko E, Meggyes M, Bogar B, *et al*. Involvement of Galectin-9/TIM-3 pathway in the systemic inflammatory response in early-onset preeclampsia. PLoS One 2013; 8: e71811.
300. Gebhardt S, Bruiners N, Hillermann R. A novel exonic variant (221delT) in the LGALS13 gene encoding placental protein 13 (PP13) is associated with preterm labour in a low risk population. J Reprod Immunol 2009; 82: 166-73.
301. Shimizu H, Sekizawa A, Purwosunu Y, *et al*. PP13 mRNA expres-

sion in the cellular component of maternal blood as a marker for preeclampsia. Prenat Diagn 2009; 29: 1231-6.
302. Farina A, Zucchini C, Sekizawa A, *et al*. Performance of messenger RNAs circulating in maternal blood in the prediction of preeclampsia at 10-14 weeks. Am J Obstet Gynecol 2010; 203: 575.e1-7.
303. Huppertz B, Meiri H, Gizurarson S, Osol G, Sammar M. Placental protein 13 (PP13): a new biological target shifting individualized risk assessment to personalized drug design combating pre-eclampsia. Hum Reprod Update 2013; 19: 391-405.
304. Khalil A, Cowans NJ, Spencer K, Goichman S, Meiri H, Harrington K. First trimester maternal serum placental protein 13 for the prediction of pre-eclampsia in women with a priori high risk. Prenat Diagn 2009; 29: 781-9.
305. Audibert F, Boucoiran I, An N, *et al*. Screening for preeclampsia using first-trimester serum markers and uterine artery Doppler in nulliparous women. Am J Obstet Gynecol 2010; 203: 383.e1-8.
306. Akolekar R, Syngelaki A, Sarquis R, Zvanca M, Nicolaides KH. Prediction of early, intermediate and late pre-eclampsia from maternal factors, biophysical and biochemical markers at 11-13 weeks. Prenat Diagn 2011; 31: 66-74.
307. Odibo AO, Zhong Y, Goetzinger KR, *et al*. First-trimester placental protein 13, PAPP-A, uterine artery Doppler and maternal characteristics in the prediction of pre-eclampsia. Placenta 2011; 32: 598-602.
308. Di Lorenzo G, Ceccarello M, Cecotti V, *et al*. First trimester maternal serum PIGF, free beta-hCG, PAPP-A, PP-13, uterine artery Doppler and maternal history for the prediction of preeclampsia. Placenta 2012; 33: 495-501.
309. El Sherbiny WS, Soliman A, Nasr AS. Placental protein 13 as an early predictor in Egyptian patients with preeclampsia, correlation to risk, and association with outcome. J Investig Med 2012; 60: 818-22.
310. Moslemi Zadeh N, Naghshvar F, Peyvandi S, Gheshlaghi P, Ehetshami S. PP13 and PAPP-A in the First and Second Trimesters: Predictive Factors for Preeclampsia? ISRN Obstet Gynecol 2012; 2012: 263871.
311. Myatt L, Clifton RG, Roberts JM, *et al*. First-trimester prediction of preeclampsia in nulliparous women at low risk. Obstet Gynecol 2012; 119: 1234-42.
312. Schneuer FJ, Nassar N, Khambalia AZ, *et al*. First trimester screening of maternal placental protein 13 for predicting preeclampsia and small for gestational age: in-house study and systematic review. Placenta 2012; 33: 735-40.
313. Svirsky R, Meiri H, Herzog A, Kivity V, Cuckle H, Maymon R. First trimester maternal serum placental protein 13 levels in singleton vs. twin pregnancies with and without severe pre-eclampsia. J Perinat Med 2013; 41: 561-6.
314. Cuckle HS. Screening for pre-eclampsia: lessons from aneuploidy screening. Placenta 2011; 32 Suppl: S42-8.
315. Spencer K, Cowans NJ, Chefetz I, Tal J, Kuhnreich I, Meiri H. Second-trimester uterine artery Doppler pulsatility index and maternal serum PP13 as markers of pre-eclampsia. Prenat Diagn 2007; 27: 258-63.
316. Kuc S, Wortelboer EJ, van Rijn BB, Franx A, Visser GH, Schielen PC. Evaluation of 7 serum biomarkers and uterine artery Doppler ultrasound for first-trimester prediction of preeclampsia: a systematic review. Obstet Gynecol Surv 2011; 66: 225-39.
317. Nicolaides KH. Turning the pyramid of prenatal care. Fetal Diagn Ther 2011; 29: 183-96.
318. Than NG, Balogh A, Romero R, *et al*. Placental protein 13 (PP13): a placental immunoregulatory galectin protecting pregnancy. Front Immunol 2014; 5: 348.
319. Grimpel YI, Kivity V, Cohen A, *et al*. Effects of calcium, magnesium, low-dose aspirin and low-molecular-weight heparin on the release of PP13 from placental explants. Placenta 2011; 32 Suppl: S55-64.
320. Sammar M, Nisemblat S, Fleischfarb Z, *et al*. Placenta-bound and body fluid PP13 and its mRNA in normal pregnancy compared to preeclampsia, HELLP and preterm delivery. Placenta 2011; 32 Suppl: S30-6.

Journal of Pathology and Translational Medicine 2015; 49: 209-217
http://dx.doi.org/10.4132/jptm.2015.04.09

■ REVIEW ■

Advances in the Endoscopic Assessment of Inflammatory Bowel Diseases: Cooperation between Endoscopic and Pathologic Evaluations

Jae Hee Cheon

Department of Internal Medicine,
Yonsei University College of Medicine,
Seoul, Korea

Received: March 30, 2015
Accepted: April 9, 2015

Corresponding Author
Jae Hee Cheon, M.D., Ph.D.
Department of Internal Medicine and
Institute of Gastroenterology, Yonsei University
College of Medicine, 50-1 Yonsei-ro,
Seodaemun-gu, Seoul 120-752, Korea
Tel: +82-2-2228-1990
Fax: +82-2-393-6884
E-mail: geniushee@yuhs.ac

Endoscopic assessment has a crucial role in the management of inflammatory bowel disease (IBD). It is particularly useful for the assessment of IBD disease extension, severity, and neoplasia surveillance. Recent advances in endoscopic imaging techniques have been revolutionized over the past decades, progressing from conventional white light endoscopy to novel endoscopic techniques using molecular probes or electronic filter technologies. These new technologies allow for visualization of the mucosa in detail and monitor for inflammation/dysplasia at the cellular or subcellular level. These techniques may enable us to alter the IBD surveillance paradigm from four quadrant random biopsy to targeted biopsy and diagnosis. High definition endoscopy and dye-based chromoendoscopy can improve the detection rate of dysplasia and evaluate inflammatory changes with better visualization. Dye-less chromoendoscopy, including narrow band imaging, iScan, and autofluorescence imaging can also enhance surveillance in comparison to white light endoscopy with optical or electronic filter technologies. Moreover, confocal laser endomicroscopy or endocytoscopy have can achieve real-time histology evaluation *in vivo* and have greater accuracy in comparison with histology. These new technologies could be combined with standard endoscopy or further histologic confirmation in patients with IBD. This review offers an evidence-based overview of new endoscopic techniques in patients with IBD.

Key Words: Inflammatory bowel diseases; High definition endoscopy; Chromoendoscopy; Narrow band imaging; Microscopy, confocal; iScan; Autofluorescence imaging; Endocytoscopy

Inflammatory bowel disease (IBD) includes Crohn's disease (CD) and ulcerative colitis (UC), is a chronic, relapsing inflammatory disease in the gastrointestinal tract. The cause of IBD is unknown. It has been suggested that genetic, environmental, and immunologic factors are involved in the pathogenesis of IBD, but the precise etiologic mechanisms remain unclear.

Diagnostic and therapeutic approaches for IBD have evolved over the past decades, but precise diagnosis and assessment of disease status is still an important matter of concern for physicians and IBD specialists. Precise diagnosis and assessment of patients with IBD is particularly difficult because medical therapies, surgical approaches, and long-term prognosis differ by IBD subtypes, even if patients have similar signs and symptoms.

The most valuable tool for primary diagnosis of IBD is endoscopic assessment with tissue sampling.[1,2] It can be used to observe inflammatory changes in the intestinal mucosa, evaluate the extent of disease. It also plays a role in assessing treatment efficacy in terms of mucosal healing and the risk of postsurgical recurrence. Importantly, colonoscopy with random biopsy is essential to endoscopic diagnosis, management, and treatment of IBD. The relationship between longstanding IBD and increased colorectal cancer (CRC) risk has been well established.[3] CRC is regarded as the primary cause of death in up to 15% of IBD patients. The overall rate of CRC in UC patients is 3.7% with cumulative probabilities of 18% by 30 years, according to a meta-analysis of 116 studies on the subject.[4] There is also a 2–3 fold increased risk of CRC in CD than in patients without IBD 18.3 years after initial CD diagnosis.[5] Recent studies suggest a decreased risk of CRC in IBD patients as highly developed endoscopic surveillance techniques have been adopted. According to a one time-trend study, the relative risk of CRC decreased from 1.34 in 1979–1988 to 0.57 in 1999–2008.[6] In this sense, proper cancer surveillance with conventional and novel endoscopic techniques has major clinical implications for patients with IBD.[7]

Generally, the standard recommendations for random biopsy in surveillance colonoscopy for IBD patients include four quadrant biopsies taken every 10 cm. These biopsies generally begin 8 to 10 years after diagnosis. Extra biopsies can be obtained from strictured, raised, or color changed areas in the colorectum.[8-13]

pISSN 2383-7837
eISSN 2383-7845

However, these biopsies can be time consuming and laborious. Recent endoscopic techniques are evolving with the aim of visualizing detailed surface architecture of the mucosa, vascular patterns, and even the cellular and subcellular structures in real time. Precise observation and targeted biopsy are possible with the progress of technologies such as high definition endoscopy, narrow band imaging, chromoendoscopy, confocal endomicroscopy, etc. The present review focuses on novel endoscopic technologies and diagnostic strategies for inflammation and dysplasia in IBD patients.

RECENT DEVELOPMENT OF TECHNIQUES FOR ENDOSCOPY IN INFLAMMATORY BOWEL DISEASE

Endoscopic techniques have led to improved observation of mucosal details, which may lead to reduced random biopsies since biopsies will be able to be targeted for histological evaluation. These techniques include image enhancement with modifying conventional endoscopy and improvement in mucosal imaging with magnification or several optical techniques (Table 1).

Each of these techniques is at a different stage of development and use in clinical medicine. Some of the equipment, such as probe-based or scope-based confocal laser techniques or endocytoscopy, are available only in specialized academic centers, whereas high definition endoscopy has become the standard and is widely used in clinical practice. In addition, specialized training and adequate clinical experience are necessary to adequately perform these novel endoscopies. In the case of image-enhanced endoscopy, it is important to prepare the patient with bowel cleansing in order to ensure the efficacy and safety of the procedure prior to use. This technique should be used to visualize a specific area in detail rather than for observation of the entire colon. Each of the advanced endoscopies has their own advantages and limitations. These techniques are far from being used as the gold standard in IBD, and some studies have been controversial. Thus, it requires more experience before implementing them in clinical practice and cautious use for patients on clinical use.

Table 1. Categories of endoscopic techniques used in inflammatory bowel disease

Category	Endoscopic technique
White light endoscopy	Standard definition colonoscopy High definition colonoscopy Water immersion colonoscopy
Dye-based image enhanced endoscopy	Chromoendoscopy with absorptive agents, contrast agents, tattooing, reactive staining agents
Dye-less image enhanced endoscopy	Narrow band imaging i-Scan Autofluorescence imaging
Other emerging endoscopic techniques	Confocal laser endomicroscopy Balloon assisted enteroscopy Endocytoscopy Molecular imaging Spectroscopy

High definition endoscopy

High definition or high resolution endoscopy presents signal images with 850,000 to 1 million pixels, while standard definition signals offer 100,000 to 400,000 pixels on an SD format.[14,15] High resolution endoscopy results in visualization of subtle mucosal details and improves the sensitivity and specificity of dysplastic lesion detection. Furthermore, it facilitates endoscopic resection by delineating borders of neoplastic lesions in IBD patients.

The majority of published data comes from non-IBD patients and found high definition endoscopy to be superior compared with conventional endoscopy. A retrospective study with 160 colonoscopies including long-standing (> 7 years) colonic IBD patients demonstrated 2.21 greater likelihood (95% confidence interval [CI], 1.09 to 4.45) adjusted prevalence ratio of detecting any dysplastic lesions and 2.99 (95% CI, 1.16 to 7.79) of detecting dysplastic lesions on targeted biopsy with high definition colonoscopy compared to conventional endoscopy.[16] There was also a 3-fold higher neoplasia detection rate with high definition endoscopy when compared with standard definition endoscopy in IBD patients.

Chromoendoscopy

Chromoendoscopy is considered a cost-effective technique intended to enhance visualization of mucosal detail, submucosal vascular patterns, and lesion characterization. In particular, chromoendoscopy can facilitate the identification of flat lesions harboring intraepithelial neoplasia. With this, it can guide biopsies and reduces the number of biopsies. It is divided into dye-based and dye-less imaging techniques.

Dye-based chromoendoscopy has been used for over a decade and increases the rate of dysplastic lesion detection, especially in patients with long-standing IBD (Fig. 1A). In addition, Dye-based chromoendoscopy allows for improved assessment of disease severity and extent. Absorptive agents (e.g., Lugol solution, methylene blue, toludine blue, and cresyl violet), contrast agents (e.g., indigo carmine and acetic acid), agents for tattooing (e.g., India ink, Indocyanine green, and methylene blue), and reactive

http://dx.doi.org/10.4132/jptm.2015.04.09

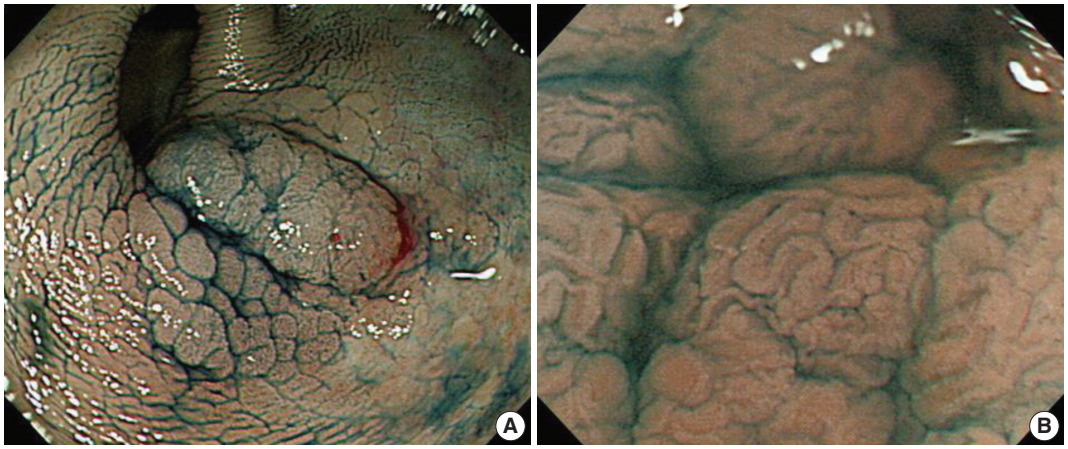

Fig. 1. Chromoendoscopy using indigocarmine (A) and combined with magnification technique (B) for colonic dysplasia in ulcerative colitis (Courtesy of Dr. Jeong-Sik Byeon at Asan Medical Center).

staining agents (e.g., congo red and phenol red) can be used in dye-based chromoendoscopy.[17,18] Several studies have shown the superiority of chromoendoscopy compared to conventional white light endoscopy. Dye-based chromoendoscopy has a moderate to high sensitivity for diagnosis, improved dysplasia detection, and prediction of mucosal change using magnification techniques (Fig. 1B). Two meta-analyses also demonstrated the superiority of targeted biopsy with dye-based chromoendoscopy in diagnosing and assessing mucosal ulcerations and dysplasia[19,20] while reducing the number of biopsies. Most recently, Soetikno *et al.*[20] included 665 patients from 6 studies and confirmed that the rate of detection of any dysplasia was approximately 9 times higher with dye-based chromoendoscopy with targeted biopsy than using white light endoscopy, with an 8.9 pooled odds ratio (95% CI, 3.4 to 23.0). When comparing the difference in the mean procedure time, dye-based chromoendoscopy is 10.9 minutes shorter than white light endoscopy, including the time spent on random biopsies.

Dye-less chromoendoscopy is a novel imaging technology that allows for a detailed examination of both the mucosal surface and the mucosal vascular pattern by pushing a button on the handle of the endoscope, thereby enabling high-contrast imaging of the mucosal surface in real time without the use of special equipment. These dye-less chromoendoscopy techniques are divided into two types. One is an optical filter system including narrow band imaging (NBI) from Olympus, Tokyo, Japan and Compound Band Imaging from Aohua, Shanghai, China, and the other is digital chromoendoscopy with a post-processing system including i-Scan from Pentax, Tokyo, Japan and FICE (Fuji intelligent color enhancement from Fujinon, Tokyo, Japan).[21,22]

Optical chromoendoscopy techniques are based on optical lenses integrated within the light source of the endoscope, usually in front of the excitation white light source, to narrow the bandwidth in the blue and green regions of the spectrum.[23,24] In contrast, digital chromoendoscopy uses digital postprocessing of endoscopic images made in real-time by the video processor.[25] Recent studies indicate that dye-less chromoendoscopy, including optical and digital ones, are useful and practical for the differentiation of adenoma versus hyperplastic colon polyps and have good histological correlations.[26-28]

Narrow band imaging

NBI is the most recognized among the virtual chromoendoscopy. This *in vivo* method uses optical filters in front of the light source to narrow the wavelength of the projected light to a 30 nm wide blue (415 nm) and green (540 nm) spectra, which enables visualization of micro-vessel morphological changes in superficial neoplastic lesions. NBI enhances the visibility of the small irregularities that accompany non-neoplastic inflammatory changes using the same logic as dye-based chromoendoscopy (Fig. 2).

However, the role of NBI in detecting dysplasia in IBD remains somewhat uncertain due to conflicting results in the literature. A paper by East *et al.*[29] was the first to describe the use of NBI to distinguish dysplastic from nondysplastic mucosa in patients with longstanding. Subsequent to this case report, several randomized controlled studies have been published. Dekker *et al.*[30] demonstrated that NBI does not improve the detection rate of neoplasia in UC compared with high-definition white light endoscopy with a randomized crossover study of 42 patients. Of 11 patients with neoplastic lesions, four were detected with both modalities, four with NBI alone, and three with standard

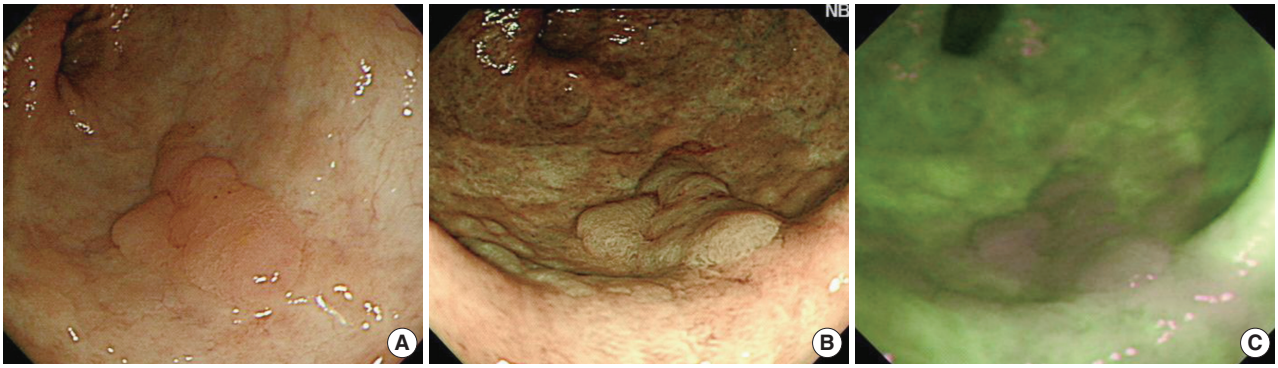

Fig. 2. Observation findings of colonic dysplasia using white light endoscopy (A), narrow band imaging technique (B), and autofluorescence imaging technique (C) in ulcerative colitis (Courtesy of Dr. Jeong-Sik Byeon at Asan Medical Center).

white light colonoscopy alone.

Two additional randomized trials comparing NBI to white light endoscopy also found no significant difference in the detection of neoplastic lesions. Random background biopsies were also ineffective in detecting dysplasia. According to Ignjatovic *et al.*,[31] dysplasia detection was 9% in each arm and the yield of dysplasia detection from random nontargeted biopsies was 0.04%. Van den Broek *et al.*[32] found 13 of 16 neoplastic lesions (81%) using high definition-NBI compared with 11 of 16 neoplastic lesions (69%) using high definition -white light endoscopy. A study using a new-generation NBI system compared with dye based chromoendoscopy for the early detection of colitis-associated dysplasia and cancer in patients with longstanding colonic IBD demonstrated that NBI is less time-consuming (26.87 ± 9.89 minutes vs 15.74 ± 5.62 minutes, $p < .01$), but has no advantages over conventional endoscopy for the detection of intraepithelial neoplasia.[33] However, NBI has some advantages over dye-based chromoendoscopy, as it does not require additional dye agents and is easier to use in practice. These findings have led to controversy regarding the real role of NBI in dysplasia detection in IBD patients.

i-Scan

Currently, two virtual chromoendoscopy techniques are available, including FICE and i-Scan is a new endoscopic system using post processing light filter technology based on software algorithms with real time image mapping. It enhances different elements of the mucosa by three different image processes such as surface enhancement, tone enhancement, and contrast enhancement. Activation between different modes is done by pushing a button on the handle of the endoscope.[34,35] To date, most randomized trials have not shown that NBI or FICE can improve the detection of colorectal neoplasia when comparing colonoscopy with and without filter enhancement.

A randomized controlled study was conducted on 78 IBD patients in Germany to identify whether i-Scan has the potential to enhance assessment of disease severity and extent in mild or inactive IBD patients. The average duration of the examination for high definition—white light endoscopy and i-Scan groups was 18 and 20.5 minutes, respectively, but these differences were not statistically significant. When comparing the endoscopic prediction of inflammatory extent and activity with the histological results, there was overall agreement of 48.71% and 53.85% in the high definition—white light endoscopy group and 92.31% and 89.74% in the i-Scan group ($p < .001$ and $p = .066$).[36]

Patients with intestinal food allergy present with lymphoid hyperplasia, slight mucosal edema, and blurred mucosal vascular pattern in the colon. Based on this, an observational study reported on the potential of i-Scan for prediction of mucosal changes with suspected food allergy. Positive and negative predictive values for i-Scan to predict food allergy were 92% and 80%, respectively. Moreover, i-Scan predicted food allergy with a sensitivity, specificity, and accuracy of 85%, 89%, and 86%, respectively.[37]

Confocal laser endomicroscopy

Observation and characterization of the colonic mucosal surface and abnormalities of blood vessel architecture are crucial in predicting histology, and this can be performed more efficiently with chromoendoscopy. However, histologic confirmation is needed to determine whether the presence of mucosal abnormalities is a result of IBD or not. This can be accomplished by confocal endomicroscopy *in vivo*, which may provide images similar to histologic findings in real time (Fig. 3). Endomicroscopy is regarded as optical biopsy that can achieve an image of

 http://dx.doi.org/10.4132/jptm.2015.04.09

the cellular structure of the mucosa with 1,500 fold magnification.[38] Currently, two endomicroscopy systems are available including an integrated endoscopy system (iCLE, Pentax) and a probe-based system (pCLE, Cellvizio, Mauna Kea Technologies, Paris, France). *In vivo* CLE uses an excitation wavelength of 488 nm with a single line laser; the laser power output is up to 1 mW at the tissue surface. Images are collected at a scan rate of 0.8 frames per second at a resolution of 1,024 × 1,024 pixels or 1.6 frames per second with 1,024 × 512 pixels.[39] It can capture the z axis which enables interrogation of the epithelium and lamina propria 0–250 mm below the surface layer.[40] The pCLE-system uses a fixed laser power and a fixed image plane depth. The purpose of the system is to observe mucosal microarchitecture with an increased field of view (4 × 2 mm) through postpocessing with Cellvio Viewer (Fig. 4A). It enables virtual staining of mucosal structures to further enhance tissue contrast. The probe requires an accessory channel of 2.8 mm and has a resolution of 1 μm with a field of view of 240 μm and a fixed image plane depth varying between 55–65 μm (Fig. 4B).

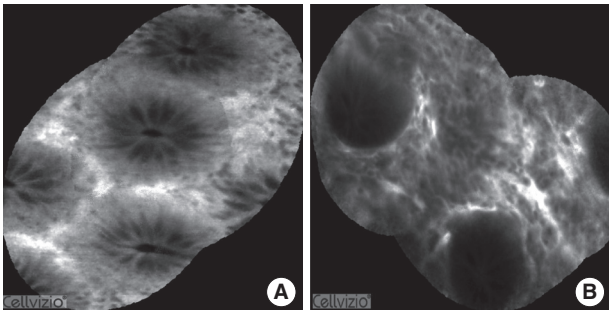

Fig. 3. Confocal laser endomicroscopic findings for normal mucosa (A) and mucosa in active ulcerative colitis (B). In ulcerative colitis, lamina propria widening, inflammatory infiltrates, goblet cell depletion, and crypt distortion are observed.

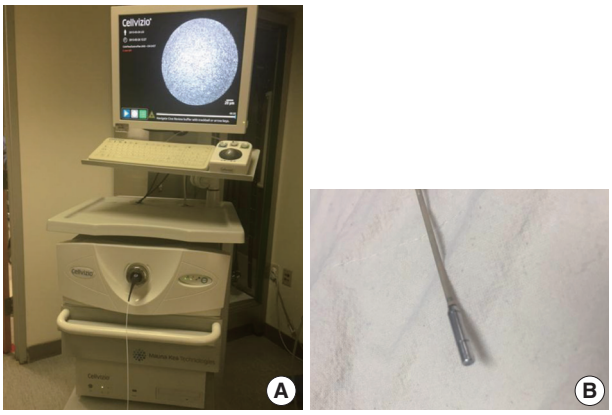

Fig. 4. Cellvizio system for probe based confocal laser endomicroscopy (A) and a probe (B).

Crypt architecture, microvascular alterations, fluorescein leakage, and cellular infiltrates within the lamina propria are important observational markers in CLE evaluation.[12,41-44] CLE can aid in demonstrating mucosal healing in terms of deep remission beyond the absence of mucosal ulceration.

Watanabe *et al.*[45] investigated the features of CLE in the inflamed and noninflamed rectal mucosa of 17 UC patients and compared these results to standard histology. In this study, the crypts of colonic mucosa in active UC were large, variously shaped and irregular in arrangement. Numerous inflammatory cells and capillaries were visible in the lamina propria with CLE. Li *et al.*[42] also assessed crypt architecture, fluorescein leakage, and microvascular alterations in 73 consecutive UC patients and showed a correlation with histological results ($p < .001$). On post-CLE objective assessment, subjective architectural classifications were supported by the number of crypts per image ($p < .001$), but not fluorescein leakage results by gray scale ($p = .194$). Most recently, CLE also proved a sensitive tool in predicting UC relapse. In this study, 17 of 20 patients (85%) with histologically confirmed normal or chronic inflammation were diagnosed as having nonactive inflammation by real-time CLE. Twenty two of 23 patients (96%) with histologically confirmed acute inflammation were diagnosed as having active inflammation by CLE. The results of CLE were highly consistent with those of conventional histology (kappa value = 0.812). Eleven percent of patients in the nonactive inflammation group relapsed, while 64% of patients in the active inflammation group relapsed. The relapse rate of patients with active inflammation was significantly higher than of those with nonactive inflammation ($p < .001$).

Neumann *et al.*[46] proposed the Crohn's Disease Endomicroscopic Activity Score for assessing CD activity *in vivo* from comparison data between CD patients and a normal control group with standard white-light endoscopy followed by CLE. Active CD patients showed a higher proportion of increased colonic crypt tortuosity, enlarged crypt lumens, microerosions, augmented vascularization, and increased cellular infiltrates within the lamina propria. In the case of quiescent CD patients, there was a significant increase in crypt and goblet cell number compared with controls.

Autofluorescence imaging

Autofluorescence imaging (AFI) is a technique using the natural principle that cells contain molecules that become fluorescent when excited by UV/Vis radiation of a certain wavelength. Among the endogenous fluorophores, collagen and elastin have

a relatively high quantum yield, so the extracellular matrix usually contributes to the autofluorescence emission more than cellular components. Autofluorescence imaging videoendoscopy produces real-time pseudo-color images based on tissue autofluorescence emitted by excitation of endogenous tissue fluorophores.

It is well known that cell and tissue state change resulting from modifications of the amount and distribution of endogenous fluorophores and the chemical-physical properties of their microenvironment during physiological and/or pathological processes. Therefore, AFI can be utilized in order to obtain information about the morphological and physiological state of cells and tissues (Fig. 2).

AFI has been used to highlight various lesions, such as neoplastic tissue, minimal changes in reflux esophagitis, the extent of chronic atrophic fundal gastritis, and Barrett's esophagus.[47-50] AFI improves detection rates of neoplasia in patients with IBD and decreases the number of random biopsies needed. In a randomized, comparative study with 50 UC patients, neoplasia miss-rates for AFI and white light endoscopy were 0% and 50%, respectively ($p = .036$).[51] AFI had 100% of sensitivity since all neoplasia was colored purple on AFI, while NBI had a 75% of sensitivity according to the Kudo classification.

AFI also has the ability to detect inflammatory lesions, including microscopic activity, in the colonic mucosa. Osada *et al.*[52] evaluated 572 images from 42 UC patients including white light endoscopy and AFI to validate the clinical relevance of AFI endoscopy for the assessment of the severity of inflammation. The green color component of AFI corresponded more closely with mucosal inflammation sites ($r = -0.62$, $p < .01$) than the red ($r = 0.52$, $p < .01$) or blue ($r = 0.56$, $p < .01$) color components. There were significant differences in green color components between limited (0.399 ± 0.042) and extensive (0.375 ± 0.044) ($p = .014$) polymorphonuclear cell infiltration within MES-0. It was observed that the green color component of AFI decreased as the severity of the mucosal inflammation increased.

Endocytoscopy

Endocytoscopy (Olympus, Tokyo, Japan) is a new technique, enabling observation of the gastrointestinal mucosa at the cellular level. Microscopic imaging for the gut mucosal layer can be observed at a magnification up to 1,400-fold with a contact light microscope.[53] It requires preparation of the mucosal layer with absorptive contrast agents like methylene blue or toluidine blue. Thus, endoscopists can distinguish architectural details such as epithelial structure, cellular features, and vascular patterns in terms of size, leakage, and tortuosity.[54-56]

Some studies suggest that endocytoscopy has a potential role in *in vivo* evaluation. A study in patients who have colorectal aberrant crypt foci demonstrated that endocystoscopy was able to detect tissue abnormalities in the normal mucosa surrounding CRC and to identify neoplasia in aberrant crypt foci with 91.4% sensitivity.[56] A pilot study with IBD patients showed that endocytoscopy could reliably distinguish single inflammatory cells with high sensitivities and specificities (neutrophilic [60% and 95%], basophilic [74.43% and 94.44%], eosinophilic granulocytes [75% and 90.48%], and lymphocytes [88.89% and 93.33%]). It also showed that the concordance between endocytoscopy and histopathology for grading intestinal disease activity in IBD was 100%.[54] This new imaging technique introduces possibilities for the development of *in vivo* research while allowing surface magnification at cellular and subcellular resolution, but little data is currently available on endocytoscopy.

CONCLUSION

Diagnostic techniques in the field of IBD including endoscopy, molecular pathology, genetics, epigenetics, metabolomics, and proteomics have emerged over the past few decades. An improvement in endoscopic techniques has enabled precise diagnosis and identification of dysplasia with advanced image processing software and optical filter technology. The two major advances provide better recognition of abnormalities enabling a refined classification and characterize the extent and depth of the inflammation or mucosal healing, facilitating targeted biopsy. Real-time microscopy during the ongoing endoscopy at a subcellular resolution is noninvasive and timesaving. These features provide high diagnostic accuracy for the detection of disease activity, location, severity, and complications and can provide valuable guidance for choosing medical and surgical treatments (Table 2).

Despite the promising data, the generalizability of the proce-

Table 2. Potential clinical use of image-enhanced endoscopy in inflammatory bowel disease

	Disease severity and extent	Detection of dysplasia
High definition endoscopy	+	++
Chromoendoscopy (dye-based)	+	+++
Narrow band imaging	++	± or +
i-Scan	+ or ++	++
Confocal laser endomicroscopy	++	++
Autofluorescence imaging	±	++
Endocytoscopy	++	± or +

http://dx.doi.org/10.4132/jptm.2015.04.09

dure should be confirmed with more well designed clinical investigations. Moreover, the utility of these techniques are dependent on the skill of the observers, so it is practically impossible to avoid "intra-observer variation" and "inter-observer variation."

The new endoscopic imaging modalities used in clinical practice still warrant further investigation. In addition, even if endoscopy in IBD patients is clear, final diagnosis of intraepithelial neoplasia and disease activity still remains on histopathology. It will be important to identify the challenges associated with implementing these advanced endoscopy techniques in clinical practice.

Conflicts of Interest

No potential conflict of interest relevant to this article was reported.

REFERENCES

1. Hommes DW, van Deventer SJ. Endoscopy in inflammatory bowel diseases. Gastroenterology 2004; 126: 1561-73.
2. Stange EF, Travis SP, Vermeire S, *et al.* European evidence based consensus on the diagnosis and management of Crohn's disease: definitions and diagnosis. Gut 2006; 55 Suppl 1: i1-15.
3. Rubin DC, Shaker A, Levin MS. Chronic intestinal inflammation: inflammatory bowel disease and colitis-associated colon cancer. Front Immunol 2012; 3: 107.
4. Eaden JA, Abrams KR, Mayberry JF. The risk of colorectal cancer in ulcerative colitis: a meta-analysis. Gut 2001; 48: 526-35.
5. Laukoetter MG, Mennigen R, Hannig CM, *et al.* Intestinal cancer risk in Crohn's disease: a meta-analysis. J Gastrointest Surg 2011; 15: 576-83.
6. Jess T, Simonsen J, Jørgensen KT, Pedersen BV, Nielsen NM, Frisch M. Decreasing risk of colorectal cancer in patients with inflammatory bowel disease over 30 years. Gastroenterology 2012; 143: 375-81.e1.
7. Cheon JH, Kim WH. Recent advances of endoscopy in inflammatory bowel diseases. Gut Liver 2007; 1: 118-25.
8. Rutter MD, Saunders BP, Wilkinson KH, *et al.* Thirty-year analysis of a colonoscopic surveillance program for neoplasia in ulcerative colitis. Gastroenterology 2006; 130: 1030-8.
9. Panaccione R. The approach to dysplasia surveillance in inflammatory bowel disease. Can J Gastroenterol 2006; 20: 251-3.
10. Biancone L, Michetti P, Travis S, *et al.* European evidence-based consensus on the management of ulcerative colitis: special situations. J Crohns Colitis 2008; 2: 63-92.
11. Eaden JA, Mayberry JF; British Society for Gastroenterology; Association of Coloproctology for Great Britain and Ireland. Guidelines for screening and surveillance of asymptomatic colorectal cancer in patients with inflammatory bowel disease. Gut 2002; 51 Suppl 5: V10-2.
12. Kiesslich R, Goetz M, Lammersdorf K, *et al.* Chromoscopy-guided endomicroscopy increases the diagnostic yield of intraepithelial neoplasia in ulcerative colitis. Gastroenterology 2007; 132: 874-82.
13. Hlavaty T, Huorka M, Koller T, *et al.* Colorectal cancer screening in patients with ulcerative and Crohn's colitis with use of colonoscopy, chromoendoscopy and confocal endomicroscopy. Eur J Gastroenterol Hepatol 2011; 23: 680-9.
14. ASGE Technology Committee. High-definition and high-magnification endoscopes. Gastrointest Endosc 2014; 80: 919-27.
15. Udagawa T, Amano M, Okada F. Development of magnifying video endoscopes with high resolution. Dig Endosc 2001; 13: 163-9.
16. Subramanian V, Ramappa V, Telakis E, *et al.* Comparison of high definition with standard white light endoscopy for detection of dysplastic lesions during surveillance colonoscopy in patients with colonic inflammatory bowel disease. Inflamm Bowel Dis 2013; 19: 350-5.
17. Kiesslich R, Neurath MF. Chromoendoscopy in inflammatory bowel disease. Gastroenterol Clin North Am 2012; 41: 291-302.
18. Canto MI. Staining in gastrointestinal endoscopy: the basics. Endoscopy 1999; 31: 479-86.
19. Subramanian V, Mannath J, Ragunath K, Hawkey CJ. Meta-analysis: the diagnostic yield of chromoendoscopy for detecting dysplasia in patients with colonic inflammatory bowel disease. Aliment Pharmacol Ther 2011; 33: 304-12.
20. Soetikno R, Subramanian V, Kaltenbach T, *et al.* The detection of nonpolypoid (flat and depressed) colorectal neoplasms in patients with inflammatory bowel disease. Gastroenterology 2013; 144: 1349-52.e1-6.
21. Goetz M, Kiesslich R. Advanced imaging of the gastrointestinal tract: research vs. clinical tools? Curr Opin Gastroenterol 2009; 25: 412-21.
22. Amateau SK, Canto MI. Enhanced mucosal imaging. Curr Opin Gastroenterol 2010; 26: 445-52.
23. Kuznetsov K, Lambert R, Rey JF. Narrow-band imaging: potential and limitations. Endoscopy 2006; 38: 76-81.
24. Subramanian V, Bisschops R. Image-enhanced endoscopy is critical in the surveillance of patients with colonic IBD. Gastrointest Endosc Clin N Am 2014; 24: 393-403.
25. Tontini GE, Vecchi M, Neurath MF, Neumann H. Review article: newer optical and digital chromoendoscopy techniques vs. dye-based chromoendoscopy for diagnosis and surveillance in inflammatory bowel disease. Aliment Pharmacol Ther 2013; 38: 1198-208.
26. van den Broek FJ, Reitsma JB, Curvers WL, Fockens P, Dekker E. Systematic review of narrow-band imaging for the detection and

differentiation of neoplastic and nonneoplastic lesions in the colon (with videos). Gastrointest Endosc 2009; 69: 124-35.
27. Pohl J, Nguyen-Tat M, Pech O, May A, Rabenstein T, Ell C. Computed virtual chromoendoscopy for classification of small colorectal lesions: a prospective comparative study. Am J Gastroenterol 2008; 103: 562-9.
28. Teixeira CR, Torresini RS, Canali C, *et al.* Endoscopic classification of the capillary-vessel pattern of colorectal lesions by spectral estimation technology and magnifying zoom imaging. Gastrointest Endosc 2009; 69(3 Pt 2): 750-6.
29. East JE, Suzuki N, von Herbay A, Saunders BP. Narrow band imaging with magnification for dysplasia detection and pit pattern assessment in ulcerative colitis surveillance: a case with multiple dysplasia associated lesions or masses. Gut 2006; 55: 1432-5.
30. Dekker E, van den Broek FJ, Reitsma JB, *et al.* Narrow-band imaging compared with conventional colonoscopy for the detection of dysplasia in patients with longstanding ulcerative colitis. Endoscopy 2007; 39: 216-21.
31. Ignjatovic A, East JE, Subramanian V, *et al.* Narrow band imaging for detection of dysplasia in colitis: a randomized controlled trial. Am J Gastroenterol 2012; 107: 885-90.
32. van den Broek FJ, Fockens P, van Eeden S, *et al.* Narrow-band imaging versus high-definition endoscopy for the diagnosis of neoplasia in ulcerative colitis. Endoscopy 2011; 43: 108-15.
33. Pellisé M, López-Cerón M, Rodríguez de Miguel C, *et al.* Narrow-band imaging as an alternative to chromoendoscopy for the detection of dysplasia in long-standing inflammatory bowel disease: a prospective, randomized, crossover study. Gastrointest Endosc 2011; 74: 840-8.
34. Hoffman A, Sar F, Goetz M, *et al.* High definition colonoscopy combined with i-Scan is superior in the detection of colorectal neoplasias compared with standard video colonoscopy: a prospective randomized controlled trial. Endoscopy 2010; 42: 827-33.
35. Kodashima S, Fujishiro M. Novel image-enhanced endoscopy with i-scan technology. World J Gastroenterol 2010; 16: 1043-9.
36. Neumann H, Vieth M, Günther C, *et al.* Virtual chromoendoscopy for prediction of severity and disease extent in patients with inflammatory bowel disease: a randomized controlled study. Inflamm Bowel Dis 2013; 19: 1935-42.
37. Neumann H, Vieth M, Tontini GE, *et al.* 33 High-definition endoscopy with virtual chromoendoscopy for prediction of food allergy in real-time: a prospective, randomized study with cross-over design. Gastroenterology 2014; 146(5 Suppl 1): S-9-S-10.
38. Liu JT, Loewke NO, Mandella MJ, Levenson RM, Crawford JM, Contag CH. Point-of-care pathology with miniature microscopes. Anal Cell Pathol (Amst) 2011; 34: 81-98.
39. Dunbar K, Canto M. Confocal endomicroscopy. Curr Opin Gastroenterol 2008; 24: 631-7.
40. Iacucci M, Panaccione R, Ghosh S. Advances in novel diagnostic endoscopic imaging techniques in inflammatory bowel disease. Inflamm Bowel Dis 2013; 19: 873-80.
41. Watanabe O, Ando T, Maeda O, *et al.* Confocal endomicroscopy in patients with ulcerative colitis. J Gastroenterol Hepatol 2008; 23 Suppl 2: S286-90.
42. Li CQ, Xie XJ, Yu T, *et al.* Classification of inflammation activity in ulcerative colitis by confocal laser endomicroscopy. Am J Gastroenterol 2010; 105: 1391-6.
43. Kiesslich R, Burg J, Vieth M, *et al.* Confocal laser endoscopy for diagnosing intraepithelial neoplasias and colorectal cancer *in vivo*. Gastroenterology 2004; 127: 706-13.
44. Li CQ, Liu J, Ji R, Li Z, Xie XJ, Li YQ. Use of confocal laser endomicroscopy to predict relapse of ulcerative colitis. BMC Gastroenterol 2014; 14: 45.
45. Watanabe C, Sumioka M, Hiramoto T, *et al.* Magnifying colonoscopy used to predict disease relapse in patients with quiescent ulcerative colitis. Inflamm Bowel Dis 2009; 15: 1663-9.
46. Neumann H, Vieth M, Atreya R, *et al.* Assessment of Crohn's disease activity by confocal laser endomicroscopy. Inflamm Bowel Dis 2012; 18: 2261-9.
47. Asaoka D, Nagahara A, Kurosawa A, *et al.* Utility of autofluorescence imaging videoendoscopy system for the detection of minimal changes associated with reflux esophagitis. Endoscopy 2008; 40 Suppl 2: E172-3.
48. Inoue T, Uedo N, Ishihara R, *et al.* Autofluorescence imaging videoendoscopy in the diagnosis of chronic atrophic fundal gastritis. J Gastroenterol 2010; 45: 45-51.
49. Asaoka D, Nagahara A, Oguro M, *et al.* Utility of autofluorescence imaging videoendoscopy in screening for Barrett's esophagus. Endoscopy 2009; 41 Suppl 2: E113.
50. Nakaniwa N, Namihisa A, Ogihara T, *et al.* Newly developed autofluorescence imaging videoscope system for the detection of colonic neoplasms. Dig Endosc 2005; 17: 235-40.
51. van den Broek FJ, Fockens P, van Eeden S, *et al.* Endoscopic trimodal imaging for surveillance in ulcerative colitis: randomised comparison of high-resolution endoscopy and autofluorescence imaging for neoplasia detection; and evaluation of narrow-band imaging for classification of lesions. Gut 2008; 57: 1083-9.
52. Osada T, Arakawa A, Sakamoto N, *et al.* Autofluorescence imaging endoscopy for identification and assessment of inflammatory ulcerative colitis. World J Gastroenterol 2011; 17: 5110-6.
53. Neumann H, Vieth M, Neurath MF. Image of the month. Endocytoscopy-based detection of focal high-grade intraepithelial neopla-

sia in colonic polyps. Clin Gastroenterol Hepatol 2011; 9: e13.
54. Neumann H, Vieth M, Neurath MF, Atreya R. Endocytoscopy allows accurate *in vivo* differentiation of mucosal inflammatory cells in IBD: a pilot study. Inflamm Bowel Dis 2013; 19: 356-62.
55. Pohl H, Rosch T, Tanczos BT, Rudolph B, Schlüns K, Baumgart DC. Endocytoscopy for the detection of microstructural features in adult patients with celiac sprue: a prospective, blinded endocytoscopy-conventional histology correlation study. Gastrointest Endosc 2009; 70: 933-41.
56. Cipolletta L, Bianco MA, Rotondano G, *et al.* Endocytoscopy can identify dysplasia in aberrant crypt foci of the colorectum: a prospective *in vivo* study. Endoscopy 2009; 41: 129-32.

Journal of Pathology and Translational Medicine 2015; 49: 218-229
http://dx.doi.org/10.4132/jptm.2015.04.15

■ REVIEW ■

Pathology-MRI Correlation of Hepatocarcinogenesis: Recent Update

Jimi Huh[1] · Kyung Won Kim[1,2]
Jihun Kim[2,3] · Eunsil Yu[2,3]

[1]Department of Radiology, [2]Asan Liver Center,
[3]Department of Pathology, Asan Medical Center,
University of Ulsan College of Medicine,
Seoul, Korea

Received: April 7, 2015
Accepted: April 14, 2015

Corresponding Author
Kyung Won Kim, M.D., Ph.D.
Department of Radiology, Asan Medical Center,
University of Ulsan College of Medicine,
88 Olympic-ro 43-gil, Songpa-gu, Seoul 138-736,
Korea
Tel: +82-2-3010-4377
Fax: +82-2-3010-8724
E-mail: medimash@gmail.com

Understanding the important alterations during hepatocarcinogenesis as well as the characteristic magnetic resonance imaging (MRI) and histopathological features will be helpful for managing patients with chronic liver disease and hepatocellular carcinoma. Recent advances in MRI techniques, such as fat/iron quantification, diffusion-weighted images, and gadoxetic acid-enhanced MRI, have greatly enhanced our understanding of hepatocarcinogenesis.

Key Words: Hepatocarcinogenesis; Magnetic resonance image; Carcinoma, hepatocellular; Pathology

Hepatocellular carcinoma (HCC) is the sixth most common cancer worldwide and the third most common cause of death from cancer.[1] Asia is an endemic area of HCC. It is estimated that approximately 75%–80% of the HCC cases worldwide develop in Asia.[2] The primary etiological factor in Asia is the hepatitis B virus; however, the proportion of hepatitis C virus–related HCC has been increasing.[3] In chronic hepatitis B or C, multistep hepatocarcinogenesis, in which dysplastic nodules progress to early HCC and eventually advanced HCC, is widely accepted as the main mechanism of HCC development.[4]

Knowledge of the mechanism of hepatocarcinogenesis is important, as it may contribute to improved detection of HCC at an early stage and more successful therapeutic outcomes. In fact, the 5-year survival rate for patients with HCC has improved over the past several decades, and the early detection of HCC is one of the most important contributing factors.[5] In particular, the nationwide surveillance for HCC among high-risk individuals has allowed small HCCs less than 2 cm in diameter to be easily detected.[4] Furthermore, the rapid development of noninvasive imaging technology, including the rapidly developing, high-quality magnetic resonance (MR) techniques using new, cell-specific contrast agents, may allow further improvement of the detection and characterization of small nodules in cirrhotic livers.[6] As a result, we are currently able to diagnose more early-stage HCCs. Pathologists and radiologists should be aware of the variable imaging features of these early-stage HCCs, as they frequently show different characteristics than advanced HCC. In this study, we review the important changes in magnetic resonance imaging (MRI) and histopathologic features during multistep hepatocarcinogenesis as well as the recent developments in MRI technology for detecting and characterizing hepatocellular nodules.

MULTISTEP HEPATOCARCINOGENESIS: HISTOLOGIC CHANGE

Multistep hepatocarcinogenesis is characterized by progressive dedifferentiation of phenotypically abnormal nodular lesions in the liver and the emergence of successively more advanced precancerous, early cancerous, and overtly cancerous lesions (Fig. 1).[7,8] Chronic inflammation causes repeated injury to liver cells and regeneration of injured tissue, both of which promote accumulation of genetic and epigenetic alterations.[9-12] These alterations begin from the early preneoplastic phase and progress par-

pISSN 2383-7837
eISSN 2383-7845

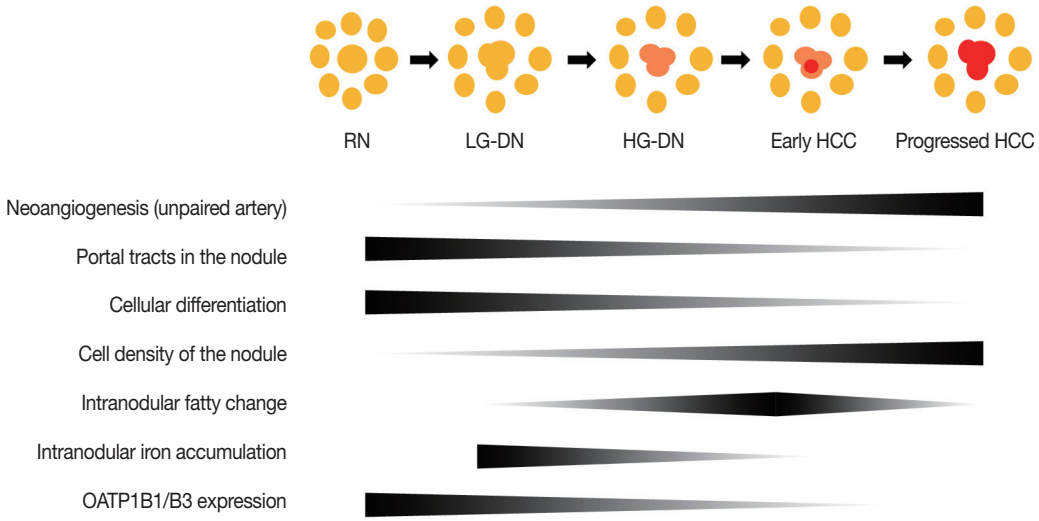

Fig. 1. Schematic view of multistep hepatocarcinogenesis. Unpaired arterial supply replaces portal supply progressively from regenerative nodules to progressed hepatocellular carcinoma (yellow, nodules with portal supply; red, nodules with unpaired arterial supply). Degrees of various pathologic components are depicted as gradient bars. DN, dysplastic nodule; HCC, hepatocellular carcinoma; HG, high grade; LG, low grade; RN, regenerative nodule.

allel to the evolution of hepatic fibrosis or cirrhosis.[13,14]

This linear, repetitive, and successive process of the expansion and development of less differentiated, aberrant clonal populations of hepatocytes causes their evolution over time.[15] These dedifferentiated clonal populations eventually completely replace those of the more differentiated environment. Repetitive clonal growth and expansion ultimately generates nodules of the malignant phenotype. The dedifferentiated evolution process occurs in serial order as a biologic continuum *in vivo*; however, these processes are divided into discrete steps for clinical use.[16]

In 1995, after the stepwise development of HCC from regenerating nodules of liver cirrhosis was proposed, the International Working Party (IWP) of the World Congress of Gastroenterology defined regenerative nodules (RNs), low-grade dysplastic nodules (DNs), high-grade DNs, and HCC as steps from regeneration to cancer.[17,18] In addition, the IWP defined small HCCs as tumors less than 2 cm in diameter. However, there had been debate regarding the definition of small HCC, as these tumors can be divided into early HCCs, i.e., an early stage of hepatocarcinogenesis, and progressed HCCs, i.e., advanced HCC less than 2 cm in diameter. In addition, the accurate pathological definition of early HCCs differentiated from DNs was not established until recently. Finally, in 2009 the International Consensus Group for Hepatocellular Neoplasia (ICGHN) reached a consensus regarding the pathological criteria of early HCCs, as discussed below.[19] These international efforts have contributed greatly to the standardization of the nomenclature regarding nodules during hepatocarcinogenesis.

Regenerative nodules

A RN, also known as a cirrhotic nodule, is a well-defined nodular region surrounded by fibrotic/scar tissue, which has emerged from the regenerative process of the injured liver tissue. In RNs, the cells are histologically normal and lack clonal features.[18] A RN is considered a benign hepatocellular nodule.

Dysplastic nodules

DNs are small nodules which are in the precancerous stage between benign RNs and malignant HCC. DNs usually differ from the surrounding liver parenchyma in color, texture, and cellular change.[18] DNs are subdivided into low-grade DN and high-grade DN.

Low-grade DNs show features suggestive of a clonal cell population without significant architectural or cellular atypia (Fig. 2A). Occasionally, low-grade DNs demonstrate large cell change, although they do not show small cell change. Low-grade DNs can show a mild increase in cell density with a monotonous pattern. A nodule-in-nodule pattern is not present in low-grade DNs.[18,20]

In contrast, high-grade DNs show cytological and architectural atypia, although those changes are insufficient for a diagnosis of malignancy.[18] Small cell change is the most frequently seen cytological atypia. The architectural atypia observed in high-grade DNs includes the thick cell plates up to three cells thick and/or pseudoglandular structures (Fig. 2B). The cell den-

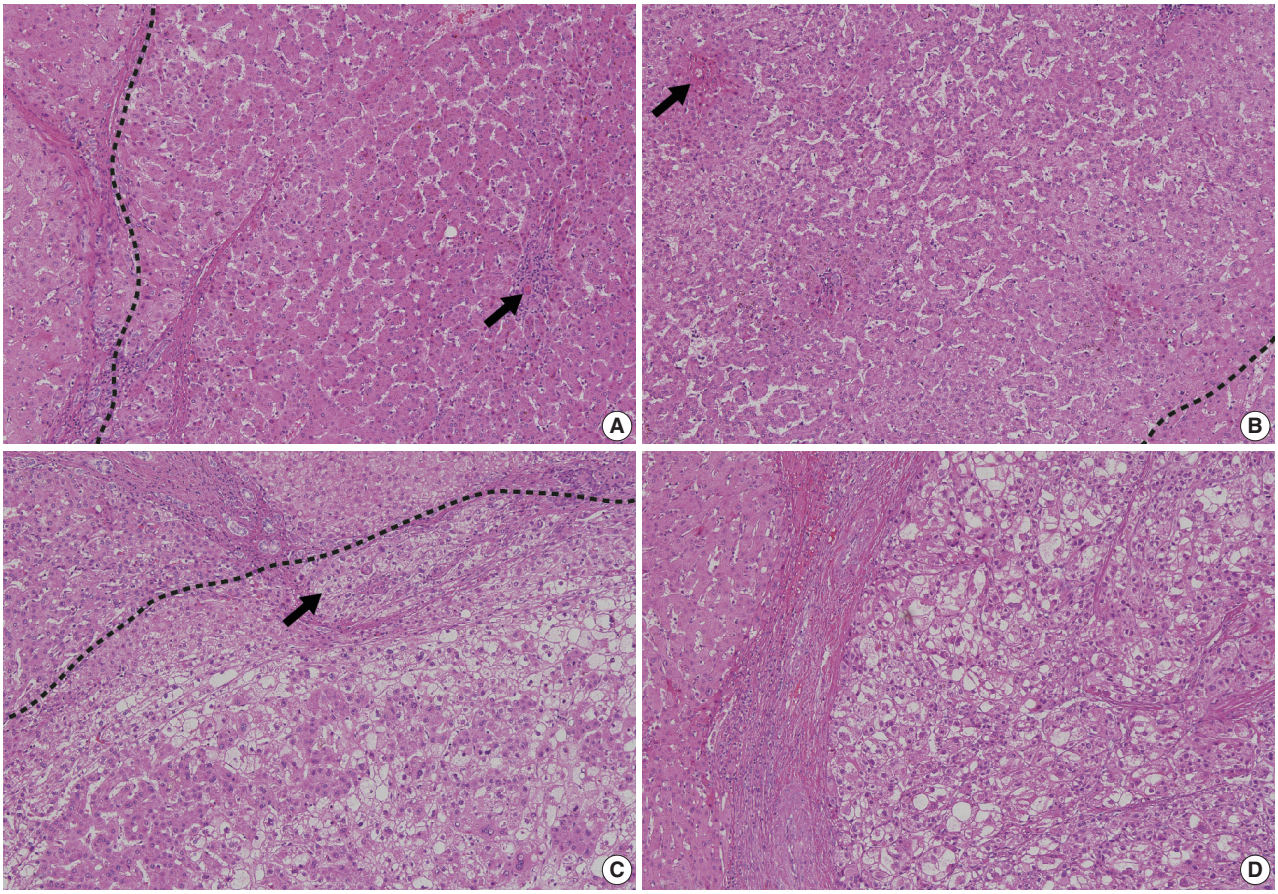

Fig. 2. Representative pathologic images of multistep hepatocarcinogenesis. (A) Low-grade dysplastic nodule (right of the dashed line) shows increased cellularity, and residual portal tracts (arrow) are easily identifiable within the nodule. (B) High-grade dysplastic nodule (left of the dashed line) shows further increased cellularity and frequent unpaired arteries (arrow). (C) Early hepatocellular carcinoma (below the dashed line) is poorly demarcated but shows unequivocal cytological atypia and stromal invasion (arrow). (D) Advanced hepatocellular carcinoma is well demarcated by a thick capsule and shows overt features of malignancy.

sity of these lesions is usually 1.3–2 times greater than that of the adjacent cirrhotic parenchyma.[19]

Early HCC

In 2009, the ICGHN made a consensus for the definition of early HCC.[19] Early HCCs are considered "*in situ* carcinoma" showing well-differentiated proliferation.[18,20] Early HCCs are referred to as 'small HCC of the vaguely nodular type.' The most important histologic feature that distinguishes early HCCs from high-grade DNs is stromal invasion, defined as the presence of tumor cells invading the portal tracts or fibrous septa (Fig. 2C). Early HCCs also show various combinations of the following histologic features: "(1) increased cell density more than two times that of the surrounding liver parenchyma and with an increased nuclear/cytoplasm ratio and irregular, thin trabecular pattern; (2) varying numbers of portal tracts within the nodule (intratumoral portal tracts); (3) a pseudoglandular pattern; (4) diffuse fatty change; and (5) various numbers of unpaired arteries."[19]

There may be confusion regarding the terminology of early HCC and small HCC. By the definition of the IWP consensus in 1995, small HCC is a tumor less than 2 cm, whereas early HCC refers to well-differentiated HCC of the vaguely nodular type during the hepatocarcinogenesis process. The question has remained for small HCCs with moderate or poor differentiation. After much debate, such tumors are now termed "small progressed HCC" or "small HCC of the distinctively nodular type." In Table 1, the terminology and histologic characteristics of these small, hepatocellular lesions are summarized.

Progressed HCC

Progressed HCCs are overtly malignant hepatocellular lesions. Small lesions with a maximum diameter less than 2 cm usually have distinctly nodular macroscopic features,[19] while

 http://dx.doi.org/10.4132/jptm.2015.04.15

Table 1. Terminology and histologic characteristics of these small (less than 2 cm) hepatocellular lesions

Terminology	Feature	Histologic characteristic
Regenerative nodules	Gross	Well-defined rounded regions of the cirrhotic parenchyma surrounded by scar tissue
	Microscopic	Phenotypically normal cells
Dysplastic nodules	Gross	Distinctly nodular lesions which differ from adjacent cirrhotic parenchyma with regard to size, color, texture, and degree of bulging at the cut surface
	Microscopic	Divided into low-grade DNs and high-grade DNs – Low-grade DN: a clonal cell population without significant architectural atypia and with a mild increase in cell density – High-grade DN: a clonal cell population with cytological and architectural atypia although not sufficient for a diagnosis of malignancy
Early HCCs (=small HCCs of the vaguely nodular type)	Gross	Vaguely nodular lesions with indistinct margins
	Microscopic	Well-differentiated histology of HCC with increased cell density and an irregular, thin-trabecular pattern; the stromal invasion is the most helpful feature to differentiate early HCC from high-grade DN
Progressed HCCs (=small HCCs of the distinctly nodular type)	Gross	Distinctly nodular lesions
	Microscopic	Well (G1) to moderately (G2) differentiated histology of HCC

DN, dysplastic nodule; HCC, hepatocellular carcinoma.

large lesions greater than 2 cm in diameter, which are termed "large HCCs," have variable macroscopic features. Although three common macroscopic patterns of large HCCs have been proposed,[21] six macroscopic patterns, which were proposed by the Korean Liver Cancer Study Group, are more widely accepted in Korea.[22] Briefly, expanding nodular pattern is defined by one single, dominant mass and is the most common type. In these tumors, mosaic architecture is frequently observed, characterized by the multiple sub-nodules separated by fibrous septations and foci of hemorrhage or necrosis.[23] Nodular and perinodular extension type and infiltrative pattern show a dominant mass with infiltration into adjacent hepatic parenchyma along < 50% of tumor border in the former and ≥50% in the latter. Those tumors are usually associated with poorly differentiated cancer cells that spread into the surrounding sinusoids and cell plates.[17,24] Cirrhotomimetic pattern represents widespread infiltration by innumerable small nodules that frequently replace the whole liver.[21] In addition, multinodular confluent type and pedunculated type have also been described.[22] These progressed HCCs with both small and large lesions frequently show macroscopic vascular invasion with involvement of portal veins and less frequently hepatic veins. Sometimes, bile duct invasion may be seen macroscopically.

On histology, the main hallmark of HCC is that the malignant cells resemble the normal liver, both in architecture and cytology. Progressed HCCs can show different degrees of hepatocellular differentiation ranging from well-differentiated to poorly differentiated. Based on the degree of nuclear anaplasia, the Edmondson and Steiner system was proposed and is widely used to divide HCC into four grades from I to IV.[17,25] The common histological patterns include (1) trabecular pattern, where tumor cells with hepatocellular differentiation are arranged in plates of various thickness, separated by sinusoid vascular spaces (Fig. 2D); (2) pseudoglandular pattern, where gland-like dilatation of the canaliculi are present between tumor cells forming the lumen; (3) compact pattern, which is composed of thick trabeculae compressed into a compact mass; (4) scirrhous pattern, where desmoplastic stroma divides tumor cell masses into smaller nests; and (5) fibrolamellar pattern, which shows characteristic lamellar collagen bundles running between large glassy tumor cells.

RECENT ADVANCES IN MAGNETIC RESONANCE IMAGING TECHNIQUES

Recently, the diagnosis of hepatocellular carcinoma has become primarily based on imaging.[26] In clinical practice, computed tomography (CT) is the most widely used imaging modality to diagnose HCC. With the dramatic technical advances in MRI, it is currently more useful than other imaging modalities for diagnosing HCC because it provides better soft-tissue contrast and information regarding cellularity, tissue components, and hemodynamic changes of the hepatocellular nodules. In the recent past, the spatial resolution and scan speed were generally better on CT than on MRI;[27,28] however, recently developed MRI units have fast scanning with high spatial resolution, comparable to CT scanning. Therefore, the use of MRI for the diagnosis of HCC has greatly increased.

Nonradiologist physicians may not be familiar with MRI sequences and the information that can be obtained from those sequences. Indeed, there are many sequences of liver MRI which may cause confusion. In addition, the interpretation of MRI largely depends on which contrast agent is used. We summarize

the commonly used sequences in Table 2 and illustrate the representative images of such sequences in Fig. 3.

T2-weighted images

T2-weighted imaging (T2-WI) highlights the differences in the T2 relaxation time of tissues. Sequences for T2-WI are the basic components of MRI, and are quite helpful for the differential diagnosis of liver tumors. For example, hepatic cysts and hemangiomas show very high T2 hyperintensity, while HCCs show intermediately high T2 hyperintensity (Fig. 3A).[29]

For routine liver MRI, two kinds of T2-WI sequences are used: sequences moderately weighting T2, including fast spin-

Table 2. Commonly used MRI sequences for liver imaging

MRI sequences	Information
T2-weighted images	Helpful for differential diagnosis Hepatic cysts and hemangiomas show very high T2 hyperintensity, while HCCs show intermediately high T2 hyperintensity
T1-weighted dual gradient-echo images (in-phase and opposed-phase)	Helpful for detecting the intralesional fat component
Multiphasic dynamic imaging (arterial phase, portal-venous phase, and three-minute equilibrium phase)	Evaluate the hemodynamic pattern of hepatic tumors HCCs typically show arterial enhancement and delayed washout
Hepatobiliary phase imaging (i.e., 20-minute delayed image)	When gadoxetic acid is used as a contrast agent, the hepatobiliary phase is used to improve the detection and characterization of hepatocellular nodules
Diffusion-weighted imaging	Helpful for the detection and characterization of hepatocellular nodules

MRI, magnetic resonance imaging; HCC, hepatocellular carcinoma.

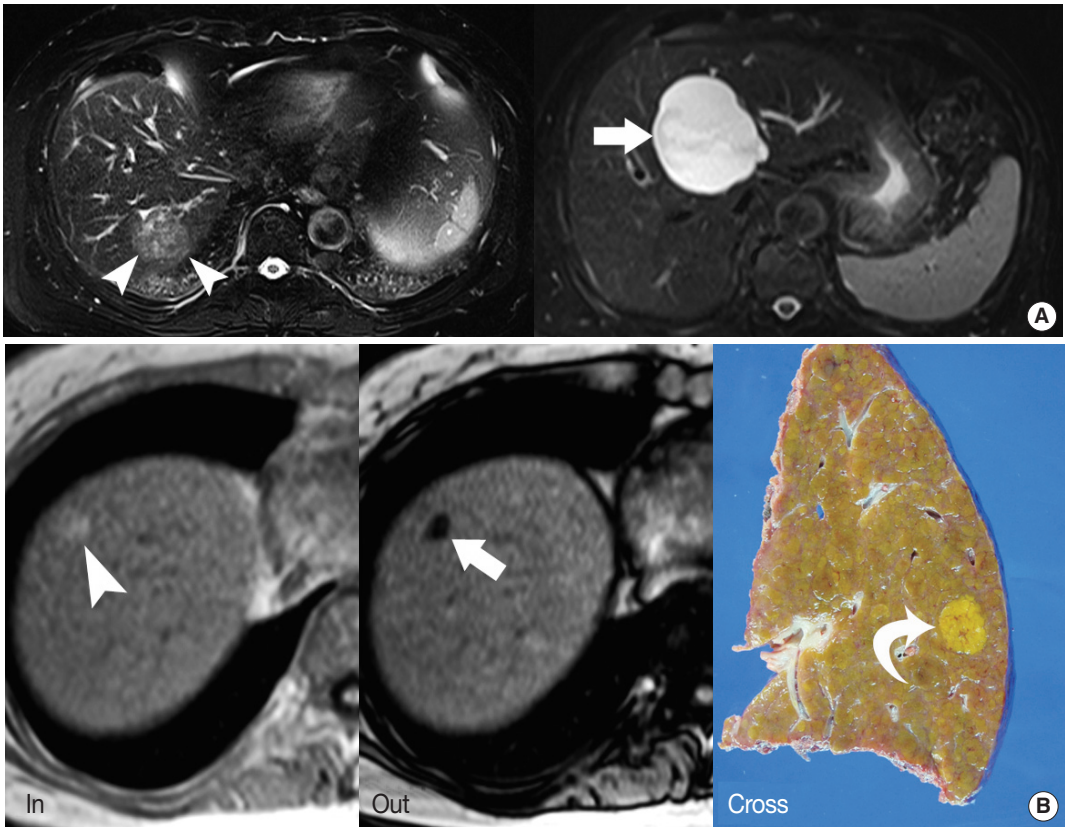

Fig. 3. Routine magnetic resonance imaging sequences. (A) T2-weighted imaging is helpful for the differential diagnosis of liver tumors. Hepatocellular carcinoma (HCC) usually shows intermediate high-signal intensity (arrowheads on the left), whereas hepatic cysts show bright high-signal intensity (arrow on the right). (B) In-phase and opposed-phase images provide information regarding the fat or iron content of hepatocellular nodules. The fat component of a nodule is seen as high-signal intensity on in-phase imaging (arrowhead on the left) and as low-signal intensity on opposed-phase imaging (arrow on the middle). On histology of the resected specimen, the nodule is confirmed as a fat-containing HCC.

(Continued to the next page)

http://dx.doi.org/10.4132/jptm.2015.04.15

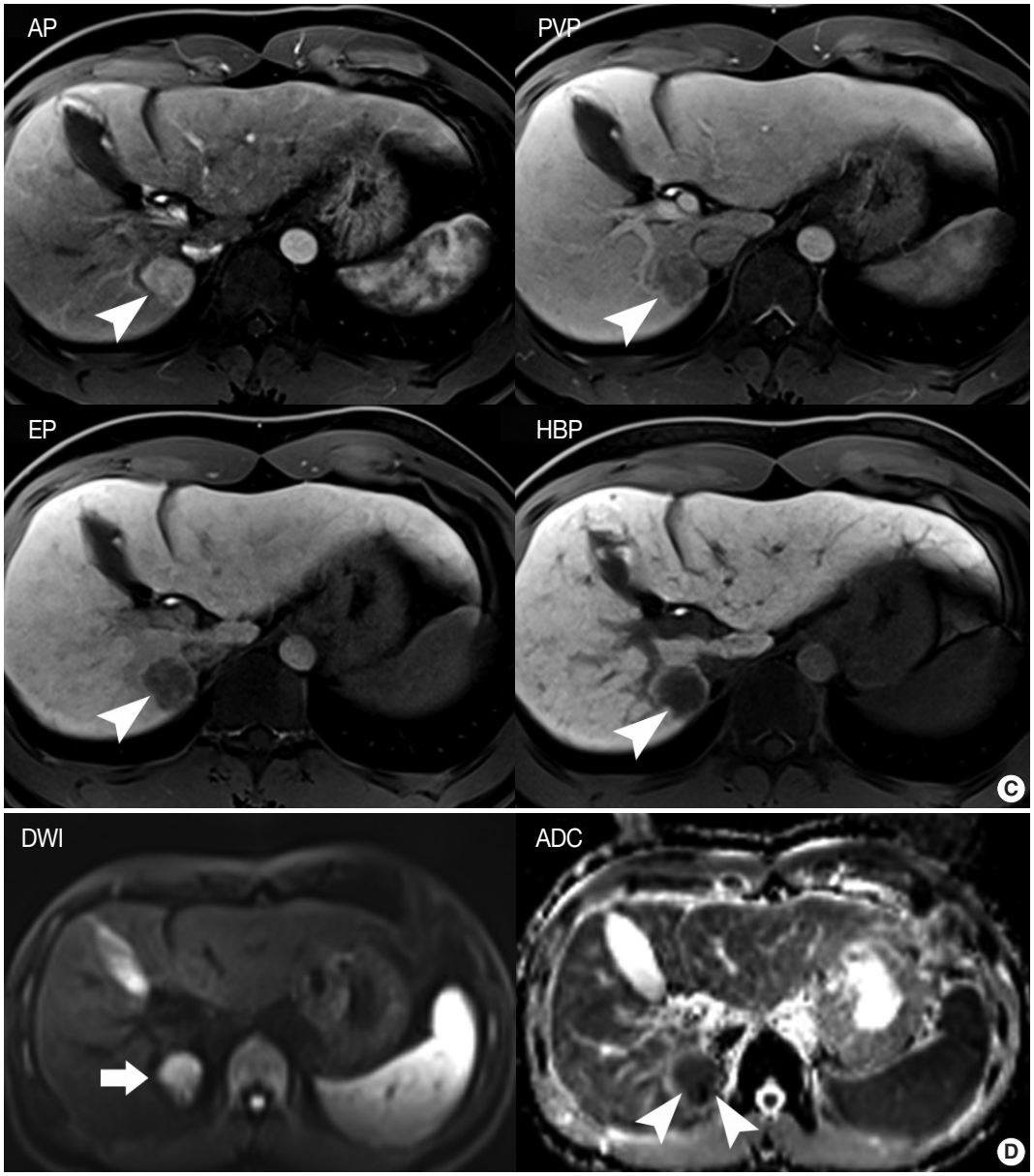

Fig. 3. *(Continued)* (C) Multiphasic dynamic images and hepatobiliary-phase images. After contrast injection, T1-weighted images are obtained in the arterial phase (AP), portal-venous phase (PVP), three-minute, delayed equilibrium phase (EP), and 20-minute, delayed hepatobiliary phase (HBP) to provide hemodynamic information regarding liver tumors. An HCC (arrowheads) shows typical hemodynamic features, including enhancement on AP, and washout on PVP and EP. On HBP, the HCC is seen as a hypodense mass. (D) Diffusion-weighted imaging (DWI) and the apparent diffusion coefficient (ADC) map are helpful for evaluating the cellularity of a liver tumor. HCC mostly shows high signal intensity on DWI (arrow on the left) and low signal on the ADC map (arrowheads on the right).

echo or turbo spin-echo, and sequences exaggerating T2 of tissues, including single-shot fast spin-echo or half-Fourier acquisition single-shot turbo spin-echo.[29]

T1-weighted, dual gradient-echo sequence (in-phase and oppposed-phase)

A T1-weighted, dual gradient-echo sequence is composed of an in-phase image and an opposed-phase image. These images are routine components of the liver MRI protocol, as they can evaluate the fat content of tissues.[30] They are primarily used to identify diffuse or focal hepatic steatosis or to detect the fatty component of liver tumors, such as fat-containing, dysplatic nodules or HCC. When comparing the signal intensity (SI) between in-phase and opposed-phase images, the fatty component

of tissue shows a signal drop in the opposed-phase (Fig. 3B).

This sequence is also helpful for detecting the iron component of tissues using the dual-echo approach. In contrast to the fatty component, the iron component shows a signal drop on in-phase images compared to opposed-phase images. Therefore, the pathological conditions, such as hemochromatosis or hemosiderosis, can be identified.[7] It is also helpful to detect iron-containing liver tumors, such as siderotic nodules or iron-containing hepatocellular lesions.

Multiphasic dynamic imaging

In liver MRI, contrast agents have crucial roles in the detection and characterization of HCC, based on evaluation of the hemodynamic pattern of liver tumors and liver parenchyma. Multiphasic dynamic imaging consists of repeated acquisition of T1-weighted images (T1-WIs) after contrast agent injection and is composed of the arterial phase, portal-venous phase, and three minutes of the equilibrium phase (Fig. 3C). Enhancement in the arterial phase and washout in the portal or equilibrium phase is regarded as a characteristic feature of HCC on both dynamic CT and dynamic MRI.[31]

Hepatobiliary phase images

The hepatobiliary phase refers to a 20-minute delayed phase following injection of gadoxetic acid (Fig. 3C). Therefore, the hepatobiliary phase is only performed when gadoxetic acid is used as the contrast agent. Gadoxetic acid is a dual-function agent allowing both dynamic imaging and hepatobiliary-phase imaging. It has characteristics like extracellular contrast agents and can be used in dynamic MRI within three minutes after contrast agent injection. In the hepatobiliary phase, gadoxetic acid is taken up by cells that express the OATP receptor. Normal hepatocytes usually express abundant OATP receptors, while HCCs or liver metastases lack OATP receptors. This results in improved lesion-to-liver contrast because normal liver parenchyma shows high SI while liver tumors show dark SI in the hepatobiliary phase of gadoxetic-acid–enhanced MRI.[32]

Gadoxetic acid is excreted into the biliary system. In the hepatobiliary phase it is possible to observe the biliary excretion of gadoxetic acid, which thus allows functional biliary imaging. In liver tissue in which the bile duct is obstructed, biliary excretion is not observed. Regarding liver tumor evaluation, the hepatobiliary phase is sometimes helpful for obtaining a differential diagnosis. For example, focal nodular hyperplasia (FNH) has a functioning, hepatocyte-expressing OATP receptor, although it has no biliary excretion system. Therefore, gadoxetic acid is retained for a long time within an FNH nodule. FNH shows high SI in the hepatobiliary phase, which is helpful for differentiating FNH from HCC.[8]

Diffusion-weighted imaging

Diffusion-weighted imaging is a sequence to map the diffusion process of molecules, primarily water molecules, in biological tissues. Diffusion is a random motion of water molecules. In tissues or cells, diffusion of water molecules is restricted due to the interactions of molecules.[33] The degree of diffusion restriction varies across tissues, thus reflecting the microscopic details of biological tissues. The apparent diffusion coefficient (ADC) is a quantitative parameter of diffusion restriction calculated from diffusion-weighted images. The ADC map, together with diffusion-weighted images, is quite helpful for visual assessment and quantitative analysis of a liver tumor (Fig. 3D).

The diffusion of water molecules is highly restricted in dense cellular tissue such as HCC, compared to that of normal liver parenchyma, whereas necrosis or nonviable tumor tissues cause increased membranous permeability allowing free diffusion of water molecules.[34] Therefore, diffusion-weighted images are helpful for detecting highly cellular tumors and for differentiating malignant lesions from benign lesions.

MAGNETIC RESONANCE IMAGING OF ALTERATIONS DURING HEPATOCARCINOGENESIS

During multistep hepatocarcinogenesis, the important changes in hepatocellular nodules are neo-angiogenesis, cellular differentiation and density, fat or iron accumulation, and biliary drainage dysfunction (Fig. 1). Recent advances in MR technology allow the evaluation of these pathological and functional changes.[6,35]

Alteration of hepatic vasculature

During hepatocarcinogenesis, hemodynamic change occurs in hepatocellular nodules and can be visualized by radiologic imaging and histopathology.[36] The blood flow of RNs is supplied from both the portal vein (75%–80%) and the hepatic artery (20%–25%), as with normal liver parenchyma. As the hepatocellular nodules evolve from low-grade DN through high-grade DN to early HCC, both the intranodular portal blood supply and the hepatic arterial blood supply tend to decrease.[37] The majority of these nodules are still hypovascular on dynamic MRI.[9] As the grade of HCCs increases, i.e., Edmondson grade II or

 http://dx.doi.org/10.4132/jptm.2015.04.15

greater, the intranodular portal supply definitely decreases, whereas the intranodular arterial supply tends to progressively increase. This increased intranodular arterial input is due to neoangiogenesis of the unpaired artery in the lesion.[10] Therefore, the majority of advanced HCCs show typical hemodynamic features of arterial enhancement and portal/delayed washout (Fig. 3C).

Cellular change in hepatocellular nodules

As hepatocellular nodules evolve from DNs to HCCs, several cellular changes occur, including small cell change, increased cell density, and nodule-in-nodule growth. These cellular changes can be detected in T2-WI and diffusion-weighted images.[35]

First, cell density can be evaluated by diffusion-weighted imaging and T2-WI. Low-grade DNs show a mild increase in cell density, and high-grade DNs show a moderate increase in cell density, i.e., as much as twice that of the surrounding liver parenchyma.[11] However, these cellular changes of DNs are usually insufficient to show overt high SI on diffusion-weighted images and T2-WI. In contrast, in HCCs, an increase in cell density is usually sufficiently detectable on diffusion-weighted images or T2-WIs.[38] Small cell change is frequently observed in HCC and may also contribute to diffusion restriction of water molecules in the malignant cells seen on diffusion-weighted images (Fig. 3D).

Secondly, the nodule-in-nodule pattern is one of the typical histologic and imaging features of HCC, although it is uncommon. Usually, cirrhotic nodules and low-grade DNs are seen as distinct single nodules, while some high-grade DNs contain sub-nodules which are usually HCC foci, i.e., clones of malignant-transformed cells from DNs during hepatocarcinogenesis. The nodule-in-nodule pattern can be depicted by either T2-WI or dynamic MRI.[39] If the sub-nodule within the DN shows arterial enhancement, it is easily detected in the arterial phase of dynamic MRI (Fig. 4).

Thirdly, the tumor capsule is a characteristic feature of progressed HCCs.[39] It is usually seen as a thin rim of low SI on non-contrast T1-WI. On contrast-enhanced MRI, the tumor capsule can be progressively enhanced following injection of gadolinium contrast agent, as the tumor capsule is generally composed of fibrous tissue containing compressed vessels (Fig. 5).[12] On T2-WI, the tumor capsule may show variable SI as either low SI or high SI. Although the tumor capsule is regarded as a characteristic finding of progressed HCCs, it may be present in large DNs and may not be seen in small HCCs. For the diagnosis of HCC, the presence of a tumor capsule is helpful, although not essential.

Alterations of the fat/iron composition in hepatocellular nodules

During hepatocarcinogenesis, iron may accumulate in low-grade DNs and in some high-grade DNs. These nodules containing an iron deposit are referred to as 'siderotic nodules' (Fig. 6). In hepatocytes of siderotic nodules, the iron-transporter system, such as the transferrin transporter, are upregulated.[14] However, as these nodules progress into HCCs, the iron-transportation system also alters, and iron utilization increases, thus causing iron deficiency in HCCs.[15] Therefore, with progression to HCC, iron usually decreases.

These alterations of the fat composition in DNs and HCCs are often helpful for characterizing hepatocellular nodules on MRI. On T2-WI or T2*-WI, the iron component is seen as

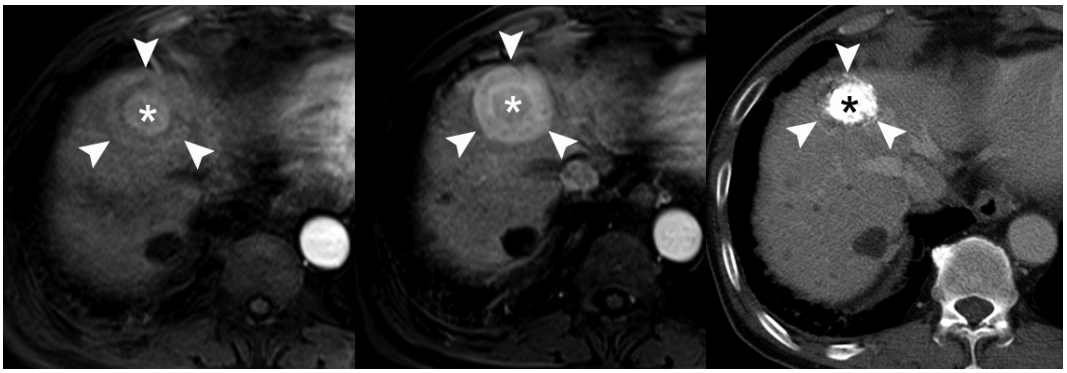

Fig. 4. Nodule-in-nodule pattern of hepatocellular carcinoma (HCC). On a multiphasic, dynamic magnetic resonance imaging of a 50-year-old patient with HCC, there is a large mass without arterial hypervascularity (arrowheads on the left) and a sub-nodule with strong arterial hypervascularity (asterisk on the left) on the arterial-phase image, i.e., the so-called nodule-in-nodule pattern. The central sub-nodule shows washout on the portal-venous phase (asterisk in the middle). After the patient was treated with transarterial chemoembolization, lipiodol was taken up only in the sub-nodule (asterisk on the right). These findings suggest the presence of HCC as a sub-nodule arising from a large dysplastic nodule.

dark SI. On T1-weighted, dual gradient-echo images, the iron component shows a signal drop in in-phase images compared to that of opposed-phase images. Iron-containing, hepatocellular nodules are usually DNs and are unlikely to be HCCs. The development of an iron-deficient sub-nodule within a siderotic nodule indicates HCC foci arising from the DN. Likewise, if a siderotic nodule is seen to be iron-free on a follow-up study, it may suggest its transformation into HCC.[17]

Fat accumulation within hepatocellular nodules is also altered during hepatocarcinogenesis. In low-grade DNs, high-grade DNs, and early HCCs, fat can accumulate focally or diffusely in the nodules. The intralesional fat accumulation peaks in the early HCC stage and regresses according to the increasing size and grade of HCCs. Usually, poorly differentiated HCCs or large HCCs > 3 cm rarely show intralesional fat accumulation.[13] The fat component can be evaluated on T1-weighted, dual gradient-echo images. The fatty component of tissue shows a signal drop in opposed-phase images compared to in-phase images (Fig. 3B).

MAGNETIC RESONANCE IMAGING FINDINGS OF HEPATOCARCINOGENESIS

Regenerative nodules

On MRI, most RNs are imperceptible and isointense on unenhanced T1-WIs and T2-WIs. Some of these nodules may be differentiated by unusual imaging features, such as hyperintensity on T1-WIs and hypointensity on T2-WIs. When enhanced with contrast material, most RNs demonstrate a similar degree of enhancement with that of the adjacent parenchyma, although occasionally mild, delayed-phase hypoenhancement or hepatobiliary phase hyperintensity may be seen.[27,40]

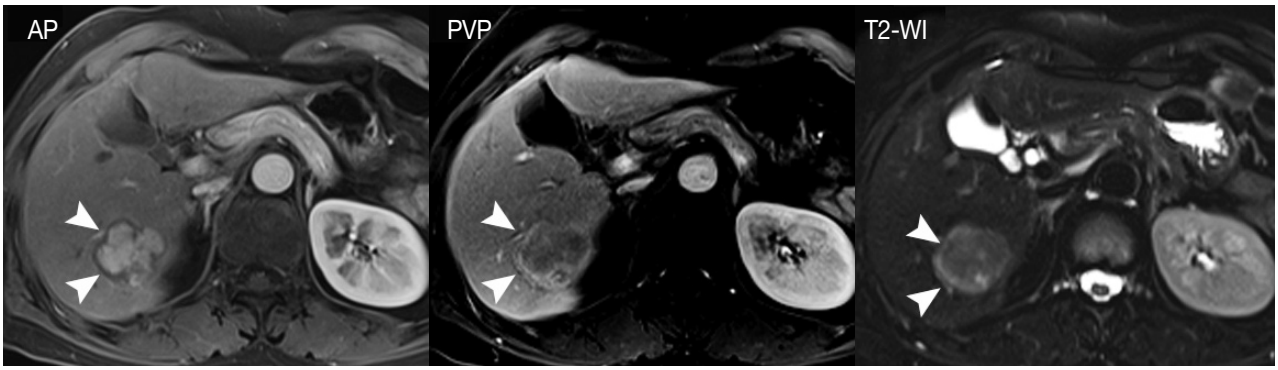

Fig. 5. Tumor capsule of the hepatocellular carcinoma (HCC). The tumor capsule (arrowheads) is seen as a hypointense rim on the arterial-phase (AP) image (left) and as an enhancing rim on the portal-venous phase (PVP) image (middle), indicating a delayed and persistent enhancement pattern. On T2-weighted imaging (T2-WI), the tumor capsule is seen as a hyperintense rim (right).

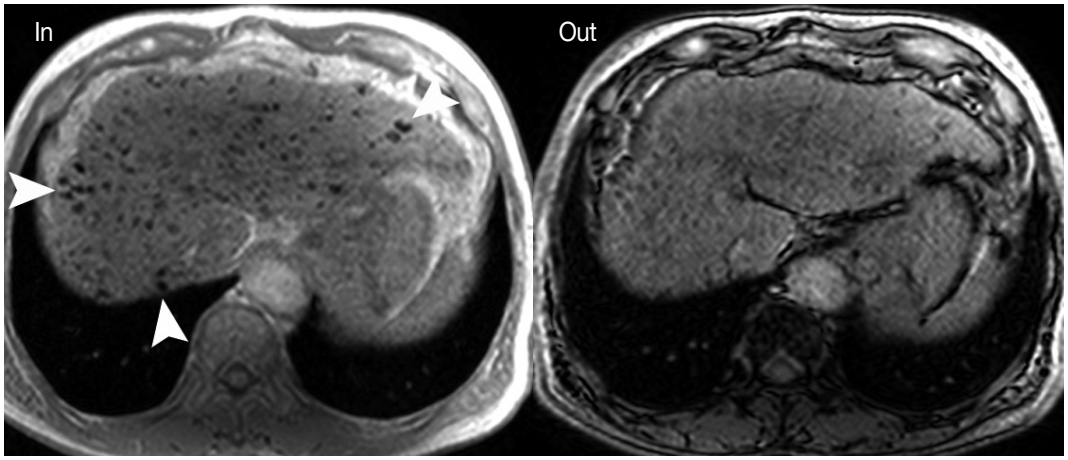

Fig. 6. Siderotic nodule. A 60-year-old patient with liver cirrhosis underwent liver magnetic resonance imaging. On in-phase images, there are many nodules with low signal intensity (arrowheads on the left), which are not clearly demonstrable on opposed-phase images (right). This signal drop of nodules on the in-phase image suggests that these nodules contain an iron component (so-called siderotic nodules).

 http://dx.doi.org/10.4132/jptm.2015.04.15

Dysplastic nodules

Common imaging findings of DNs are hyperintensity on T1-WIs and isointensity or hypointensity on T2-WIs.[27,41] The T1 hyperintensity can be explained by the fact that DNs accumulate copper or iron, which are paramagnetic materials leading to T1 hyperintensity depending on the concentration. Such intranodular copper or iron accumulation may lead to T2 hypointensity due to the T2-shortening effects. Some DNs, especially high-grade DNs, may show fatty change manifested as T1 hyperintensity on MRI.

After contrast agent injection, most DNs are usually isointense to the liver parenchyma in the hepatic arterial, portal venous, and hepatobiliary phases. As some DNs show washout or capsular enhancement in the delayed phase and hypointensity in the hepatobiliary phase, these findings may be good predictors of pre-malignancy.[27]

Early HCC

Most early HCCs are either isointense or hyperintense on T1-WIs and are mostly isointense on T2-WIs.[42] In addition, most early HCCs are hypovascular, and only 5% of the early HCCs show arterial hypervascularity on dynamic MRI. These characteristics are nonspecific, suggesting that it is difficult to accurately diagnose early HCC using conventional MRI.

In particular, differentiating early HCC from high-grade DN on MRI is quite challenging. There are a few differential points. First, high SI on diffusion-weighted images almost always indicates early HCC. DNs are almost never hyperintense on T2-WI and diffusion-weighted images.[17] Second, nodule hypointensity on the hepatobiliary phase of gadoxetic-acid-enhanced MRI favors early HCC rather than high-grade DN, as a substantial number of such hypointense nodules show hypervascularity during the follow-up period (Fig. 7).[43]

Progressed HCC

The typical MRI findings of HCC, which have been extensively investigated in numerous research studies, mostly apply to progressed HCC rather than early HCC. The hallmarks of HCC are arterial hypervascularity and washout on the portal-venous phase and/or equilibrium phase of multiphasic dynamic

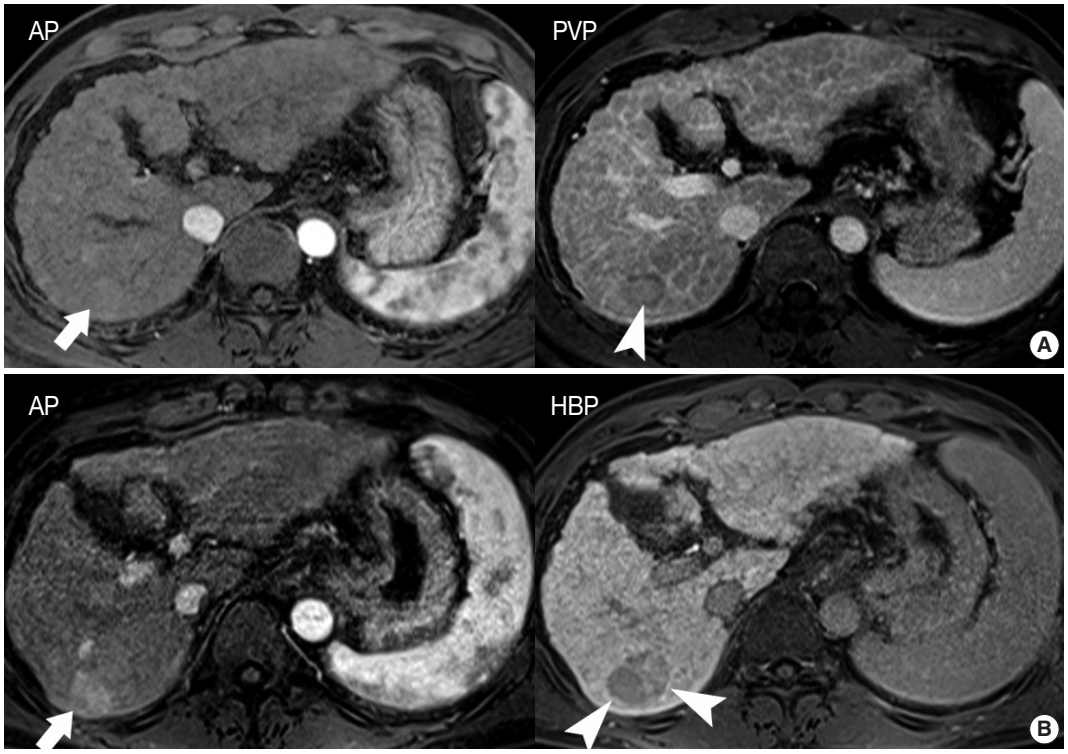

Fig. 7. A 65-year-old patient with a liver nodule. (A) On the initial magnetic resonance imaging (MRI), there is a 1.4 cm, hypointense nodule on the portal-venous phase (PVP, arrowhead) without arterial hypervascularity (arrow) on the arterial phase (AP). This nodule was regarded as a high-grade dysplastic nodule or early hepatocellular carcinoma (HCC). (B) On the one-year follow-up MRI, the nodule had increased in size. The nodule showed hypointensity on the hepatobiliary phase (HBP, arrowheads) and arterial hypervascularity on the AP (arrow), which suggests development of HCC.

CT or MRI.[4,37] This finding is due to the predominant vascular supply to HCCs from unpaired hepatic arteries and the absence of the portal vein supply. These hemodynamic changes are apparent in the progressed HCC rather than the early HCC. Therefore, it is very helpful to differentiate small progressed HCC from early HCC. In addition, the nodule margin seen on MRI is also helpful to differentiate small, progressed HCC, because it is more distinctly nodular than early HCC with its indistinct margin. Indeed, the tumor capsule is a characteristic feature of progressed HCCs and is seen as a persistent enhancing rim at the periphery of the tumor.[39]

Progressed HCCs can present as infiltrative masses as well as expansile nodules/masses. In infiltrative masses, the tumor cells may infiltrate through the tumor capsule into the surrounding parenchyma.[17] These infiltrative HCCs frequently show vascular invasion or biliary invasion, thus leading to a poor patient prognosis.

Vascular invasion is common in progressed HCCs, including portal vein invasion or hepatic vein invasion. As vascular invasion is rarely observed in other types of liver malignancies, this is a helpful characteristic for diagnosing HCC. Vascular invasion generally indicates a poor prognosis for the patients, as it is a route of tumor spread through the liver and of systemic metastasis.[26]

CONCLUSION

The incidence of small HCCs has recently been increasing due to a nationwide surveillance program and advances in imaging techniques. It is difficult to correctly diagnose such small HCCs during histological and radiological examinations. Understanding the important alterations during hepatocarcinogenesis as well as the characteristic MRI and histopathological features will be helpful for managing patients with chronic liver disease and HCC. There is no doubt that special MRI techniques, such as fat/iron quantification, diffusion-weighted images, and gadoxetic-acid-enhanced MRI, have greatly enhanced our understanding of hepatocarcinogenesis.

Conflicts of Interest

No potential conflict of interest relevant to this article was reported.

Acknowledgments

This research was supported by a grant of the Korea Health Technology R&D Project through the Korea Health Industry Development Institute (KHIDI), funded by the Ministry of Health & Welfare, Republic of Korea (Grant No. HI14C1090).

REFERENCES

1. Song P, Tang W, Tamura S, *et al.* The management of hepatocellular carcinoma in Asia: a guideline combining quantitative and qualitative evaluation. Biosci Trends 2010; 4: 283-7.
2. Kudo M, Han KH, Kokudo N, *et al.* Liver Cancer Working Group report. Jpn J Clin Oncol 2010; 40 Suppl 1: i19-27.
3. Lee SH, Choi HC, Jeong SH, *et al.* Hepatocellular carcinoma in older adults: clinical features, treatments, and survival. J Am Geriatr Soc 2011; 59: 241-50.
4. Kudo M. Multistep human hepatocarcinogenesis: correlation of imaging with pathology. J Gastroenterol 2009; 44 Suppl 19: 112-8.
5. Yoo HJ, Lee JM, Lee MW, *et al.* Hepatocellular carcinoma in cirrhotic liver: double-contrast-enhanced, high-resolution 3.0T-MR imaging with pathologic correlation. Invest Radiol 2008; 43: 538-46.
6. Choi BI, Lee JM. Advancement in HCC imaging: diagnosis, staging and treatment efficacy assessments: imaging diagnosis and staging of hepatocellular carcinoma. J Hepatobiliary Pancreat Sci 2010; 17: 369-73.
7. Henninger B, Zoller H, Rauch S, *et al.* Automated two-point dixon screening for the evaluation of hepatic steatosis and siderosis: comparison with R2*-relaxometry and chemical shift-based sequences. Eur Radiol 2015; 25: 1356-65.
8. Suh CH, Kim KW, Kim GY, Shin YM, Kim PN, Park SH. The diagnostic value of Gd-EOB-DTPA-MRI for the diagnosis of focal nodular hyperplasia: a systematic review and meta-analysis. Eur Radiol 2015; 25: 950-60.
9. Krinsky G. Imaging of dysplastic nodules and small hepatocellular carcinomas: experience with explanted livers. Intervirology 2004; 47: 191-8.
10. Fournier LS, Cuenod CA, de Bazelaire C, *et al.* Early modifications of hepatic perfusion measured by functional CT in a rat model of hepatocellular carcinoma using a blood pool contrast agent. Eur Radiol 2004; 14: 2125-33.
11. Roncalli M, Terracciano L, Di Tommaso L, *et al.* Liver precancerous lesions and hepatocellular carcinoma: the histology report. Dig Liver Dis 2011; 43 Suppl 4: S361-72.
12. Ishigami K, Yoshimitsu K, Nishihara Y, *et al.* Hepatocellular carcinoma with a pseudocapsule on gadolinium-enhanced MR images: correlation with histopathologic findings. Radiology 2009; 250: 435-43.
13. Kutami R, Nakashima Y, Nakashima O, Shiota K, Kojiro M. Pathomorphologic study on the mechanism of fatty change in small hepatocellular carcinoma of humans. J Hepatol 2000; 33: 282-9.

14. Pascale RM, De Miglio MR, Muroni MR, *et al.* Transferrin and transferrin receptor gene expression and iron uptake in hepatocellular carcinoma in the rat. Hepatology 1998; 27: 452-61.
15. Holmstrom P, Gåfvels M, Eriksson LC, *et al.* Expression of iron regulatory genes in a rat model of hepatocellular carcinoma. Liver Int 2006; 26: 976-85.
16. Libbrecht L, Craninx M, Nevens F, Desmet V, Roskams T. Predictive value of liver cell dysplasia for development of hepatocellular carcinoma in patients with non-cirrhotic and cirrhotic chronic viral hepatitis. Histopathology 2001; 39: 66-73.
17. Choi JY, Lee JM, Sirlin CB. CT and MR imaging diagnosis and staging of hepatocellular carcinoma: part I. Development, growth, and spread: key pathologic and imaging aspects. Radiology 2014; 272: 635-54.
18. International Working Party. Terminology of nodular hepatocellular lesions. Hepatology 1995; 22: 983-93.
19. International Consensus Group for Hepatocellular Neoplasia; The International Consensus Group for Hepatocellular Neoplasia. Pathologic diagnosis of early hepatocellular carcinoma: a report of the International Consensus Group for Hepatocellular Neoplasia. Hepatology 2009; 49: 658-64.
20. Park YN. Update on precursor and early lesions of hepatocellular carcinomas. Arch Pathol Lab Med 2011; 135: 704-15.
21. Okuda K, Peters RL, Simson IW. Gross anatomic features of hepatocellular carcinoma from three disparate geographic areas: proposal of new classification. Cancer 1984; 54: 2165-73.
22. Korean Liver Cancer Study Group. Pathology for prediction of liver. General rules for the study of primary liver cancer. Seoul: Korean Liver Cancer Study Group, 2004; 39-40.
23. Choi BI, Lee GK, Kim ST, Han MC. Mosaic pattern of encapsulated hepatocellular carcinoma: correlation of magnetic resonance imaging and pathology. Gastrointest Radiol 1990; 15: 238-40.
24. Demirjian A, Peng P, Geschwind JF, *et al.* Infiltrating hepatocellular carcinoma: seeing the tree through the forest. J Gastrointest Surg 2011; 15: 2089-97.
25. Edmondson HA, Steiner PE. Primary carcinoma of the liver: a study of 100 cases among 48,900 necropsies. Cancer 1954; 7: 462-503.
26. Bruix J, Sherman M; American Association for the Study of Liver Diseases. Management of hepatocellular carcinoma: an update. Hepatology 2011; 53: 1020-2.
27. Lee JM, Choi BI. Hepatocellular nodules in liver cirrhosis: MR evaluation. Abdom Imaging 2011; 36: 282-9.
28. Zech CJ, Reiser MF, Herrmann KA. Imaging of hepatocellular carcinoma by computed tomography and magnetic resonance imaging: state of the art. Dig Dis 2009; 27: 114-24.
29. Bitar R, Leung G, Perng R, *et al.* MR pulse sequences: what every radiologist wants to know but is afraid to ask. Radiographics 2006; 26: 513-37.
30. Kang BK, Yu ES, Lee SS, *et al.* Hepatic fat quantification: a prospective comparison of magnetic resonance spectroscopy and analysis methods for chemical-shift gradient echo magnetic resonance imaging with histologic assessment as the reference standard. Invest Radiol 2012; 47: 368-75.
31. Ayyappan AP, Jhaveri KS. CT and MRI of hepatocellular carcinoma: an update. Expert Rev Anticancer Ther 2010; 10: 507-19.
32. Sun HY, Lee JM, Shin CI, *et al.* Gadoxetic acid-enhanced magnetic resonance imaging for differentiating small hepatocellular carcinomas (< or =2 cm in diameter) from arterial enhancing pseudolesions: special emphasis on hepatobiliary phase imaging. Invest Radiol 2010; 45: 96-103.
33. Taouli B, Ehman RL, Reeder SB. Advanced MRI methods for assessment of chronic liver disease. AJR Am J Roentgenol 2009; 193: 14-27.
34. Taouli B, Koh DM. Diffusion-weighted MR imaging of the liver. Radiology 2010; 254: 47-66.
35. Bartolozzi C, Battaglia V, Bozzi E. HCC diagnosis with liver-specific MRI: close to histopathology. Dig Dis 2009; 27: 125-30.
36. Hayashi M, Matsui O, Ueda K, *et al.* Correlation between the blood supply and grade of malignancy of hepatocellular nodules associated with liver cirrhosis: evaluation by CT during intraarterial injection of contrast medium. AJR Am J Roentgenol 1999; 172: 969-76.
37. Choi BI. Hepatocarcinogenesis in liver cirrhosis: imaging diagnosis. J Korean Med Sci 1998; 13: 103-16.
38. Han JK, Eun HW, Kim SH. Radiologic findings of dysplastic nodule. Korean J Hepatol 2008; 14: 231-4.
39. Hanna RF, Aguirre DA, Kased N, Emery SC, Peterson MR, Sirlin CB. Cirrhosis-associated hepatocellular nodules: correlation of histopathologic and MR imaging features. Radiographics 2008; 28: 747-69.
40. Trevisani F, Cantarini MC, Wands JR, Bernardi M. Recent advances in the natural history of hepatocellular carcinoma. Carcinogenesis 2008; 29: 1299-305.
41. Aravalli RN, Cressman EN, Steer CJ. Cellular and molecular mechanisms of hepatocellular carcinoma: an update. Arch Toxicol 2013; 87: 227-47.
42. Thorgeirsson SS, Grisham JW. Molecular pathogenesis of human hepatocellular carcinoma. Nat Genet 2002; 31: 339-46.
43. Ichikawa T, Sano K, Morisaka H. Diagnosis of pathologically early HCC with EOB-MRI: experiences and current consensus. Liver Cancer 2014; 3: 97-107.

Journal of Pathology and Translational Medicine 2015; 49: 230-235
http://dx.doi.org/10.4132/jptm.2015.03.21

■ REVIEW ■

Effectiveness and Limitations of Core Needle Biopsy in the Diagnosis of Thyroid Nodules: Review of Current Literature

Jung Hyun Yoon · Eun-Kyung Kim
Jin Young Kwak · Hee Jung Moon

Department of Radiology, Severance Hospital, Research Institute of Radiological Science, Yonsei University College of Medicine, Seoul, Korea

Received: March 5, 2015
Accepted: March 20, 2015

Corresponding Author
Eun-Kyung Kim, M.D., Ph.D.
Department of Radiology, Severance Hospital, Research Institute of Radiological Science, Yonsei University College of Medicine, 50-1 Yonsei-ro, Seodaemun-gu, Seoul 120-752, Korea
Tel: +82-2-2228-7400
Fax: +82-2-393-3035
E-mail: ekkim@yuhs.ac

Fine needle aspiration (FNA) is currently accepted as an easy, safe, and reliable tool for the diagnosis of thyroid nodules. Nonetheless, a proportion of FNA samples are categorized into non-diagnostic or indeterminate cytology, which frustrates both the clinician and patient. To overcome this limitation of FNA, core needle biopsy (CNB) of the thyroid has been proposed as an additional diagnostic method for more accurate and decisive diagnosis for thyroid nodules of concern. In this review, we focus on the effectiveness and limitations of CNB, and what factors should be considered when CNB is utilized in the diagnosis of thyroid nodules.

Key Words: Thyroid; Neoplasm; Core needle biopsy; Ultrasonography

At present, thyroid nodules are a common problem. With advances in diagnostic technology and the widespread usage of high-resolution ultrasonography (US), approximately 19%–67% of otherwise healthy, asymptomatic individuals will eventually be found to have thyroid nodules.[1] Out of the vast amount of thyroid nodules detected, only 7%–16% of them will be eventually diagnosed as malignant.[1] Therefore, an accurate and efficient diagnostic tool is critical for triaging patients with nodular disease of the thyroid. Fine needle aspiration (FNA), especially under US guidance, is considered the gold standard for differential diagnosis of thyroid nodules, due to its simplicity, safety, cost-effectiveness, and diagnostic accuracy. Most authoritative guidelines recommend FNA for thyroid nodules detected on US as the next step in diagnosis.[1,2] FNA has been reported to have diagnostic sensitivity of 83%–98% and specificity of 70%–92% by various studies.[1-3]

One major drawback of FNA is non-diagnostic and indeterminate cytology results (including atypia of undetermined significance/follicular lesion of undetermined significance [AUS/FLUS], follicular neoplasm or suspicious for a follicular neoplasm [FN/SFN], and suspicious for malignancy), which comprises approximately 10%–33.6% and 15%–42% of all FNA samples,[4-7] respectively. According to the Bethesda System for Reporting Thyroid Cytopathology,[3] repeat ultrasonography-guided fine needle aspiration (US-FNA) is recommended for nodules with non-diagnostic or indeterminate cytology results, as repeat aspiration provides conclusive results in most of these nodules. However, about 9.9%–50% of nodules with initial non-diagnostic cytology,[8-10] and 38.5%–43% of nodules with indeterminate nodules[11,12] will once again be diagnosed with inconclusive results, which induces frustration and anxiety in the patient and leads to confusion in patient management and additional diagnostic medical costs.

Core needle biopsy (CNB) of the thyroid gland has been proposed as an additional diagnostic method to US-FNA, mainly to overcome the limitations of inconclusive cytologic diagnosis. CNB provides a large amount of tissue which enables histologic diagnosis, and additional immunohistochemical staining, if needed. Several studies have shown the usefulness of CNB in providing definitive diagnosis for thyroid nodules.[12-15] Neverthe-

pISSN 2383-7837
eISSN 2383-7845

less, there currently remains a lack of evidence and no definite guideline on how CNB should be used in the diagnosis of thyroid nodules. The American Association of Clinical Endocrinologists, Associazione Medici Endocrinologi, and European Thyroid Association (AACE/AME/ETA) guideline is the only authoritative guideline that mentions using CNB, and only in selective cases with inadequate cytology,[2] but the actual usage of CNB in clinical practice varies among institutions and radiologists. In this paper, we will review previous studies evaluating the diagnostic performance of CNB in order to discuss the effectiveness and limitations of CNB in the diagnosis of thyroid nodules.

EFFECTIVENESS

CNB in thyroid nodules with initial non-diagnostic cytology

Although FNA has been established as an accurate diagnostic method for thyroid nodules by many authorized guidelines,[1-3] the diagnostic accuracy of FNA has been known to vary according to (1) the experience of the operator, (2) intrinsic characteristics of the targeted nodule, and (3) cytology interpretation.[16] These factors in particular, have significant influence on non-diagnostic cytology. As non-diagnostic aspirates are common causes of false-negative FNA results, the current guidelines recommend repeat FNA under US guidance,[1-3] yet approximately 20.4%–38.4% will once again be diagnosed as non-diagnostic.[2,10] Surgery is recommended for solid nodules with repeated non-diagnostic results for diagnostic purposes,[1-3] which seems rather extreme when considering the relatively low malignancy rates (6.6%–39.5%) of nodules with non-diagnostic cytology.[4,8,17] Hence, CNB has been used as an adjunctive diagnostic tool in nodules with initial non-diagnostic cytology; recent studies have reported diagnostic or conclusive results in 86%–98.9% of non-diagnostic nodules, and significantly lower non-diagnostic rates in CNB compared to repeat US-FNA (Table 1).[12,13,15,17,18] In reports that provide the diagnostic performances of CNB, high specificity and positive predictive values of 100% were commonly observed in CNB, suggesting that CNB enables malignancy-specific results, even in nodules with prior non-diagnostic results. Higher diagnostic rates obtained with CNB are only natural since CNB can obtain larger tissue samples that provide histopathologic information of the targeted nodule and the surrounding thyroid parenchyma. However, presently, only the AACE/AME/ETA guideline considers using US-CNB in "selected cases with inadequate FNA results."[2] Otherwise, no specific recommendation or indications have been established on using CNB as a follow-up diagnostic tool in nodules with non-diagnostic cytology. In addition, based on the low malignancy rates from repeat US-FNA (0.5%) or surgical resection (1.8%) in thyroid nodules with initial non-diagnostic cytology, a more conservative approach such as clinical or US follow-up has been proposed as a more appropriate alternative to additional invasive procedures such as follow-up FNA.[19] Thus, the role of CNB in contributing meaningful information in non-diagnostic nodules is still unclear.

CNB in nodules with indeterminate cytology

Indeterminate cytology, including AUS/FLUS, FN/SFN, and suspicious for malignancy categories of the Bethesda System for Reporting Thyroid Cytopathology,[3] is a diagnostic challenge since it harbors a higher risk of malignancy (5%–75%) but not sufficiently high to directly consider surgery. There have been continual efforts to improve the accurate detection of malignancy among these lesions, including US features and molecular analysis such as *BRAF* mutations.[7,20] CNB has been utilized in the diagnosis of thyroid nodules with indeterminate cytology;[12,14,21-24] in most studies, CNB is used to direct indeterminate nodules to either surgery or conservative management. Park *et al*.[21] showed a high detection rate of benign nodules in CNB (77.8%), compared to repeat FNA (35.2%) and surgery (38.7%), with high diagnostic accuracy. In addition, inconclusive rates of CNB (17.6%) have been reported to be significantly lower than repeat FNA (37.3%) in another study which included AUS nodules.[24]

Table 1. Results of the diagnostic performances of rFNA and CNB in thyroid nodules diagnosed as non-diagnostic on prior cytology

Reference	Total	rFNA	CNB	rFNA-ND (%)	CNB-ND (%)	Diagnostic performance of CNB				
						Sensitivity (%)	Specificity (%)	PPV (%)	NPV (%)	Accuracy (%)
Samir *et al*.[18] (2012)	90	90 (100)	90 (100)	53	23	-	-	-	-	-
Na *et al*.[12] (2012)	64	64 (100)	64 (100)	28.1	1.6	71.4	100	100	88.6	91.1
Yeon *et al*.[15] (2013)	155	-	155	-	1.3	94.6	100	100	97.5	98.3
Lee *et al*.[17] (2014)	514	389 (75.7)	125 (24.3)	33.2	2.4	70	100	100	97.3	-
Choi *et al*.[13] (2014)	360	180 (50.0)	180 (50.0)	40.0	1.1	95.7	100	100	97.6	98.4

Values are presented as number (%) unless otherwise indicated.
rFNA, repeat fine needle aspiration; CNB, core needle biopsy; ND, non-diagnostic; PPV, positive predictive value; NPV, negative predictive value.

This information facilitates accurate patient management and reduces unnecessary surgery.

Few studies have investigated the efficacy of US-CNB in the diagnosis of FN of the thyroid gland.[23,25,26] CNB has been known to have advantages over FNA cytology in the diagnosis of FN in that the CNB specimen provides tissue samples which (1) visualizes the microscopic monotonous follicular proliferation and presence of fibrous capsules, and (2) enables additional immunohistochemical staining for differential diagnosis. Nasrollah *et al*.[26] introduced a new biopsy technique that uses targeting to include the nodular tissue, surrounding fibrous capsule, and extranodular parenchyma; based on this method, a recent study demonstrated the utility of CNB in preoperative diagnosis of FN with a significantly lower false-positive rate, unnecessary surgery rate, and higher malignancy rates compared to FNA.[25] However, in contrast, Hakala *et al*.[6] showed that while the sensitivity of CNB may be superior in the diagnosis of papillary thyroid carcinoma or other non-follicular thyroid lesions, CNB does not confer as much benefit as in the diagnosis of follicular tumors. Additionally, a meta-analysis by Novoa *et al*.[27] showed that FN was the reason for a high number of false-positive results from CNB in the thyroid when compared to other head and neck neoplasms, since CNB cannot differentiate between follicular adenoma and follicular carcinoma. Tissue sampling including obtaining an adequate amount of fibrous capsule and surrounding normal parenchyma, which is required for the diagnosis of FN[26] is not easy, even under US-guidance, and confounds the diagnosis between benign hyperplastic nodule and FN. In addition, for the diagnosis of follicular carcinoma, evaluation of the entire nodular capsule is required to detect the presence of capsular/vascular invasion, limiting the role of CNB as well as FNA as supported by the results of a prior study,[23] which showed that although the diagnosis of neoplasm was significantly higher in CNB, the overall malignancy rates did not show significant differences between CNB and FNA (46% to 48%, respectively). Presently, even with its ability to provide larger tissue volume for additional immunohistochemical staining, CNB, like FNA, has limited value in the differential diagnosis among subtypes of FN, serving only as a 'screening test,' rather than diagnostic for FN. Thus, CNB is not recommended for use in the differential diagnosis of FN since it does not provide additional diagnostic information, which is specified in the AACE/AME/ETA guidelines.[2]

CNB as a first-line diagnosis for thyroid nodules

At most institutions, CNB is used as a second-line diagnostic method, either as an adjunct or alternative to repeat FNA.[5,12-14,17,18,26,28] However, recently several studies have applied CNB in first-line diagnosis of thyroid nodules showing suspicious US features,[29,30] concluding that CNB has high conclusive rates and reduces false-negative or inconclusive results of FNA in solid nodules that carry high levels of suspicion for malignancy. Both studies were from single institutions with a limited number of patients. More evidence from a large study population is warranted before considering the application of CNB as a first-line

Table 2. Inconclusive rates of CNB in published literature

Reference	Reason for CNB	CNB-ND	CNB-AUS/FLUS	CNB-FN/SFN	Total inconclusive
Khoo *et al*.[31] (2008)	Referred for CNB by clinicians	-	-	-	37/320 (10.9)
Park *et al*.[21] (2011)	Prior indeterminate cytology	1/54 (1.8)	-	-	1/54 (1.8)
Sung *et al*.[14] (2012)	Previous non-diagnostic or indeterminate FNA result, suspected malignancy with benign cytology results, repeated scanty or bloody aspirates, thyroid malignancy other than differentiated cancer suspected	8/555 (1.4)	63/555 (11.4)	11/555 (2.0)	82/555 (14.8)
Na *et al*.[12] (2012)	Prior ND cytology	1/64 (1.6)	7/64 (10.9)	6/64 (9.4)	14/64 (21.9)
Na *et al*.[12] (2012)	Prior AUS/FLUS cytology	5/161 (3.1)	38/161 (23.6)	8/161 (5.0)	51/161 (31.7)
Ha *et al*.[5] (2013)	Suspicious US features, benign cytology	0/85 (0.0)	1/85 (1.2)	7/85 (8.2)	8/85 (9.4)
Yeon *et al*.[15] (2013)	Prior ND cytology	2/155 (1.3)	18/155 (11.6)	3/155 (1.9)	23/155 (14.8)
Lee *et al*.[17] (2014)	Prior ND cytology	3/125 (2.4)	5/125 (4.0)	11/125 (8.8)	19/125 (15.2)
Choi *et al*.[22] (2014)	Prior AUS cytology	1/84 (1.2)	13/84 (15.5)	5/84 (6.0)	19/84 (22.6)
Choi *et al*.[22] (2014)	Prior FLUS cytology	0/107 (0.0)	23/107 (21.5)	11/107 (10.3)	34/107 (31.8)
Choi *et al*.[13] (2014)	Prior ND cytology	2/180 (1.1)	11/180 (6.1)	3/180 (1.7)	16/180 (8.9)
Ha *et al*.[32] (2014)	Calcified nodules on US	2/272 (0.7)	25/272 (9.2)	12/272 (4.4)	39/272 (14.3)
Zhang *et al*.[30] (2014)	First-line diagnosis of thyroid nodules	4/369 (1.1)	7/369 (1.9)	11/369 (3.0)	22/369 (6.0)

Values are presented as number (%).
CNB, core needle biopsy; AUS/FLUS, atypia of undetermined significance/follicular lesion of undetermined significance; ND, non-diagnostic; FN/SFN, follicular neoplasm/suspicious for follicular neoplasm; FNA, fine needle aspiration; US, ultrasonography.

diagnostic tool.

Khoo *et al.*[31] showed that no significant differences existed in the non-diagnostic rates between US-FNA alone and US-FNA combined to CNB, but there was a trend towards increased complications in US-FNA combined to CNB. This study concluded that the addition of CNB to US-FNA does not decrease non-diagnostic results, and may only increase morbidity from the procedure. A recent meta-analysis by Li *et al.*[33] showed similar results: the area under the receiving operator characteristics curves did not show significant differences between FNA (Az, 0.905) and CNB (Az, 0.745) in the preoperative diagnosis of thyroid nodules and Az values even lower in CNB. However, in some cases, especially in the diagnosis of lymphoma or anaplastic carcinoma, CNB has been reported to be helpful in specific diagnosis.[28] Hence, the clinical and imaging features of the patient must also be considered when deciding which patients will benefit from CNB when applied in the diagnosis of thyroid lesions.

LIMITATIONS AND FURTHER CONSIDERATIONS NEEDED FOR CORE NEEDLE BIOPSY

Complications from CNB

Commonly known complications that can occur after CNB are post-biopsy hematomas, bleeding from the incision site, pain, infections, transient hemoptysis, and nerve injuries.[27,34,35] Reported complication rates are low, ranging from 0.5%–1.0%,[27] with similar patient tolerability and discomfort between FNA and CNB.[36] However, CNB is not always technically feasible, especially in nodules located posteriorly or in close approximation to important structures such as the carotid artery or trachea. Therefore, complications are bound to occur with CNB, even under US-guidance. Bergeron and Beaudoin[34] reported an iatrogenic arteriovenous fistula formation after CNB causing tinnitus. From this case report, we can see that although complication rates are low, CNB can lead to severe and critical complications. While US-FNA may be more feasible for relatively less experienced operators, CNB must be performed with experienced radiologists with dedicated training who are familiar with the radiologic features of important anatomic structures within the cervical region to minimize major complications.

Inconclusive results on CNB

Based on the tissue samples obtained from CNB, higher conclusive rates are reported in the majority of the studies mentioned above. Even so, inconclusive results are unavoidable in thyroid CNB with reported rates ranging from 6.4%–26.7%,[12,13,15,17,22,28] reaching 31.8% when including FN in the inconclusive category (Table 2). As larger tissue samples are provided for histologic diagnosis, higher conclusive results are naturally expected. Yet, similar to FNA, a considerable proportion of thyroid nodules are once again diagnosed as inconclusive on CNB; in fact, a recent study from our institution suggested that 72.7% may be FN.[37] This is important and must always be considered when choosing CNB as the next step for thyroid nodules with prior inconclusive results.

Lack of standardization in CNB pathologic classification

Management guidelines are established based on the clinical outcomes of non-diagnostic, AUS/FLUS, or FN/SFN cytology,[1-3] but currently, there are no reporting systems that can be used as a reference for CNB specimens as in the Bethesda System for Reporting Thyroid Cytopathology nor further management guidelines according to the diagnostic results from CNB. For appropriate application of CNB in the diagnosis of thyroid nodules, a systematic diagnostic approach and definitive management guidelines need to be established first to minimize confusion on the indications for CNB and further management as needed.

CONCLUSION

CNB may have a complementary role to FNA especially in nodules with inconclusive cytologic diagnosis by providing definitive diagnosis that helps to triage patients who need surgery and minimize unnecessary invasive procedures. CNB withholds a considerable proportion of inconclusive results which must be acknowledged. In addition, it must be performed by an experienced radiologist to minimize severe complications from procedures. There should be careful selection of patients who may benefit from CNB. Ultimately, we must keep in mind that CNB is still a complementary diagnostic tool to FNA and not an alternative.

Conflicts of Interest

No potential conflict of interest relevant to this article was reported.

REFERENCES

1. American Thyroid Association (ATA) Guidelines Taskforce on Thyroid Nodules and Differentiated Thyroid Cancer, Cooper DS, Doherty GM, *et al.* Revised American Thyroid Association management guidelines for patients with thyroid nodules and differen-

tiated thyroid cancer. Thyroid 2009; 19: 1167-214.
2. Gharib H, Papini E, Paschke R, *et al*. American Association of Clinical Endocrinologists, Associazione Medici Endocrinologi, and European Thyroid Association medical guidelines for clinical practice for the diagnosis and management of thyroid nodules: executive summary of recommendations. J Endocrinol Invest 2010; 33(5 Suppl): 51-6.
3. Cibas ES, Ali SZ. The Bethesda System for Reporting Thyroid Cytopathology. Thyroid 2009; 19: 1159-65.
4. Yoon JH, Moon HJ, Kim EK, Kwak JY. Inadequate cytology in thyroid nodules: should we repeat aspiration or follow-up? Ann Surg Oncol 2011; 18: 1282-9.
5. Ha EJ, Baek JH, Lee JH, *et al*. Sonographically suspicious thyroid nodules with initially benign cytologic results: the role of a core needle biopsy. Thyroid 2013; 23: 703-8.
6. Hakala T, Kholová I, Sand J, Saaristo R, Kellokumpu-Lehtinen P. A core needle biopsy provides more malignancy-specific results than fine-needle aspiration biopsy in thyroid nodules suspicious for malignancy. J Clin Pathol 2013; 66: 1046-50.
7. Yoon JH, Kwak JY, Kim EK, *et al*. How to approach thyroid nodules with indeterminate cytology. Ann Surg Oncol 2010; 17: 2147-55.
8. Choi YS, Hong SW, Kwak JY, Moon HJ, Kim EK. Clinical and ultrasonographic findings affecting nondiagnostic results upon the second fine needle aspiration for thyroid nodules. Ann Surg Oncol 2012; 19: 2304-9.
9. Renshaw AA. Significance of repeatedly nondiagnostic thyroid fine-needle aspirations. Am J Clin Pathol 2011; 135: 750-2.
10. Richards ML, Bohnenblust E, Sirinek K, Bingener J. Nondiagnostic thyroid fine-needle aspiration biopsies are no longer a dilemma. Am J Surg 2008; 196: 398-402.
11. Ho AS, Sarti EE, Jain KS, *et al*. Malignancy rate in thyroid nodules classified as Bethesda category III (AUS/FLUS). Thyroid 2014; 24: 832-9.
12. Na DG, Kim JH, Sung JY, *et al*. Core-needle biopsy is more useful than repeat fine-needle aspiration in thyroid nodules read as nondiagnostic or atypia of undetermined significance by the Bethesda system for reporting thyroid cytopathology. Thyroid 2012; 22: 468-75.
13. Choi SH, Baek JH, Lee JH, *et al*. Thyroid nodules with initially nondiagnostic, fine-needle aspiration results: comparison of core-needle biopsy and repeated fine-needle aspiration. Eur Radiol 2014; 24: 2819-26.
14. Sung JY, Na DG, Kim KS, *et al*. Diagnostic accuracy of fine-needle aspiration versus core-needle biopsy for the diagnosis of thyroid malignancy in a clinical cohort. Eur Radiol 2012; 22: 1564-72.
15. Yeon JS, Baek JH, Lim HK, *et al*. Thyroid nodules with initially nondiagnostic cytologic results: the role of core-needle biopsy. Radiology 2013; 268: 274-80.
16. Haider AS, Rakha EA, Dunkley C, Zaitoun AM. The impact of using defined criteria for adequacy of fine needle aspiration cytology of the thyroid in routine practice. Diagn Cytopathol 2011; 39: 81-6.
17. Lee SH, Kim MH, Bae JS, Lim DJ, Jung SL, Jung CK. Clinical outcomes in patients with non-diagnostic thyroid fine needle aspiration cytology: usefulness of the thyroid core needle biopsy. Ann Surg Oncol 2014; 21: 1870-7.
18. Samir AE, Vij A, Seale MK, *et al*. Ultrasound-guided percutaneous thyroid nodule core biopsy: clinical utility in patients with prior nondiagnostic fine-needle aspirate. Thyroid 2012; 22: 461-7.
19. Anderson TJ, Atalay MK, Grand DJ, Baird GL, Cronan JJ, Beland MD. Management of nodules with initially nondiagnostic results of thyroid fine-needle aspiration: can we avoid repeat biopsy? Radiology 2014; 272: 777-84.
20. Kim SY, Kim EK, Kwak JY, Moon HJ, Yoon JH. What to do with thyroid nodules showing benign cytology and *BRAF*(V600E) mutation? A study based on clinical and radiologic features using a highly sensitive analytic method. Surgery 2015; 157: 354-61.
21. Park KT, Ahn SH, Mo JH, *et al*. Role of core needle biopsy and ultrasonographic finding in management of indeterminate thyroid nodules. Head Neck 2011; 33: 160-5.
22. Choi YJ, Baek JH, Ha EJ, *et al*. Differences in risk of malignancy and management recommendations in subcategories of thyroid nodules with atypia of undetermined significance or follicular lesion of undetermined significance: the role of ultrasound-guided core-needle biopsy. Thyroid 2014; 24: 494-501.
23. Min HS, Kim JH, Ryoo I, Jung SL, Jung CK. The role of core needle biopsy in the preoperative diagnosis of follicular neoplasm of the thyroid. APMIS 2014; 122: 993-1000.
24. Lee KH, Shin JH, Oh YL, Hahn SY. Atypia of undetermined significance in thyroid fine-needle aspiration cytology: prediction of malignancy by US and comparison of methods for further management. Ann Surg Oncol 2014; 21: 2326-31.
25. Yoon RG, Baek JH, Lee JH, *et al*. Diagnosis of thyroid follicular neoplasm: fine-needle aspiration versus core-needle biopsy. Thyroid 2014; 24: 1612-7.
26. Nasrollah N, Trimboli P, Guidobaldi L, *et al*. Thin core biopsy should help to discriminate thyroid nodules cytologically classified as indeterminate: a new sampling technique. Endocrine 2013; 43: 659-65.
27. Novoa E, Gurtler N, Arnoux A, Kraft M. Role of ultrasound-guided core-needle biopsy in the assessment of head and neck lesions: a meta-analysis and systematic review of the literature. Head Neck 2012; 34: 1497-503.
28. Hahn SY, Shin JH, Han BK, Ko EY, Ko ES. Ultrasonography-guided core needle biopsy for the thyroid nodule: does the procedure hold

any benefit for the diagnosis when fine-needle aspiration cytology analysis shows inconclusive results? Br J Radiol 2013; 86: 20130007.
29. Trimboli P, Nasrollah N, Guidobaldi L, *et al*. The use of core needle biopsy as first-line in diagnosis of thyroid nodules reduces false negative and inconclusive data reported by fine-needle aspiration. World J Surg Oncol 2014; 12: 61.
30. Zhang M, Zhang Y, Fu S, Lv F, Tang J. Thyroid nodules with suspicious ultrasound findings: the role of ultrasound-guided core needle biopsy. Clin Imaging 2014; 38: 434-8.
31. Khoo TK, Baker CH, Hallanger-Johnson J, *et al*. Comparison of ultrasound-guided fine-needle aspiration biopsy with core-needle biopsy in the evaluation of thyroid nodules. Endocr Pract 2008; 14: 426-31.
32. Ha EJ, Baek JH, Lee JH, *et al*. Core needle biopsy can minimise the non-diagnostic results and need for diagnostic surgery in patients with calcified thyroid nodules. Eur Radiol 2014; 24: 1403-9.
33. Li L, Chen BD, Zhu HF, *et al*. Comparison of pre-operation diagnosis of thyroid cancer with fine needle aspiration and core-needle biopsy: a meta-analysis. Asian Pac J Cancer Prev 2014; 15: 7187-93.
34. Bergeron M, Beaudoin D. Simple core-needle biopsy for thyroid nodule, complicated tinnitus. Eur Thyroid J 2014; 3: 130-3.
35. Chen BT, Jain AB, Dagis A, *et al*. Comparison of the efficacy and safety of ultrasound-guided core needle biopsy versus fine-needle aspiration for evaluating thyroid nodules. Endocr Pract 2015; 21: 128-35.
36. Nasrollah N, Trimboli P, Rossi F, *et al*. Patient's comfort with and tolerability of thyroid core needle biopsy. Endocrine 2014; 45: 79-83.
37. Kim YH, Kwon HJ, Kim EK, Kwak JY, Moon HJ, Yoon JH. Applying US-guided core needle biopsy (CNB) in the diagnosis of thyroid masses: preliminary results of a single institution. J Ultrasound Med 2015 Forthcoming.

Journal of Pathology and Translational Medicine 2015; 49: 236-242
http://dx.doi.org/10.4132/jptm.2015.03.16

■ ORIGINAL ARTICLE ■

Proposal of an Appropriate Decalcification Method of Bone Marrow Biopsy Specimens in the Era of Expanding Genetic Molecular Study

Sung-Eun Choi · Soon Won Hong
Sun Och Yoon

Department of Pathology, Yonsei University College of Medicine, Seoul, Korea

Received: January 27, 2015
Revised: February 24, 2015
Accepted: March 16, 2015

Corresponding Author
Sun Och Yoon, M.D., Ph.D.
Department of Pathology,
Yonsei University College of Medicine,
50-1 Yonsei-ro, Seodaemun-gu,
Seoul 120-752, Korea
Tel: +82-2-2228-1763
Fax: +82-2-2227-7939
E-mail: revita@naver.com

Background: The conventional method for decalcification of bone specimens uses hydrochloric acid (HCl) and is notorious for damaging cellular RNA, DNA, and proteins, thus complicating molecular and immunohistochemical analyses. A method that can effectively decalcify while preserving genetic material is necessary. **Methods:** Pairs of bilateral bone marrow biopsies sampled from 53 patients were decalcified according to protocols of two comparison groups: EDTA versus HCl and RDO GOLD (RDO) versus HCl. Pairs of right and left bone marrow biopsy samples harvested from 28 cases were allocated into the EDTA versus HCl comparison group, and 25 cases to the RDO versus HCl comparison group. The decalcification protocols were compared with regards to histomorphology, immunohistochemistry, and molecular analysis. For molecular analysis, we randomly selected 5 cases from the EDTA versus HCl and RDO versus HCl groups. **Results:** The decalcification time for appropriate histomorphologic analysis was the longest in the EDTA method and the shortest in the RDO method. EDTA was superior to RDO or HCl in DNA yield and integrity, assessed via DNA extraction, polymerase chain reaction, and silver *in situ* hybridization using DNA probes. The EDTA method maintained intact nuclear protein staining on immunohistochemistry, while the HCl method produced poor quality images. Staining after the RDO method had equivocal results. RNA *in situ* hybridization using kappa and lambda RNA probes measured RNA integrity; the EDTA and RDO method had the best quality, followed by HCl. **Conclusions:** The EDTA protocol would be the best in preserving genetic material. RDO may be an acceptable alternative when rapid decalcification is necessary.

Key Words: Decalcification technique; Ethylenediaminetetraacetic acid disodium salt dehydrate; Hydrochloric acid; RDO GOLD; Bone marrow

Sampling bone tissue is usually performed for the diagnosis of hematologic malignancy, metastatic tumor, or primary bone tumor. The processing of bone specimens usually follows decalcification and microtome sectioning in pathology laboratories. Inorganic acids such as nitric acid or HCl are used in decalcification, and limit diagnostic options by damaging DNA and RNA. As a result, gene testing is usually not plausible with these decalcified bone specimens, even though certain cancers need further genetic studies for diagnostic and therapeutic purposes. Therefore, there is a growing need for new decalcification agents that adequately preserve DNA and RNA.[1-3]

A variety of molecular testing techniques are necessary to diagnose hematologic malignancies. Fluorescence *in situ* hybridization, gene rearrangement studies of immunoglobulin and T cell receptor genes, and *in situ* hybridization for kappa and lambda light chains and Epstein-Barr virus–encoded small RNAs are commonly used molecular tools in diagnosis of hematologic malignancies. However, further molecular study from bone marrow biopsy specimens is often impossible due to DNA or RNA damage by decalcification. Furthermore, immunohistochemistry may be required for differentiating and subtyping hematolymphoid lesions in conjunction with histomorphologic features of paratrabecular, interstitial, intrasinusoidal, or intravascular aggregates within bone marrow structures. HCl degrades both protein quality and quantity, resulting in poor immunohistochemical staining that cannot be used for accurate diagnosis.

With consideration of these limitations, we evaluated modified bone marrow decalcification protocols and compared them to the HCl method.

MATERIALS AND METHODS

This was a prospective study. To eliminate bias due to variables among cases, cases were enrolled when pairs of bilaterally

pISSN 2383-7837
eISSN 2383-7845

biopsied bone marrow specimens were available. Among bone marrow specimens sampled from the right and left iliac crests between January 2013 and July 2014 at Gangnam Severance Hospital, 53 cases were finally included. For the 53 selected cases, 28 right and left bone marrow samples were allocated to the EDTA (Sigma-Aldrich, St. Louis, MO, USA) protocol and HCl (Calci-Clear Rapid, National Diagnostics, Atlanta, GA, USA) protocol, respectively. Samples from the 25 remaining cases were assigned to the RDO GOLD (RDO) group (Apex Engineering Products Corporation, Aurora, IL, USA) protocol and HCl protocol. Concentration, processing time, and temperature are summarized in Table 1.

To test DNA quality, five cases were randomly selected from each of the three groups (EDTA, HCl, and RDO). DNA was extracted, and the quantity and quality were confirmed using NanoDrop ND-2000 spectrophotometer (Thermo Fisher Scientific Inc., Waltham, MA, USA). The *BRAF* PNA clamping method (Panagene, Daejeon, Korea) and comparison with Ct values of internal controls were used to evaluate the efficacy of polymerase chain reaction (PCR) DNA amplification. To evaluate the efficacy of DNA *in situ* hybridization, HER2 dual color silver *in situ* hybridization (Ventana, Tucson, AZ, USA) was applied to 10 pairs of bone marrow samples. RNA *in situ* hybridization and immunohistochemical studies were performed prospectively. According to the potential differential diagnoses for suspicious lesions observed within bone marrow, appropriate RNA probes or protein antibodies were applied. For immunohistochemistry, the following primary antibodies were used and the details are summarized in Table 2: cyclin D1, Ki67, Bcl2, Bcl6, TdT, CD138, CD20, CD79a, CD3, CD5, CD23, CD10, CD30, and myeloperoxidase. To state the process, after deparaffinization and rehydration, the sections were incubated in BenchMark XT automated slide stainer (Ventana) for 16 minutes at 37°C and then counterstained with hematoxylin reagent. Two pathologists reviewed the hematoxylin and eosin (H&E), immunohistochemistry, and *in situ* hybridization slides. The quality of immunohistochemistry and RNA *in situ* hybridization were assessed using a 3-tiered grading scale: good, equivocal, or poor. HER2 silver *in situ* hybridization was assessed by

Table 1. The decalcification protocols of three methods

Solution	Processing time (hr)	Processing temperature
HCl (100%)	3	Room temperature
EDTA (12.5%)	3 or 24[a]	Room temperature
RDO (100%)	0.5–1	Room temperature

HCl, hydrochloric acid; EDTA, ethylenediaminetetraacetic acid disodium salt dehydrate; RDO, RDO GOLD.
[a]The processing time of EDTA method was mostly 3 hours. It was 24 hours for few cases that contained more cortical bone due to the oblique direction when inserting biopsy-needle.

Table 2. Primary antibodies used

Product name	Dilution	Clonality	Clone	Company
Cyclin D1 (SP4)	1:50	Monoclonal	SP4	LabVision[a]
Ki67	1:1,000	Monoclonal	MIB-1	DAKO[b]
Bcl2 Bond-III	1:50	Monoclonal	bcl2/100/D5	Novocastra[c]
Bcl6	Prediluent	Monoclonal	LN22	Novocastra
TdT	1:100	Polyclonal	-	Cell Marque[d]
CD138	Prediluent	Monoclonal	ML15	DAKO
CD20	1:400	Monoclonal	L26	Novocastra
CD79a (B cell)	1:100	Monoclonal	JCB117	DAKO
CD3	1:200	Monoclonal	SP7	LabVision
CD5	1:100	Monoclonal	4C7	Novocastra
CD23	1:100	Monoclonal	SP23	LabVision
CD10	1:75	Monoclonal	56C6	Novocastra
CD30	1:50	Monoclonal	Ber-H2	DAKO
Myeloperoxidase	1:2,000	Polyclonal	-	DAKO

[a]Lab vision, Waltham, MA; [b]DAKO, Carpinteria, CA; [c]Novocastra, Buffalo Grave, IL; [d]Cell Marque, Rocklin, CA.

Table 3. Quantity and quality of DNA according to decalcification protocols

		DNA yield (median, range)	p-value	Ct value (median, range)	p-value
EDTA vs HCl	EDTA	25 (11.0–37.0)	.168	25.0 (24.6–27.2)	<.001
	HCl	12 (11.0–28.0)		32.7 (28.9–33.3)	
RDO vs HCl	RDO	14.7 (10.9–15.0)	.753	33.6 (33.0–34.1)	.754
	HCl	13.4 (10.0–15.3)		33.5 (33.2–35.2)	

Mann-Whitney U test was used to compare the median of each variables.
HCl, hydrochloric acid; EDTA, ethylenediaminetetraacetic acid disodium salt dehydrate; RDO, RDO GOLD.

detecting two signals of HER2 and CEP17 per nucleus from the normal hematopoietic cells of bone marrow.

The differences in variables were analyzed using the Mann-Whitney U test. All statistical analyses were carried out by SPSS ver. 20.0 for Windows (IBM Co., Armonk, NY, USA).

RESULTS

Isolated DNA quality

DNA quantity, purity, and Ct values of internal controls after real-time PCR in the EDTA versus HCl group and RDO versus

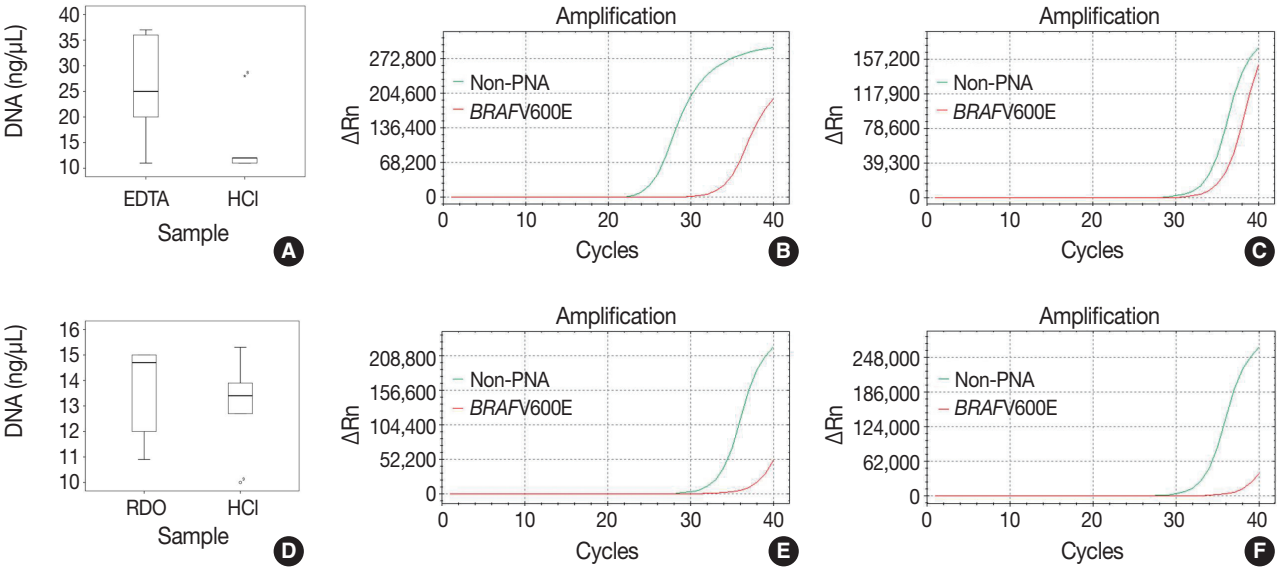

Fig. 1. The quality, quantity, and feasibility of real time PCR study is compared between EDTA, RDO, and HCl protocols. The first row demonstrates EDTA versus HCl, and the second row RDO versus HCl (A, D, DNA yield; B, PCR result of EDTA; E, PCR result of RDO; C, F, PCR results of HCl). D, PCR result of RDO. PCR, polymerase chain reaction; EDTA, ethylenediaminetetraacetic acid disodium salt dehydrate; RDO, RDO GOLD; HCl, hydrochloric acid; PNA, peptide nucleic acid.

Table 4. Comparison of the immunohistochemical results

Item	EDTA vs HCl		RDO vs HCl	
	EDTA	HCl	RDO	HCl
HER2/CEP17 SISH	5/5 (100)[a]	0/5 (0)	0/5 (0)	0/5 (0)
Kappa ISH	7/7 (100)	4/7 (57.1)	2/3 (66.7)	2/3 (66.7)
Lambda ISH	5/5 (100)	1/5 (20)	2/2 (100)	0/2 (0)
CyclinD1	9/9 (100)	2/9 (22.2)	3/3 (100)	1/3 (33.3)
Ki67	9/9 (100)	5/9 (55.6)	10/10 (100)	6/10 (45.5)
Bcl2	1/1 (100)	1/1 (100)	4/4 (100)	4/4 (100)
Bcl6	No data	No data	1/1 (100)	1/1 (100)
TdT	No data	No data	1/1 (100)	0/1 (0)
CD138	7/7 (100)	7/7 (100)	3/3 (100)	3/3 (100)
CD20	9/9 (100)	9/9 (100)	9/9 (100)	9/9 (100)
CD79a (B cell)	No data	No data	2/2 (100)	2/2 (100)
CD3	5/5 (100)	5/5 (100)	4/4 (100)	4/4 (100)
CD5	No data	No data	3/3 (100)	3/3 (100)
CD23	No data	No data	1/1 (100)	1/1 (100)
CD10	1/1 (100)	1/1 (100)	1/1 (100)	1/1 (100)
CD30	1/1 (100)	1/1 (100)	No data	No data
Myeloperoxidase	1/1 (100)	1/1 (100)	2/2 (100)	2/2 (100)

HCl, hydrochloric acid; EDTA, ethylenediaminetetraacetic acid disodium salt dehydrate; RDO, RDO GOLD; SISH, silver *in situ* hybridization; ISH, *in situ* hybridization.

[a]Case number showing intact stain result among overall case number stained with each item (%). Positive expression in the indicated tumor cells or internal controls was considered as intact stain. For example, positive expression of cyclin D1 in mantle cell lymphoma cells or endothelial cells was interpreted as intact stain result.

http://dx.doi.org/10.4132/jptm.2015.03.16

HCl group are depicted in Table 3 and Fig. 1. Although differences were not statistically significant, the DNA yield of the EDTA protocol was about 2 times higher than the HCl protocol. In addition, the Ct value of the former protocol was significantly lower than that of the latter ($p < .001$) with the estimated difference being about 7. Furthermore, the Ct values of EDTA processed samples were lower than 30, demonstrating that the amount of intact DNA feasible for PCR with the EDTA protocol is better preserved by a factor of 2^7 than the HCl protocol.

There were no significant differences between DNA yield and Ct values of RDO and HCl methods. The yield of extracted DNA after RDO decalcification was similar to that of HCl. The Ct values of both protocols were above 33, indicating that the amount of intact DNA feasible for PCR was very small.

Morphological comparison of DNA, RNA, and protein expression

The morphological comparison and quality assessment of H&E stain, HER2/CEP17 dual color silver *in situ* hybridization, kappa/lambda *in situ* hybridization, and immunohistochemistry studies were analyzed. The rates of high quality staining for each study were compared between the three protocols. The results are summarized in Table 4.

There was no difficulty in microtome dissection of 4 μm or less in thickness in any of the three methods. The morphological quality of H&E slide was similar in all three protocols, showing well-preserved histological features of the bone marrow (Fig. 2).

All five cases in the RDO versus HCl group had severe DNA breakdown on HER2/CEP17 dual color silver *in situ* hybridization, revealing no HER2 or CEP17 nuclear signal in bone marrow hematopoietic cells. However, in the EDTA versus HCl group, all 5 cases in the EDTA protocol showed two HER2 and CEP17 nuclear signals from almost all of the hematopoietic cells, whereas nearly no nuclear signal was detected in samples from the HCl protocol (Fig. 3).

Bone marrow specimens from the EDTA and RDO protocols that underwent kappa/lambda RNA *in situ* hybridization showed well preserved RNA signal in the nuclei of plasma cells, while those in the HCl group had severe breakdown of RNA signals (Fig. 4).

Nuclear proteins such as Ki67, cyclin D1, and TdT were relatively better preserved on immunohistochemistry with both EDTA and RDO protocols, while samples from the HCl protocol showed breakdown and lower quality of nuclear protein staining (Fig. 5A–H). Immunohistochemistry targeting the cytoplasmic membrane or cytoplasmic CD markers was well preserved in all three protocols (Fig. 5I–L).

DISCUSSION

There have been several studies comparing several types of decalcification protocols to date. Some retrospective studies compared the morphology of *in situ* hybridization or immunohistochemistry by using stored tissues containing bone. Other studies

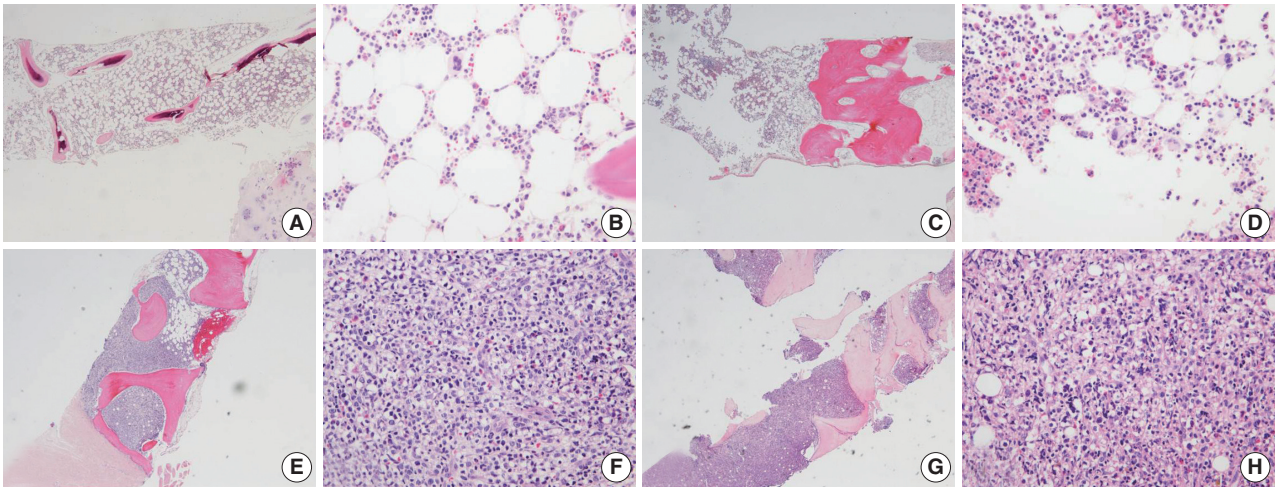

Fig. 2. In EDTA versus HCl comparison of a pair of bone marrow sampled from the same patient (A–D, EDTA versus HCl group; A, B, EDTA protocol; C, D, HCl protocol), and in RDO versus HCl comparison of a pair of bone marrow sampled from the same patient (E–H, RDO versus HCl group; E, F, RDO protocol; G, H, HCl protocol), all the three methods of EDTA, RDO, and HCl protocols demonstrate intact and well-preserved histological features of bone marrow. EDTA, ethylenediaminetetraacetic acid disodium salt dehydrate; HCl, hydrochloric acid; RDO, RDO GOLD.

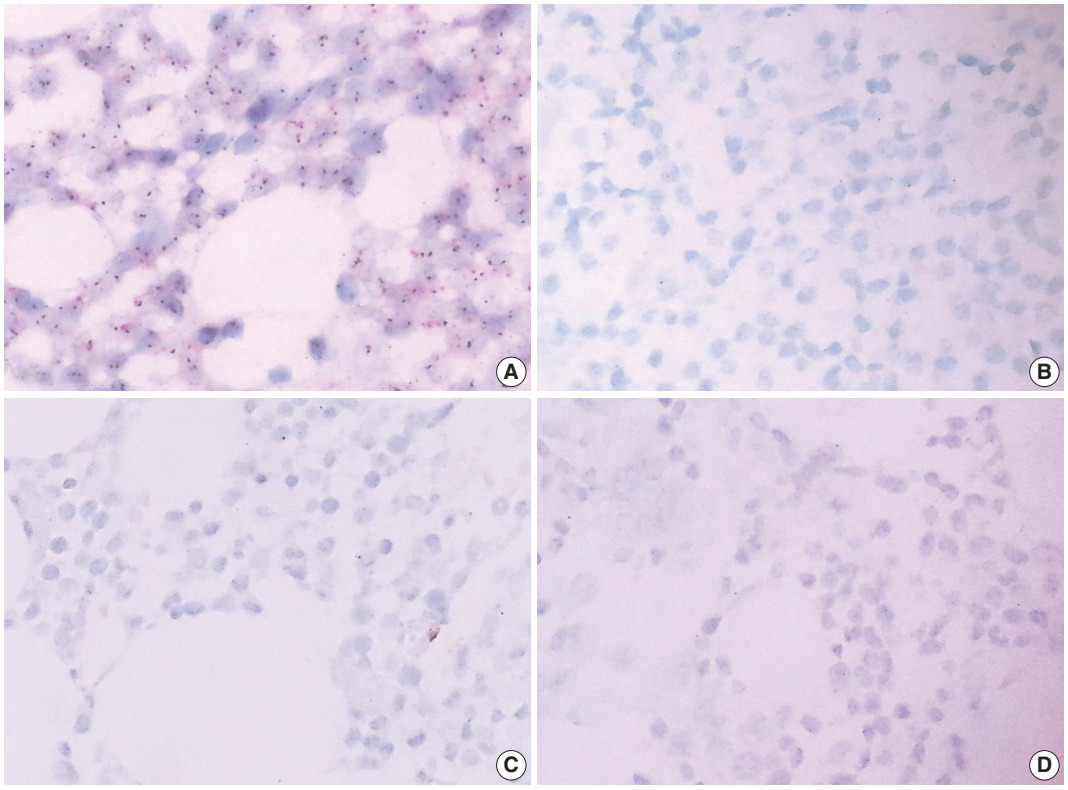

Fig. 3. In HER2 dual color silver *in situ* hybridization study, almost every nucleus in cases of EDTA protocol demonstrates two intact signals of HER2 and CEP17, while cases of RDO or HCl protocol barely demonstrate HER2 or CEP17 signals from the nucleus due to the severe breakdown of DNA (A, B, comparison of EDTA versus HCl in a pair of bone marrow from the same patients; C, D, comparison of RDO versus HCl in a pair of bone marrow from the same patients). EDTA, ethylenediaminetetraacetic acid disodium salt dehydrate; RDO, RDO GOLD; HCl, hydrochloric acid.

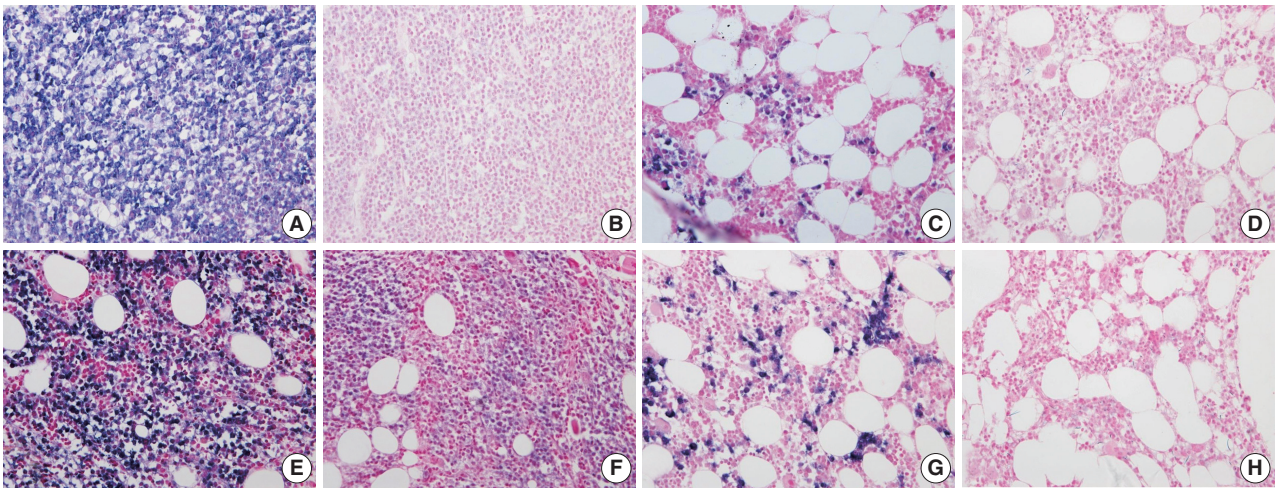

Fig. 4. The quality of RNA is compared in kappa light chain (A–D) and lambda light chain (E–H) RNA *in situ* hybridization using a pair of bone marrow specimens from the same patient. In a case of kappa light chain-restricted plasma cell myeloma, EDTA protocol (A) reveals intact quality while HCl (B) protocol shows poor quality in kappa light chain RNA *in situ* hybridization. In a case of lambda light chain-restricted plasma cell myeloma, EDTA protocol (E) reveals intact quality while HCl (F) protocol shows poor quality. In a case of polyclonal plasma cell infiltration within the bone marrow, the EDTA and RDO protocol (C and G, respectively) reveal intact quality while HCl (D, H) protocol show poor quality in kappa and lambda light chain RNA *in situ* hybridization, respectively. EDTA, ethylenediaminetetraacetic acid disodium salt dehydrate; HCl, hydrochloric acid; RDO, RDO GOLD.

 http://dx.doi.org/10.4132/jptm.2015.03.16

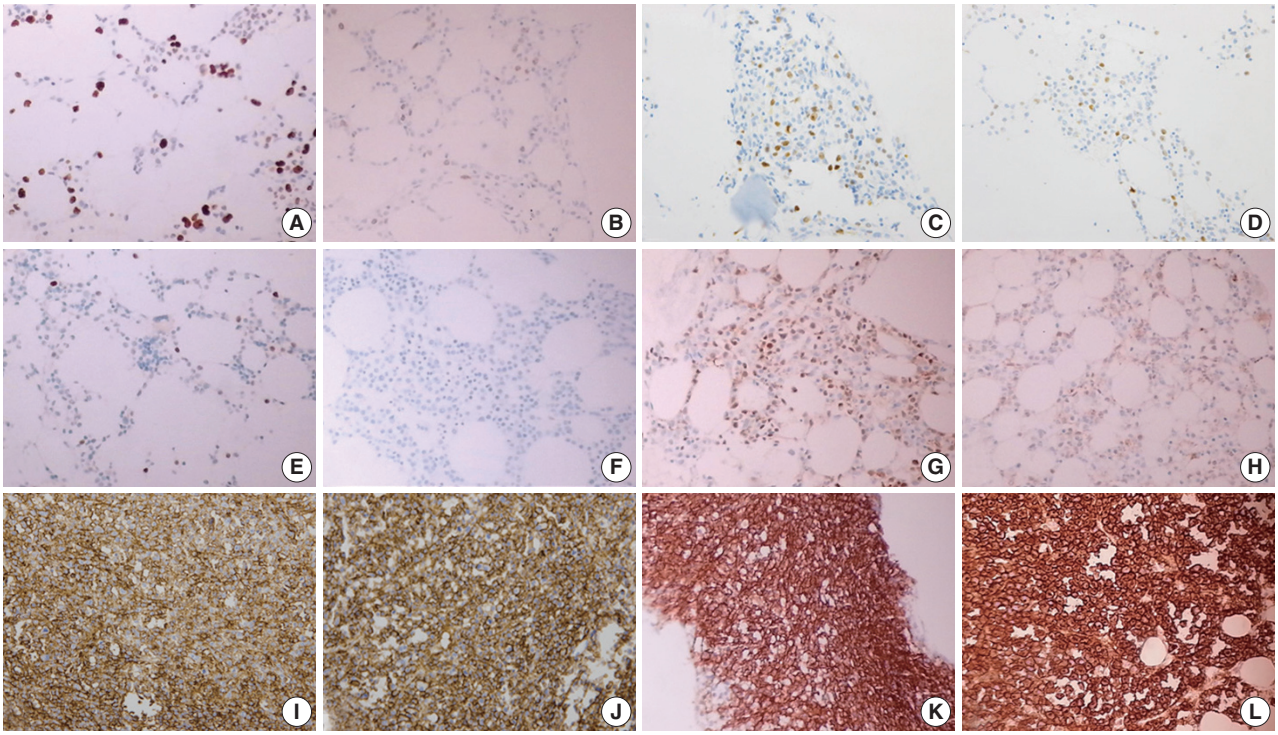

Fig. 5. In immunohistochemistry of Ki67 (A–D), EDTA (A) shows intact quality while HCl (B) shows poor quality in a pair of bone marrow sample from the same patient. A similar result is noted in comparison of RDO (C) versus HCl (D). Nuclear staining of cyclin D1 is intact in EDTA (E), while it is not in HCl (F) of a paired bone marrow from the same patient. Nuclear staining of TdT is intact in RDO (G), while it is poor in HCl (H) of a paired bone marrow from the same patient. Cytoplasmic membrane staining of CD138 (I–L) reveals intact quality in all three protocols: EDTA (I), RDO (K), and HCl (J, L). EDTA, ethylenediaminetetraacetic acid disodium salt dehydrate; HCl, hydrochloric acid; RDO, RDO GOLD.

extracted nucleic acid from stored tissues containing bone and compared the quantity, purity, and Ct value of the DNA and/or RNA after real-time PCR.[1-4] Few studies have used specimens sampled with diagnostic purpose in clinical practice. We investigated the quality of nucleic acid and protein in decalcified bone marrow tissue employing several types of genetic tools, immunohistochemistry, and morphological assessments. In addition, we compared the effect of decalcification protocol while limiting bias variance, which may be caused by sampling from different patients and cell degeneration from long-term storage. We prospectively investigated pairs of bone marrow biopsy specimens from the same patients sampled for diagnostic purposes in a clinical setting. To our knowledge, this is one of the first studies utilizing clinical samples to assess decalcification protocols.

We compared the conventional protocol using HCl, the well-known alternative protocol using EDTA, and the new protocol using RDO.

All three methods had equally good performance with respect to microtome dissection and preservation of cytomorphologic and histomorphologic features. The EDTA protocol was superior in preserving nucleic acid (DNA and RNA), allowing for the feasibility of genetic studies, such as real time PCR and *in situ* hybridization. The EDTA protocol would be an appropriate option for genetic studies in bone-contained tissues. The present study also confirmed that the HCl protocols are inappropriate for genetic studies due to the severe damage of genetic material. The quality of nucleic acids in the RDO group was equivocal, but this method also didn't seem to be suitable for genetic studies. In immunohistochemistry targeting nuclear protein, both EDTA and RDO were relatively superior to the HCl protocol. All three methods showed intact staining in immunohistochemistry targeting cytoplasmic membranes or cytoplasm. EDTA protocols seem to be the most appropriate in that comprehensive immunohistochemical stains can be applied to the specimens processed by this protocol. The feasibility of immunohistochemistry using specimens processed with the HCl protocol would be limited in many cases, especially when immunostaining for nuclear proteins is necessary. Immunohistochemical markers can be more widely applied in samples processed with the RDO protocol than with the HCl protocol, but diagnostic options are still more limited than the EDTA protocol.

In this study, the EDTA protocol was the most feasible method for several types of genetic studies and immunohistochemistry. Such advantages of EDTA decalcification protocol are already widely known.[1,5-7] The present study confirms again the superiority of the EDTA protocol in a wide range of ancillary tests for pathologic diagnosis. The potential of the RDO protocol is higher than the conventional HCl protocol; however, it is not superior to the EDTA protocol and thus, it cannot be considered an alternative to EDTA protocols, particularly when genetic studies are needed.

When choosing decalcification agents, cost-effectiveness and turn-around time from biopsy to final pathologic diagnosis are important issues. HCl costs less and requires less time than using EDTA. Small bone tissues like bone marrow take about three to twenty four hours for decalcification in EDTA protocol, but most of the other bone specimens need more time when using the same protocol. RDO protocols can shorten decalcification time, but this agent is also expensive.

In many cases, bone biopsies are needed for diagnosis of hematologic cancer, metastatic tumors, and primary bone sarcoma; these types of cancers usually need further gene-based diagnosis. Bone marrow biopsy is widely performed in patients with hematologic malignancies and pediatric sarcomas or blastomas. Therefore, preserving genetic materials is critical in handling bone marrow tissues, and cost and turn-around time may be less important in such cases. Preserving intact nucleic acid, as well as intact proteins, is critical to providing not only accurate pathologic diagnosis but also diverse therapeutic options to the patients. Considering this, in this study the EDTA protocol was the most appropriate method for handling bone marrow specimens. RDO may also be useful in that it requires less decalcification time and it enables more ancillary tests than HCl, but its usefulness is limited by less potential for genetic studies in processed samples than EDTA.

In this era of expanding genetic molecular study, better tissue handling methods are needed. The present study suggests an appropriate approach in handling bone marrow tissues, and this approach should be expanded to other types of tissue specimens.

Conflicts of Interest

No potential conflict of interest relevant to this article was reported.

Acknowledgments

This study was supported by a faculty research grant of Yonsei University College of Medicine for 2014 (6-2014-0133).

REFERENCES

1. Singh VM, Salunga RC, Huang VJ, *et al*. Analysis of the effect of various decalcification agents on the quantity and quality of nucleic acid (DNA and RNA) recovered from bone biopsies. Ann Diagn Pathol 2013; 17: 322-6.
2. Reineke T, Jenni B, Abdou MT, *et al*. Ultrasonic decalcification offers new perspectives for rapid FISH, DNA, and RT-PCR analysis in bone marrow trephines. Am J Surg Pathol 2006; 30: 892-6.
3. Brown RS, Edwards J, Bartlett JW, Jones C, Dogan A. Routine acid decalcification of bone marrow samples can preserve DNA for FISH and CGH studies in metastatic prostate cancer. J Histochem Cytochem 2002; 50: 113-5.
4. Alers JC, Krijtenburg PJ, Vissers KJ, van Dekken H. Effect of bone decalcification procedures on DNA in situ hybridization and comparative genomic hybridization. EDTA is highly preferable to a routinely used acid decalcifier. J Histochem Cytochem 1999; 47: 703-10.
5. Adegboyega PA, Gokhale S. Effect of decalcification on the immunohistochemical expression of ABH blood group isoantigens. Appl Immunohistochem Mol Morphol 2003; 11: 194-7.
6. Castania VA, Silveira JW, Issy AC, *et al*. Advantages of a combined method of decalcification compared to EDTA. Microsc Res Tech 2015; 78: 111-8.
7. Wickham CL, Sarsfield P, Joyner MV, Jones DB, Ellard S, Wilkins B. Formic acid decalcification of bone marrow trephines degrades DNA: alternative use of EDTA allows the amplification and sequencing of relatively long PCR products. Mol Pathol 2000; 53: 336.

Journal of Pathology and Translational Medicine 2015; 49: 243-248
http://dx.doi.org/10.4132/jptm.2015.03.30

■ ORIGINAL ARTICLE ■

Smad1 Expression in Follicular Lymphoma

Jai Hyang Go

Department of Pathology,
Dankook University College of Medicine,
Cheonan, Korea

Received: February 25, 2015
Revised: March 20, 2015
Accepted: March 30, 2015

Corresponding Author
Jai Hyang Go, M.D.
Department of Pathology,
Dankook University College of Medicine,
119 Dandae-ro, Dongnam-gu,
Cheonan 330-997, Korea
Tel: +82-41-550-6972
Fax: +82-41-561-9127
E-mail: cyjy555@ hanmail.net

Background: Follicular lymphomas present with various immunohistologic patterns. The immunohistochemical markers used in the diagnosis of follicular lymphoma show variable degrees of sensitivity and specificity, and thus, additional germinal center markers are required. Smad1 has been reported to be overexpressed in follicular lymphoma, but little is known regarding the expression patterns of Smad proteins in human lymphoid tissue. **Methods:** In the present study, we performed immunohistochemistry for traditional germinal center markers and for Smad1 in human reactive lymphoid and follicular lymphoma tissues to investigate Smad1's usefulness in the diagnosis of follicular lymphoma. **Results:** In the reactive germinal centers, most cells were positive for Smad1. Among the 27 follicular lymphoma cases, 17 of 21 (80%) were Smad1 positive, 17 of 27 (63%) were positive for CD10, and 23 of 27 (85%) were positive for Bcl6. Notably, three cases expressed CD10 only, and one only expressed Bcl6. All these cases were grade 3 tumors and showed follicular and diffuse growth patterns. **Conclusions:** These results indicate that Smad1 is a candidate as a germinal center marker. Furthermore, they suggest that the Smad signaling pathway might be involved in follicular lymphoma.

Key Words: Smad1; Bcl6; Lymphoma; Follicular

Follicular lymphoma (FL) is the neoplastic counterpart of normal germinal center (GC) B-cells and can present with various immunohistologic patterns which make them difficult to distinguish from other B-cell lymphomas.[1] Of the GC markers used in the diagnosis of FL, CD10 is a traditional marker of GC B cells and has long been regarded as a reliable marker of both GCs and FL.[2] The reported CD10 positivity rates in FL vary widely, though most reports indicate positivity rate of 60% to 90%.[3] Furthermore, CD10 showed less expression in grade 3 FL than in indolent grades 1 or 2 FL.[4]

Another marker for GC B cells is the Bcl6 protein. The intense and diffuse staining for this protein can also identify tumors arising from follicular GCs.[5] Bcl6 expression is most prominent in FL and displays an expression pattern similar to that of GCs.[2] Immunohistochemical staining for Bcl6 and CD10 can identify tumors of GC B-cell origin, and their co-expression has generally been used as a marker of tumors with a GC B-cell origin.[2]

The immunohistochemical markers typically used in the diagnosis of FL, such as CD10 and Bcl6, show variable degrees of sensitivity and specificity and lack concordance of expression.[1] Thus, additional GC markers are needed. Recently, several other markers such as human GC associated lymphoma (HGAL), LIM-only transcriptional factor 2 (LMO2), and interferon regulatory factor 8 (IRF 8), have been explored.[1] In the search for new GC markers, Smad1 was found to be overexpressed in FL compared to normal GC B cells in a gene expression profiling study, suggesting its possible utility.[6] In the present study, we performed immunohistochemistry for Smad1 in human FL tissues to investigate its usefulness for the diagnosis of FL, and we compared these findings to other traditional GC markers.

MATERIALS AND METHODS

Cases

We retrieved paraffin-embedded tissue blocks of 27 FL cases from the surgical files at our hospital. All cases were diagnosed according to the World Health Organization (WHO) criteria.[7] The B-cell nature of these tumors was confirmed by the immunohistochemical detection of B-cell (CD20) and T-cell (CD3) markers in the paraffin-embedded sections. Tumors were graded as grade 1, 2, or 3 according to the proportion of large cells (centroblasts). In addition, tumors were classified as follicular, follicular and diffuse, or focally follicular according to the proportion of follicular pattern present. To distinguish large, confluent follicles or interfollicular involvement from diffuse areas,

pISSN 2383-7837
eISSN 2383-7845

we stained for follicular dendritic cells using CD21. The study subjects consisted of 17 male and 10 female patients with ages ranging from 23 to 68 years (mean, 47 years). Twenty-one tumors were located in lymph nodes and six were in extranodal sites (tonsil, 5; maxilla, 1). Reactive lymph node tissues were used as a control.

Immunohistochemistry

Immunohistochemical analysis was performed using formalin-fixed, paraffin-embedded materials with primary antibodies to CD10 (1:100, Novocastra Laboratories Ltd., Newcastle upon Tyne, UK), Bcl6 (1:600, Novocastra Laboratories Ltd.), and Smad1 (1:400, Santa Cruz Biotechnology Inc., Santa Cruz, CA, USA). Briefly, sections were deparaffinized in xylene, rehydrated, washed in distilled water, immersed in 10 mM citrate buffer (pH 6), and either microwaved or autoclaved. They were then treated with 3% hydrogen peroxide solution to reduce endogenous peroxidase activity, washed in phosphate-buffered saline, and incubated with the primary antibodies. Bound antibodies were detected by the streptavidin biotin method using an LSAB kit (Dako Co., Carpinteria, CA, USA). The sections were then treated with diaminobenzidine and counterstained with Mayer hematoxylin. Tumor cells were considered positive only when we observed distinct membranous or cytoplasmic staining for CD10 and Smad1 or distinct nuclear staining for Bcl6. Marker expression was considered positive when more than 20% of the neoplastic lymphocytes were stained.

RESULTS

Histologic findings

The morphologic findings of the 27 FL cases are summarized in Table 1. There are seventeen grade 3 tumors, nine tumors with a follicular and diffuse growth pattern, and one tumor with a focally follicular growth pattern.

Immunohistochemical findings

In reactive GCs, most cells (centrocytes and centroblasts) were

Table 1. Morphologic and immunohistochemical findings for follicular lymphomas

Case No.	Sex	Age (yr)	Location	Pattern	Grade	CD10	Bcl6	Smad1
1	F	34	LN-N	F	2	+	+	+
2	F	68	Tonsil	F&D	3	+	–	–
3	F	66	LN-N	FF	3	–	+	+
4	F	50	LN-N	F	1	+	+	+
5	M	48	LN-N	F	2	+	+	+
6	M	57	LN-I	F	3	+	+	+
7	M	35	LN	F	3	+	+	+
8	F	47	LN	F	3	–	+	+
9	M	52	LN-SM	F	3	–	+	+
10	F	37	LN-N	F	1	+	+	+
11	M	23	LN-SM	F	3	+	+	+
12	M	42	LN-N	F&D	3	+	–	–
13	M	42	Tonsil	F&D	3	+	–	–
14	F	40	Tonsil	F&D	3	–	+	+
15	M	62	Maxilla	F&D	3	–	+	+
16	M	48	Tonsil	F&D	3	–	+	+
17	F	45	Tonsil	F&D	3	–	+	–
18	M	60	LN-M	F	1	+	+	+
19	F	53	LN-S	F&D	3	–	+	+
20	M	47	LN-N	F&D	3	–	+	+
21	M	35	LN	F	1	+	+	+
22	F	38	LN-N	F	1	+	+	ND
23	M	60	LN-M	F	1	+	–	ND
24	M	45	LN-N	F	3	–	+	ND
25	M	41	LN-A	F	2	+	+	ND
26	M	34	LN-R	F	2	+	+	ND
27	M	61	LN-N	F	3	+	+	ND

LN, lymph node; N, neck; I, inguinal; SM, submental; M, mediastinal; S, salivary; A, axillary; R, retroperitoneal; F, follicular; F&D, follicular and diffuse; FF, focally follicular; +, positive; –, negative; ND, not-done.

http://dx.doi.org/10.4132/jptm.2015.03.30

positive for Smad1. No other cells expressed Smad1, with the exception of scattered plasma cells, which were more strongly positive than the GC cells (Fig. 1). Smad1 immunostaining was not performed in six cases of FLs because of a shortage of Smad1 antibody. Of the tested FL cases, 17 of 21 (80%) were Smad1+ (Fig. 2A). When we tested common GC markers, 17 of 27 (63%) were positive for CD10 (Fig. 2B) and 23 of 27 (85%) were positive for Bcl6 (Table 2, Fig. 2C). Of the 21 cases immunostained for all three antibodies, all of the grade 1 and 2 tumors were positive for Smad1, CD10, and Bcl6. For the 15 grade 3 tumors, three were positive for all three markers, eight co-expressed Smad1 and Bcl6, three expressed CD10 only and one expressed Bcl6 only (Table 3). Most tumors with a follicular growth pattern were positive for Smad1, CD10, and Bcl6 (9 of 11, 82%), and the remaining were positive for Smad1 and Bcl6 (n = 2). However, of the nine tumors with a follicular and diffuse pattern, five co-expressed Smad1 and Bcl6, three expressed CD10 only, and one expressed Bcl6 only. The one case with a focally follicular pattern was positive for Smad1 and Bcl6 but was negative for CD10 (Table 4).

DISCUSSION

This immunohistochemical study was undertaken to investigate the usefulness of Smad1 for the diagnosis of FL in human reactive lymphoid and FL tissues and to compare Smad1 to the traditional GC markers. Our results indicate the Smad signaling pathway is involved in the maintenance of homeostasis in human lymphoid follicles, and our results demonstrate that Smad1 is a candidate GC marker. In addition, they suggest that the Smad signaling pathway might be functionally active in FL.

CD10 is a cell surface metalloproteinase that reduces the cellular responses to peptide hormones and is found on neutrophils, B lymphoblasts, some T lymphoblasts, normal follicular center cells, follicular helper T cells, and some nonhematopoietic cells.[1,3] CD10 is a traditional marker of GC B cells and has long been regarded as a reliable marker for both GC and FL.[2] Furthermore, its expression is well correlated with the t(14;18)(q32;q21) chromosomal translocation, which is the most reliable diagnostic criterion for FL.[8] DNA microarray analysis has also confirmed the association between CD10 and other genes

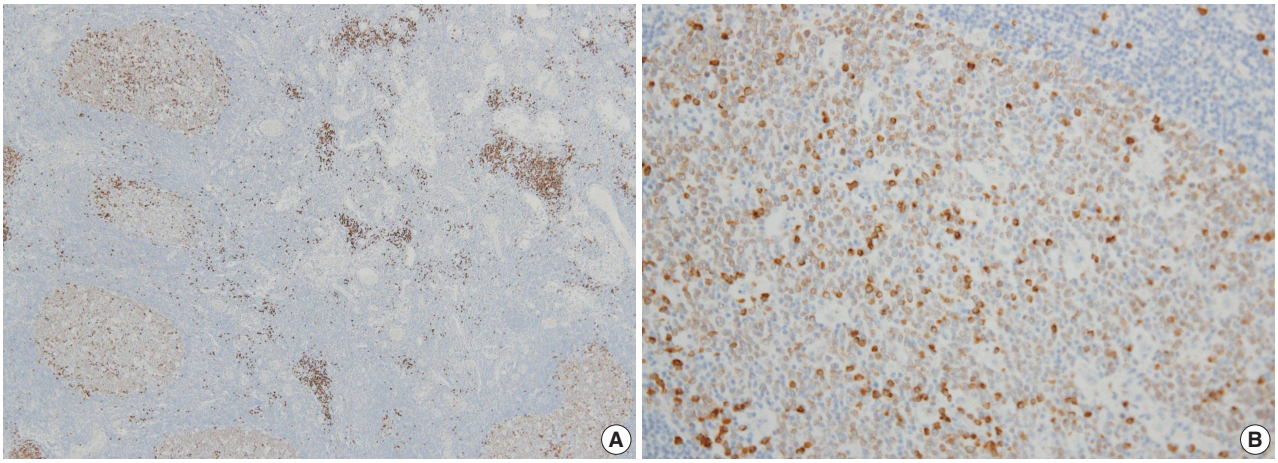

Fig. 1. Immunohistochemical pattern of Smad1 in reactive germinal centers. Most centrocytes and centroblasts are positive for Smad1 with moderate intensity. Scattered plasma cells are more strongly positive than germinal center cells (A, B).

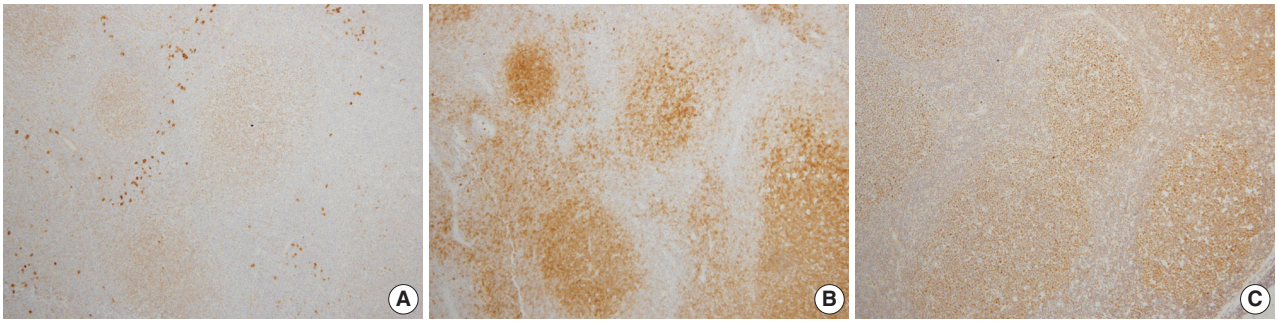

Fig. 2. Immunohistochemical pattern of follicular lymphoma. The tumor cells are positive for Smad1 (A), CD10 (B), and Bcl6 (C).

Table 2. Summary of Immunohistologic results for follicular lymphomas

	CD10	Bcl6	Smad1
Positive	17	23	17
Negative	10	4	4
Positive rate (%)	63	85	80

Table 3. Immunohistologic results according to tumor grade for 21 follicular lymphomas

Grade	Triple (+)	Double (+) Bcl6/Smad1	Single (+) CD10, Bcl6
1	4	0	0
2	2	0	0
3	3	8	3 (CD10), 1 (Bcl6)
Total	9	8	4

Triple (+): Bcl6+, Smad1+, CD10+.

Table 4. Immunohistologic results according to growth pattern for 21 follicular lymphomas

Growth pattern	Triple (+)	Double (+) Bcl6/Smad1	Single (+) CD10, Bcl6
Follicular	9	2	0
Follicular and diffuse	0	5	3 (CD10), 1 (Bcl6)
Focally follicular	0	1	0
Total	9	8	4

Triple (+): Bcl6+, Smad1+, CD10+.

associated with GC cells.[9] However, CD10 positivity in FL varies widely, and most reports on the topic indicate that 60% to 90% of tumors are CD10 positive.[3] Furthermore, CD10 expression is frequently weak to negative in WHO grade 3 FLs,[10] and in one study, CD10 was detected in only 20% of these tumors.[1] Therefore, the lack of CD10 expression does not preclude FL[1] or exclude the possibility that neoplastic lymphocytes originated from follicular center cells in diffuse large B-cell lymphoma (DLBCL).[10] In the present study, CD10 was positive in 63% of the 27 FL cases as follows: grade 1 (6 of 6, 100%), grade 2 (4 of 4, 100%), and grade 3 (7 of 17, 41%); follicular (14 of 17, 82%), follicular and diffuse (3 of 9, 33%), and focally follicular (0 of 1, 0%). Our findings are consistent with other studies[1] and confirm that CD10 expression is frequently weak to absent in high grade FL or in FL with a diffuse growth pattern.

Bcl6 protein is another GC B-cell marker,[10] and its expression, which is independent of Bcl6 gene rearrangement, is largely restricted to GC B cells (centroblasts and centrocytes) in normal human lymphoid tissues.[1,5] Intense and diffuse staining for this protein can also identify tumors arising from follicular GCs.[5] In B-cell lymphoma, Bcl6 expression is most prominent in FL and Burkitt's lymphoma, in which it displays a pattern of expression similar to that of GCs. Bcl6 staining has been useful in detecting tumors of GC B-cell derivation in DLBCL.[2] In addition, staining for Bcl6 and CD10 in combination can identify tumors of GC B-cell origin in archival specimens, and their co-expression is generally used as a tumor marker of tumor of GC B-cell origin.[2] Furthermore, Bcl6's expression has been reported in CD10 negative, MUM1-positive FL, which frequently presents as high grade FL in the absence of the t(14:18) translocation. Bcl6 is a useful adjunct for the diagnosis of CD10 and/or Bcl2-negative FL[1] and is a more reliable marker than CD10, as it is conserved in high grade, interfollicular, and diffuse areas.[11] In the present study, Bcl6 was expressed in 85% of 27 FL cases as follows: grade 1 (5 of 6, 83%), grade 2 (4 of 4, 100%), and grade 3 (14 of 17, 82%); follicular (16 of 17, 94%), follicular and diffuse (6 of 9, 67%), and focally follicular (1 of 1, 100%). These results suggest that Bcl6 is superior to CD10, especially for the diagnosis of high grade FL or FL without a predominant follicular pattern.

Smad proteins play a key role in signal transduction of transforming growth factor beta (TGF-β) family members, including TGF-β and bone morphogenetic proteins.[12,13] Lymphoid tissues and stromal cells (in a mouse model), and T-cells of the developing thymus show widespread expression of the common mediator, Smad4, and show moderate expression of the TGF-β–specific Smads 2 and 3.[14] Using gene expression profiling, Smad1 was found to be the most differentially overexpressed gene in FL compared to normal GC B cells.[6] However, little is known about the expression pattern of Smad proteins in human lymphoid tissue. In the present study, most GC cells (centrocytes and centroblasts) were positive for Smad1 in reactive GCs, and although scattered plasma cells were more strongly positive than GC cells, no other cells expressed Smad1. Furthermore, Smad1 expression was observed in 17 of 21 cases (80%) of FL, which is similar to the positive expression rate of Bcl6. Smad1 was positive in all grade 1 and 2 tumors and in 11 of 15 grade 3 tumors (73%). Regarding growth patterns, all tumors with a follicular pattern (11 of 11, 100%) and five of nine tumors with a follicular and diffuse pattern (56%) were Smad1-positive. One tumor showing a focally follicular growth pattern was also positive for Smad1. Therefore, the addition of Smad1 to the routine diagnostic panel for FL might be useful, especially for the diagnosis of high-grade tumors without a predominant follicular growth pattern. These findings can be extended to the identification of follicular origin tumors in DLBCL. Further studies are needed to determine that Smad1 expression shows higher sensitivity and specificity in FL than those in other B-cell lymphomas, including mantle cell lymphoma, MALT lymphoma,

 http://dx.doi.org/10.4132/jptm.2015.03.30

small lymphocytic lymphoma.

TGF-β is a potent growth inhibitor of most cells, and cellular insensitivity to growth inhibition by TGF-β is a hallmark in the genesis and progression of human cancer. This can be directly linked to inactivating mutations or the loss of expression of various signaling molecules. Therefore, TGF-β and its signaling proteins are regarded as widely established tumor suppressors.[15] The major effects of TGF-β in B-cells are the inhibition of DNA synthesis and the induction of cell cycle arrest, in addition to the induction of apoptosis in some B-cell lines.[6] FLs are the neoplastic counterparts of normal GC B cells,[1] and the overexpression of Bcl-2 in FL cells due to t(14;18)[16] may prevent TGF-β–induced apoptosis.[6]

Although extensively investigated in solid tumors, there have not been many reports of the Smad-associated pathways in B-cell lymphoma.[17] Using gene expression profiling, Smad1 was found to be the most differentially overexpressed gene in FL compared to the normal GC B cells.[6] The overexpression of Smad1 may increase the sensitivity of FL cells to the effects of TGF-β and contribute to the hypoproliferative nature of these cells.[6] One study reported that 13 of 29 (45%) FL or transformed FL samples showed weak to moderate intensity nuclear staining in more than 10% of cells by immunostaining for phosphospecific Ser463/465 Smad1 (Smad1-P) antibody (Cell Signaling Technology, Beverly, MA, USA), which is not presently commercially available. Normal lymphoid tissue was wholly negative or rarely positive for GC cells. In that study, the presence of an active Smad1 pathway was suggested in FL but not in reactive B cells.[16] In the present study, Smad1 expression was observed in 17 of 21 FL cases (80%), using Smad1 (A-4) antibody (sc-7965), which detects cytoplasmic Smad1. Furthermore, many Smad1-positive tumors (10 of 21, 48%) showed strong or moderate positivity in the majority of the tumor cells.

TGF-β signaling through a family of transmembrane receptors and ligand binding to type II receptors results in the recruitment and transphsphorylation of type I receptors that then signal downstream responses and induce phosphorylation of Smad proteins.[15] Once phosphorylated, R-Smads, such as Smad1, associate with Smad4, translocate to the nucleus, and regulate the TGF-β pathway.[16] However, a part of the phosphorylated Smad1 remains in the cytoplasm as well. Taken together, these results suggest that the Smad signaling pathway might be involved in this type of lymphoma. Investigation of the expression of other proteins in the Smad signaling pathway and molecular studies are warranted to determine the mechanisms of the Smad1-specific pathway in FL.

Conflicts of Interest

No potential conflict of interest relevant to this article was reported.

REFERENCES

1. Younes SF, Beck AH, Lossos IS, Levy R, Warnke RA, Natkunam Y. Immunoarchitectural patterns in follicular lymphoma: efficacy of HGAL and LMO2 in the detection of the interfollicular and diffuse components. Am J Surg Pathol 2010; 34: 1266-76.
2. Kwon MS, Go JH, Choi JS, *et al*. Critical evaluation of Bcl-6 protein expression in diffuse large B-cell lymphoma of the stomach and small intestine. Am J Surg Pathol 2003; 27: 790-8.
3. King BE, Chen C, Locker J, *et al*. Immunophenotypic and genotypic markers of follicular center cell neoplasia in diffuse large B-cell lymphomas. Mod Pathol 2000; 13: 1219-31.
4. Borovecki A, Korać P, Nola M, Ivanković D, Jaksić B, Dominis M. Prognostic significance of B-cell differentiation genes encoding proteins in diffuse large B-cell lymphoma and follicular lymphoma grade 3. Croat Med J 2008; 49: 625-35.
5. Ree HJ, Yang WI, Kim CW, *et al*. Coexpression of Bcl-6 and CD10 in diffuse large B-cell lymphomas: significance of Bcl-6 expression patterns in identifying germinal center B-cell lymphoma. Hum Pathol 2001; 32: 954-62.
6. Husson H, Carideo EG, Neuberg D, *et al*. Gene expression profiling of follicular lymphoma and normal germinal center B cells using cDNA arrays. Blood 2002; 99: 282-9.
7. Harris NL, Swerdlow SH, Jaffe ES, *et al*. Follicular lymphoma. In: Swerdlow SH, Campo E, Harris NL, *et al*., eds. WHO classification of tumors of haematopoietic and lymphoid tissues. 4th ed. Lyon: IARC Press, 2008; 220-6.
8. Straka C, Mielke B, Eichelmann A, Trede I, Ho AD, Möller P. Bcl-2 gene rearrangements in primary B-cell lymphoma of the gastrointestinal tract reveal follicular lymphoma as a subtype. Leukemia 1993; 7: 268-73.
9. Alizadeh AA, Eisen MB, Davis RE, *et al*. Distinct types of diffuse large B-cell lymphoma identified by gene expression profiling. Nature 2000; 403: 503-11.
10. Eshoa C, Perkins S, Kampalath B, Shidham V, Juckett M, Chang CC. Decreased CD10 expression in grade III and in interfollicular infiltrates of follicular lymphomas. Am J Clin Pathol 2001; 115: 862-7.
11. Goteri G, Lucarini G, Zizzi A, *et al*. Comparison of germinal center markers CD10, BCL6 and human germinal center-associated lymphoma (HGAL) in follicular lymphomas. Diagn Pathol 2011; 6: 97.
12. Yue J, Frey RS, Mulder KM. Cross-talk between the Smad1 and

Ras/MEK signaling pathways for TGFbeta. Oncogene 1999; 18: 2033-7.
13. Kretzschmar M, Liu F, Hata A, Doody J, Massagué J. The TGF-beta family mediator Smad1 is phosphorylated directly and activated functionally by the BMP receptor kinase. Genes Dev 1997; 11: 984-95.
14. Flanders KC, Kim ES, Roberts AB. Immunohistochemical expression of Smads 1-6 in the 15-day gestation mouse embryo: signaling by BMPs and TGF-betas. Dev Dyn 2001; 220: 141-54.
15. Schiemann WP, Pfeifer WM, Levi E, Kadin ME, Lodish HF. A deletion in the gene for transforming growth factor beta type I receptor abolishes growth regulation by transforming growth factor beta in a cutaneous T-cell lymphoma. Blood 1999; 94: 2854-61.
16. Munoz O, Fend F, de Beaumont R, Husson H, Astier A, Freedman AS. TGFbeta-mediated activation of Smad1 in B-cell non-Hodgkin's lymphoma and effect on cell proliferation. Leukemia 2004; 18: 2015-25.
17. Go JH. Expression pattern of Smad proteins in diffuse large B-cell lymphomas. Korean J Pathol 2004; 38: 301-5.

 http://dx.doi.org/10.4132/jptm.2015.03.30

Journal of Pathology and Translational Medicine 2015; 49: 249-256
http://dx.doi.org/10.4132/jptm.2015.03.27

■ ORIGINAL ARTICLE ■

MUC2 Expression Is Correlated with Tumor Differentiation and Inhibits Tumor Invasion in Gastric Carcinomas: A Systematic Review and Meta-analysis

Jung-Soo Pyo · Jin Hee Sohn
Guhyun Kang[1] · Dong-Hoon Kim
Kyungeun Kim · In-Gu Do
Dong Hyun Kim

Department of Pathology, Kangbuk Samsung Hospital, Sungkyunkwan University School of Medicine, Seoul; [1]Department of Pathology, Inje University Sanggye Paik Hospital, Seoul, Korea

Received: February 25, 2015
Revised: March 23, 2015
Accepted: March 26, 2015

Corresponding Author
Jin Hee Sohn, M.D.
Department of Pathology, Kangbuk Samsung Hospital, Sungkyunkwan University School of Medicine, 29 Saemunan-ro, Jongno-gu, Seoul 110-746, Korea
Tel: +82-2-2001-2391
Fax: +82-2-2001-2398
E-mail: jhpath.sohn@samsung.com

Background: While MUC2 is expressed in intestinal metaplasia and malignant lesions, the clinicopathological significance of MUC2 expression is not fully elucidated in gastric carcinoma (GC). **Methods:** The present study investigated the correlation between MUC2 expression and clinicopathological parameters in 167 human GCs. In addition, to confirm the clinicopathological significance of MUC2 expression, we performed a systematic review and meta-analysis in 1,832 GCs. **Results:** MUC2 expression was found in 58 of 167 GCs (34.7%). MUC2-expressing GC showed lower primary tumor (T), regional lymph node (N), and tumor node metastasis (TNM) stages compared with GCs without MUC2 expression ($p=.001$, $p=.001$, and $p=.011$, respectively). However, MUC2 expression was not correlated with Lauren's classification and tumor differentiation. In meta-analysis, MUC2 expression was significantly correlated with differentiation and lower tumor stage (odds ratio [OR], 1.303; 95% confidence interval [CI], 1.020 to 1.664; $p=.034$ and OR, 1.352; 95% CI, 1.055 to 1.734; $p=.017$, respectively) but not with Lauren's classification, pN stage, or pTNM stage. **Conclusions:** MUC2 expression was correlated with a lower tumor depth and lower lymph node metastasis in our study; the meta-analysis showed a correlation of MUC2 expression with tumor differentiation and lower tumor depth.

Key Words: Gastric carcinoma; MUC2; Clinicopathological significance; Meta-analysis

Mucin expression shows variable patterns in the gastrointestinal tract based on organ and specific conditions. Gastric markers, such as MUC1, MUC5AC, and MUC6 are expressed in the stomach, and intestinal markers, such as MUC2, may be expressed in cases of intestinal metaplasia or malignant lesions, although MUC2 is not constitutively expressed in normal gastric mucosa.[1-4] Based on the pattern of intestinal and gastric mucin expression, gastric carcinomas (GCs) are subclassified into gastric, intestinal, mixed, or null phenotypes.[4] Although many studies have reported the significance of mucin expression and mucin phenotypes and their correlation with tumor behavior and prognosis, the clinicopathological significance has not been fully elucidated in GC.

In gastric mucosa with incomplete intestinal metaplasia (type II or III), which are considered to be precancerous lesions of GC, MUC2 is expressed in both goblet and columnar cells.[5,6] In addition, MUC2-expressing GCs are believed to result from intestinal metaplasia-dysplasia-carcinoma cascades,[5,6] although the complete understanding of its regulatory mechanisms and clinicopathological significance is yet to be elucidated.

In the present study, we investigated the correlation between MUC2 expression and clinicopathological parameters in 167 surgically resected GCs using tissue-microarray slides. Systematic review and meta-analysis were performed additionally to confirm the clinicopathological significance of MUC2 expression in all available studies, including the present study.

MATERIALS AND METHODS

Patients

The files of 167 patients who had undergone surgical resection of GCs in Kangbuk Samsung Hospital, Sungkyunkwan

pISSN 2383-7837
eISSN 2383-7845

University School of Medicine (Seoul, Korea), from January 1, 1992, to December 31, 1996, were analyzed. We evaluated clinicopathological characteristics, such as age, gender, location of tumor, Lauren's classification, tumor differentiation, lymphatic invasion, nodal metastasis, and pathologic tumor node metastasis (pTNM) stages, by reviewing medical charts, pathological records, and glass slides. The patients had undergone curative resection, subtotal gastrectomy or total gastrectomy. This protocol was reviewed and approved by the Institutional Review Board of Kangbuk Samsung Hospital (approval No. KBC12125).

Tissue array methods

Seven array blocks containing a total of 167 tissue cores of resected GCs obtained from patients were prepared. Briefly, tissue cores (2 mm in diameter) were taken from individual paraffin-embedded GCs (donor blocks) and arranged in recipient paraffin blocks (tissue-array block) using a trephine apparatus. The staining results of the different intra-tumoral areas in these tissue-array blocks showed excellent agreement. A core was chosen from each case for analysis. We defined an adequate case as a tumor occupying more than 10% of the core area. Each block contained internal controls consisting of non-neoplastic gastric tissue. Sections 4 μm in thickness were cut from each tissue-array block, deparaffinized, and dehydrated.

Immunohistochemical staining and evaluation

Sections were deparaffinized and hydrated by a routine xylene-alcohol series. For antigen retrieval, sections were treated with 0.01 M citrate buffer (pH 6.0) for 5 minutes in a microwave oven followed by treatment with 3% H_2O_2 to quench endogenous peroxidase. Sections were treated with normal serum of the host animal of the secondary antibody to block nonspecific binding. Sections were then incubated with anti-MUC2 antibody (1:200, Leica Biosystems, Newcastle upon Tyne, UK) as described previously.[7] Immunohistochemical stains were performed using a compact polymer method using a Bond Intense Detection Kit (Leica Biosystems). Visualization was performed by treatment with 3,3'-diaminobenzidine (Vector Laboratories, Burlingame, CA, USA). To confirm the reaction specificity of the antibody, a negative control stain without primary antibody was utilized. All immunostained sections were lightly counterstained with Mayer's hematoxylin.

Immunohistochemical stainings were evaluated by two pathologists. MUC2 showed immunoreactivity in the cytoplasm or cell membrane of tumor cells. Immunostaining results were considered positive if more than 5% of tumor cells were stained.

Published studies search and selection criteria

Relevant articles were obtained by searching the PubMed and Web of Science databases up to September 30, 2014. Searches were performed using the following keywords: 'MUC2,' 'gastric carcinoma,' and 'immunohistochemistry.' The title and abstract of all searched articles were screened for exclusion. Review articles were also screened to find additional eligible studies. The search results were then scanned according to the following inclusion and exclusion criteria: (1) MUC2 expression was investigated in human GC tissue, (2) the correlation between MUC2 expression and clinicopathological parameters was included, (3) case reports were excluded, and (4) all were English-language publications.

Data extraction

Data from all eligible studies were extracted by two pathologists. The following data were extracted from each of the eligible studies: the first author's name, year of publication, manufacturer and dilution ratio of each MUC2 antibody, MUC2 cut-off value, number of patients analyzed, tumor differentiation, and pTNM stage.

Statistical analysis

Statistical analyses were performed using SPSS ver. 18.0 (SPSS Inc., Chicago, IL, USA). The significance of the correlation between the expression of MUC2 and the clinicopathological parameters was determined by either the χ^2 test or the Fisher exact test (two-sided). The results were considered statistically significant when $p < .05$. Moreover, to perform the meta-analysis, the Comprehensive Meta-Analysis software package (Biostat, Engelwood, NJ, USA) was used. Odds ratios (ORs) with a 95% confidence interval (CI) were calculated by a fixed-effects model and used to evaluate the correlation between MUC2 expression and clinicopathological parameters. The fixed-effect model was selected in the current meta-analysis, because we analysed correlation between immunoexpression and the clinicopathological parameters by single-effect-event (positive or negative), but not by mean. Heterogeneity between studies was evaluated with the Q test, I^2 statistics and p-values. For assessment of publication bias, Begg's funnel plot and Egger's test were performed. The results were two-sided and considered statistically significant when $p < .05$.

RESULTS

Clinicopathological features of MUC2-expressing GCs

MUC2 was expressed in 58 (34.7%) of 167 GCs in the im-

http://dx.doi.org/10.4132/jptm.2015.03.27

munohistochemical study (Fig. 1). MUC2 expression was significantly higher in early GCs compared to advanced GCs (p = .001). In addition, GCs expressing MUC2 showed significantly lower rates of lymphatic invasion, lymph node metastasis, and pTNM stages (p = .010, p = .001, and p = .011, respectively). However, there was no correlation of MUC2 expression with other clinicopathological parameters such as age, gender, location of tumor, Lauren's classification, or tumor differentiation in our study (Table 1).

Systematic review and meta-analysis

To confirm the clinicopathological significances of MUC2 expression, we performed a systematic review and meta-analysis. In the current meta-analysis, 195 studies were identified through database searches and were screened. Of these studies, 88 reports were excluded due to insufficient information for correlation between clinicopathological parameters and MUC2 expression. In addition, 32 reports were non-adenocarcinoma studies and 42 reports were non-stomach studies. An additional 22 reports were excluded because they were studies using animal or cell lines, duplicated reports, or case reports. The current meta-analysis included 12 eligible studies, including our data (Fig. 2).[1,3,8-16] The number of total patients was 1,832, including 167 patients from our study.

MUC2 expression was found in 827 of 1,832 GCs (45.1%), and the range in eligible studies was 22.9%–90.7% (Table 2). MUC2 expression was significantly correlated with tumor differentiation (OR, 1.303; 95% CI, 1.020 to 1.664; p = .034; I^2 = 79.3%) (Fig. 3A) and lower tumor depth (pT1) (OR, 1.352; 95% CI, 1.055 to 1.734; p = .017; I^2 = 65.7%) (Fig. 4A). However, Lauren's classification was not correlated with MUC2 expression (OR, 1.245; 95% CI, 0.933 to 1.661; p = .137; I^2 = 83.2%) (Fig. 3B), consistent with our immunohistochemical study. Unlike our result, meta-analysis showed no significant correlation between MUC2 expression and nodal stage or TNM stage (OR, 0.872; 95% CI, 0.689 to 1.104; p = .256; I^2 = 68.4% and OR, 1.208; 95% CI, 0.940 to 1.552; p = .139; I^2 = 21.3%, respectively) (Fig. 4B, C). Significant heterogeneities between studies were identified in tumor differentiation, Lauren's classification, tumor depth and nodal stage but not TNM stage. In Begg's funnel plots,

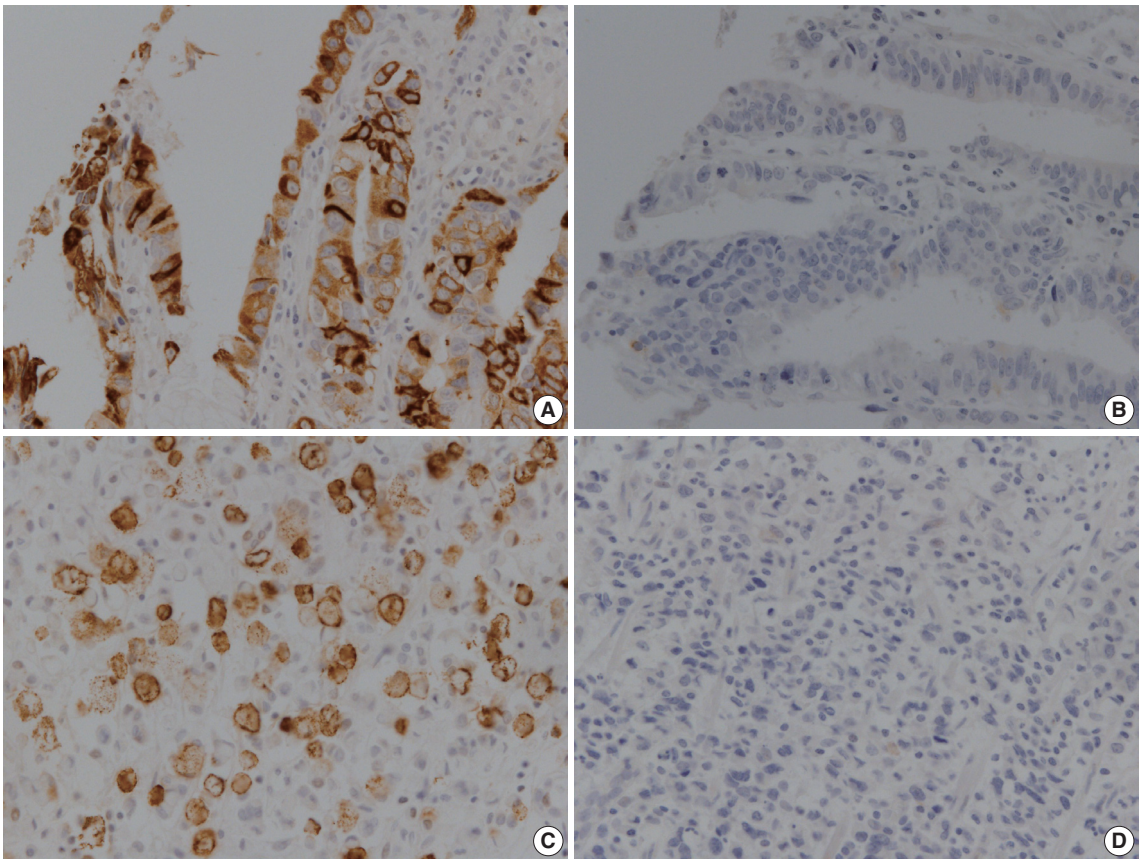

Fig. 1. Representative images showing immunoreactivity for MUC2 in human gastric carcinoma. (A, B) Well-differentiated gastric adenocarcinoma. (C, D) Poorly differentiated gastric adenocarcinoma.

no definite asymmetry was identified (data not shown). Moreover, Egger's test showed no evidence of publication bias (Table 3).[1,3,8-16]

Table 1. The correlation between the MUC2 expression and clinicopathological parameters in gastric carcinomas

Parameter	MUC2-negative	MUC2-positive	p-value
Total (n = 168)	109 (65.3)	58 (34.7)	
Age (yr)			.573
0–39	12 (60.0)	8 (40.0)	
40–65	77 (64.2)	43 (35.8)	
66–99	20 (74.1)	7 (25.9)	
Gender			.365
Male	77 (60.4)	37 (32.5)	
Female	32 (67.5)	21 (39.6)	
Location of tumor			.42
Antrum	53 (62.4)	32 (37.6)	
Body, cardia	56 (68.3)	26 (31.7)	
Lauren's classification			.114
Intestinal	65 (68.4)	30 (31.6)	
Diffuse	40 (65.6)	21 (34.4)	
Mixed	4 (36.4)	7 (63.6)	
Tumor differentiation			.419
Well or moderate	34 (36.6)	59 (63.4)	
Poorly	22 (30.6)	50 (69.4)	
EGC	28 (48.3)	30 (51.7)	.001
AGC	81 (74.3)	28 (25.7)	
Lymphatic invasion			.01
Present	42 (79.2)	11 (20.8)	
Absent	67 (58.8)	47 (41.2)	
Lymph node metastasis			.001
Present	62 (77.5)	18 (22.5)	
Absent	47 (54.0)	40 (46.0)	
pTNM stage			.011
I	38 (52.8)	34 (47.2)	
II	36 (76.6)	11 (23.4)	
III	34 (75.6)	11 (24.4)	
IV	1 (33.3)	2 (66.7)	

Values are presented as number (%).
EGC, early gastric carcinoma; AGC, advanced gastric carcinoma.

DISCUSSION

While various mucins are expressed in GCs, the correlation between MUC2 expression and clinicopathological characteristics remains controversial. In addition, MUC2 could be expressed in benign lesions as well as GC. Therefore, a systemic review and meta-analysis is useful for the elucidation of the clinicopathological significance of MUC2 expression in GCs.

MUC2, an intestinal mucin marker, is not expressed in normal gastric mucosa,[17,18] unlike other gastric mucin markers such as MUC1, MUC5AC, and MUC6.[19] The roles of induced MUC2 expression in GC are not fully elucidated and have been controversial in previous studies. In our immunohistochemical study, MUC2 expression was significantly correlated with lower tumor depth (p = .001), lower nodal metastasis rate (p = .001), and lower pTNM stage (p = .011). Unlike our results, the correlations between MUC2 expression and pathologic primary tumor (pT), regional lymph node (pN), and pTNM stage are controversial.[1,3,8-16] These discrepancies might be caused by various factors, such as composition of tumor types and differences by country. Therefore, it is difficult to determine the clinicopathological significance of MUC2 via our study alone, which led us to analyze previous studies by systematic review and meta-analysis for confirmation of our data.

In the current meta-analysis, MUC2 expression was significantly correlated with lower pT stage, consistent with our results. In our published *in vitro* study data, MUC2-expressing GC cells showed lower rates of tumor invasion and migration than non-MUC2–expressing GC cells.[20] This result reinforces the finding that MUC2 expression seems to be associated with lower pT stage. On the other hand, a meta-analysis of colorectal

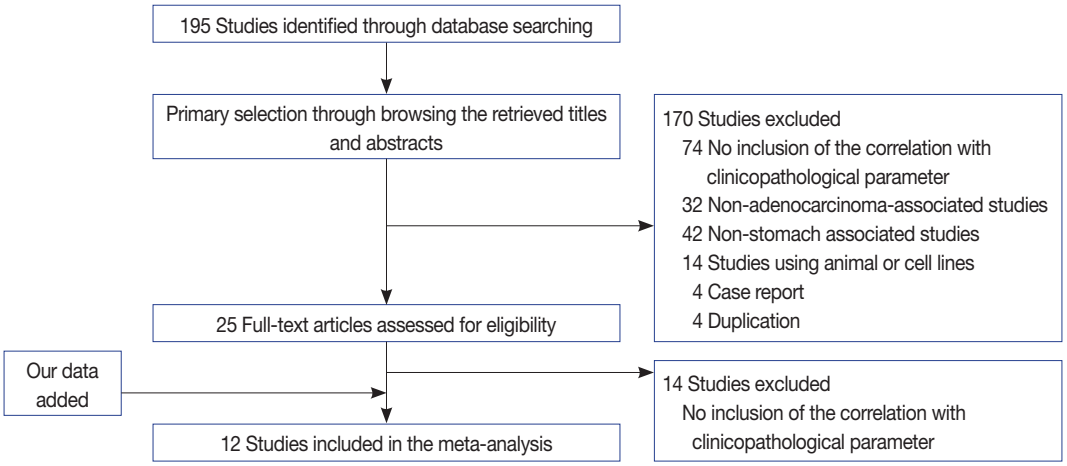

Fig. 2. Flow chart for study search and selection.

http://dx.doi.org/10.4132/jptm.2015.03.27

cancer reported that MUC2 positivity was significantly correlated with higher pT3 and pT4 stages.[21] Correlation with nodal metastasis was controversial in both GC and colon cancer meta-analysis, while our current immunohistochemical study showed a correlation between MUC2 expression and lower nodal metastasis in GC. Further study is needed to define this relationship. Taken together, our results and previous reports suggest that induction of MUC2 may carry out dissimilar functions through different mechanisms according to the specific organ.

Lauren's classification and World Health Organization tumor differentiation are usually used for evaluation of GC in practice. In the current immunohistochemical study, there were no significant correlations between MUC2 expression and Lauren's classification or tumor differentiation. However, the current meta-analysis showed that MUC2 positivity was significantly correlated with degree of GC differentiation, unlike our result. This discrepancy might also be caused by various factors such as composition of tumor types, differences in number of cases analyzed,

Table 2. Main characteristics of the eligible studies

Source	Country	Antibody corporation	Dilution ratio	Cut off (%)	No. of patients	No. of MUC2-positive
Akyürek *et al.*[8] (2002)	Turkey	Novacastra	1:100	5	143	60
Baldus *et al.*[9] (1998)	Germany	Donation	1:1,000	5	128	49
Barresi *et al.*[10] (2006)	Italy	Novacastra	1:100	5	40	20
Ilhan *et al.*[1] (2010)	Turkey	Neomarkers	1:100	5	257	233
Lee *et al.*[3] (2001)	Korea	Santa Cruz	1:100	20	300	82
Lee *et al.*[11] (2007)	Korea	Neomarker	-	-	98	53
Shiratsu *et al.*[12] (2014)	Japan	Novacastra	1:200	5	214	49
Tanaka *et al.*[13] (2003)	Japan	Santa Cruz	1:100	30	209	83
Utsunomiya *et al.*[14] (1998)	Japan	Novacastra	1:600	5	136	48
Wang and Fang[15] (2003)	China	-	1:150	10	46	31
Zhang *et al.*[16] (2004)	China	Shenzhen Jingmei Biot	-	-	94	61
Our study	Korea	Novacastra	1:100	5	167	58

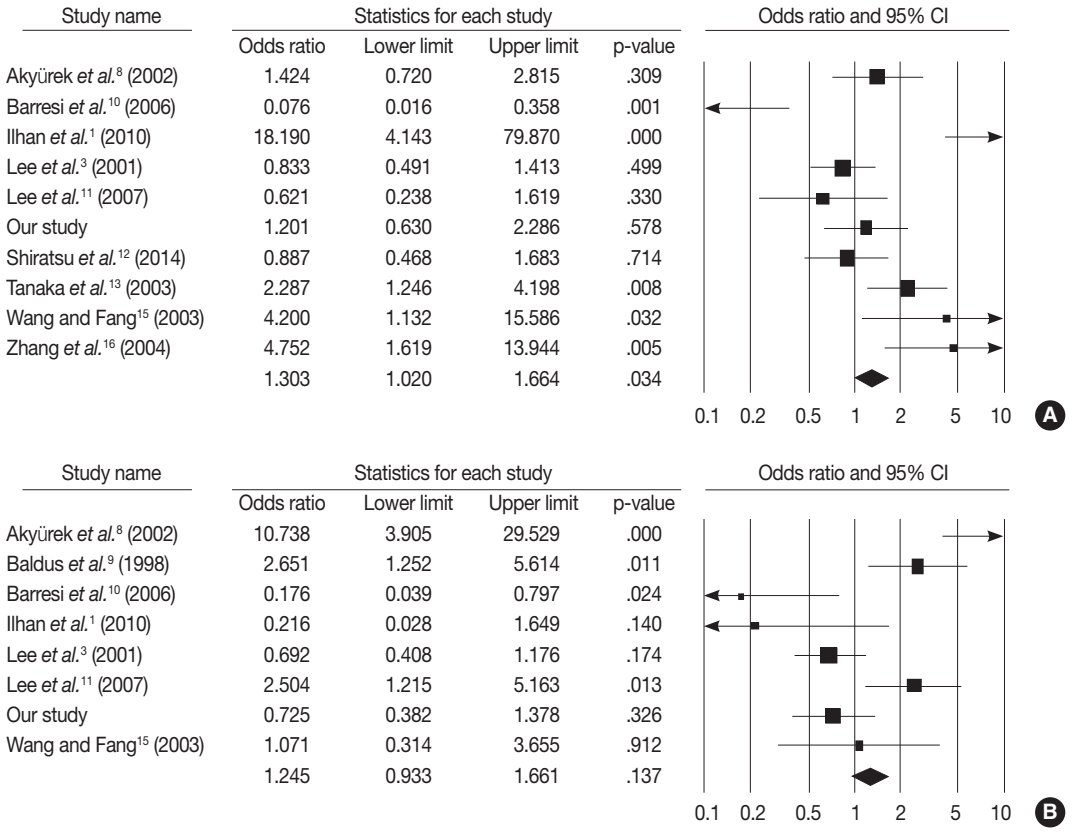

Fig. 3. Forest plot diagram for tumor differentiation (A) and Lauren's classification (B). CI, confidence interval.

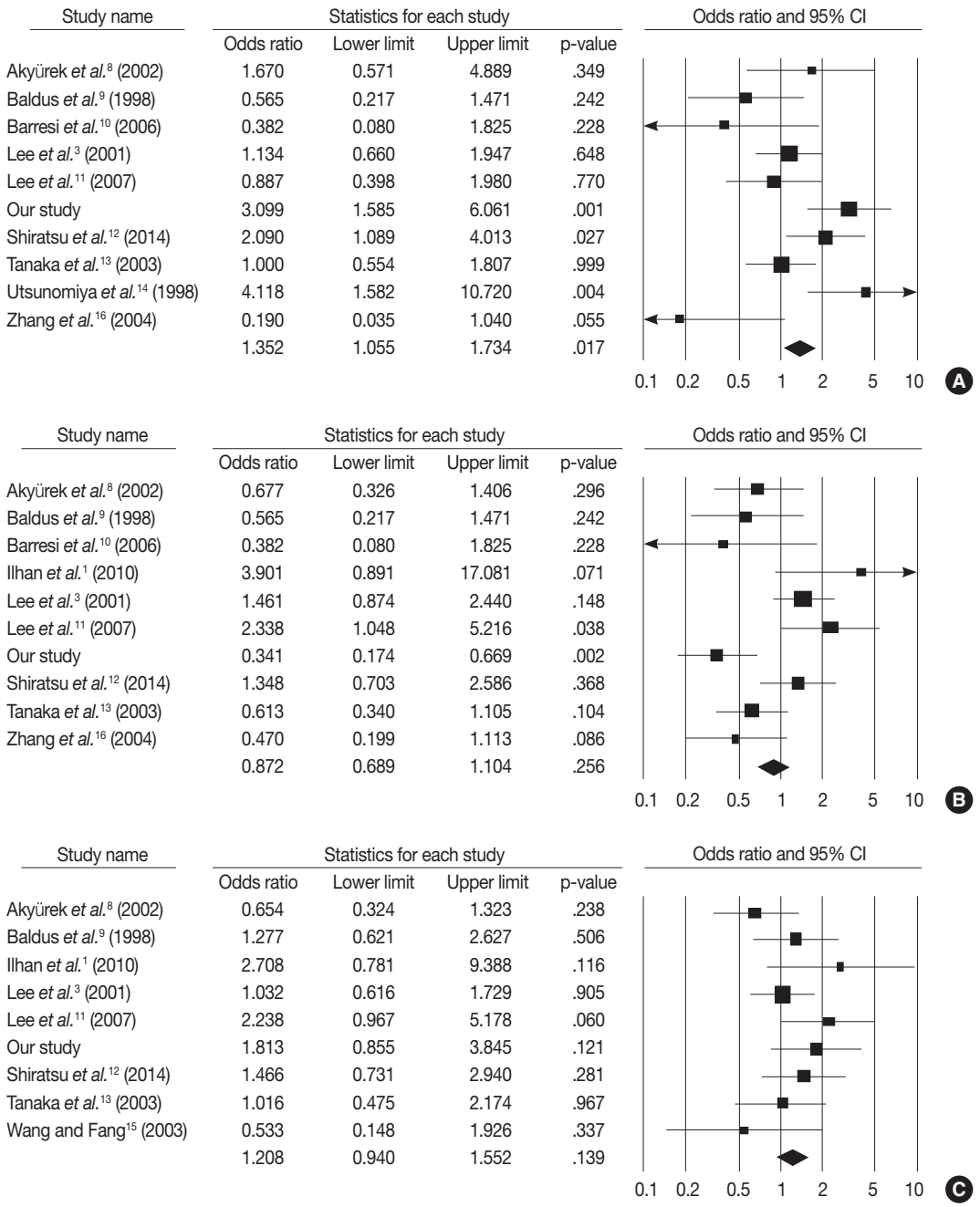

Fig. 4. Forest plot diagram for pathologic primary tumor (A), regional lymph node (B), and tumor node metastasis (C) stages. CI, confidence interval.

differences by country, and heterogeneity of MUC2 positivity. In addition, whether MUC2 expression is associated with tumor differentiation in GC has not been fully elucidated. Nevertheless, based on previous studies and meta-analysis, MUC2 expression was correlated with differentiation and progression and may be considered to be a representative feature of differentiated cells.[14,22]

In the current meta-analysis, MUC2 expression was shown in 22.9%–90.7% of GCs.[1,3,8-16] This wide variability may have been induced by variable dilution ratios and manufacturers of these antibodies. In addition, various cut-off values (5%–30%) were used for evaluation of MUC2 expression, and many studies (6 of 11 studies) used a 5% cut-off value, including ours. MUC2 expression showed significantly higher rates in studies with a 5% cut-off value than other studies ($p < .001$, data not shown). However, the rates of MUC2 expression in subgroups with 5%

cut-off value and other cut-off values overlapped at 22.9%–90.7% and 27.3%–67.4%, respectively. Whether a difference in cut-off value could have an effect on the positive rate of MUC2 expression was not clear in our current systematic review. Moreover, each study included various types of GCs and different compositions. In addition, because some studies used tissue microarray, heterogeneity of MUC2 expression should be considered. These differences may have an effect on the discrepancies of MUC2 positivity between studies. Further studies are needed for confirmation of the clinicopathological significance of MUC2 expression with more eligible criteria and a larger number of patients.

Eligible studies included studies in Korea (3 studies), Japan (3 studies), China (2 studies), Turkey (2 studies), Germany (1 study), and Italy (1 study); eight of twelve studies were conducted in East Asia. According to country, MUC2 positivity was significantly higher in Europe than in East Asia (63.7% vs. 36.8%, $p < .001$, data not shown). The results of meta-analysis in pT and pN stages differed between European and East Asian patients. MUC2 expression was significantly correlated with lower depth of invasion in East Asian patients but not significantly correlated in European patients (OR, 1.484; 95% CI, 1.134 to 1.941; $p = .004$ and OR, 0.746; 95% CI, 0.448 to 1.243; $p = .261$, respectively). However, there was no correlation between MUC2 expression and lymph node metastasis in both East Asian and European patients. Differences in ethnicity and country may affect the discrepancies in the roles of MUC2 expression. The precise mechanisms are not yet fully understood, and more studies including *in vitro* study are needed.

In conclusion, our meta-analysis showed that MUC2 expression was significantly correlated with tumor differentiation and depth. However, the correlation between MUC2 expression and other clinicopathological characteristics is controversial. Further studies are needed in order to elucidate the role of MUC2 expression as a prognostic predictor in GC.

Conflicts of Interest

No potential conflict of interest relevant to this article was reported.

REFERENCES

1. İlhan Ö, Han Ü, Önal B, Çelik SY. Prognostic significance of MUC1, MUC2 and MUC5AC expressions in gastric carcinoma. Turk J Gastroenterol 2010; 21: 345-52.
2. Kim JY, Shin NR, Kim A, *et al.* Microsatellite instability status in gastric cancer: a reappraisal of its clinical significance and relationship with mucin phenotypes. Korean J Pathol 2013; 47: 28-35.
3. Lee HS, Lee HK, Kim HS, Yang HK, Kim YI, Kim WH. MUC1, MUC2, MUC5AC, and MUC6 expressions in gastric carcinomas: their roles as prognostic indicators. Cancer 2001; 92: 1427-34.
4. Wakatsuki K, Yamada Y, Narikiyo M, *et al.* Clinicopathological and prognostic significance of mucin phenotype in gastric cancer. J Surg Oncol 2008; 98: 124-9.
5. Busuttil RA, Boussioutas A. Intestinal metaplasia: a premalignant lesion involved in gastric carcinogenesis. J Gastroenterol Hepatol 2009; 24: 193-201.
6. Reis CA, David L, Correa P, *et al.* Intestinal metaplasia of human stomach displays distinct patterns of mucin (MUC1, MUC2, MUC5AC, and MUC6) expression. Cancer Res 1999; 59: 1003-7.
7. Pyo JS, Kang G, Kim DH, *et al.* Activation of nuclear factor-kappaB contributes to growth and aggressiveness of papillary thyroid carcinoma. Pathol Res Pract 2013; 209: 228-32.
8. Akyürek N, Akyol G, Dursun A, Yamaç D, Günel N. Expression of MUC1 and MUC2 mucins in gastric carcinomas: their relationship with clinicopathologic parameters and prognosis. Pathol Res Pract 2002; 198: 665-74.
9. Baldus SE, Zirbes TK, Engel S, *et al.* Correlation of the immunohistochemical reactivity of mucin peptide cores MUC1 and MUC2 with the histopathological subtype and prognosis of gastric carcinomas. Int J Cancer 1998; 79: 133-8.
10. Barresi V, Vitarelli E, Grosso M, Tuccari G, Barresi G. Relationship between immunoexpression of mucin peptide cores MUC1 and MUC2 and Lauren's histologic subtypes of gastric carcinomas. Eur J Histochem 2006; 50: 301-9.
11. Lee HW, Yang DH, Kim HK, *et al.* Expression of MUC2 in gastric carcinomas and background mucosae. J Gastroenterol Hepatol 2007; 22: 1336-43.
12. Shiratsu K, Higuchi K, Nakayama J. Loss of gastric gland mucin-specific O-glycan is associated with progression of differentiated-type adenocarcinoma of the stomach. Cancer Sci 2014; 105: 126-33.
13. Tanaka M, Kitajima Y, Sato S, Miyazaki K. Combined evaluation of mucin antigen and E-cadherin expression may help select patients with gastric cancer suitable for minimally invasive therapy. Br J Surg 2003; 90: 95-101.
14. Utsunomiya T, Yonezawa S, Sakamoto H, *et al.* Expression of MUC1 and MUC2 mucins in gastric carcinomas: its relationship with the prognosis of the patients. Clin Cancer Res 1998; 4: 2605-14.
15. Wang RQ, Fang DC. Alterations of MUC1 and MUC3 expression in gastric carcinoma: relevance to patient clinicopathological features. J Clin Pathol 2003; 56: 378-84.
16. Zhang HK, Zhang QM, Zhao TH, Li YY, Yi YF. Expression of mu-

cins and E-cadherin in gastric carcinoma and their clinical significance. World J Gastroenterol 2004; 10: 3044-7.

17. Audie JP, Janin A, Porchet N, Copin MC, Gosselin B, Aubert JP. Expression of human mucin genes in respiratory, digestive, and reproductive tracts ascertained by *in situ* hybridization. J Histochem Cytochem 1993; 41: 1479-85.
18. Chang SK, Dohrman AF, Basbaum CB, *et al.* Localization of mucin (MUC2 and MUC3) messenger RNA and peptide expression in human normal intestine and colon cancer. Gastroenterology 1994; 107: 28-36.
19. Kocer B, Soran A, Kiyak G, *et al.* Prognostic significance of mucin expression in gastric carcinoma. Dig Dis Sci 2004; 49: 954-64.
20. Pyo JS, Ko YS, Kang G, *et al.* Bile acid induces MUC2 expression and inhibits tumor invasion in gastric carcinomas. J Cancer Res Clin Oncol 2014 Dec 5 [Epub]. http://dx.doi.org/10.1007/s00432-014-1890-1.
21. Li L, Huang PL, Yu XJ, Bu XD. Clinicopathological significance of mucin 2 immuno-histochemical expression in colorectal cancer: a meta-analysis. Chin J Cancer Res 2012; 24: 190-5.
22. Gong L, Debruyne PR, Witek M, *et al.* Bile acids initiate lineage-addicted gastroesophageal tumorigenesis by suppressing the EGF receptor-AKT axis. Clin Transl Sci 2009; 2: 286-93.

Journal of Pathology and Translational Medicine 2015; 49: 257-261
http://dx.doi.org/10.4132/jptm.2015.04.14

■ ORIGINAL ARTICLE ■

IDH Mutation Analysis in Ewing Sarcoma Family Tumors

Ki Yong Na · Byeong-Joo Noh[1]
Ji-Youn Sung[2] · Youn Wha Kim[2]
Eduardo Santini Araujo[3]
Yong-Koo Park[2]

Department of Pathology, Central Physical Examination Agency, Daegu; [1]Department of Pathology, Graduate School of Medicine, Kyung Hee University, Seoul; [2]Department of Pathology, Kyung Hee University College of Medicine, Seoul, Korea; [3]Orthopedic Pathology Laboratory, Buenos Aires, Argentina

Received: April 2, 2015
Accepted: April 14, 2015

Corresponding Author
Yong-Koo Park, M.D.
Department of Pathology, Kyung Hee University Hospital, 23 Kyungheedae-ro, Dongdaemun-gu, Seoul 130-872, Korea
Tel: +82-2-958-8742
Fax: +82-2-958-8740
E-mail: ykpark@khmc.or.kr

Background: Isocitrate dehydrogenase (IDH) catalyzes the oxidative decarboxylation of isocitrate to yield α-ketoglutarate (α-KG) with production of reduced nicotinamide adenine dinucleotide (NADH). Dysfunctional IDH leads to reduced production of α-KG and NADH and increased production of 2-hydroxyglutarate, an oncometabolite. This results in increased oxidative damage and stabilization of hypoxia-inducible factor α, causing cells to be prone to tumorigenesis. **Methods:** This study investigated IDH mutations in 61 Ewing sarcoma family tumors (ESFTs), using a pentose nucleic acid clamping method and direct sequencing. **Results:** We identified four cases of ESFTs harboring IDH mutations. The number of *IDH1* and *IDH2* mutations was equal and the subtype of IDH mutations was variable. Clinicopathologic analysis according to IDH mutation status did not reveal significant results. **Conclusions:** This study is the first to report IDH mutations in ESFTs. The results indicate that ESFTs can harbor IDH mutations in previously known hot-spot regions, although their incidence is rare. Further validation with a larger case-based study would establish more reliable and significant data on prevalence rate and the biological significance of IDH mutations in ESFTs.

Key Words: Isocitrate dehydrogenase; Sarcoma, Ewing; PNA clamping

Ewing sarcoma (ES) is the second most common primary bone sarcoma of those that typically develop in children and young adults. It is also called ES family tumor (ESFT) and includes extraskeletal ES and primitive neuroectodermal tumor.[1] ESFT is an aggressive tumor with metastases present at diagnosis in 20%–25% of cases. With current therapeutic options, the 5-year survival rate for non-metastatic disease is as high as 70%. However, survival for patients who have metastasis is approximately 20%, and for those who develop relapsed or refractory disease, the survival rate is less than 10%. There is a need to identify alternative therapeutic agents that appropriately target the biomolecular mechanisms of this disease.[1]

There is a group of tumors and tumor syndromes that carry mutations in metabolic enzymes involved in the tricarboxylic acid cycle, especially enzymes in the isocitrate dehydrogenase (IDH) family. IDH catalyzes the oxidative decarboxylation of isocitrate to yield α-ketoglutarate (α-KG) with production of reduced nicotinamide adenine dinucleotide (NADH). Dysfunctional IDH leads to reduced production of α-KG and NADH and increased production of 2-hydroxyglutarate, an oncometabolite. Together, this results in increased oxidative damage and stabilization of hypoxia-inducible factor α, causing cells to be prone to tumorigenesis.[2] A functional study proved that *IDH2* mutations in mesenchymal cells can induce malignant transformation.[3] Mutations in *IDH1* are reported to cluster at a single hotspot locus (R132), whereas *IDH2* mutations occur primarily at two loci (R140 and R172).[2] Recurrent somatic *IDH1/2* mutations have been described in gliomas and secondary glioblastomas.[4] Similar *IDH1/2* mutations have been detected in acute myeloid leukemia[5] and myelodysplastic disorders.[6] Recently, IDH mutations have been reported in a large proportion of cartilaginous tumors,[7] a small number of osteosarcomas,[8] and in giant cell tumors.[9] The fact that these mutations appear to be present in these relatively common bone tumors led us to investigate *IDH1/2* mutations in ESFTs.

pISSN 2383-7837
eISSN 2383-7845

MATERIALS AND METHODS

Patient and tissue samples

Formalin-fixed, paraffin-embedded tissue samples from 61 patients with primary localized ESFTs were obtained in Korea, Brazil, and Argentina. Fifty-five of the 61 tissue samples were obtained by surgical biopsy and the other six were obtained by surgical excision. At the time of tissue sampling, none of the patients had a history of chemotherapy or radiation therapy and there was no evidence of metastatic disease. The disease was diagnosed according to World Health Organization (WHO) criteria.[10] Briefly, they are small round cell sarcomas showing diffuse membranous CD99 immunostaining, cytoplasmic periodic acid–Schiff staining, and *EWSR1* gene translocation as demonstrated with fluorescence *in situ* hybridization (ZytoLight SPEC EWSR1 Dual Color Break Apart Probes, ZytoVision, Bremerhaven, Germany). However, lack of an *EWSR1* gene translocation was not considered as grounds for exclusion if a tumor showed the typical immunophenotypes, which are inconsistent with other small round cell tumors in the differential diagnosis of diseases such as lymphoma and rhabdomyosarcoma.

After histological diagnosis, the patients received standard multidrug chemotherapy in combination with surgery. Data, including the follow-up period and overall survival, were available for 48 patients. During follow-up, assessment of distant metastasis was available in 38 patients. The patients were grouped into dead of disease, alive with disease, and no evidence of disease (NED). The classification of patients as NED was established when the follow-up period had passed more than 24 months. Our study protocol was reviewed and approved by the Kyung Hee University Institutional Review Board.

Pentose nucleic acid–mediated clamping polymerase chain reaction for detection of *IDH1/2* mutations

IDH1/2 mutations were tested using the pentose nucleic acid (PNA) Clamp *IDH1/2* Mutation Detection Kit (Panagene, Daejeon, Korea). All reactions had a total reaction volume of 20 μL and contained template DNA, primer and PNA probe sets, and fluorescent polymerase chain reaction (PCR) master mix. All required reagents were included with the kit. Real-time PCR reactions of PNA-mediated clamping PCR were performed using a CFX 96 (Bio-Rad, Hercules, CA, USA). PCR cycling conditions were as follows: 5 minutes at 94°C followed by 40 cycles of 94°C for 30 seconds, 70°C for 20 seconds, 63°C for 30 seconds, and 72°C for 30 seconds. In this assay, PNA probes and DNA primers were used together in the clamping reaction. Positive signals were detected by intercalation of fluorescent dye. The PNA probe, which is complementary to the wild-type sequence, suppresses amplification of the wild-type target. This suppression results in preferential amplification of mutant sequences by competitively inhibiting the binding of DNA primers to wild-type DNA. PCR efficiency was determined by measuring the threshold cycle (Ct) value. Ct values for control and mutant assays were obtained from fluorescent amplification plots. Calculations of the delta Ct (ΔCt) value were done as follows: ΔCt1=(Standard Ct)−(Sample Ct), ΔCt2=(Sample Ct)−(Non-PNA mix Ct). The gene was considered to be mutated when ΔCt1 values were more than 2.0. When ΔCt1 values were between 0 and 2, a ΔCt2 value was then calculated. The gene was considered to be mutated if the calculated ΔCt2 value was ≤4.

Direct sequencing

Genomic PCR for sequencing was performed in 20-μL volumes using 30 ng of template DNA and 2× Taq PCR Smart Mix (Solgent, Daejeon, Korea). The PCR primers used for *IDH1/2* amplification were as follows: *IDH1* forward primer (5'-CGGTCTTCAGAGAAGCCATT-3') and *IDH1* reverse primer (5'-GCAAAATCACATTATTGCCAAC-3'). *IDH2* forward primer (5'-CCAATGGAACTATCCG-3') and *IDH2* reverse primer (5'-CTCCACCCTGGCCTACCTG-3'). PCR cycling commenced with a 10 minutes hold at 95°C, followed by 40 cycles of 95°C for 30 seconds, 58°C for 40 seconds, and 72°C for 60 seconds, terminating with 72°C for 5 minutes. Each amplified product was purified using a PCR clean-up kit (Macherey-Nagel, Duren, Germany) and sequenced in duplicate, in both the forward and reverse directions, using a BigDye Terminator Kit (Applied Biosystems, Carlsbad, CA, USA) on an ABI Prism 3100 station (Applied Biosystems), according to the manufacturer's instructions. Sequences were compared with the GenBank-archived sequence of human *IDH1/2*.

Immunohistochemistry

The primary antibody that is specific for the *IDH1* R132H point mutation (1:200, Histonova DIA-H09, Dianova, Ham-

Table 1. Results of *IDH1/2* mutation analysis using PNA clamping and direct sequencing

	PNA clamping	Direct sequencing
Wild type	57	59
Mutant		
IDH1	2	1
IDH2	1	1
Equivocal	1	0

PNA, pentose nucleic acid.

http://dx.doi.org/10.4132/jptm.2015.04.14

Table 2. Summary of four cases bearing *IDH1/2* mutations, including clinicopathologic characteristics

Case No.	PNA clamping	Direct sequencing	DIA-H09	Race	Age (yr)	Sex	Site	F/U (mo)	Met
1	R132	R132H	(+)	Korea	47	M	Face	NED 32	No
2	R132	Wild	(–)	Brazil	12	F	Foot	DOD 48	No
3	R172	Wild	(–)	Korea	14	F	Ilium	NED 72	No
4	Equivocal	R172K	(–)	Korea	19	M	Femur	NED 48	No

R132H, CGT>CAT; R172K, AGG>AAG.
PNA, pentose nucleic acid; F/U, follow-up; Met, metastasis; M, male; NED, no evidence of disease; F, female; DOD, dead of disease.

Table 3. Clinicopathologic analysis according to *IDH1/2* mutation status

Characteristic	Gene profile		
	Wild	Mutant	p-value
Race			
Argentina	12	0	.009
Brazil	37	1	
Korea	8	3	
Age (yr)			
<20	29	3	.614
>20	28	1	
Sex			
Female	24	2	>.999
Male	33	2	
Tumor site			
Central	21	1	>.999
Peripheral	36	3	
Distant metastasis			
Yes	9	0	.554
No	25	4	

burg, Germany) was used for the samples bearing *IDH1* mutations, revealed by either direct PCR or PNA clamping. The Bond Polymer Intense Detection System (Vision Biosystems, Melbourne, Australia) was used according to the manufacturer's instructions with minor modifications. Nuclei were counterstained with hematoxylin. Paraffin-embedded tissues of brain astrocytomas were used as a positive control.

Statistics

Statistical analyses were performed using SPSS Software (SPSS Inc., Chicago, IL, USA). Pearson's chi-square test or Fisher exact test were performed to determine correlations between IDH mutation status and clinicopathological parameters. Statistical significance was defined as a p-value less than .05.

RESULTS

Using the PNA clamping method, *IDH1/2* mutations were detected in three of the 61 patients (5%). Of these three samples, two were *IDH1* mutants and one sample was an *IDH2* mutant. By direct sequencing, *IDH1/2* mutations were detected in two of the 61 patients (3%), of which, one sample was an *IDH1* mutant and one sample was an *IDH2* mutant. In total, four cases out of 61 (6%) harbored *IDH1/2* mutations by at least one of the two methods employed, and the numbers of *IDH1* and *IDH2* mutants were equal (Table 1).

Table 2 summarizes the clinicopathologic characteristics of the four mutant cases. In one of four cases, the *IDH1* mutation was found by both the PNA clamping method and direct sequencing (case No. 1) (Fig. 1A). In two of four cases, the *IDH1/2* mutation was found only by the PNA clamping method (cases Nos. 2 and 3). In one of four cases, examination by the PNA clamping method showed equivocal results, but direct sequencing showed an *IDH2* mutation (case No. 4) (Fig. 1C). The overall concordance rate of both methods was over 95% (58 of 61) and the discordance rate was less than 5% (3 of 61). In mutant cases, the concordance rate was 25% (1 of 4) and the discordance rate was 75% (3 of 4), although case No. 4 showed equivocal results by the PNA clamping method. Immunohistochemistry with antibody to DIA-H09 in the four cases bearing *IDH1/2* mutations showed positive reactions only in case No. 1 (Fig. 1B).

In the four cases bearing *IDH1/2* mutations, three patients were Korean and one patient was Brazilian, and the male/female ratio was 1:1. Three of the four patients were in their second decade and one patient was in the fifth decade. There was no evidence of distant metastasis in all patients and only one patient died during follow-up.

Statistical analyses showed that *IDH1/2* mutant cases had stronger associations with Korean patients than with South American patients (p=.009). There was no significant association between *IDH1/2* mutations and any of the other characteristics of tumors or patients (Table 3).

DISCUSSION

Research on *IDH1/2* mutations in human tumors has been active in recent years and has revealed that various tumors of different origins bear *IDH1/2* mutations.[2] Following increased in-

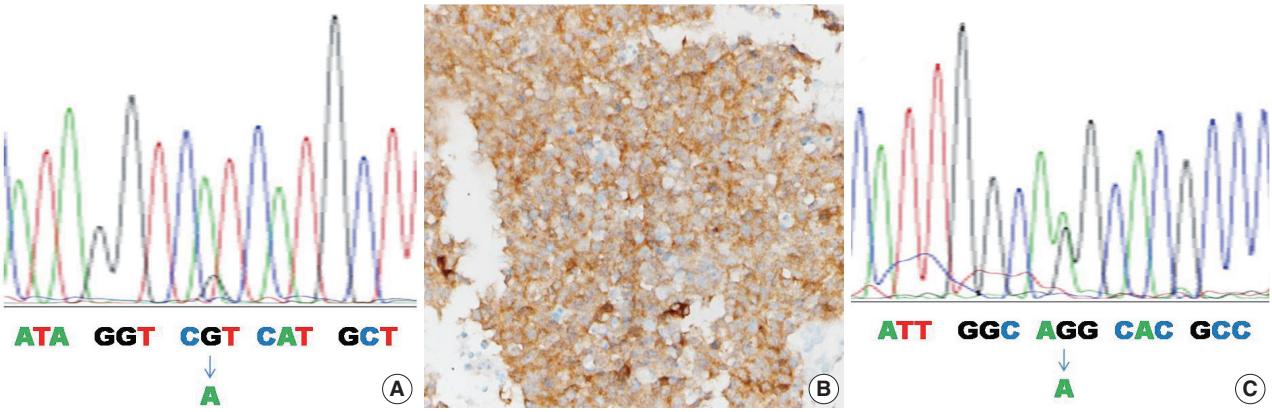

Fig. 1. The case No. 1 sample shows *IDH1* R132H mutation by direct sequencing (A) and positive immunoreactivity with antibody clone H09 (B). The case No. 4 sample shows *IDH2* R172K mutation (C).

terest in *IDH1/2* mutations in soft tissue tumors, a rudimentary study on sarcoma cell lines demonstrated IDH mutations in fibrosarcoma.[11] Subsequently, a study on chondrogenic tumors demonstrated *IDH1/2* mutations in 81 of 145 (56%) cases with an *IDH1*:*IDH2* mutation ratio of 10.6:1. This study also included the evaluation of *IDH1/2* mutations in 222 osteosarcomas, 79 chordomas, and 25 ESFTs, and no mutations were found.[7] Therefore, IDH mutations are considered to be found exclusively in chondrogenic tumors. Furthermore, previous studies support the value of examining IDH mutations for the purpose of differentiating chondrosarcoma from chondroblastic osteosarcoma[12] and chordoma.[13] However, a recent study in Japan showed that three of 12 osteosarcomas (25%)[8] and 16 of 20 giant cell tumors (80%) harbor *IDH2* mutations,[9] suggesting the possibility of *IDH1/2* mutations in various soft tissue tumors in addition to chondrogenic tumors.

We demonstrated that four of 61 ESFTs (6%) possessed IDH mutations. The PNA clamping method is known to be sensitive, rapid, and simple to perform and can detect mutant alleles when present at levels 100-fold lower than those of wild-type alleles. In contrast, the minimum percentage of mutant DNA required for analysis by direct sequencing is more than 25%.[14] The two cases harboring IDH mutations, found only by PNA clamping, might have had less than 25% mutant DNA. It is worth noting that three osteosarcomas bearing IDH mutations were found in Japanese,[8] and three ESFT bearing IDH mutations were found in Korean patients. However, evaluation of the same tumors from American patients revealed no mutations.[7] Although it is still early to remark on the background responsible for these findings, it is possible that Asian populations may be predisposed to IDH mutations in these tumors and therefore should be further evaluated.

Variation in the most prevalent mutation type according to tumor has been observed. *IDH1* R132H represents the most common type in gliomas,[4] and *IDH2* R140Q is exclusively found in acute myeloid leukemia.[5] Whereas *IDH1* R132C represents the most common type in cartilaginous tumors,[13] *IDH2* R172S is the dominant type in osteosarcomas[8] and giant cell tumors.[9] In our study, ESFTs demonstrated equal numbers of *IDH1* and *IDH2* mutations in which one case of R132H and one case of R172K were found. A previous study on cartilaginous tumors demonstrated that IDH mutations are frequent in acral-based tumors without any other association with other factors.[7] IDH mutations in osteosarcomas and giant cell tumors did not show any association with other clinical parameters.[8,9] Our study also did not find a significant association between IDH mutations and clinical parameters of ESFTs.

In conclusion, our study is the first report to demonstrate IDH mutations in ESFTs. It provides evidence that ESFTs can harbor IDH mutations in previously known hot-spot regions, although its incidence is rare. To provide generalized knowledge, our study is still lacking enough data about these mutations in ESFTs. Further validation with a larger case-based study would establish more reliable and significant data on prevalence rate and the biological significance of *IDH1/2* mutation status in ESFTs.

Conflicts of Interest

No potential conflict of interest relevant to this article was reported.

REFERENCES

1. van Maldegem AM, Hogendoorn PC, Hassan AB. The clinical use of biomarkers as prognostic factors in Ewing sarcoma. Clin Sarco-

ma Res 2012; 2: 7.
2. Schaap FG, French PJ, Bovée JV. Mutations in the isocitrate dehydrogenase genes *IDH1* and *IDH2* in tumors. Adv Anat Pathol 2013; 20: 32-8.
3. Lu C, Venneti S, Akalin A, *et al*. Induction of sarcomas by mutant *IDH2*. Genes Dev 2013; 27: 1986-98.
4. Yan H, Parsons DW, Jin G, *et al*. *IDH1* and *IDH2* mutations in gliomas. N Engl J Med 2009; 360: 765-73.
5. Abbas S, Lugthart S, Kavelaars FG, *et al*. Acquired mutations in the genes encoding *IDH1* and *IDH2* both are recurrent aberrations in acute myeloid leukemia: prevalence and prognostic value. Blood 2010; 116: 2122-6.
6. Abdel-Wahab O, Manshouri T, Patel J, *et al*. Genetic analysis of transforming events that convert chronic myeloproliferative neoplasms to leukemias. Cancer Res 2010; 70: 447-52.
7. Amary MF, Bacsi K, Maggiani F, *et al*. *IDH1* and *IDH2* mutations are frequent events in central chondrosarcoma and central and periosteal chondromas but not in other mesenchymal tumours. J Pathol 2011; 224: 334-43.
8. Liu X, Kato Y, Kaneko MK, *et al*. Isocitrate dehydrogenase 2 mutation is a frequent event in osteosarcoma detected by a multi-specific monoclonal antibody MsMab-1. Cancer Med 2013; 2: 803-14.
9. Kato Kaneko M, Liu X, Oki H, *et al*. Isocitrate dehydrogenase mutation is frequently observed in giant cell tumor of bone. Cancer Sci 2014; 105: 744-8.
10. Fletcher CD, Bridge JA, Hogendoorn PC, Mertens F. WHO classification of tumours of soft tissue and bone. 4th ed. Lyon: IARC Press, 2013.
11. Rasheed S, Nelson-Rees WA, Toth EM, Arnstein P, Gardner MB. Characterization of a newly derived human sarcoma cell line (HT-1080). Cancer 1974; 33: 1027-33.
12. Kerr DA, Lopez HU, Deshpande V, *et al*. Molecular distinction of chondrosarcoma from chondroblastic osteosarcoma through *IDH1/2* mutations. Am J Surg Pathol 2013; 37: 787-95.
13. Arai M, Nobusawa S, Ikota H, Takemura S, Nakazato Y. Frequent *IDH1/2* mutations in intracranial chondrosarcoma: a possible diagnostic clue for its differentiation from chordoma. Brain Tumor Pathol 2012; 29: 201-6.
14. Lee HJ, Xu X, Kim H, *et al*. Comparison of direct sequencing, PNA clamping-real time polymerase chain reaction, and pyrosequencing methods for the detection of *EGFR* mutations in non-small cell lung carcinoma and the correlation with clinical responses to EGFR tyrosine kinase inhibitor treatment. Korean J Pathol 2013; 47: 52-60.

Journal of Pathology and Translational Medicine 2015; 49: 262-266
http://dx.doi.org/10.4132/jptm.2015.03.26

■ CASE STUDY ■

Follicular Proliferative Lesion Arising in Struma Ovarii

Min Jee Park · Min A Kim
Mi Kyung Shin[1] · Hye Sook Min[2]

Department of Pathology, Seoul National University College of Medicine, Seoul; [1]Department of Pathology, Hallym University College of Medicine, Seoul; [2]Department of Epidemiology and Preventive Medicine, Graduate School of Public Health, Seoul National University, Seoul, Korea

Received: February 25, 2015
Revised: March 21, 2015
Accepted: March 26, 2015

Corresponding Author
Hye Sook Min, M.D., Ph.D.
Department of Epidemiology and Preventive Medicine, Graduate School of Public Health, Seoul National University, 1 Gwanak-ro, Gwanak-gu, Seoul 151-742, Korea
Tel: +82-2-880-2743
Fax: +82-2-762-9105
E-mail: lilloa@snu.ac.kr

Malignant struma ovarii is extremely rare and difficult to diagnose histologically, particularly in cases of follicular carcinoma. This case study is intended to describe three cases of follicular proliferative lesion arising in struma ovarii that we experienced. The first case was clearly malignant given the clinical picture of multiple recurrences, but there was little histological evidence of malignancy. Our second case featured architectural and cellular atypia and necrosis and was diagnosed as malignant despite the absence of vascular and stromal invasion. Our third case exhibited solid microfollicular proliferation without any definite evidence of malignancy (even the molecular data was negative); however, we could not completely exclude malignant potential after conducting a literature review. In cases such as our third case, it has been previously suggested that a diagnostic term recognizing the low-grade malignant potential, such as "proliferative stromal ovarii" or "follicular proliferative lesion arising in the stromal ovarii" would be appropriate.

Key Words: Follicular proliferative lesion; Adenocarcinoma, follicular; Malignant struma ovarii

A struma ovarii is a monodermal variant of an ovarian mature teratoma containing thyroid tissue, either exclusively or predominantly.[1] Malignant change in a struma ovarii is a rare event, and the criteria used to detect such changes are identical to those used to evaluate the thyroid gland. In some cases, diagnosis of malignant struma ovarii is not straightforward, particularly when a proliferative follicular pattern is evident. Here, we report on three cases of follicular proliferative lesions arising in struma ovarii and discuss their clinicopathological and molecular characteristics.

CASE REPORT

A 35-year-old female visited the hospital complaining of abdominal discomfort, and pelvic magnetic resonance imaging (MRI) scan revealed multiple nodules in the peritoneum and omentum with a large volume of ascitic fluid. She had a history of surgery to treat struma ovarii in the left ovary 9 years ago. The mass was removed under the suspicion of struma ovarii recurrence. Three months later, multiple enhanced nodules in the adnexa, omentum, perihepatic space, and peritoneum (Fig. 1A) were evident on follow-up imaging, and the patient underwent re-surgery, total thyroidectomy, and radioactive iodine (RAI) therapy. The histological features of nodules from the second and third surgeries were similar. The nodules exhibited mixed micro- and macro-follicular proliferation, with scattered lymphocytic infiltration, and were covered with thin fibrous capsules (Fig. 1B). The tumor cell nuclei were round, uniform, and normochromatic; neither mitosis nor necrosis was evident (Fig. 1C). Immunohistochemically, galectin-3, cyclin D1, and HBME1 were focally positive, and HBME1 expression was limited principally to regions of microfollicular proliferation (Fig. 1D). The Ki-67 positivity level was enhanced by up to 10%, in the microfollicles. The cervical thyroid showed features of chronic lymphocytic thyroiditis but there was no evidence of malignancy. We reviewed all slides of the struma ovarii initially operated on to compare later lesions with the initial ovarian mass. The original mass had both solid and cystic components, and was fibrotically encapsulated (Fig. 1E). Follicles of variable size and papillary structure were

pISSN 2383-7837
eISSN 2383-7845

observed, and one microscopic focus of vascular invasion was observed after meticulous examination (Fig. 1E, inset). No mutation in any of *BRAF* (V600E) or *RAS* (*HRAS* codon 61, *NRAS* codon 61, and *KRAS* codon 12/13), and no *PPARγ* rearrangement (explored using fluorescence *in situ* hybridization), was evident in the recurring nodules. The lesion was diagnosed as follicular carcinoma arising in the struma ovarii, based on the clinical and pathological findings, and the patient underwent RAI therapy (200 mCi). There has not been local recurrence or distant metastasis in the 25 months of follow-up to date.

The second case was an 80-year-old female who visited the hospital complaining of acute abdominal discomfort. A 20 cm-

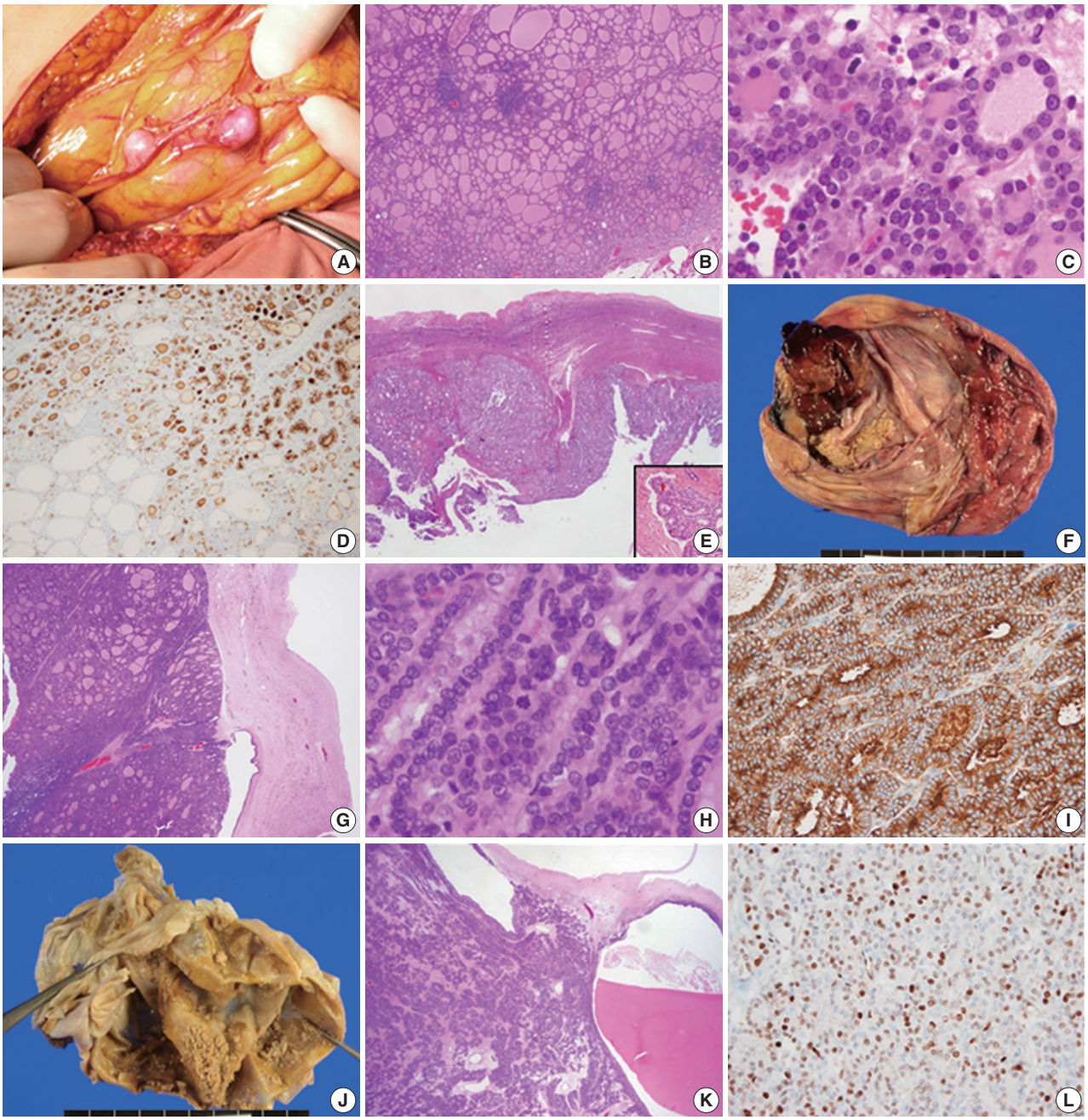

Fig. 1. Peritoneal nodules found intraoperatively (A) and the microscopic findings (B, C). HBME1 positivity of microfollicles of the first case (D) is observed and the initial ovarian lesion of the first case (E) shows vascular invasion (E, inset). The gross features of the second case (F) and the histological findings (G, H) are suggestive of malignancy, and HBME1 status is positive only in the cytoplasm (I). In the third case, the solid regions are tiny and scattered (J). Microscopically, microfollicles are predominant (K), and cyclin D1 expression is increased (L).

diameter mass was observed in the right ovary on pelvic computed tomography and was thought to be a mature cystic teratoma. The tumor was removed with no evidence of peritoneal adhesions, ascites, or seeding nodules apparent intraoperatively. The mass was grossly multicystic and partially solid (~10%) (Fig. 1F). Histologically, the cystic wall was composed of normal thyroid tissue (>50%), skin, and fat tissue. However, the solid portion was surrounded by fibrotic tissue (separating the solid portion from the ovarian stroma), and exhibited proliferation of macro- and micro-follicles (Fig. 1G), crowded nuclei, occasional mitosis (Fig. 1H), and necrosis. However, there was no evidence of vascular invasion. The solid region was galectin-3–negative, but HBME1-positive in the cytoplasm but not the cytoplasmic membrane (Fig. 1I). Cyclin D1 and Ki-67 levels were focally increased in the solid portion of the mass (by ~10%) and thyroglobulin expression was retained. No *BRAF* or *RAS* mutation was present and *PPARγ* was not rearranged. The lesion was diagnosed as a follicular carcinoma arising in struma ovarii, which might progress to a poorly differentiated carcinoma requiring RAI therapy and close follow-up. There was no local recurrence or distant metastasis during 20 months of follow-up.

The last case was a 58-year-old female with a palpable pelvic mass. MRI revealed a 16 cm-diameter multiloculated, solid cystic mass in the left ovary, without adhesions, ascites, or peritoneal seeding. On removal, the tumor was grossly multicystic and filled with thick brownish fluid; small yellowish solid portions were scattered within the inner cystic wall (Fig. 1J). These exhibited a microfollicular proliferation pattern admixed with occasional macrofollicles. No capsule was evident (Fig. 1K). The nuclei were uniformly round and mildly atypical, but there was no evident necrosis or vascular invasion. The mass was HBME1 and p53 negative, but focally positive for galectin-3 and cyclin D1 (Fig. 1L). The Ki-67 positivity rate was approximately 1%–3%. All molecular studies were negative. This lesion was diagnosed as a follicular proliferative lesion arising in the struma ovarii, requiring regular long-term follow-up. There was no recurrence or metastasis noted during 18 months of follow-up.

Results of clinicopathological studies on the three aforementioned patients are summarized in Table 1.

DISCUSSION

Some earlier cases reported as malignant struma ovarii are now recognized to have been strumal carcinoids.[2] Malignant struma ovarii currently refers to thyroid-type carcinomas, including papillary and follicular carcinomas. Follicular carcinoma is the second most common type of malignant struma ovarii. The age range for patients with malignant struma ovarii is 22 to 70 years.[3] Typical follicular carcinomas commonly metastasize to distant sites including the lung, liver, bone, and central nervous system,[3] as do thyroid gland carcinomas.

However, histological diagnosis of follicular carcinoma arising in struma ovarii is rather difficult; it is not clear whether the malignant criteria for the thyroid gland are wholly transferable to the struma ovarii.[4] Capsular invasion is the major criterion for thyroid malignancy, but the normal ovary usually lacks a capsule. Furthermore, many struma ovarii associated with distant metastases lacked tumor capsules.[5] Thus, invasion of the surrounding ovarian stroma and/or serosa and vascular invasion have been regarded as histological evidence for follicular carcinoma of the ovary.[3,6] However, it is difficult to define the term "invasion into the stroma and serosa"; some authors consider invasion to be when infiltrating tumor cells are surrounded by thin fibrotic tissue, not by thickened ovarian cortical tissue.[4] The concept of vascular invasion is also somewhat controversial; some authors consider this to be present only when more than three invasive foci are found[7] or, indeed, only when many well-separated vessels are involved.[8] Also, less-differentiated forms of follicular carcinoma can exhibit architectural abnormalities of the trabecular pattern, nuclear atypia, and increased mitotic activity.[5]

Table 1. Summary of patient clinicopathological features

Variable	Case 1	Case 2	Case 3
Age (yr)	35	80	58
Tumor diameter (cm)	NA	20	16
Progression	Peritoneal seeding	None	None
Follow-up (mo)	25	20	18
Histologic feature	Micro-/macrofollicles	Micro-/macrofollicles, necrosis	Predominantly micro-follicles
Invasion of the ovarian stroma	–	–	–
Vascular invasion	+	–	–
Galectin-3/HBME1/cyclin D1	f+/f+/f+	–/f+ (cytoplasm)/f+	f+/–/f+

NA, not applicable; f+, focal positive; –, negative.

 http://dx.doi.org/10.4132/jptm.2015.03.26

A new subtype of follicular carcinoma of the ovary, described by Roth and Karseladze,[9] presents an even greater diagnostic challenge. Highly differentiated follicular carcinoma of ovarian origin (HDFCO) was previously considered to reflect extra-ovarian dissemination of normal thyroid tissue, and was termed "peritoneal strumosis." However, based on both clinical experience and a literature review,[3,9] the authors suggested that the term peritoneal strumosis should be replaced by HDFCO, as these lesions behaved as did other thyroid-type carcinomas except that HDFCO was of a much low grade. In line with this suggestion, Robboy *et al*.[4] reported on 15 cases of biological malignancy (thus characterized by recurrence and metastasis) that exhibited histologically normal thyroid patterns, and/or normal micro- or macro-follicular proliferative patterns, without any definite histological evidence of malignancy. The cited authors and others[7,8] argued that the histological patterns of follicular lesions were not predictive of clinical behavior, and proposed that the diagnostic term "proliferative struma ovarii" should be used to describe a proliferative follicular lesion of the ovary without evident malignant features; the term aptly recognized the latent malignant potential of these masses.

Since microscopic features do not predict the clinical outcomes of malignant struma ovarii, pathologists cannot be certain that a follicular proliferative lesion in the struma ovarii is benign. Instead, we should consider clinical behavior suggestive of malignancy, such as extraovarian spread, adhesion to adjacent organs, significant volume of ascites (1 L or more), a stromal diameter >5 cm, and a lesion comprised of >50% proliferative thyroid tissue.[8]

Our first case was obviously malignant, given the mutiple recurrences. However, initially, it was difficult to diagnose a malignant struma ovarii because the lesion exhibited no histological evidence of stromal/serosal invasion or vascular invasion. Although no ascites or peritoneal adhesion was evident during the first surgery, the tumor diameter was presumed to be over 5 cm and follicular proliferations (of various patterns) constituted more than half of the lesion. Thus, the lesion was a "proliferative strumal ovarii" according to the terminology defined by Robboy *et al*.,[4] although this terminology is not universally employed. The second case exhibited necrosis and features of a less-differentiated follicular carcinoma including architectural and nuclear atypia, and there was no difficulty with a diagnosis of malignant stromal ovarii. The third case exhibited rather innocuous histological features. Microfollicular proliferation was observed in most regions of the solid lesion; however, the tumor was largely cystic and the solid portions were tiny and scattered, so it was unclear whether proliferative thyroid tissue constituted >50% of the lesion. Both ascites and adhesion were absent, and the tumor diameter was far greater than 5 cm due to its cystic nature. We could not completely exclude malignant potential, and we diagnosed the lesion as a "follicular proliferative lesion, requiring long-term follow-up."

Although *BRAF* and *RAS* mutations and *RET/PTC* rearrangement have been reported in malignant struma ovarii exhibiting histological features of papillary carcinoma,[10] we did not find any molecular studies that examined follicular proliferative lesions of struma ovarii in the literature. Previous results on papillary carcinoma suggested that the pathogenesis of malignant struma ovarii might be similar to that of carcinoma of the thyroid gland. Thus, we analyzed tissue samples for *BRAF* and *RAS* mutations and *PPARγ* rearrangements, but the results were negative in each of the three cases.

In summary, a follicular proliferative lesion in struma ovarii, including typical follicular carcinoma, HDFCO, and follicular proliferation without evident malignant features, is extremely rare. Diagnoses are not straightforward, and pathologists should be cautious in diagnosing such lesions as benign because a malignant potential may co-exist with innocuous histological features. In particular, even if a follicular proliferative lesion lacks evident malignant features, a diagnostic term recognizing low-grade malignant potential should be used. The literature review suggests that "proliferative sturmal ovarii" or "follicular proliferative lesion arising in the stromal ovarii" would be appropriate.

Conflicts of Interest

No potential conflict of interest relevant to this article was reported.

Acknowledgments

This study was approved by the Institutional Review Board of Seoul National University Hospital (IRB No. H-1502-065-648).

REFERENCES

1. Kurman RJ, Carcangiu ML, Herrington CS, Young RH. WHO classification of tumours of female reproductive organs. 4th ed. Lyon: IARC Press, 2014.
2. Kurman RJ, Ellenson LH, Ronnett BM. Blaustein's pathology of the female genital tract. 6th ed. New York: Springer, 2010.
3. Roth LM, Miller AW 3rd, Talerman A. Typical thyroid-type carcinoma arising in struma ovarii: a report of 4 cases and review of the literature. Int J Gynecol Pathol 2008; 27: 496-506.
4. Robboy SJ, Shaco-Levy R, Peng RY, *et al*. Malignant struma ovarii:

an analysis of 88 cases, including 27 with extraovarian spread. Int J Gynecol Pathol 2009; 28: 405-22.
5. Zhang X, Axiotis C. Thyroid-type carcinoma of struma ovarii. Arch Pathol Lab Med 2010; 134: 786-91.
6. Roth LM, Talerman A. The enigma of struma ovarii. Pathology 2007; 39: 139-46.
7. Shaco-Levy R, Bean SM, Bentley RC, Robboy SJ. Natural history of biologically malignant struma ovarii: analysis of 27 cases with extraovarian spread. Int J Gynecol Pathol 2010; 29: 212-27.
8. Shaco-Levy R, Peng RY, Snyder MJ, *et al*. Malignant struma ovarii: a blinded study of 86 cases assessing which histologic features correlate with aggressive clinical behavior. Arch Pathol Lab Med 2012; 136: 172-8.
9. Roth LM, Karseladze AI. Highly differentiated follicular carcinoma arising from struma ovarii: a report of 3 cases, a review of the literature, and a reassessment of so-called peritoneal strumosis. Int J Gynecol Pathol 2008; 27: 213-22.
10. Boutross-Tadross O, Saleh R, Asa SL. Follicular variant papillary thyroid carcinoma arising in struma ovarii. Endocr Pathol 2007; 18: 182-6.

 http://dx.doi.org/10.4132/jptm.2015.03.26

Journal of Pathology and Translational Medicine 2015; 49: 267-269
http://dx.doi.org/10.4132/jptm.2015.03.20

■ BRIEF CASE REPORT ■

Traumatic Bowel Perforation and Inguinal Hernia Masking a Mesenteric Calcifying Fibrous Tumor

Dong Hyun Kim* · Kyueng-Whan Min[1]* · Dong-Hoon Kim · Seoung Wan Chae
Jin Hee Sohn · Jung-Soo Pyo · Sung-Im Do · Kyungeun Kim · Hyun Joo Lee

Department of Pathology, Kangbuk Samsung Hospital, Sungkyunkwan University School of Medicine, Seoul;
[1]Department of Pathology, Hallym University Sacred Heart Hospital, Hallym University College of Medicine, Anyang, Korea

Calcifying fibrous tumors (CFTs) are uncommon benign tumors occurring in children and young adults. They arise in various anatomic sites, including subcutaneous and deep soft tissue, pleura, and peritoneum. Histologically, the tumor appears as a relatively well-circumscribed mass consisting of hypocellular hyalinized collagen and bland spindle cells, showing patchy lymphoplasmacytic infiltration and dystrophic calcifications. CFT of the gastrointestinal tract is extremely rare, and it can be difficult to distinguish from other spindle cell lesions that are more common. Moreover, its presence may be obscured by other clinical disorders. We report a case of incidentally detected mesenteric CFT during surgical treatment for bowel perforation and hernia.

CASE REPORT

A 71-year-old man visited our hospital for progressive abdominal pain after a fall. He also complained of nausea, vomiting, and abdominal discomfort for the previous 2 hours and had a medical history of hypertension, diabetes, and stroke. Physical examination revealed abdominal tenderness with mild rigidity. Abdominal computerized tomography revealed diffuse wall thickening of the distal ileum with free air and fluid collections and two inguinal hernias (Fig. 1). Additionally, there was a small amount of fluid collection and an air bubble in the right inguinal canal, suspicious for abscess or fecal spillage. An exploratives laparoscopy was performed under the impression of bowel perforation associated with inguinal hernia. Laparoscopy revealed a 2-cm-sized bowel perforation located at 15 cm above the ileocecal valve in the right inguinal herniated lesion. Intriguingly, a hard mass was noted near the perforation site. The patient underwent small bowel resection and herniorrhaphy.

Segmental resection revealed a firm, 1.1×1.1×0.7-cm-sized mass located at 2 cm from the perforation. The cut surface demonstrated a solid, well-demarcated, gray-brown mass in the mesentery. The remaining mucosal surface was edematous with congestion (Fig. 2A). Microscopically, the mass showed hypocellular sclerosis with wavy collagenous stroma, microcalcifications, and scattered inflammatory cells (Fig. 2B, C). Immunohistochemical staining results were negative for c-kit, smooth muscle actin, desmin, S-100 protein, and CD34 in the stromal cells. The Ki-67 labeling index was less than 1%. Pathological diagnosis thus confirmed a CFT. IgG and IgG4 immunohistochemical stains were also performed for this lesion to determine if the tumor was associated with an IgG4-related disease. IgG stain was positive, but IgG4 stain was negative. At the 6-month postoperative follow-up visit, the patient remained well without complications.

DISCUSSION

CFT can occur in a wide range of ages and may arise from dif-

Corresponding Author
Dong-Hoon Kim, M.D., Ph.D.
Department of Pathology, Kangbuk Samsung Hospital, Sungkyunkwan University School of Medicine, 29 Saemunan-ro, Jongno-gu, Seoul 110-746, Korea
Tel: +82-2-2001-2392, Fax: +82-2-2001-2398, E-mail: idavid.kim@samsung.com

*Dong Hyun Kim and Kyueng-Whan Min contributed equally to this work.

Received: December 31, 2014 **Revised:** March 11, 2015
Accepted: March 20, 2015

pISSN 2383-7837
eISSN 2383-7845

ferent sites. It is often detected incidentally, but visceral CFT has occasionally presented as a painful mass due to mass effect. Most cases of CFT in the small intestine have been reported as pain inducing lesion. Emanuel *et al.*[1] described presentation with abdominal symptoms (intussusception, abdominal pain) in four patients. Mesenteric CFT presenting with acute peritonitis has also been documented.[2] CFT needs to be distinguished from gastrointestinal stromal tumors, desmoid tumors and myomas, which have varying clinical outcomes. The typical radiographic findings in CFT are a well circumscribed, homogeneous mass, but these findings are nonspecific, so biopsy with histologic confirmation is needed prior to treatment.[3]

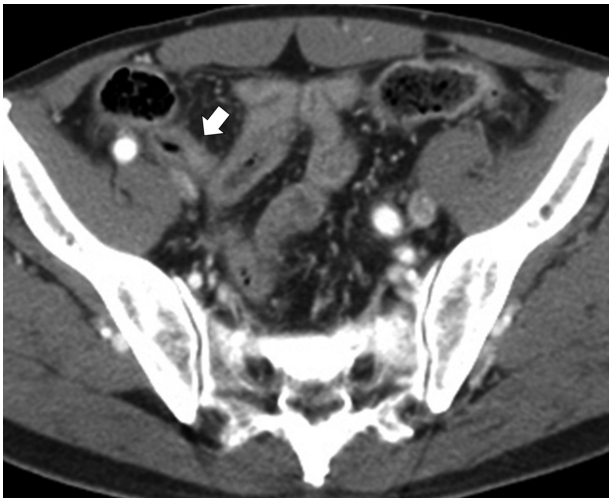

Fig. 1. Abdominal contrast-enhanced computed tomography scan reveals diffuse enhancing wall thickening (arrow) without an obvious mass-like lesion.

The mechanism of CFT development is thought to be reactive pseudotumoral. Previous reports suggested that CFT is a late sclerosing stage of inflammatory myofibroblastic tumors (IMT).[4,5] However, Sigel *et al.*[6] reported that anaplastic lymphoma kinase (ALK) stain, which is positive in IMT, was negative in their CFT patients. Nascimento *et al.*[7] also reported that CD34 was positive and ALK-1 was negative in their CFT patients. These studies do not support a relationship between CFT and IMT. Other studies described CFT associated with IgG4+ plasma cells. IgG4+ plasma cells were increased in a case of disseminated abdominal CFT associated with sclerosing angioma-

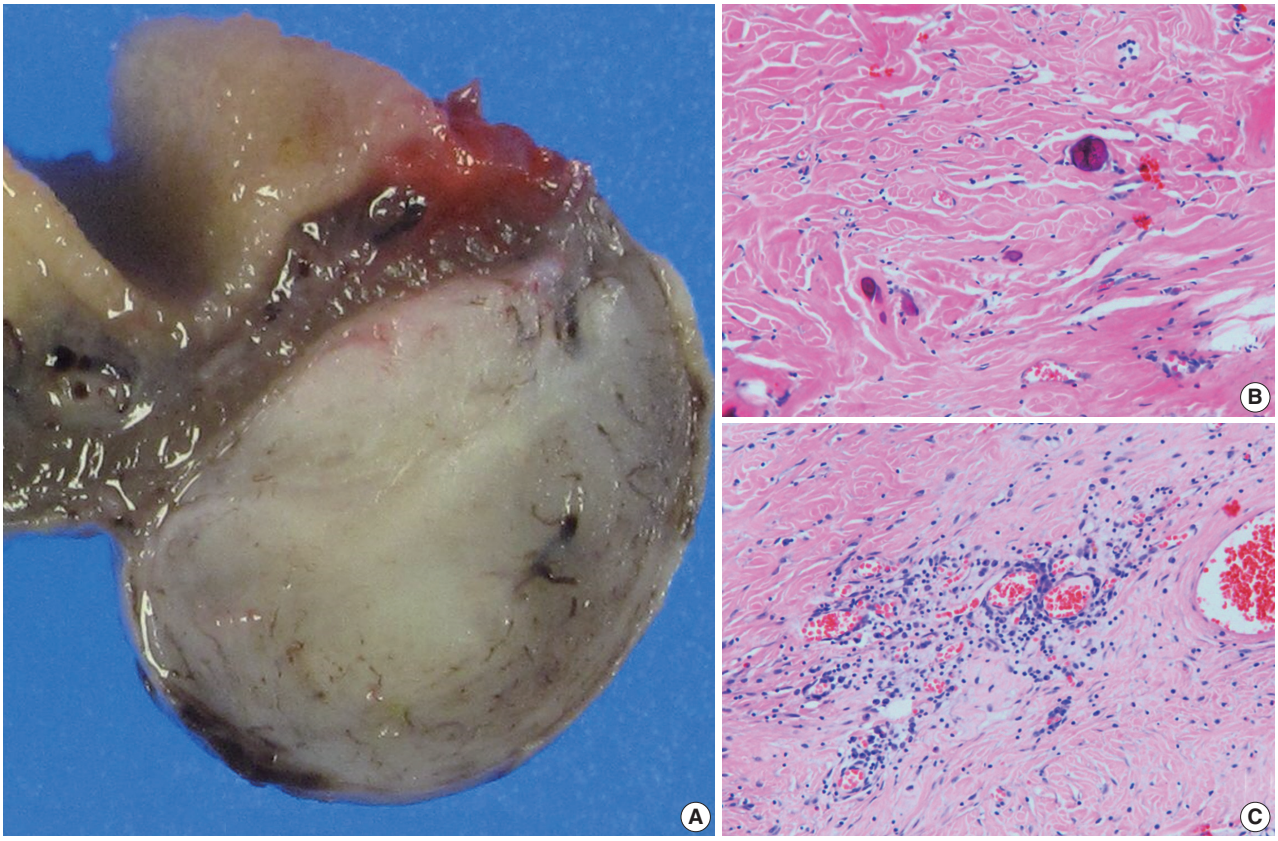

Fig. 2. (A) Viewed grossly, a well-demarcated gray-brown firm solid mass is confined to the mesenteric fat (right). (B) Microscopically, there are dispersed sparse spindle cells and occasional dystrophic calcification among thick wavy collagen bundles (left upper). (C) Patchy lymphoplasmacytic infiltrations are found throughout the tumor.

 http://dx.doi.org/10.4132/jptm.2015.03.20

toid nodular transformation of the spleen.[8] A study of gastric CFT reported that IgG4+ plasma cells were seen in this tumor.[9] Larson *et al*.[10] also suggested that CFT could be an IgG4 related disease. Although these reports support that CFT might be IgG4 related, our case was negative for IgG4 stain. Thus, more work needs to be done to better understand the mechanism of CFT development.

In the present case, the mesenteric CFT was slow-growing and asymptomatic, but abdominal symptoms appeared abruptly after trauma. Bowel perforation and hernia masked the solitary mass from radiological detection, but laparoscopy revealed a solid mass 2 cm from the bowel perforation. Considering the solid mass near the perforation and the patient's history of trauma, bowel perforation may have been caused by herniation of the CFT. Although it is rare for inguinal herniation and bowel perforation due to trauma to occur simultaneously with CFT, this case indicates that unusual clinical findings can be important for early detection and presurgical planning.

Conflicts of Interest

No potential conflict of interest relevant to this article was reported.

REFERENCES

1. Emanuel P, Qin L, Harpaz N. Calcifying fibrous tumor of small intestine. Ann Diagn Pathol 2008; 12: 138-41.
2. Ben-Izhak O, Itin L, Feuchtwanger Z, Lifschitz-Mercer B, Czernobilsky B. Calcifying fibrous pseudotumor of mesentery presenting with acute peritonitis: case report with immunohistochemical study and review of literature. Int J Surg Pathol 2001; 9: 249-53.
3. Giardino AA, Ramaiya NH, Shinagare AB, Jagannathan JP, Stachler MD, Raut CP. Case report: Calcifying fibrous tumor presenting as an asymptomatic pelvic mass. Indian J Radiol Imaging 2011; 21: 306-8.
4. Van Dorpe J, Ectors N, Geboes K, D'Hoore A, Sciot R. Is calcifying fibrous pseudotumor a late sclerosing stage of inflammatory myofibroblastic tumor? Am J Surg Pathol 1999; 23: 329-35.
5. Pomplun S, Goldstraw P, Davies SE, Burke MM, Nicholson AG. Calcifying fibrous pseudotumour arising within an inflammatory pseudotumour: evidence of progression from one lesion to the other? Histopathology 2000; 37: 380-2.
6. Sigel JE, Smith TA, Reith JD, Goldblum JR. Immunohistochemical analysis of anaplastic lymphoma kinase expression in deep soft tissue calcifying fibrous pseudotumor: evidence of a late sclerosing stage of inflammatory myofibroblastic tumor? Ann Diagn Pathol 2001; 5: 10-4.
7. Nascimento AF, Ruiz R, Hornick JL, Fletcher CD. Calcifying fibrous 'pseudotumor': clinicopathologic study of 15 cases and analysis of its relationship to inflammatory myofibroblastic tumor. Int J Surg Pathol 2002; 10: 189-96.
8. Kuo TT, Chen TC, Lee LY. Sclerosing angiomatoid nodular transformation of the spleen (SANT): clinicopathological study of 10 cases with or without abdominal disseminated calcifying fibrous tumors, and the presence of a significant number of IgG4+ plasma cells. Pathol Int 2009; 59: 844-50.
9. Agaimy A, Bihl MP, Tornillo L, Wünsch PH, Hartmann A, Michal M. Calcifying fibrous tumor of the stomach: clinicopathologic and molecular study of seven cases with literature review and reappraisal of histogenesis. Am J Surg Pathol 2010; 34: 271-8.
10. Larson BK, Balzer B, Goldwasser J, Dhall D. Calcifying fibrous tumor: an unrecognized IgG4: related disease? APMIS 2015; 123: 72-6.

Journal of Pathology and Translational Medicine 2015; 49: 270-273
http://dx.doi.org/10.4132/jptm.2015.04.01

■ BRIEF CASE REPORT ■

Cytomegalovirus-Associated Intussusception with Florid Vascular Proliferation in an Infant

Heejung Park · Sanghui Park[1] · Young Ju Hong[2] · Sun Wha Lee[3] · Min-Sun Cho[1]

Department of Pathology, National Health Insurance Service Ilsan Hospital, Goyang; Departments of [1]Pathology, [2]Surgery, and [3]Radiology, Ewha Womans University School of Medicine, Seoul, Korea

Intussusception is usually idiopathic, with no pathologic lead point except for the presence of reactive lymphoid hyperplasia, which is probably associated with gastrointestinal infection or a reaction to newly introduced food proteins. Viral infections, such as those caused by non-enteric adenovirus, human herpes virus (HHV)-6, HHV-7, and Epstein-Barr virus, are known etiologic factors of intussusception. Cytomegalovirus (CMV)-associated intussusception has been reported rarely; there have been three case reports in immunocompetent and human immunodeficiency virus–infected infants.[1-3] None of these three case reports described a detailed histologic pattern, except ischemic necrosis of the small intestine due to a prolonged clinical history and delayed surgery. Here, we report a case of a CMV-associated inflammatory polyp with unique gross and microscopic findings as a leading cause of ileoileal intussusception in an 8-week-old healthy female.

CASE REPORT

An 8-week-old healthy female infant was admitted to the hospital following 10 episodes of repeated vomiting and poor oral intake for one day. She was born by normal vaginal delivery at 40 weeks without any perinatal problems and with a birth weight of 3.98 kg. At admission, her height was 63.1 cm and her body weight was 6 kg, which was 89.4% of her ideal body weight. Her body temperature was 37.2°C. The results of the laboratory examination were unremarkable. Ultrasonography (US) on admission showed ileocolic intussusception at the hepatic flexure of the colon, which was successfully reduced by US-guided saline reduction. However, vomiting continued, although at a reduced rate, and bloody diarrhea developed intermittently. Follow-up US the next day revealed a newly developed ileoileal intussusception, which persisted until additional follow-up US (Fig. 1A). Five days after symptoms developed, an exploratory laparotomy and segmental resection of the ileum was performed.

The resected ileum contained a roughly ovoid, sessile, polypoid mass, measuring 4×2×1 cm. On the mucosal side of the mass, an aggregation of multiple small round polyps was observed, which had a cobblestone-like or nodule-aggregating appearance (Fig. 1B). The cut surface revealed multiple round-to-ovoid solid nodules with focal hemorrhages scattered from the submucosal to the subserosal connective tissue (Fig. 1C).

Upon histological examination, each mucosal polyp appeared to represent variably expanded and fused mucosal folds of the plicae circulares (Fig. 1D). The surface villi were flattened, multifocally, and covered with fibrinopurulent exudate. The crypts were irregularly deformed and cystically dilated. The lamina propria showed exuberant granulation tissue-type small vessel proliferation and fibroblastic reaction, with inflammatory infiltrates composed of plasma cells, small and large lymphoid cells, eosinophils, and histiocytes (Fig. 2A). The muscularis propria were partly disorganized and fused with the muscularis mucosae, suggesting a stretched intestinal wall of intussusception. The deeper layer showed multiple well-defined solid nodules, in which proliferated florid vessels were intermixed with fibroblasts and inflammatory cell infiltrates (Fig. 2B). Some of the nodules

Corresponding Author
Min-Sun Cho, M.D.
Department of Pathology, Ewha Womans University Mokdong Hospital, 1071 Anyangcheon-ro, Yangcheon-gu, Seoul 158-710, Korea
Tel: +82-2-2650-5044, Fax: +82-2-2650-2789, E-mail: mcho1124@ewha.ac.kr

Received: February 5, 2015 **Revised:** March 25, 2015
Accepted: April 1, 2015

pISSN 2383-7837
eISSN 2383-7845

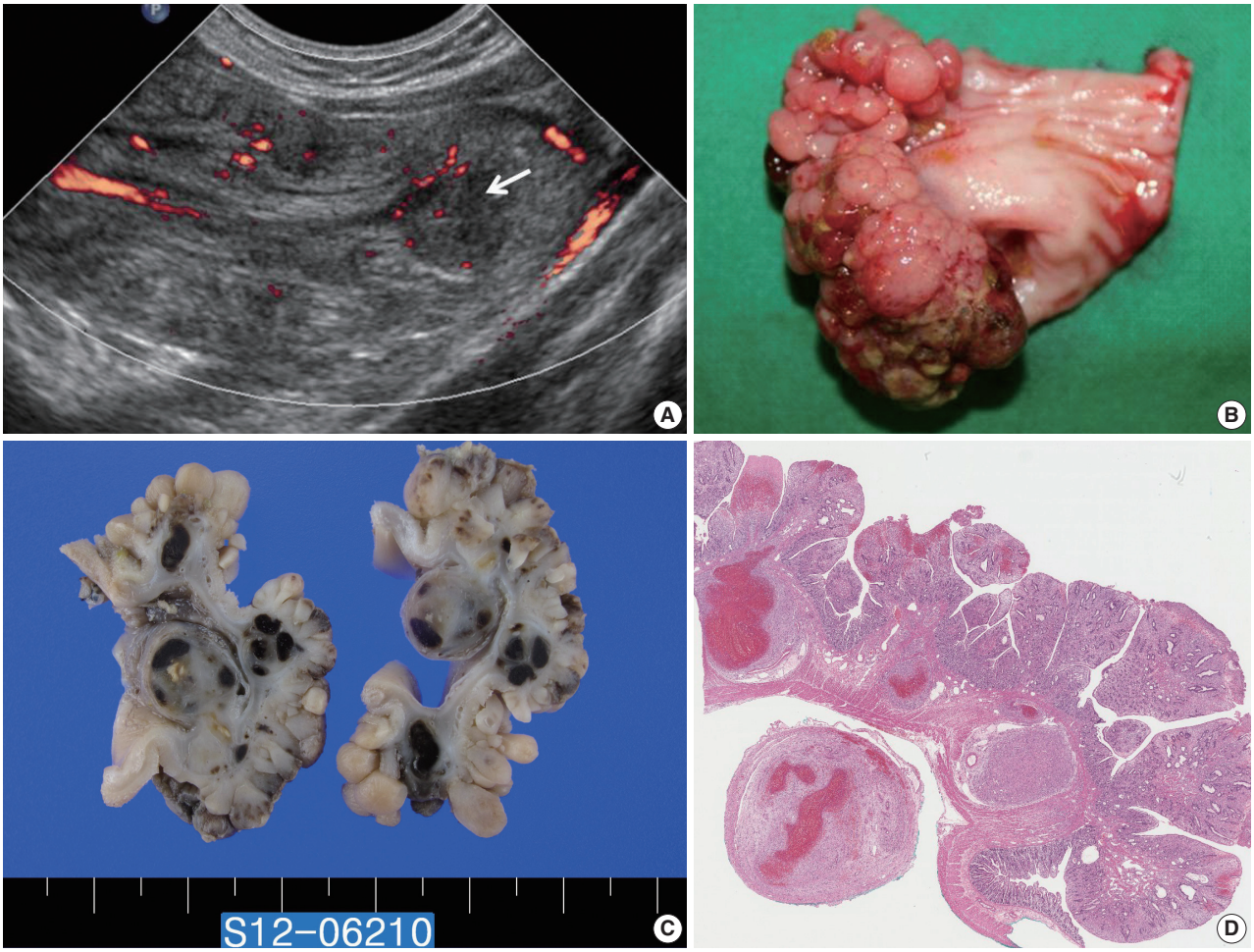

Fig. 1. (A) Longitudinal ultrasonography of the lower abdomen with a Doppler study shows an ovoid mass with alternating thick hypoechoic and thin hyperechoic layers, indicating ileoileal intussusception and Doppler flow signals at the intussusceptum. A round hypoechoic lesion (arrow) indicating a lead point of intussusception is identified. (B) The ileum reveals a 4×2×1 cm, roughly ovoid, sessile, polypoid mass with a conglomerated nodular or nodule-aggregating appearance. (C) The cut surface shows thickened mucosa and multiple round solid nodules with focal hemorrhages at deeper layers. (D) The polyp is composed of enlarged plicae circulares having dilated and distorted crypt glands with expanded lamina propria.

showed multifocal hemorrhages with fibroblastic proliferation, resembling reorganizing thrombus (Fig. 2C). Careful searching revealed that a few capillary endothelial cells and stromal cells exhibited characteristic eosinophilic intranuclear and cytoplasmic viral inclusions beneath and around the eroded mucosal surface in the focal area (Fig. 2D). These cells displayed positive immunostaining for CMV. After surgery, the CMV antigen was not detected in peripheral blood but was isolated from a stool culture in additional laboratory tests.

DISCUSSION

CMV infection occurs throughout the gastrointestinal tract, with ulceration as the most common morphologic change.[4,5] Gastrointestinal CMV infection presenting as a polyp is unusual, and only a few cases have been reported.[2,6,7] The lesions exhibit features like those of inflammatory or juvenile polyps, including surface ulceration, distention and shape irregularity of the crypt glands, and granulation tissue-type small capillary proliferation with inflammatory cell infiltration. Therefore, based on the dominant histologic pattern in the biopsy, CMV-associated polyps could be variably diagnosed as inflammatory fibroid polyps, inflamed hyperplastic polyps, inflammatory myofibroblastic tumors or even vascular tumors, etc.[2,6,7] In our case, the polyp had histologic features reminiscent of a juvenile polyp. However, glandular change and the preserved plicae circulares structure did not fit the diagnosis of a juvenile polyp. Thorough microscopic observation identified cells with CMV inclusion bodies.

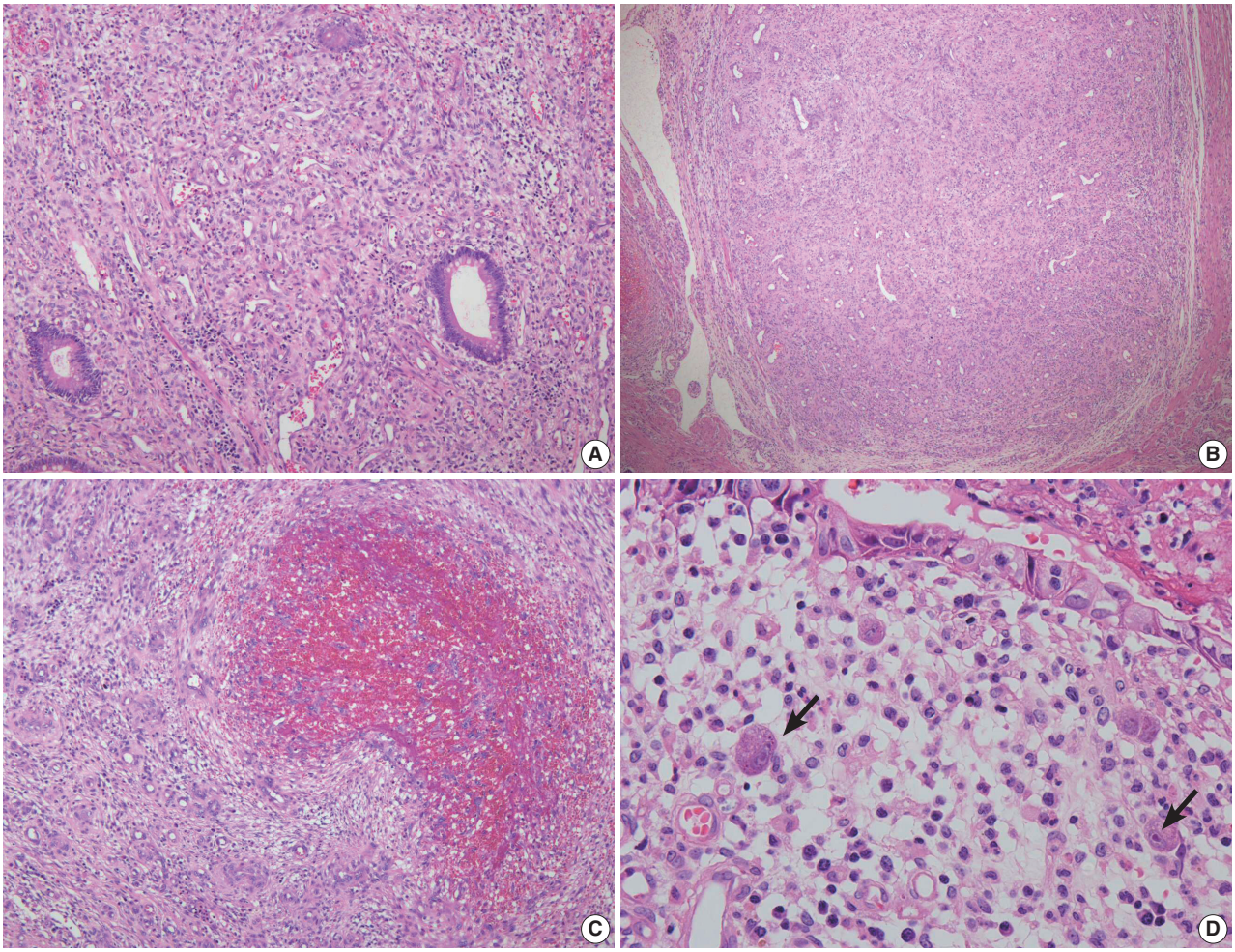

Fig. 2. (A) The lamina propria shows granulation tissue-type small vessel proliferation. (B) The nodules at deeper layers are composed of proliferated florid small vessels and fibroblasts. (C) Organizing-thrombus-like areas are noted focally in the nodules. (D) A few stromal cells with intranuclear and cytoplasmic cytomegalovirus inclusions are present beneath the eroded mucosal surface.

Recurrent intussusception produces variable nonspecific histologic changes, including disorganization of the muscularis propria, fusion of the muscularis mucosae with the muscularis propria, focal submucosal fibrosis, telangiectasia, fibrous serosal adhesion, localized mucosal hyperplasia, etc.[8] In addition, florid small vascular proliferation has been reported, which may be so pronounced as to raise the possibility of primary vascular neoplasm.[9,10] Although the mechanisms underlying the development of such vascular lesions are difficult to ascertain, repeated mechanical forces applied to the bowel wall during long-term mucosal prolapse associated with intussusception trigger angiogenesis, resulting in an exuberant form of highly vascularized granulation tissue. The clinical history of prolonged intussusceptions may explain the granuloma pyogenicum-like solid nodules scattered at deeper layers with focal hemorrhages, and the organizing thrombus-like features of this case.

In summary, it is considered that CMV-induced mucosal inflammation acted as a lead point of intussusception, and persistent prolonged intussusception caused nodular florid vascular proliferation of deeper layers, in this case with unique microscopic and gross findings.

Conflicts of Interest

No potential conflict of interest relevant to this article was reported.

Acknowledgments

This study was supported by a grant from the Memorial Research Foundation for the 50th anniversary of the Medical College of Ewha Womans University, Medical College of Ewha Womans University Alumnae Association.

REFERENCES

1. Ma R, Alam M, Pacilli M, Hook E, Nagy A, Carroll D. A rare case of neonatal intussusception caused by cytomegalovirus. Eur J Pediatr Surg 2014; 24: 184-6.
2. Agaimy A, Mudter J, Markl B, Chetty R. Cytomegalovirus infection presenting as isolated inflammatory polyps of the gastrointestinal tract. Pathology 2011; 43: 440-6.
3. Zupancic JA, Pennie RA, Issenman R. Intussusception in a child with cytomegalovirus infection. Pediatr Infect Dis J 1994; 13: 548-9.
4. Chetty R, Roskell DE. Cytomegalovirus infection in the gastrointestinal tract. J Clin Pathol 1994; 47: 968-72.
5. Seo TH, Kim JH, Ko SY, *et al*. Cytomegalovirus colitis in immunocompetent patients: a clinical and endoscopic study. Hepatogastroenterology 2012; 59: 2137-41.
6. Kelesidis T, Tozzi S, Mitty R, Worthington M, Fleisher J. Cytomegalovirus pseudotumor of the duodenum in a patient with AIDS: an unrecognized and potentially treatable clinical entity. Int J Infect Dis 2010; 14: e274-82.
7. Lin WR, Su MY, Hsu CM, *et al*. Clinical and endoscopic features for alimentary tract cytomegalovirus disease: report of 20 cases with gastrointestinal cytomegalovirus disease. Chang Gung Med J 2005; 28: 476-84.
8. Noffsinger A, Fenoglio-Preiser CM, Maru D, Gilinsky N. Gastrointestinal diseases: atlas of nontumor pathology. Washington, DC: American Registry of Pathology, 2008.
9. Ramsden KL, Newman J, Moran A. Florid vascular proliferation in repeated intussusception mimicking primary angiomatous lesion. J Clin Pathol 1993; 46: 91-2.
10. Bavikatty NR, Goldblum JR, Abdul-Karim FW, Nielsen SL, Greenson JK. Florid vascular proliferation of the colon related to intussusception and mucosal prolapse: potential diagnostic confusion with angiosarcoma. Mod Pathol 2001; 14: 1114-8.

Journal of Pathology and Translational Medicine 2015; 49: 274-278
http://dx.doi.org/10.4132/jptm.2015.03.12

■ BRIEF CASE REPORT ■

A Case of Primary Subpleural Pulmonary Microcystic Myxoma Coincidentally Occurred with Pulmonary Adenocarcinoma

Jungsuk Ahn · Na Rae Kim · Seung Yeon Ha · Keun-Woo Kim[1] · Kook Yang Park[1] · Yon Mi Sung[2]

Departments of Pathology, [1]Thoracic Surgery, and [2]Radiology, Gachon University Gil Medical Center, Incheon, Korea

Myxoma occurs most commonly in the heart, which is regarded as the origin of primitive mesenchymal cells that differentiate into multiple tissues. Up to 18% of cardiac myxomas are located in the right atrium and are frequently diagnosed after recurrent pulmonary embolism.[1] Extracardiac myxomas have been reported in the subcutaneous tissue, muscle, and lung.[2,3] Nine cases of primary pulmonary myxoma have been described.[4,5] Due to its rarity, clinical and histologic review of pulmonary myxoma is limited in number.

To the best of our knowledge, this is the first report describing cytologic features of a primary pulmonary microcystic myxoma.

CASE REPORT

A 71-year-old Korean man was admitted for an incidentally detected pulmonary mass. The initial chest X-ray and subsequent computed tomography (CT) showed a subpleurally located, well-defined, round and smooth mass in the left upper lobe, measuring 1.0×0.8×0.7 cm in size (Fig. 1A). The surrounding parenchyma showed mild volume loss and focal consolidation, measuring about 2.0×2.0×1.8 cm. A poorly enhanced soft tissue lesion, measuring 3.5×3.0×2.0 cm in size, was also found in the anterior thymic area. Cardiac echographic findings were as follows; normal-sized cardiac chambers, normal left ventricular systolic function, normal left ventricle filling pattern, and no motional abnormalities or regional wall abnormalities. Under the impression of pulmonary hamartoma, a wedge resection of the subpleural mass and partial thymectomy through video-assisted thoracoscopic surgery was performed. A 3-month follow up was planned for the parenchymal consolidation.

Grossly, the wedge-resected lung showed a well-delineated, glistening, round, and gray subpleural mass (Fig. 1B). The cut surface of the mass was gelatinous mucoid, grayish yellow without a capsule. Intraoperative touch imprints were made using Papanicolaou and hematoxylin and eosin stains. The smears were paucicellular showing copious amounts of viscous pinkish mucoid material and scattered inflammatory cells (Fig. 2A). Scattered inflammatory cells such as macrophages containing foamy granular cytoplasm with occasional hemosiderin-laden macrophages were found. Cracking and a pleated pattern were observed on thickly smeared slides. Sparse capillaries were also found. There were a few loose aggregates of bland, monomorphic spindle cells with oval nuclei and no distinct nucleoli, and these spindle cells had long, thin, and tapered cytoplasmic processes (Fig. 2B). The nuclei were round to oval with indistinct nucleoli, and the cytoplasm was vacuolated and granular with a well-delineated cell border (Fig. 2C). Differential diagnoses for the frozen section were myxoid tumors including pulmonary hamartoma.

The specimen was fixed with 10% formalin, and paraffin-embedded tissue was stained with hematoxylin and eosin. Microscopically, the pulmonary mass was composed of scattered spindle-shaped mesenchymal cells with chronic inflammatory cells, embedded in a rich basophilic gelatinous myxoid matrix (Fig. 2D). Stellate cells with vacuolated bubbly cytoplasm were observed. Neither mitosis nor cytologic atypia was found in the stellate cells. In the abundant basophilic mucoid matrix, there were no cellular elements other than chronic inflammatory cells

Corresponding Author
Na Rae Kim, M.D.
Department of Pathology, Gachon University Gil Medical Center, 21 Namdong-daero 774 beon-gil, Namdong-gu, Incheon 405-760, Korea
Tel: +82-32-460-3847, Fax: +82-32-460-2394, E-mail: clara_nrk@gilhospital.com

Received: February 7, 2015 **Revised:** March 10, 2015
Accepted: March 12, 2015

pISSN 2383-7837
eISSN 2383-7845

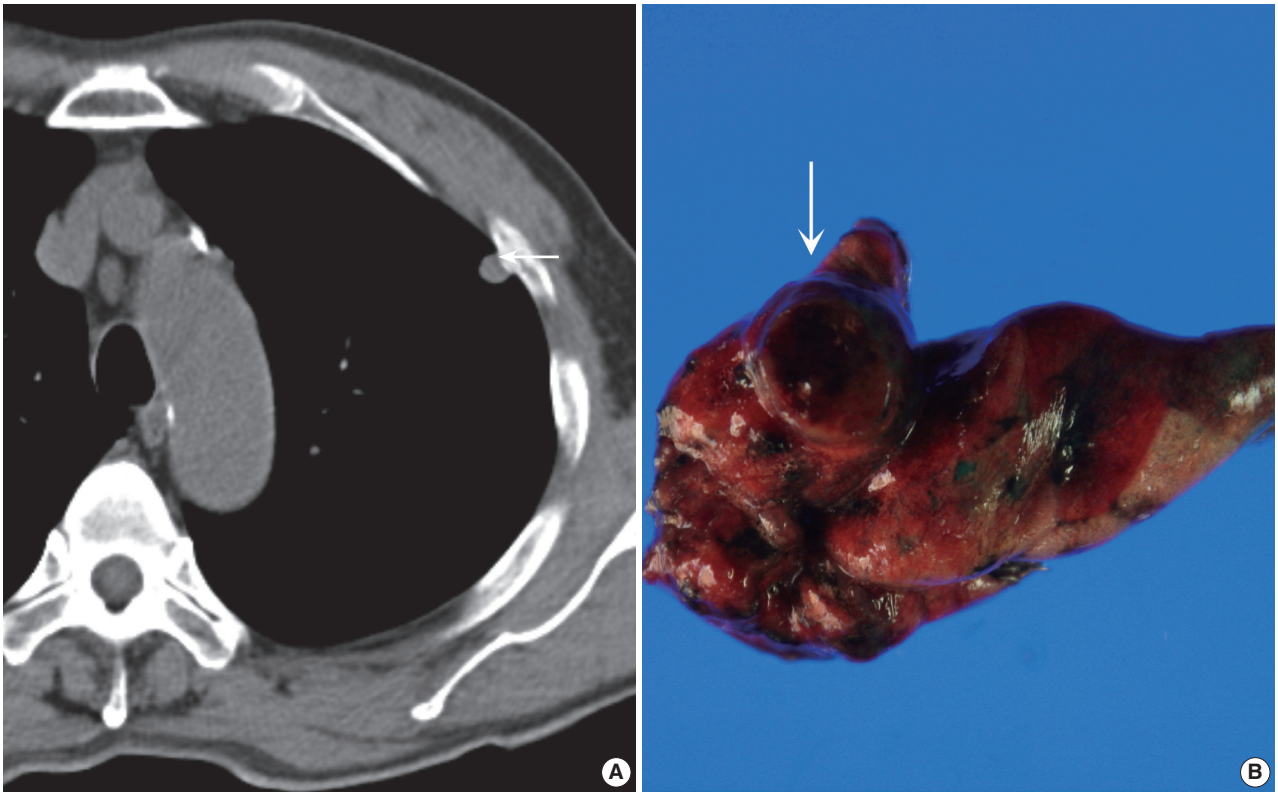

Fig. 1. (A) Precontrast chest computed tomography shows a well-delineated low-attenuated oval mass (arrow) with slightly high density delete the portion in the subpleural area. (B) Gross photo shows a well-demarcated ovoid mass (arrow) with a mucous gelatinous texture with focal hemorrhage.

and some neutrophils (Fig. 2E). The mass had predominantly microcytic changes lined by attenuated flattened cells or no lining of cells and the cystic spaces were empty or filled with myxid materials (Fig. 2F, left). Size of the cystic spaces ranged from 300 μm to 1.2 mm. Visceral pleura was free of tumor. The surrounding pulmonary parenchyma was normal. The fragmented partial thymectomy specimen showed a cystic structure, lined with cylindrical ciliated epithelial cells with surrounding normal-appearing thymic tissue with Hassall's corpuscles in the cyst wall. It was diagnosed as a unilocular thymic cyst.

Immunohistochemically, the spindle cells were positive for vimentin (prediluted, V9, Dako, Glostrup, Denmark) (Fig. 2F, right). They were all negative for matrix metalloproteinase (MMP)-2 (1:250, 4D3, Santa Cruz Biotechnology, Santa Cruz, CA, USA), MMP-9 (1:250, 2C3, Santa Cruz Biotechnology), pancytokeratin (prediluted, A1/A3, Dako), D2-40 (1:200, D2-40, Dako), TTF-1 (prediluted, 8G7G3, Dako), c-kit (1:40, T595, Novocastra, Newcastle upon Tyne, UK), S-100 protein (prediluted, polyclonal, Dako), desmin (prediluted, D33, Dako), smooth muscle actin (prediluted, 1A4, Dako), alpha-inhibin (1:50, BC/R1, Biocare Medical, Chicago, IL, USA), calretinin (prediluted, DAK-Calret1, Dako), CD34 (prediluted, QBEnd10, Dako), epithelial membrane antigen (prediluted, E29, Dako), CD68 (prediluted, PG-M1, Dako), CD99 (prediluted, 12E7, Dako), synaptophysin (prediluted, DAK-SYNAP, Dako), factor VIII-related antigen (prediluted, polyclonal, Dako), and factor XIII (1:50, E980.1, Novocastra). The myxoid stroma was stained with Alcian blue at pH 2.5 with or without hyaluronidase, periodic-acid Schiff (PAS) and diastase-resistant PAS. The Ki-67 (prediluted, MIB-1, Dako) proliferation index was less than 0.1%.

Ultrastructurally, the tumor was composed of several types of cells including spindle-shaped fibroblast-like cells (Fig. 3). The fibroblast-like spindle cells had a ruffled villus-like cell surface, and the cytoplasm was filled with rough endoplasmic reticulums, prominent Golgi complexes, and lysosomes. Amorphous flocculent and granular proteinaceous material and some collagen fibrils were observed in the extracellular spaces. Macrophages, mature lymphocytes, and some mast cells were also found. Cell junctions were not observed. Metastasis or embolic myxoma from the heart was excluded based on the absence of primary cardiac myxoma and the cytologic benignity of the pulmonary

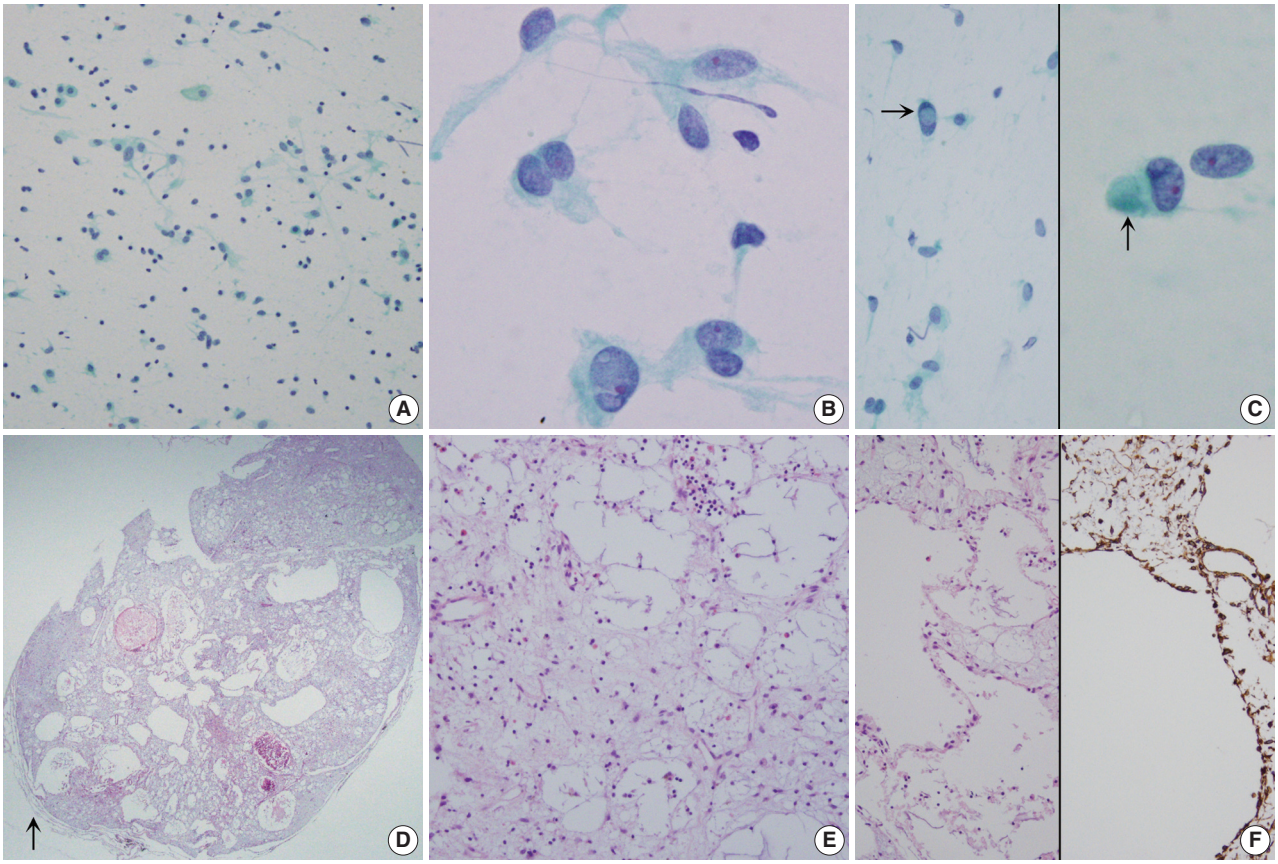

Fig. 2. (A–C) Touch imprint cytology. (A) Hypocellular smear shows many scattered inflammatory cells and macrophages. Note the background amorphous mucin-like metachromatic materials. (B) High-power view shows round to spindle cells having a moderate amount of granular cytoplasm and euchromatic round nuclei. (C) Note rare intranuclear inclusions (left, arrow) and cytoplasmic globular materials (right, arrow) (A–C, Papanicolaou stain). (D–F) Histologic findings. (D) Low-power view shows a well-demarcated bluish mass, and the mass is composed of predominantly chondromyxoid stroma. Arrow indicates normal pulmonary parenchyma. (E) High-power view shows that the mass is composed of abundant bluish chondromyxoid stroma and the paucicellular elements including scattered spindle cells, intermixed macrophages, mature lymphocytes, and some eosinophils. (F) Microcysts are surrounded by attenuated flattened cells or no lining (left, H&E stain; right, Vimentin immunostain).

mass. Primary pulmonary myxoma was the diagnosis.

Chest CT taken 2 months after the operation revealed an interval increase in the extent of parenchymal consolidative lesion in the left upper lobe, which was accompanied by left pleural effusion. Cytology through pleurocentesis revealed metastatic adenocarcinoma. Brain magnetic resonance images revealed a small parenchymal mass with focal enhancement in the left cerebellar hemisphere. Chemotherapy with pemetrexed and cisplatin was performed, and radiation therapy was planned.

DISCUSSION

Touch imprints of the current case were paucicellular with abundant gelatinous mucin showing a folded pattern and scattered mucinophages. Simple capillaries were also aspirated. The differential diagnoses based on the cytologic features were mucin-rich lesions including mesenchymal tumors such as myxoma, hamartoma, extraskeletal myxoid chondrosarcoma (EMCS) and low cellular epithelial tumors such as mucinous epithelial tumor.[1,6,7] Cytologic findings of pulmonary hamartoma are scantly cellular smears composed of bland-looking spindle and stellate cells and fibromyxoid materials in serosanguinous background.[6] Pulmonary hamartoma is composed of predominantly chondroid connective tissue, adipocytes and fibroblasts with intervening nests of bland-looking epithelial cells. Cartilaginous component is rarely aspirated. Fine needle aspirates may show highly cellular smears showing epithelial cells with fine granular chromatin, mimicking a neuroendocrine neoplasm. Benign to low-grade mucinous epithelial tumors show a predominance of epithelial cells in the cytology, but mucinous cystic epithelial

 http://dx.doi.org/10.4132/jptm.2015.03.12

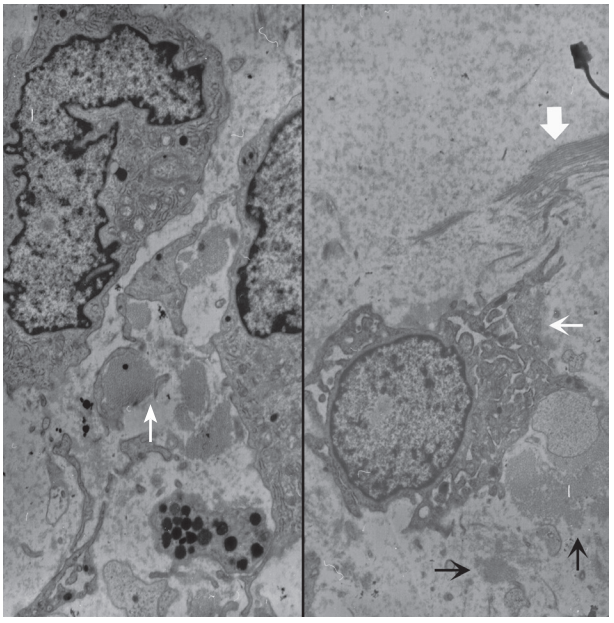

Fig. 3. Ultrastructural examination reveals spindle to round cells with round euchromatic nuclei and cytoplasm having many lysosomes, mitochondria, and rough endoplasmic reticulums. Extracellular amorphous mucin material (arrow) is observed (left, ×2,500). Multiple ruffled cell surfaces (thin arrow) and abundant collagen fibrils (thick arrow) are also observed (right, ×3,500).

tumors yield extremely low cellular mucin predominance with only a few floating epithelial cell nests. In such cases, diagnosis, particularly on scantly cellular cytology specimens, is exceedingly difficult. Mucin-rich smears must be searched carefully for clusters or single cells showing intracytoplasmic mucin vacuoles to ensure detection of mucinous cystic epithelial tumor. Cytologic findings of EMCS are composed of several fragments of polygonal to ovoid monotonous tumor cells with eccentrically located scalloped nuclei and peripheral fine cytoplasmic vacuoles embedded in a dense, metachromatic matrix as well as abundant myxoid materials.[7] Vesicular nuclei or nuclear grooves or inclusions may occasionally be found in EMCS.[8] Myxoid stroma can also be seen in myxoid liposarcoma.[9] Atypical lipoblasts have central or eccentric nuclei or scalloped and vacuolated cytoplasm with high nucleus-cytoplasmic ratio, and can be seen clustered around branching, arborizing capillaries, unlike the simple capillaries seen in the current case.

The histologic differential diagnosis of this case was limited; pulmonary hamartoma and myxoma are the main differential diagnoses. Other differential diagnoses included EMCS, and low-grade myxofibrosarcoma. Pulmonary hamartoma is an important differential diagnosis. Like cardiac myxoma, pulmonary myxoma is composed of rich connective tissue derived from fibroblasts and connective tissue mucin, whereas pulmonary hamartoma is composed of nonorganized epithelial cells and primitive mesenchymal spindle cells, including fibrous tissue, fat, smooth muscle, cartilage, and occasionally bone. Pulmonary myxoma consists of stellate or elongated fibroblast-like cells with abundant intercellular myxoid material. Variable amounts of inflammatory cell infiltration are a shared feature between myxoma and EMCS. EMCS is another important differential diagnosis, albeit extremely rare, in the lung. Pulmonary EMCS is a low-grade tumor with multilobulated growth. EMCS is a low-cellularity tumor composed of uniform oval to spindle cells arranged in short anastomosing cords in an abundant myxoid matrix. No hyaline cartilaginous differentiation is seen. Mitoses are rarely found. Microscopic characteristics important for distinguishing between EMCS and myxoma include the different nature of myxoid stroma; extracellular mucin in myxoma is hyaluronidase-sensitive, which is stained with Alcian-blue, whereas chondromyxoid type of stroma, i.e., sulfated mucopolysaccharides in (Condroitin sulphate and keratan sulphate) EMCS is stained with Alcian-blue and is hyaluronidase-resistant.

To date, 10 cases of primary pulmonary myxoma, including the current case, have been reported.[4,5] The ages of the patients ranged from 26 to 73 years (mean, 54.8 years). Five males and five females were reported. The tumor size ranged from 0.5 to 2.5 cm (mean, 1.59 cm). All except for two endobronchial lesions occurred in pulmonary parenchyma; the present case presented with subpleural parenchymal mass. Half of the cases presented with nonspecific symptoms; hemoptysis, dyspnea, shortness of breath, chest pain or exacerbation of underlying chronic obstructive pulmonary disease. The remaining lesions were found incidentally. All but two with coexisting pulmonary adenocarcinomas showed excellent clinical outcome. Complete excision was curative and metastasis was not reported in all cases. The current case is similar to three cases reported by Shilo *et al*.,[5] which were reported as microcystic fibromyxoma, a histologic variant of pulmonary myxoma. Due to rarity and the subsequent lack of cumulative data on pulmonary microcystic myxoma, we suggest that cysts negative for both vascular markers and epithelial markers may be related to increased MMP activity in a microcystic variant of pulmonary myxoma, as in cardiac myxoma, showing excessive degradation of extracellular matrix and resulting in increased potential risk for metastatic embolism.[10] Among 10 reported cases of pulmonary myxoma, metastasis had not yet been described. Accumulating prospective data on MMP-2 and MMP-9 immunoreactivities in pulmonary myxomas is necessary in order to evaluate the prognostic cor-

relation.

While preoperative fine-needle aspiration is a well-established preoperative diagnostic technique in the epithelial neoplasm, it is limited in diagnosing soft tissue lesions due to scanty cellularity and the dense nature of the soft tissue lesion. Given the rarity of myxoma in comparison to common hamartoma, cytopathologists might ignore this entity in the differential diagnosis. Acknowledging the cytology of this benign lesion, pathologists should consider the possible shared features with other myxoid lesions, including malignant tumors.

Conflicts of Interest

No potential conflict of interest relevant to this article was reported.

REFERENCES

1. Meir K, Maly A, Doviner V, Maly B. Intraoperative cytologic diagnosis of unsuspected cardiac myxoma: a case report. Acta Cytol 2004; 48: 565-8.
2. Alaiti S, Nelson FP, Ryoo JW. Solitary cutaneous myxoma. J Am Acad Dermatol 2000; 43(2 Pt 2): 377-9.
3. Nadrous HF, Krowka MJ, Myers JL, Allen MS, Sabri AN. Tracheal myxoma: a rare benign tracheal tumor. Mayo Clin Proc 2004; 79: 931-3.
4. Özdoğan S, Fidan A, Saraç G, Çağlayan B, Uçmakli E. Concomitant occurrence of lung adenocarcinoma and endobronchial myxoma: a case report. Turk Respir J 2004; 5: 124-7.
5. Shilo K, Miettinen M, Travis WD, Timens W, Nogueira R, Franks TJ. Pulmonary microcystic fibromyxoma: report of 3 cases. Am J Surg Pathol 2006; 30: 1432-5.
6. Jin MS, Ha HJ, Baek HJ, Lee JC, Koh JS. Adenomyomatous hamartoma of lung mimicking benign mucinous tumor in fine needle aspiration biopsy: a case report. Acta Cytol 2008; 52: 357-60.
7. Handa U, Singhal N, Punia RS, Garg S, Mohan H. Cytologic features and differential diagnosis in a case of extraskeletal mesenchymal chondrosarcoma: a case report. Acta Cytol 2009; 53: 704-6.
8. Insabato L, Terracciano LM, Boscaino A, Mozzi RA, Angrisani P, Pettinato G. Extraskeletal myxoid chondrosarcoma with intranuclear vacuoles and microtubular aggregates in the rough endoplasmic reticulum: report of a case with fine needle aspiration and electron microscopy. Acta Cytol 1990; 34: 858-62.
9. Munjal K, Pancholi V, Rege J, Munjal S, Bhandari V, Nahar R. Fine needle aspiration cytology in mediastinal myxoid liposarcoma: a case report. Acta Cytol 2007; 51: 456-8.
10. Orlandi A, Ciucci A, Ferlosio A, Pellegrino A, Chiariello L, Spagnoli LG. Increased expression and activity of matrix metalloproteinases characterize embolic cardiac myxomas. Am J Pathol 2005; 166: 1619-28.

 http://dx.doi.org/10.4132/jptm.2015.03.12

pISSN: 2383-7837
eISSN: 2383-7845

Executive Members

The Korean Society of Pathologists

The Korean Society for Cytopathology

Journal of Pathology and Translational Medicine

Volume 49 • Number 3 • May 2015 (bimonthly)
Published since 1967
Printed on 11 May 2015 Published on 15 May 2015

J Pathol Transl Med
pISSN: 2383-7837
eISSN: 2383-7845

Aims & Scope

The Journal of Pathology and Translational Medicine is an open venue for the rapid publication of major achievements in various fields of pathology, cytopathology, and biomedical and translational research. The Journal aims to share new insights into the molecular and cellular mechanisms of human diseases and to report major advances in both experimental and clinical medicine, with a particular emphasis on translational research. The investigations of human cells and tissues using high-dimensional biology techniques such as genomics and proteomics will be given a high priority. Articles on stem cell biology are also welcome. The categories of manuscript include original articles, review and perspective articles, case studies, brief case reports, and letters to the editor.

Subscription Information

To subscribe to this journal, please contact the Korean Society of Pathologists/the Korean Society for Cytopathology. Full text PDF files are also available at the official website (http://jpatholtm.org). *Journal of Pathology and Translational Medicine* is indexed by PubMed, PubMed Central, Scopus, KoreaMed, KoMCI, WRPIM and CrossRef. Circulation number per issue is 700.

Contact the Korean Society of Pathologists/the Korean Society for Cytopathology

Publishers: Changsuk Kang, M.D., So Young Jin, M.D.
Editors-in-Chief: Soon Won Hong, M.D., Chong Jai Kim, M.D.
Published by the Korean Society of Pathologists/the Korean Society for Cytopathology

Editorial Office
Room 1209 Gwanghwamun Officia, 92 Saemunan-ro, Jongno-gu,
Seoul 110-999, Korea/#406 Lilla Swami Bldg, 68 Dongsan-ro,
Seocho-gu, Seoul 137-899, Korea
Tel: +82-2-795-3094/+82-2-593-6943
Fax: +82-2-790-6635/+82-2-593-6944
E-mail: office@jpatholtm.org

Printed by ML communications Co., Ltd.
Jungang Bldg. 18-8 Wonhyo-ro 89-gil, Yongsan-gu, Seoul 140-846, Korea
Tel: +82-2-717-5511 Fax: +82-2-717-5515 E-mail: ml@smileml.com

Manuscript Editing by InfoLumi Co.
210-202, 421 Pangyo-ro, Bundang-gu, Seongnam 463-926, Korea
Tel: +82-70-8839-8800 E-mail: infolumi.chang@gmail.com

Front cover image: Confocal laser endomicroscopic finding for normal mucosa. p213.

This paper meets the requirements of KS X ISO 9706, ISO 9706-1994 and ANSI/NISO Z.39.48-1992 (Permanence of Paper).
This journal was supported by the Korean Federation of Science and Technology Societies Grant funded by the Korean Government.

Journal of Pathology and Translational Medicine

J Pathol Transl Med
pISSN: 2383-7837
eISSN: 2383-7845

Volume 49, Number 3, May 2015

CONTENTS

REVIEWS

ORIGINAL ARTICLES

CASE REPORTS

CONTENTS CONTINUED

Instructions for Authors for *Journal of Pathology and Translational Medicine* are available at http://jpatholtm.org/authors/authors.php

JPTM
Journal of Pathology and Translational Medicine